Metabolic Impact of the Succinate/SUCNR1 Axis in Adipocytes: Insights into Circadian and Leptin Regulation

TERESA VILLANUEVA CARMONA

ADVERTIMENT. L'accés als continguts d'aquesta tesi doctoral i la seva utilització ha de respectar els drets de la persona autora. Pot ser utilitzada per a consulta o estudi personal, així com en activitats o materials d'investigació i docència en els termes establerts a l'art. 32 del Text Refós de la Llei de Propietat Intel·lectual (RDL 1/1996). Per altres utilitzacions es requereix l'autorització prèvia i expressa de la persona autora. En qualsevol cas, en la utilització dels seus continguts caldrà indicar de forma clara el nom i cognoms de la persona autora i el títol de la tesi doctoral. No s'autoritza la seva reproducció o altres formes d'explotació efectuades amb finalitats de lucre ni la seva comunicació pública des d'un lloc aliè al servei TDX. Tampoc s'autoritza la presentació del seu contingut en una finestra o marc aliè a TDX (framing). Aquesta reserva de drets afecta tant als continguts de la tesi com als seus resums i índexs.

ADVERTENCIA. El acceso a los contenidos de esta tesis doctoral y su utilización debe respetar los derechos de la persona autora. Puede ser utilizada para consulta o estudio personal, así como en actividades o materiales de investigación y docencia en los términos establecidos en el art. 32 del Texto Refundido de la Ley de Propiedad Intelectual (RDL 1/1996). Para otros usos se requiere la autorización previa y expresa de la persona autora. En cualquier caso, en la utilización de sus contenidos se deberá indicar de forma clara el nombre y apellidos de la persona autora y el título de la tesis doctoral. No se autoriza su reproducción u otras formas de explotación efectuadas con fines lucrativos ni su comunicación pública desde un sitio ajeno al servicio TDR. Tampoco se autoriza la presentación de su contenido en una ventana o marco ajeno a TDR (framing). Esta reserva de derechos afecta tanto al contenido de la tesis como a sus resúmenes e índices.

WARNING. Access to the contents of this doctoral thesis and its use must respect the rights of the author. It can be used for reference or private study, as well as research and learning activities or materials in the terms established by the 32nd article of the Spanish Consolidated Copyright Act (RDL 1/1996). Express and previous authorization of the author is required for any other uses. In any case, when using its content, full name of the author and title of the thesis must be clearly indicated. Reproduction or other forms of for profit use or public communication from outside TDX service is not allowed. Presentation of its content in a window or frame external to TDX (framing) is not authorized either. These rights affect both the content of the thesis and its abstracts and indexes.

Metabolic Impact of the Succinate/SUCNR1 Axis in Adipocytes: Insights into Circadian and Leptin Regulation

UNIVERSITAT ROVIRA i VIRGILI

TERESA VILLANUEVA CARMONA

Doctoral Thesis

2024

Teresa Villanueva Carmona

Metabolic Impact of the Succinate/SUCNR1 Axis in Adipocytes: Insights into Circadian and Leptin Regulation

DOCTORAL THESIS

Supervised by:

Dr. Sonia Fernández Veledo

Dr. Joan Vendrell Ortega

Dr. Lídia Cedó Giné

UNIVERSITAT ROVIRA i VIRGILI

2024

UNIVERSITAT ROVIRA i VIRGILI

Sonia Fernández Veledo, Ph.D. in Biomedicine from the University of Barcelona, senior researcher at the Pere Virgili Health Research Institute (IISPV) and Associate Professor at the Rovira I Virgili University (URV). Joan Vendrell Ortega, M.D. and Ph.D. in Medicine and Surgery from the University of Barcelona, specialist in Endocrinology and Nutrition, Director of the IISPV, and Full Professor at URV. Both are co-leaders of the IISPV´s Research Group in Diabetes and Associated Metabolic Diseases. Lídia Cedó Giné, Ph.D. in Nutrition and Metabolism from the URV, and postdoctoral researcher at the IISPV.

CERTIFY THAT

The present doctoral thesis, entitled "**Metabolic Impact of the Succinate/SUCNR1 Axis in Adipocytes: Insights into Circadian and Leptin Regulation**", presented by Teresa Villanueva Carmona has been carried out under our direct supervision at the Pere Virgili Health Research Institute and the Department of Medicine and Surgery of this university and fulfills the requirements for the award of the Doctorate degree.

This certification is signed in Tarragona on August 21, 2024, for official record and initiation of the required procedures.

Doctoral Thesis Supervisors

Dr. Sonia Fernández-Veledo Dr. Joan Vendrell Ortega Dr. Lídia Cedó Giné

A mis pilares fundamentales,

mi madre y mi padre.

Y a ti, Paco, el amor de mi vida.

ACKNOWLEDGMENTS

Después de estos cuatro años, podría decir que la tesis doctoral ha sido como subir a una montaña rusa, con subidas, bajadas y mil emociones diferentes a lo largo del trayecto. Mirando atrás, esta experiencia no sólo me ha hecho crecer profesionalmente, sino que también, y quizá más importante, a nivel personal. Esto ha sido en gran parte gracias a las personas que han estado a mi lado durante estos años, a unos centímetros, o a varios (bastantes) kilómetros de distancia. Sin lugar a duda, no podría haber llegado hasta aquí sin este apoyo, por lo que no quería dejar pasar la oportunidad de dar las gracias a todas las personas que me han acompañado durante estos emocionantes e intensos años.

Me gustaría comenzar agradeciendo a mis directores de tesis, Sonia y Joan, por confiar en mi desde el principio y guiarme durante todo el proceso. Gracias por vuestro apoyo, paciencia y consejos, tanto profesionales como personales, y por transmitirme vuestra pasión por la investigación. Todavía recuerdo la primera entrevista con Sonia, cuando le pregunté si en Tarragona había metro (claramente no sabía dónde me metía) Gracias a Lídia, no solo por ser también mi directora de tesis, sino por haber sido un apoyo fundamental en cada paso de esta etapa y por los buenos momentos que hemos compartido.

Continuaré agradeciendo a todos mis compañeros del grupo DIAMET, con quienes he compartido el día a día durante estos intensos años. Gracias por, de una manera u otra, haberme ayudado en los momentos más difíciles, pero también por todos los momentos de cafés, comilonas, y muchísimas risas que hacían más amenos los días. ¡Mil gracias!

En mi primera etapa del doctorado, quiero agradecer a Noe, quien me enseñó todo desde cero, y a Joan, de quien aprendí mucho también. Llegué a Tarragona en un verano marcado por la pandemia, una época difícil con restricciones que hicieron más complicado integrarse en una ciudad nueva. Sin embargo, desde el primer momento, ellos hicieron todo más fácil y me acogieron con los brazos abiertos. Recuerdo con cariño ese verano en el laboratorio, con trabajo intenso, pero también con recompensas, como las cervecitas de después. También quiero agradecer a Diandra, quien ha estado desde el día uno mano a mano conmigo, compartiendo mil momentos juntas: el café de las 10 de cada día, las meriendas, los momentos de gimnasio, las cervezas (que no fueron pocas), o el concierto de Coldplay. Gracias por entenderme tan bien y por ser mi ratito de desconexión. No te imaginas lo esencial que has sido para mí en esta etapa. Además, quiero agradecer al resto del "team almuerzo" de las 10: Julen, Laura, Javi, Nerea, Alejandro…esos ratitos de risa y desconexión eran indispensables para mí. No puedo continuar sin agradecer a Anna y Maria, dos personitas que se han convertido en imprescindibles en mi vida. Compartir el trabajo con amigas ha sido una suerte. Gracias por hacerme este camino más fácil, por haber estado siempre ahí, por enseñarme tanto

y darme fuerzas en mis momentos más débiles. Pero, sobre todo, gracias por todos los momentos fuera del laboratorio, las risas y todo lo que nos espera juntas. Os quiero.

Continuando con mis compañeros de trabajo, de cada una me llevo algo especial. Mar, gracias por los ratitos en el estabulario, los cafés, el viaje a Madrid, las cervezas, tus consejos, y ese concierto en Madrid. Cati, ¿qué sería del laboratorio sin ti? Gracias por enseñarme, por tu paciencia (incluso con los westerns), y por aprender lo necesario para ayudarme. Elsa, gracias por nuestras charlas, risas, y cotilleos. Gracias por ser tan sincera y por decir lo que piensas en cada momento (en ese sentido eres muy como yo). Vicky, no importa cuánta gente haya a tu alrededor, tu concentración es de otro nivel. Gracias enseñarme, ayudarme y por las risas que quitan importancia a los momentos de estrés. Ana Madeira, gracias por siempre tener una sonrisa, por alegrarte de mis logros y animarme en los momentos difíciles. Carme, por siempre reírte por todo y por ser tan auténtica, por tus historias absurdas y la tranquilidad que me aportas. Javi, gracias por tus bromas y por llenar el laboratorio de alegría con tu toque andaluz, además de entenderme tan bien, sobre todo en mis momentos de "autismo". Aleix, por tu alegría contagiosa, tu disposición siempre a ayudar y por compartir la locura del crossfit. Carlos, por las calçotadas en tu casa (aunque la lesión que me llevé boxeando no se me olvida), por tu humor único y por compartir tu pasión por el Atlético de Madrid. Y, por supuesto, mil gracias a Laura, Sergiy, Isa, Marga, Ester…¡todos habéis formado parte de esta experiencia conmigo!

Gracias a mi "Petit Comité" de Tarragona, Noe, Cris y Ash. Gracias por haber estado desde el primer día que llegué a Tarragona y por ser mi desconexión. Gracias por entenderme y acompañarme en esta etapa. Gracias por darle vida a eso de "científica de día, pero perreo de noche". Por cada brunch, cada carrera, las enchiladas de Noe, la sobrasada vegana de Cris y la rúcula de Ash. Gracias por todo. Os quiero.

Una de las mejores experiencias durante el doctorado fue la estancia en Toronto. I am super grateful to Dr. Daniel Drucker for making this experience possible, for welcoming me into your research group, always treating me as one of the team, and for everything you've taught me. Thank you for the Blue Jays game, the Christmas dinner at your home, and all the unforgettable moments you've shared with me. Through this opportunity, I have met so many wonderful people. Chusa, mi hermana gallega en Toronto. Allí, además de ser mi compañera de trabajo, fuiste mi amiga, mi compi de gimnasio, mi vecina, todo. Gracias a ti viví una experiencia increíble, y te has convertido en una persona súper importante en mi vida, siempre apoyándome y celebrando mis logros. Gracias también a Julia y a Miguel, quienes junto a ti fueron mi hogar y círculo de confianza allí, compartiendo muchos momentos como las charlas arreglando el mundo, los bubble teas, los brunchs, las cervezas o las comidas en nuestro tailandés favorito. Thanks also to all my lab colleagues there. To my essential ones (along with Chusa): Jackie and Rui. To me, this experience is defined by you two. Jackie, thank you for all the help you gave me, for being my partner in the lab, and my desk buddy. Thank you for always having a

smile, for always seeing the positive side of things, and for sending me photos of your snow-covered house just because you knew I loved it. Rui, you've been such an amazing discovery. Thank you for being so much like me, for the trust you've given me, for all the silliness and laughter we've shared. Thank you for teaching me your traditions, welcoming me into your home, and introducing me to the world of Hot Pots. Te quiero.

En esta parte, quiero agradecer a esas personitas que, a pesar de la distancia, las he sentido muy cerca. A lo mejor que me dio Badajoz: Ana Compe, Iván, Alba, Coco, Fernando, Javi, Sara, Ana Pocostales (y muchos más). Gracias por darme fuerzas, por impulsarme a seguir y por estar al otro lado del teléfono siempre que lo he necesitado. También quiero agradecer a mis amigas de toda la vida: Pas, Mery, Marta, Apa, Belén, Cris…. Gracias por ser mi refugio, por estar ahí siempre que volvía a casa y recargar energías en medio de este camino. Gracias a mis amigas de Patos, en especial a Elena, por nuestra conexión, los planes, las croquetas y las cañas de milnueve, los audios eternos, y hasta por las galletas con mayonesa. Gracias por estar en los momentos más importantes, y por hacer que, pese a la distancia, todo siga igual.

También, para mí ha sido muy importante mi etapa en Valencia y me llevo a personas increíbles. A Bea, sin duda, lo mejor del máster. Por seguir contándonos la vida, por siempre vernos mínimo 5 veces al año y por mantener esta amistad tan bonita siempre. Lo más especial que me llevo de Valencia es mi experiencia en el CIPF, la cual me ha impulsado a llegar donde estoy hoy. El laboratorio era como una familia, y el ambiente era tan increíble que cada día me despertaba con ganas de ir a trabajar. Vivir la ciencia en un entorno tan sano fue lo que me llevó a embarcarme en este camino. En este laboratorio conocí al amor de mi vida, lo cual contribuyó a que estuviera tan a gusto, para qué mentir, pero de él hablaré más adelante. Quien más me ha marcado durante esta etapa ha sido Juan: tenías una pasión por la ciencia que era contagiosa, te veía disfrutar haciendo lo que te gustaba cada día, siempre en tu despacho con ganas de bajar a almorzar, hacer una paradita para hablar de la vida, y siempre con tiempo para tus amigos. Me diste momentos inolvidables y me trataste como a una "princesita" (como tú me decías). De todos los momentos, me quedo con tu boda con Majo, un día que recordaré siempre (gracias a ti empecé mi historia con Paco, y siempre voy a estar agradecida). Después, cuando empecé mi doctorado, fuiste un apoyo muy importante y siempre me alegraba compartir mis logros contigo. Hoy, eres de mis estrellas favoritas en el cielo, y espero que estés orgulloso de lo que he logrado. A Majo la quiero mucho también, y a pesar de la distancia, siempre intentamos vernos y sacar un ratito para disfrutar de una buena cerveza, reírnos y hablar de la vida. De esta etapa también me llevo a Susana, por seguir compartiendo momentos juntas, por cuidarnos tanto cuando vamos a tu casa y por nuestros cotilleos y charlas interminables. En resumen, Valencia ha sido una etapa increíble que ha marcado mi doctorado y mi vida en todos los sentidos.

Por supuesto, no hubiera conseguido esto sin mi familia, especialmente sin mis padres. Gracias por vuestro apoyo incondicional, por todas las oportunidades que he tenido

gracias a vosotros, por vuestro esfuerzo para cuidarme y enseñarme (a pesar de que no siempre ha sido fácil). Por cada llamada en la que conseguíais transmitirme tranquilidad sólo con contarme cómo había ido vuestro día. Gracias porque, a pesar de la distancia y de estar lejos de casa, siempre me habéis apoyado en mis decisiones y animado a hacer lo que realmente quiero. Gracias también a mi hermano, por ser el alma divertida de nuestra casa y por simplemente estar ahí. Aunque no te lo diga nunca, te quiero mucho. Gracias, porque de una forma u otra, has formado parte de esta etapa de mi vida, incluso sin entender muy bien lo que estaba haciendo.

Por último, quiero dedicar el agradecimiento más especial a Paco, quien realmente ha estado a mi lado en cada momento, siendo mi roca, mi mayor motivación y mi ejemplo a seguir (siempre te lo he dicho y te lo seguiré diciendo). Empecé el doctorado en un momento complicado: tú estabas en Nueva York haciendo tu estancia y yo tenía que tomar una decisión antes de que volvieras. A pesar de tener que irme de Valencia, siempre me apoyaste y animaste a seguir mi sueño, y no puedo agradecértelo lo suficiente. Gracias también a tus padres, Paqui y Juan, que siempre han estado ahí durante esta etapa y la han vivido conmigo también. El principio del doctorado coincidió con el inicio de la pandemia, por lo que empecé tres meses más tarde de lo previsto y pude disfrutar de ti un poquito más (para mí esos meses fueron increíbles). Cuando finalmente me mudé a Tarragona, nos enfrentamos a un montón de restricciones y, aun así, encontramos la manera de vernos, aunque fuera pidiendo cita en un médico diferente cada semana solo para pasar unos días juntos. Después llegó tu gran momento: te convertiste en doctor. No pude estar más orgullosa de ti ese día, y no pudiste hacerlo mejor. Recuerdo estar más nerviosa que tú, pero lo hiciste increíble. No me voy a olvidar nunca. Unos meses después decidiste venirte a vivir conmigo a Tarragona, y no te imaginas lo feliz que me hiciste. Gracias por ser mi compañero de vida y por compartir cada momento de este camino. Gracias por creer en mí incluso cuando yo dudaba, y por recordarme siempre que puedo con todo. Por ser mi refugio en los días más duros, por sacarme una sonrisa cuando lo único que quería era tirar la toalla, y por celebrar conmigo cada logro como si fuera tuyo. Gracias por tu paciencia infinita y por entender las horas extra de trabajo (ventajas tener un novio doctor). Has soportado mis momentos de estrés, mi ausencia y mi cansancio con una paciencia y un amor que me nunca dejará de sorprenderme. Gracias por cada abrazo al volver de trabajar (no sabes cuánto me curan tus abrazos). Sólo con saber que al llegar a casa estarías tú, ya era feliz. Has sido mi pilar, mi fuente de energía, y la persona que más me ha impulsado a seguir adelante, y esta tesis es un reflejo de todo lo que hemos conseguido juntos. Cada detalle del día a día, por más simple que pareciera, ha sido esencial, y nada de esto hubiera sido posible sin ti. Gracias por ser el mejor novio que podría tener, por ser mi mejor amigo, mi familia y todo lo que quiero en mi futuro. Te amo.

TABLE OF CONTENTS

ABBREVIATIONS **1**

ABSTRACT **7**

INTRODUCTION **13**

1. THE SUCCINATE/SUCCINATE RECEPTOR 1 AXIS **15**

1.1 Origin Of Extracellular Succinate **16**

1.1.1. Host-Derived Succinate 16

1.1.2. Microbiota-Derived Succinate 17

1.2 Intracellular Roles Of Succinate Beyond Energy **20**

1.2.1. Mechanisms Leading To Succinate Accumulation 20

1.2.2. Succinate As An Intracellular Signalling Molecule 22

1.3. Succinate Transport To The Extracellular Space **25**

1.4. Circulating Succinate In Health And Disease **26**

1.4.1. Circulating Succinate In Health 26

1.4.2. Circulating Succinate In Pathology 28

1.5. The Succinate Receptor **31**

1.5.1. Succinate Receptor Structure And Ligands 31

1.5.2. Signal Mechanisms Of GPCRs 33

1.5.3. Signaling Pathways Mediated By SUCNR1 36

1.5.4. Succinate/SUCNR1 Signaling In Inflammation 40

1.5.5. Metabolic Functions Ascribed To SUCNR1 Signaling 42

2. ADIPOSE TISSUE **45**

2.1. Adipocytes **45**

2.1.1. Functions And Types 45

2.1.2. Origin Of Brown, White And Beige Adipocytes 48

2.2. White Adipose Tissue **51**

2.2.1. Functions 51

2.2.2. Distribution And Metabolic Implications 51

2.2.3. Non-Adipocyte Cellular Fraction 52

2.3. Brown Adipose Tissue **54**

2.3.1. Functions 54

2.3.2. Distribution 56

2.3.3. Cellular Composition 57
2.4. Adipose Tissue As An Energy Storage Organ 58
2.5. Adipose Tissue As An Endocrine Organ 60
2.5.1. Adipokines 60
2.5.1.1. The Biology Of Leptin 61
2.5.1.2. Leptin Roles In Physiology And Pathology 63
2.5.1.3. Leptin And Regulation Of Bone Metabolism 64
2.5.2. Other Adipocyte-Derived Factors 65
3. CIRCADIAN CLOCK 68
3.1. Mammalian Circadian System 68
3.2. Molecular Basis Of Circadian Rhythm 68
3.3. Circadian Rhythmicity Within Metabolic Tissues 71
4. OBESITY 73
4.1. Epidemiology Of Obesity 73
4.2. Pathophysiology Of Obesity 74
4.3. Obesity, Insulin Resistance And Type 2 Diabetes 74
4.4. Obesity And Phenomenon Of Leptin Resistance 75
4.5. Obesity And Circadian Rhythms 76
4.6. Obesity-Induced Changes In Adipose Tissue 78
4.6.1. Adipose Tissue Expansion 78
4.6.2. Immune Cell Infiltration 79
4.6.3. Impaired Vascular Structure And Function 81
4.6.4. Adipose Tissue Fibrosis 82
4.7. Ectopic Fat Accumulation 82
4.8. Obesity Treatments 85
HYPOTHESIS AND OBJECTIVES 89
MATERIALS AND METHODS 93
1. EXPERIMENTAL MODELS AND SUBJECT INFORMMATION 95
1.1. Human Cohorts 95
1.2. Mice Studies 95
1.2.1. Adipocyte-Cell Specific *Sucnr1* KO Mice 96
1.2.1.1. Generation 96

1.2.1.2. Genotyping 97
1.2.2. Other Mouse Models 99
1.3. Mouse AT Explants 99
1.4. Primary mASCs And Mature Adipocytes 100
1.5. Isolation And Culture Of Primary Mouse BM-MSCs 101
1.6. Primary Human ASCs 102
1.6.1. Isolation 102
1.6.2. Differentiation Into Mature Adipocytes 102
1.7. 3T3-L1 Cell Line 102
1.7.1. Cell Culture Conditions 102
1.7.2. Differentiation 103
1.7.3. Experimental Conditions 103
1.8. HEK 293 Cell Line 104
2. METHOD DETAILS 105
2.1. Indirect Calorimetry 105
2.2. Locomotor Activity And Food Intake 105
2.3. Quantitative Magnetic Resonance Imaging 105
2.3.1. Fat Mass 106
2.3.2. *In Vivo* Proton Magnetic Resonance Spectroscopy 106
2.3.3. Muscle Volume 107
2.4. Metabolic Tolerance Tests 107
2.4.1. Glucose Tolerance Test 107
2.4.2. Insulin Tolerance Test 108
2.5. Effect Of Oral Succinate On Circulating Leptin 108
2.6. *In Vivo* Lipolysis Inhibition 108
2.7. Chronic Leptin Treatment 109
2.8. Feeding Studies And Leptin Sensitivity Tests 109
2.9. Microcomputed Tomography 110
2.10. *Ex Vivo* Lipolysis Determination 110
2.11. Brown Adipocyte Differentiation Of mASCs 111
2.11.1. Culture And Differentiation 111
2.11.2. Lipid Accumulation Assessment And Imaging 111

2.12. Osteoblast Differentiation Of BM-MSCs 111
2.12.1. Culture And Differentiation 111
2.12.2. Staining Procedure And Imaging 112
2.13. Cell Fractionation Assay 112
2.14. Biochemical Parameters 113
2.14.1. Enzymatic Quantification Of Plasma Lipids 113
2.14.2. Leptin Measurement 113
2.14.3. Determination Of Succinate Levels 113
2.15. Gene Expression Analysis 113
2.15.1. Total RNA Extraction And Quantification 114
2.15.2. cDNA Synthesis And qPCR 114
2.15.3. Data Analysis And Interpretation 115
2.16. Transcriptome Analysis By RNA Sequencing 115
2.16.1. Sample Collection And Library Preparation 115
2.16.2. Sequencing And Data Analysis 116
2.17.Protein Levels Analysis By Western Blot 116
2.17.1. Protein Extraction 116
2.17.2. Protein Quantification 117
2.17.3. Western Blotting 118
2.18. Histological Analysis Methods For Mouse Tissue 121
2.18.1. Hematoxylin And Eosin Staining 121
2.18.2. Ucp1 Immunohistochemistry 121
2.18.3. Bone Histology 122
2.19. Luciferase Reporter Assay 122
2.19.1. Transfection And Treatment 122
2.19.2. Luciferase Assay And Luminescence Measurement 123
3. QUANTIFICATION AND STATISTICAL ANALYSIS 124
3.1. Statistical Analysis Methodology 124
3.2. Data Presentation Techniques 124
3.3. Regression And Model Fitting 124
3.4. Statistical Analysis For Clinical Data 124
3.5. RNA Sequencing And Bioinformatics Analysis 125

RESULTS **127**
Study 1 ..... **130**
Study 2 ..... **175**
DISCUSSION **187**
1. IMPACT OF *SUCNR1* DELETION ON METABOLIC HEALTH **191**
2. METABOLIC EFFECT OF ADIPOCYTE *SUCNR1* IN HFD MICE **194**
3. SUCCINATE AS A HORMONE-LIKE METABOLITE **195**
3.1. Leptin Regulation Via Succinate/SUCNR1 In Adipocytes **195**
3.2. Circadian Clock: Succinate/SUCNR1 Implication **196**
3.3. Impact Of The Succinate/SUCNR1 Axis In Human AT **198**
4. OBESITY-LINKED DISTURBANCES IN SUCCINATE/SUCNR1 AXIS **200**
5. RESEARCH INSIGHTS AND FUTURE DIRECTIONS **201**
CONCLUSIONS **203**
REFERENCES **207**
ANNEX **261**
1. SUPPLEMENTARY METHOD DETAILS **263**
2. POSTERS AND ORAL COMMUNICATIONS **271**
3. FELLOWSHIPS, AWARDS, AND HONORS **273**
4. RESEARCH STAYS DURING THE DOCTORAL PERIOD **274**

ABBREVIATIONS

ABBREVIATIONS

α-KG: α-ketoglutarate

α-SMA: α-smooth muscle actin

Ab/Am: Antibiotic/antimycotic

abWAT: Abdominal white adipose tissue

AC: Adenylyl cyclase

Ad-*Sucnr1* KO: Adipocyte-cell specific *Sucnr1* knockout

AICAR: 5-aminoimidazole-4-carboxamide ribonucleotide

AMP: Adenosine monophosphate

AMPK: Adenosine mono-phosphate-activated protein kinase

AOM: Anti-obesity medication

ARNT: Aryl Hydrocarbon Receptor Nuclear Translocator

ASCs: Adipose-derived stem cells

AT: Adipose tissue

ATGL: Adipocyte triglyceride lipase

ATGLi: Adipocyte triglyceride lipase inhibitor

ATM: Adipose tissue macrophage

ATP: Adenosine triphosphate

β3-AR: β3-adrenergic receptor

β-TrCP: β-Transducin Repeat Containing E3 Ubiquitin Protein Ligase

BAT: Brown adipose tissue

BBB: Blood-brain barrier

BCAAs: Branches-chain amino acids

BMAL1: Brain and muscle ARNT-like protein-1

***Bmal1* KO mice**: B6.129-*Arntl*^{tm1Bra}/J KO mice

BMI: Body mass index

BM-MSCs: Bone marrow mesenchymal stem cells

BMPs: Bone morphogenetic proteins

BSA: Bovine serum albumin

Ca^{2+}: Calcium ions

CaMKIIδ: Calcium/calmodulin dependent protein kinase IIδ

cAMP: Cyclic AMP

cDNA: Complementary DNA

c/EBP: CCAAT/enhancer-binding protein

***c*ESA**: *Cis*-epoxysuccinic acid

CLOCK: Circadian locomotor output cycles kaput

CLS: "Crown-like" structures

CNS: Central nervous system

COX-2: Cyclooxygenase-2

CoA: Coenzyme A

CRY: Cryptochrome

CVD: Cardiovascular disease

DCs: Dendritic cells

DGs: Diglycerides

DMEM: Dulbecco modified eagle medium

dNTP: Deoxyribonucleotide triphosphate

E-Boxes: Enhancer boxes

ECLs: extracellular loops

ECM: Extracellular matrix

ERK: Extracellular signal-regulated kinase

ETC: Electron transport chain

FA: Fatty acid

FAHFAs: Fatty acid esters of hydroxyl fatty acids

FBS: Fetal bovine serum

FBXL3: F-Box and leucine rich repeat protein 3

FDA: Food and drug administration

FFA: Free fatty acids

FGF: Fibroblast growth factor

Fl: Floxed

GABA: γ-aminobutyric acid

GDM: Gestational diabetes mellitus

GDP: Guanosine diphosphate

GIP: Glucose-dependent insulinotropic polypeptide

GLP-1: Glucagon-like peptide1

GLP-1RA: Glucagon-like peptide 1 receptor agonists

GPCR: G-protein-coupled receptor

GPR91: G-protein-coupled receptor 91

GRK: G-protein-coupled receptor kinase

GTP: Guanosine triphosphate

GTT: Glucose tolerance test

gWAT: Gonadal white adipose tissue

HEPES: 4-(2-hydroxyethyl)-1-piperazineethanesulfonic acid

HEK 293: Human embryonic kidney 293

HFD: High-fat diet

HIF-1α: Hypoxia-inducible factor-1α

HOMA-IR: Homeostasis model assessment of insulin resistance

HPCs: Hematopoietic progenitor cells

HSCs: Hepatic stellate cells

HSL: Hormone-sensitive lipase

HUVECs: Human umbilical vein endothelial cells

IBD: Inflammatory bowel disease

IBMX: 3-isobutyl-1-methylxanthine

ICAM-1: Intracellular adhesion molecule 1

ICLs: Intracellular loops

IFN-γ: Interferon- γ

IGN: Intestinal gluconeogenesis

IGF-1: Insulin-like growth factor 1

iMoDCs: Immature monocyte-derived DCs.

i.p.: Intraperitoneal

IL-1β: Interleukin 1 beta

IL-18: Interleukin 18

IL-6: Interleukin 6

IR: Insulin resistance

ITT: Insulin tolerance test

iWAT: Inguinal white adipose tissue

JAK: Janus kinase

JGA: Juxtaglomerular apparatus

JNK: c-Jun N-terminal kinase

KO: Knockout

KRBH: Krebs-Ringer bicarbonate HEPES

LepR: Leptin receptor

M-PER: Mammalian protein extraction reagent

MAFLD: Metabolic-associated fatty liver disease

MAPK: Mitogen-activated protein kinase

MCT: Monocarboxylate transporter

MDCK: Madin-Darby canine kidney

mDIC: Mitochondrial dicarboxylate carrier

MGs: Monoglycerides

microCT: Microcomputed tomography

miRNAs: MicroRNAs

MSCs: Mesenchymal stem cells

Myf5: Myogenic transcription factor 5

NA: Norepinephrine

NaCT: Na^+/citrate cotransporter

NAD^+: Nicotinamide adenine dinucleotide

NaDC: Sodium-dependent dicarboxylate transporter

NASH: Non-alcoholic steatohepatitis

NCD: Normal chow diet

NLRP3: NOD-like receptor protein 3

NSCs: Neural stem cells

OAT: Organic anion/dicarboxylate transporter

oWAT: Omental white adipose tissue

PAI1: Plasminogen activator inhibitor 1

PBS: Phosphate-buffered saline

PCR: Polymerase chain reaction

PDGFRα: Platelet-derived growth factor receptor α

PER: Period

PFA: Paraformaldehyde

PGC1α: Peroxisome proliferator-activated receptor gamma coactivator 1 α

PGE_2 : Prostaglandin E_2

PHD: Prolyl hydroxylase domain

PI3K: Phosphoinositide 3-kinase

PKA: Protein kinase A

PKC: Protein kinase C

PLC: Phospholipase C

PPARγ: Peroxisome proliferator-activated receptor γ

PTM: Post-translational modification

qMRI: Quantitative magnetic resonance imaging

qPCR: Quantitative real-time PCR

RER: Respiratory exchange ratio

ROIs: Regions of interest

ROR: Retinoic acid orphan receptor

RORE: Retinoic acid orphan receptor element

ROS: Reactive oxygen species

rRNA: Ribosomal RNA

RT: Room temperature

RUNX2: Runt-related transcription factor 2

rWAT: Retroperitoneal white adipose tissue

SCFA: short-chain fatty acids

SCN: Suprachiasmatic nucleus

ScWAT: Subcutaneous white adipose tissue

SDH: Succinate dehydrogenase

SIRT: Sirtuin

SLC: Solute carrier

SNS: Sympathetic nervous system

SREBP1c: Sterol regulatory element-binding protein 1c

STAT3: Signal transducer and activator of transcription 3

SUCNR1: Succinate receptor 1

SVF: Stromal vascular fraction

T2DM: Type 2 diabetes mellitus

TAE: Tris-acetate-EDTA

TBS-T: Tris-buffered saline with Tween 20

TCA: Tricarboxylic acid

TG: Triglycerides

Th: T helper

TNF-α: Tumor necrosis factor-alpha

UCP1: Uncoupling protein 1

VDAC: Voltage-dependent anion channel

VEGF: Vascular endothelial growth factor

vWAT: Visceral white adipose tissue

WAT: White adipose tissue

WHO: World Health Organization

WT: Wild-type

ABSTRACT

Adipose tissue (AT) plays a crucial role in maintaining whole-body energy homeostasis through the secretion of leptin, a master regulator of energy balance and body adiposity, in response to nutritional challenge. Extensive research has elucidated the molecular mechanisms of leptin action, enhancing our understanding of leptin resistance in obesity. However, the regulatory factors controlling leptin production by adipocytes remain largely unknown.

This doctoral thesis explores the succinate/succinate receptor 1 (SUCNR1) axis in adipocytes using an integrative and translational approach. The study highlights the extracellular signaling potential of succinate, an archetypal respiratory metabolite that can also function as a hormone-like metabolite by activating its cognate receptor SUCNR1, a G protein-coupled receptor (GPCR) that is more highly expressed than previously anticipated. Traditionally recognized as a stress indicator and a key immune response regulator with anti-lipolytic effects in AT, our research focuses on an unexplored area of metabolism where the succinate/SUCNR1 signaling pathway within adipocytes governs leptin expression and energy homeostasis.

Using a comprehensive translational approach, including the development and characterization of a unique adipocyte-specific knockout (KO) mouse, *in vitro* experiments, and a well-defined cohort study, we explored the succinate/SUCNR1 axis as an essential physiological regulator of leptin production in adipocytes. Our findings demonstrate that the specific deletion of *Sucnr1* in adipocytes improves systemic metabolic health. Specifically, adipocyte *Sucnr1* deficiency results in reduced adipose mass, promotes white AT (WAT) browning, and enhances glucose tolerance. Additionally, the adipocyte specific deletion of *Sucnr1* reveals an unexpected effect on bone mass, which might partially explain the increased body weight observed in these mice. This deficiency also impairs the leptin response to feeding, resulting in lower levels of circulating leptin, an important negative regulator of bone mass, particularly relevant during postnatal bone development.

The previously mentioned mechanisms do not appear to operate effectively under overnutrition conditions. Our findings reveal that high-fat diet (HFD)-fed mice with adipocyte-specific *Sucnr1* deletion exhibited increased hepatic fat accumulation and glucose intolerance. This study also underscores the specific impact of succinate on the dichotomous effects of *Sucnr1* deficiency: while the anti-lipolytic properties of SUCNR1 are dominant during overnutrition, its influence on leptin signaling contributes to the beneficial metabolic phenotype observed in adipocyte-specific *Sucnr1* KO mice under standard diet conditions.

Furthermore, this study identifies SUCNR1 as a novel regulator of the circadian clock in AT, with *Sucnr1* deletion disrupting core-clock gene expression. I*n vitro* experiments evidenced that SUCNR1 stimulation induces the activation of the adenosine mono-phosphate-activated protein kinase α (AMPKα)-c-Jun N-terminal kinase (JNK)-

dependent pathway, controlling brain and muscle ARNT-like protein-1 (BMAL1)-CCAAT/enhancer-binding protein α (C/EBPα)-mediated leptin expression regulation in adipocytes.

Remarkably, beyond its physiological relevance, our study also shows that obesity-associated hyperleptinemia in humans correlates with SUCNR1 overexpression in adipocytes, emerging as a major predictor of leptin expression in AT.

Overall, this thesis enhances our understanding of the succinate/SUCNR1 axis as a crucial pathway for sensing metabolites and regulating nutrient-related leptin dynamics to maintain energy homeostasis. Changes in circulating succinate levels during the transition from fasting to feeding not only impact AT by controlling lipolysis but also influence leptin signaling through SUCNR1. Disruption of this pathway in obesity uncovers a novel pathophysiological mechanism underlying obesity-related hyperleptinemia. Further research is essential to fully elucidate the role of succinate as a signal transducer of physiological processes and its potential involvement in regulating the circadian rhythm. Comprehensive investigation into the succinate/SUCNR1 axis in health and disease conditions is necessary to explore its potential as a pharmacological target.

INTRODUCTION

1. THE SUCCINATE/SUCCINATE RECEPTOR 1 AXIS

Succinate, long recognized as a critical metabolic intermediate in the tricarboxylic acid (TCA) cycle, also known as the Krebs cycle or the citric acid cycle, was identified for its role in energy metabolism in the early 20thcentury by Hans Adolf Krebs, a German-British biochemist[1]. Structurally, succinate is the anionic form derived from succinic acid, a dicarboxylic acid with the molecular formula $C_4H_6O_4$[2]. Traditionally, it was primarily viewed within the context of its role in cellular respiration and energy production. However, recent research has significantly expanded our understanding of succinate, attributing it with novel physiological roles beyond mere energy metabolism[3].

In 2004, a groundbreaking discovery revealed that succinate functions as an endogenous ligand for a previously orphan GPCR, which was subsequently renamed SUCNR1, highlighting its role as a versatile signaling molecule with both intracellular and extracellular functions[4]. The landmark discovery of succinate as the ligand for SUCNR1 has opened up new research avenues, highlighting its broad extracellular signaling capabilities and its profound impact on numerous physiological and pathological processes.

Traditionally, SUCNR1 was believed to be inactive in healthy tissues, becoming active only under pathological conditions such as hypoxia and tissue injury, which are often accompanied by elevated extracellular succinate. Consistently, SUCNR1 signaling has been primarily associated with inflammatory-related diseases, such as rheumatoid arthritis[5–7], inflammatory bowel disease (IBD)[8], age-related macular degeneration[9], and certain cancers[10–12]. Additionally, SUCNR1 plays a significant role in metabolic diseases, including obesity[13–15], diabetes[15,16], and its related complications like hypertension[17], renal[18–20] and retinal complications[21,22(p91)], as well as metabolic-associated fatty liver disease (MAFLD)[23,24]. Nonetheless, current research reveals that SUCNR1 also plays a critical role in maintaining metabolic homeostasis and regulating essential physiological processes, including blood pressure[19,20], insulin release[25], AT lipolysis[13,26,27], hepatocyte glucose and lipid metabolism[28], and skeletal muscle adaptation to exercise[29]. Even though SUCNR1 is expressed at lower levels in some tissues, its impact on these critical physiological processes highlights its potential as a therapeutic target for multiple diseases. Yet, additional studies are needed to completely understand its diverse roles, discern its mechanisms of action, and assess the potential benefits of targeting this axis in clinical applications.

In this section of the doctoral thesis, we will explore succinate and its receptor SUCNR1, weaving together both well-established knowledge and the latest discoveries to provide a comprehensive understanding of their critical roles in metabolic regulation and pathophysiological processes.

1.1 ORIGIN OF EXTRACELLULAR SUCCINATE

Succinate is not only an essential intracellular metabolite, but it also functions as a significant extracellular signaling molecule[3]. Circulating succinate levels derive from a variety of sources, including cellular metabolic processes and microbial fermentation in the gut[30]. Indeed, numerous tissues, especially under stress conditions, contribute to the pool of circulating succinate. For instance, ischemic tissues release succinate due to a shift toward anaerobic metabolism and disruptions in the TCA cycle[31]. The following sections will examine the diverse sources of succinate, including both derived from both the host and microbiota.

1.1.1. HOST-DERIVED SUCCINATE

Succinic acid, or butanedioic acid, was first identified by Georgius Agricola in 1546. However, the key role of succinate in biochemistry and energy production was revealed by Albert Szent-Györgyi, who elucidated how succinate dehydrogenase (SDH) transforms succinate into fumarate. Subsequently, Sir Hans Krebs, finalized the TCA cycle, thereby positioning succinate as a key component in one of the most critical metabolic cycles[32].

The TCA cycle is a central pathway in cellular respiration produced in the mitochondria of host cells that generally occurs under aerobic conditions to release stored energy through acetyl coenzyme A (acetyl CoA) oxidation derived from carbohydrates, lipids, and proteins[33]. In this enzymatic reaction process, succinate is produced from α-ketoglutarate (α-KG) through a two-step process. First, α-KG is decarboxylated to succinyl coenzyme A (succinyl-CoA) by α-KG dehydrogenase, followed by conversion to succinate via succinyl-CoA synthetase. This reaction represents a substrate-level phosphorylation, generating one molecule of guanosine triphosphate (GTP) or adenosine triphosphate (ATP), which depends on the specific isoform of the enzyme that is expressed in the organism. Under normal physiological conditions, succinate is promptly oxidized to fumarate by SHD or complex II of the electron transport chain (ETC), transferring electrons to activate ATP synthase through oxidative phosphorylation[34].

Under specific stress conditions or metabolic alterations, mitochondrial succinate can accumulate through several alternative pathways, including reverse activity of SDH, the purine nucleotide cycle, malate/aspartate shuttle, glutamine-dependent anaplerosis, and the γ-aminobutyric acid (GABA) shunt. The detailed mechanisms of succinate accumulation will be further explored in section 1.2.1. of this doctoral thesis.

When mitochondrial succinate levels exceed cellular requirements, it is transported into the cytosol and extracellular space via membrane transporters. Notably, succinate acts as the endogenous ligand for the receptor SUCNR1, uncovering its capacity for extensive extracellular signaling. This discovery points to succinate potential influence on various pathophysiological processes[4] (**Figure 1**).

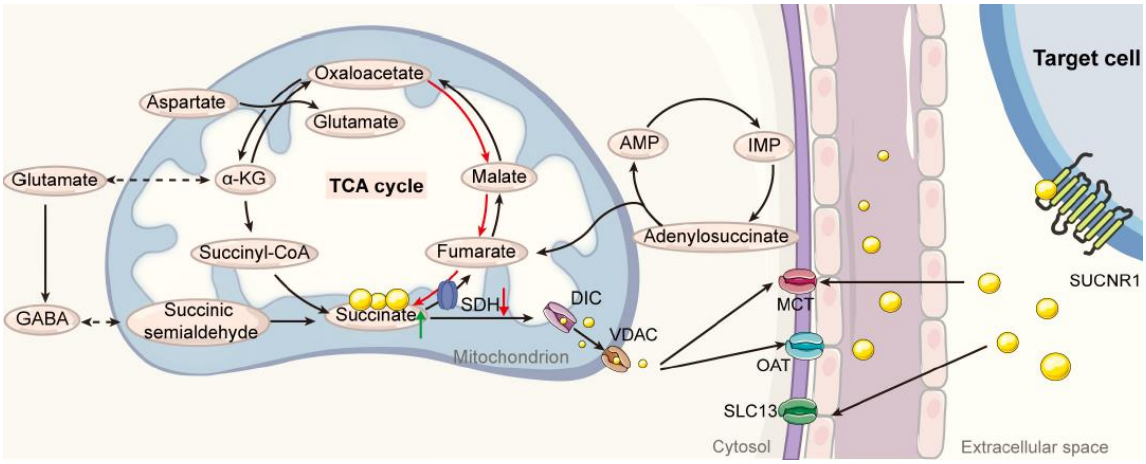

Figure 1. Schematic representation of the Krebs Cycle, succinate transport and extracellular release via SUCNR1[35].

However, a complete understanding of the succinate/SUCNR1 axis remains incomplete, suggesting that more functions of succinate are yet to be discovered. These topics, including the mechanisms of succinate release into the extracellular space and its role in signaling through SUCNR1, will be explored in greater detail from sections 1.3 to 1.5 of this doctoral thesis, providing an in-depth analysis of the current research, underlying mechanisms, and potential implications of succinate signaling in health and disease.

1.1.2. MICROBIOTA-DERIVED SUCCINATE

For many years, the scientific community largely ignored that succinate is produced not only by host cells but also by bacteria. The understanding of this process has significantly advanced, especially considering that mitochondria have an ancestral bacterial origin[36]. This connection has led researchers to further examine the role of gut microbiota in succinate production more closely[37], solidifying its status as an important microbial-derived metabolite.

The dual origin of succinate from both the host and gut microbiota places it in a unique position of being at the interface of host-gut microbiota metabolic interactions. The gut microbiota is a complex ecosystem of trillions of microorganisms residing in our gastrointestinal tract. Current evidence strongly highlights the importance of the communication between the host and its microbiota for sustaining the vital health functions of the host. Indeed, it is well known that changes in the gut microbiota, termed

dysbiosis, are associated with numerous diseases such as obesity and type 2 diabetes mellitus (T2DM)[30].

The gut microbiota metabolizes a variety of dietary fiber and host-derived nutrients, producing end products such as short-chain fatty acids (SCFAs) namely acetate, propionate and butyrate, and organic anions, like lactate and succinate. These metabolites can then be efficiently used by the intestinal mucosa and/or next host metabolism. Particularly, the primary contributors to SCFAs production are dietary non-digestible carbohydrates, which are fermented by gut microbes to produce succinate, a crucial precursor in the synthesis of propionate[30,38] (**Figure 2**).

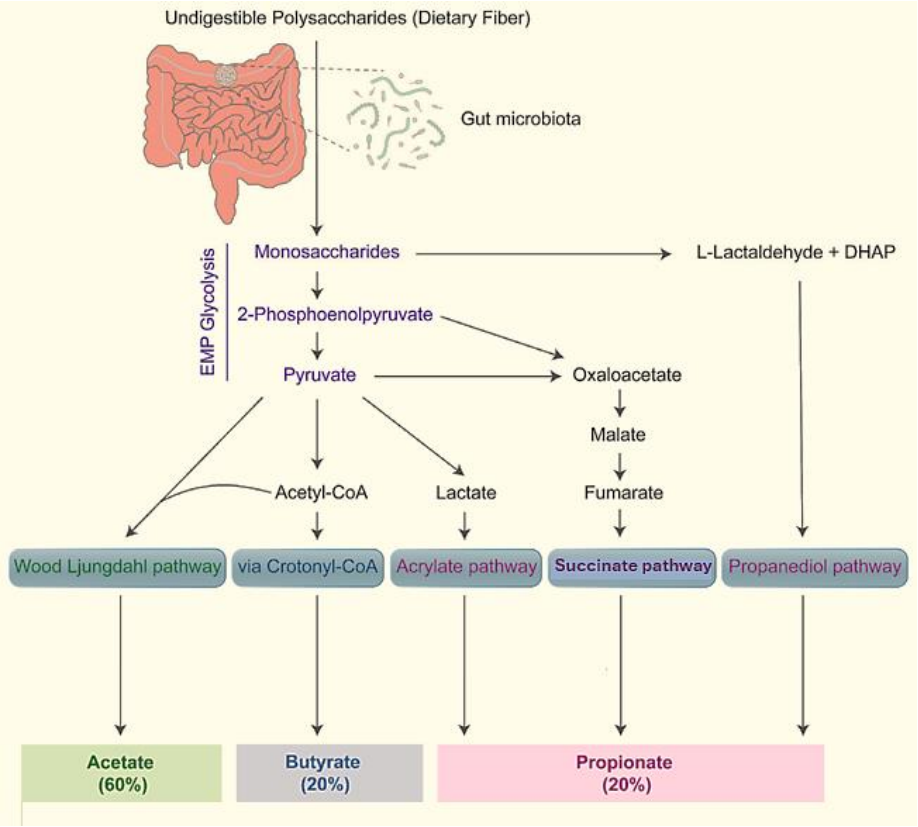

Figure 2. Pathway for succinate and SCFAs production by the bacterial gut microbiota. Image adapted[39].

Succinate was generally expected to accumulate only in small amounts due to its conversion into propionate[40]. However, a significant rinse in cecal succinate concentrations has been observed in mice with dietary fiber[41]. Human studies have shown that succinate concentrations typically range from 1–3 mM in the intestinal content and feces, although these levels can vary based on the species and the nature of the sample[42]. While mitochondria are acknowledged as a primary source of succinate, the distal gastrointestinal tract hosts a rich microbial population that generates succinate through anaerobic fermentation processes[43,44]. Research involving germ-free mice has revealed minimal to negligible levels of succinate in fecal samples compared to

conventional mice, emphasizing the crucial role of gut microbiota as the primary source of luminal succinate under normal physiological conditions[45–48].

Importantly, while some bacteria are succinate producers, others function as succinate consumers. Succinate levels are controlled by maintaining a balance between these succinate-producing and succinate-consuming bacteria[37,49]. For instance, *Bacteroides spp.*[38,50], *Prevotella spp.*[51,52], *Firmicutes spp.*[38], and other bacteria in the intestinal tract can metabolize most carbohydrates to produce succinate. In addition to being a precursor of SCFAs, succinate can also be used by certain succinate-consuming bacteria as a nutrient for proliferation[53]. Some gut bacteria, such as *Phascolarctobacterium succinatutens,* metabolize succinate directly for energy production[54], while others, like *Clostridioides difficile*, utilize succinate from other bacteria to support their survival[55], contributing to its pathogenicity.

Beyond acting as a metabolic intermediate, microbial-derived succinate can also act as signaling molecule within the gut environment. Thus, differences in succinate levels among microbial communities may indicate not only their metabolic activity and composition, but also regulate host-microbiota interactions[30]. Succinate has been demonstrated to activate dendritic cells (DCs), serving as a modulator of intestinal inflammation[56]. Moreover, it has been demonstrated that succinate produced from dietary fiber also serves as a substrate for intestinal gluconeogenesis (IGN)[41], akin to what is known for propionate and butyrate[57]. Studies in wild-type (WT) mice showed that dietary succinate enhanced glucose and insulin tolerance, but these effects were not observed in mice lacking IGN. Moreover, mice colonized with the succinate-producing bacterium *Prevotella copri* exhibited metabolic benefits, possibly through succinate-induced activation of IGN[41]. Some researchers have proposed using dietary succinate and bacteria that produce succinate to enhance glucose tolerance[58]. A recent report also revealed that administering succinate helps reduce chronic intestinal inflammation by modulating tuft cell expansion, illustrating the complexity of host-microbiota metabolic dynamics[59].

In a normal physiological state, succinate is typically present in low concentrations within the gut lumen. This is likely due to its involvement in cross-feeding interactions among gut microbes. However, some studies have observed elevated luminal succinate levels linked to alterations in gut microbiota, which can be associated with IBD or the effects of antibiotic treatments[30]. Consistent with this, research from our group has demonstrated that obesity-related disruptions in gut microbiota composition are marked by an increase presence of bacterial succinate producers, such as members of the *Prevotellaceae* and *Veillonellaceae* families, alongside a decrease in succinate consumers, including *Odoribacteraceae* and *Clostridaceae* families[37]. This particular microbiota profile was strongly correlated with the elevated levels of circulating succinate observed in obesity[48]. Notably, further studies from our group revealed lower fecal succinate levels in obese mice compared to non-obese mice, with a negative

correlation between fecal and plasma succinate in patients with obesity. Indeed, succinate can cross the epithelium into systemic circulation, negatively affecting host metabolism and inflammation[48]. Similar patterns were noted for SCFAs and bile acids in T2DM patients[60], supporting the notion of a leaky gut contributing to elevated succinate levels in the bloodstream. Moreover, evidence from our group have also demonstrated that using *Odoribacter laneus*, a bacterium that consumes succinate, can effectively neutralize these effects, highlighting its potential as a next-generation probiotic for reducing systemic succinate[48].

Overall, the origins of circulating succinate are varied and context-dependent, involving mitochondrial metabolism, gut microbiota, dietary patterns, and alternative pathways activated during cellular stress. Continued investigation of the complex interplay between succinate and different pathophysiological conditions offers potential for uncovering novel therapeutic strategies and advancing our understanding of metabolic regulation.

1.2 INTRACELLULAR ROLES OF SUCCINATE BEYOND ENERGY

As previously mentioned, succinate has traditionally been investigated primarily for its role as mediator of mitochondrial respiration and energy producer. However, recent research has unveiled that succinate is also involved in several non-energetic functions, both intracellularly and extracellularly. Its metabolism is intricately linked to various pathways, including the production of mitochondrial reactive oxygen species (ROS), the metabolism of branched-chain amino acids, haem synthesis, and the utilization of ketone bodies[32]. Moreover, succinate serves as a signaling molecule, exerting diverse functions within cells and in the extracellular environment[61]. For more detailed information on these processes, see section 1.2.2 of this doctoral thesis.

The accumulation of succinate within cells is not merely a byproduct of altered metabolic states but has profound effects on cellular physiology and pathology. This accumulation has been associated with aerobic glycolysis, TCA cycle disruption, and anaplerosis, commonly associated with hypoxia, immune cell activation, and tumorigenesis[32,62,63]. However, the roles of succinate are not limited to these pathological contexts and also involve normal physiological responses[3].

1.2.1. MECHANISMS LEADING TO SUCCINATE ACCUMULATION

The primary pathway for producing succinate under normal conditions involves mitochondrial metabolism, particularly via de TCA cycle. Nevertheless, under cellular stress or hypoxia, other metabolic pathways and anaplerotic routes may also contribute to the accumulation of succinate[63]. As previously mentioned in section 1.1.1, succinate accumulation in cells can result from a variety of mechanisms, reflecting its complex role in cellular physiology and pathophysiology (**Figure 3**).

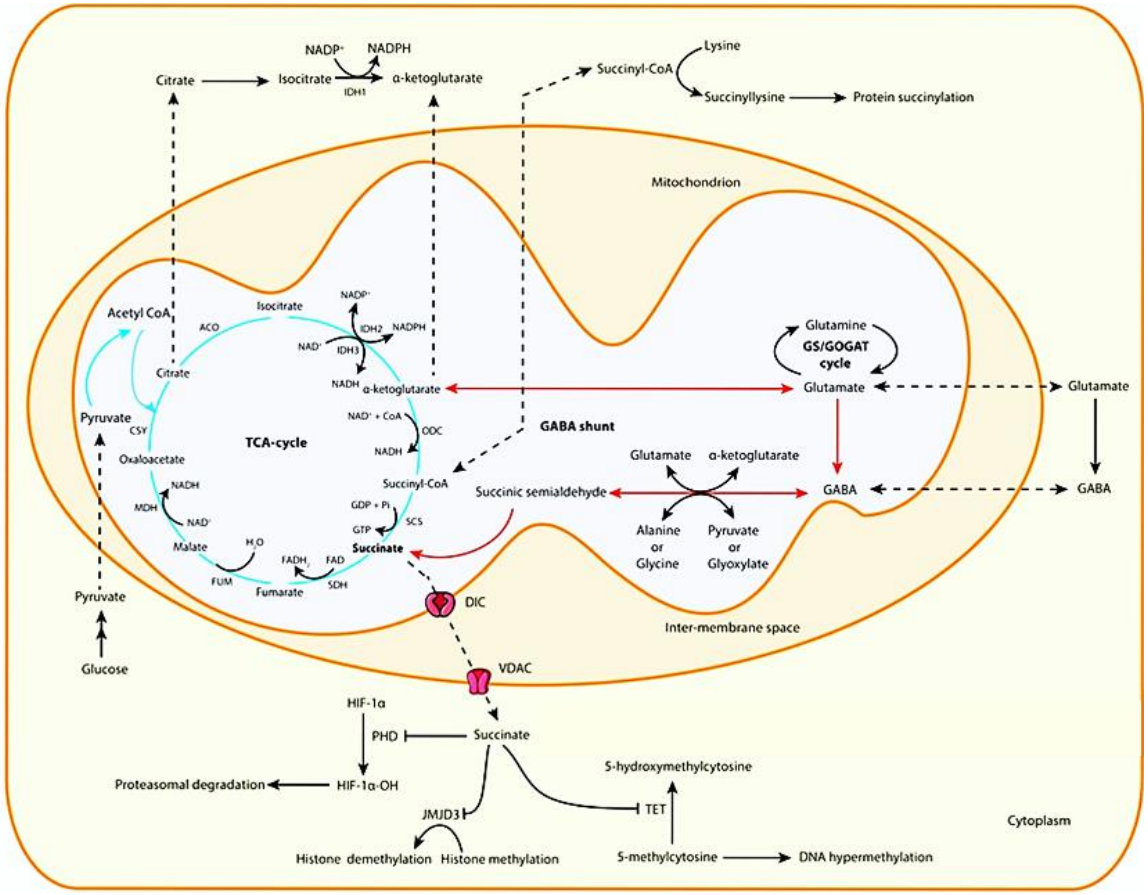

Figure 3. Succinate biosynthesis and its intracellular functions. Image adapted[64].

One primary pathway is through the disturbance of the TCA cycle under conditions such as hypoxia or mitochondrial dysfunction. Situations of reduced oxygen levels lead to an alteration in cell metabolism toward glycolysis, leading to an increased production of succinate as alternative pathways to regenerate nicotinamide adenine dinucleotide (NAD^+) from NADH, thereby avoiding the normal oxidative phosphorylation process[65].

Additionally, mutations or dysregulation of enzymes involved in the TCA cycle, such as SDH and other oxygen-dependent enzymes in the electron transport chain, can directly lead to succinate accumulation. Loss-of-function mutations in SDH, for example, result in the accumulation of succinate, which can act as an oncometabolite, contributing to the development of certain types of cancer[32].

The role of anaplerotic pathways in replenishing TCA cycle intermediates also contributes to the accumulation of succinate in cells. One example is the enzyme pyruvate carboxylase, which catalyzes the conversion of aspartate to oxaloacetate, an essential anaplerotic reaction that indirectly increases succinate levels by influencing the TCA cycle[66]. Additionally, the breakdown of branched-chain amino acids and odd-chain fatty acids through the propionyl-CoA carboxylase pathway, generates succinyl-CoA, which can be transformed into succinate[67].

Cells can also produce succinate from glutamine via the α-KG intermediate in the TCA cycle through anaplerosis. Glutamine can be converted to glutamate and then to α-KG, which can be further metabolized to succinate. This pathway, known as glutaminolysis, becomes especially important in rapidly proliferating cells, such as cancer cells, leading to increased succinate levels. Another critical pathway resulting in the increase of intracellular succinate levels is the upregulation of the GABA shunt[65]. This connects glutamate and GABA metabolism by first converting glutamate into GABA and then transforming GABA into succinate, thus playing a role in the increase of succinate[68].

Moreover, adenylosuccinate, an intermediate in purine nucleotide synthesis, contributes to succinate accumulation through its breakdown into adenosine monophosphate (AMP) and fumarate, which enters the TCA, where it is eventually converted into succinate, illustrating the link between purine metabolism and succinate production[65] .

Overall, the mechanisms leading to intracellular succinate accumulation are diverse and context-specific, encompassing canonical metabolic pathways like the TCA cycle under normal conditions, as well as other routes such as anaplerotic pathways activated under stress conditions. Additionally, dysregulation of enzymes like SDH and processes such as glutaminolysis and the GABA shunt further contribute to succinate accumulation. These pathways can disturb normal metabolism and lead to succinate buildup, influencing various physiological processes. While the dominance of these pathways in different scenarios is not fully understood, succinate plays a pivotal role as a metabolic hub connecting diverse physiological processes.

1.2.2. SUCCINATE AS AN INTRACELLULAR SIGNALLING MOLECULE

Succinate can be exported into the cytosol and extracellular space, although the precise mechanisms and conditions under which this occurs are still under investigation[3,30]. Traditionally, such release has been associated with pathological conditions such as ischemia[65], inflammation[62], and cancer[69,70]. However, there is a growing body of evidence suggesting that succinate export may also be part of a dynamic regulatory process in normal physiology. This emerging view suggests that succinate may serve as a signaling molecule, orchestrating metabolic responses among various tissues. A key pathway for this signaling involves the receptor SUCNR1, whose activation has been linked to various physiological processes, such as anti-inflammatory actions[14], AT function[13], and muscle physiology[71], which will be discussed on in section 1.5.

Succinate is a polar and charged small molecule, and specific membrane carriers are essential for its transport into the cytosol. Many of these carriers are versatile and not highly specific for succinate. The precise mechanisms for the regulation of succinate release and uptake by cells remains unknown, yet evidence consistently points to a tightly regulated process[3]. Succinate translocation from mitochondria to the cytosol depends on the mitochondrial dicarboxylate carrier (mDIC) within the inner membrane,

a member of the solute carrier (SLC) family 25 (SLC25). The expression and activity of these carriers are finely tuned in response to diverse metabolic conditions across various tissues. For instance, mDIC is involved in initiating *de novo* lipogenesis in the liver and supports glucose-stimulated insulin secretion in pancreatic β-cells[72,73]. Moreover, recent studies have revealed that modulating the efflux of succinate from the mitochondria via mDIC regulates processes such as white adipocyte lipolysis, which is dependent on SUCNR1[27]. Concurrently, the voltage-dependent anion channel (VDAC/porin) located in the outer membrane is also involved in succinate translocation to the cytosol, and plays a pivotal role in mitochondrial metabolism by regulating the flux of small molecules [70]. Emerging research has also linked VDAC/porin to apoptotic pathways, where it controls the release of apoptotic factors into the cytosol, influencing cell survival. This function underscores its potential as a novel pharmacologic target for anti-cancer drugs[74].

Once in the cytosol, succinate is involved in regulatory functions that extend beyond basic energetic processes, such as the stabilization of the hypoxia-inducible factor-1α (HIF-1α), increased production of mitochondrial ROS, epigenetic alterations, and protein succinylation[64,75] (**Figure 4**). These effects trigger responses to stress in cells and activate metabolic reprogramming pathways. Notably, the increased production of mitochondrial ROS plays a crucial role in driving these mechanisms, being directly associated with the intracellular accumulation of succinate[76].

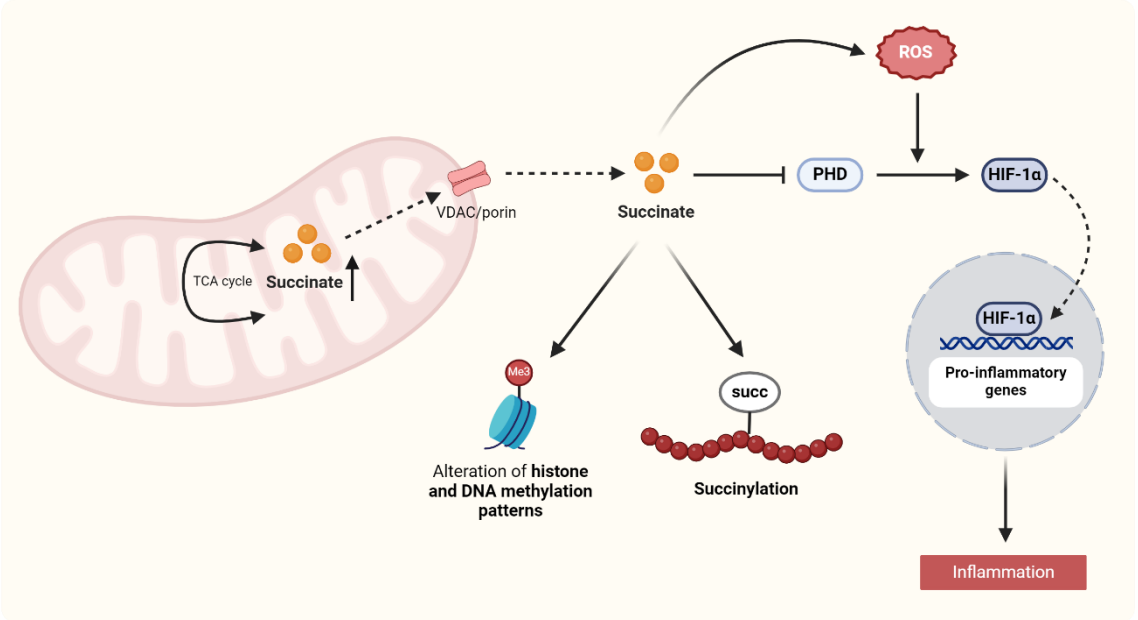

Figure 4. Intracellular roles of succinate as a signaling molecule. Image from Biorender.

The accumulation of intracellular succinate is intricately linked to inflammation via the stabilization and activation of **HIF-1α**, a transcription factor essential for regulating genes associated with angiogenesis and inflammation[7,63,77]. In normoxic conditions, prolyl hydroxylase domain (PHD) enzymes hydroxylate HIF-1α, leading to its degradation[78]. However, in low-oxygen conditions, increased succinate levels inhibit these enzymes, resulting in HIF-1α stabilization and enhanced transcriptional activity[79]. This process triggers the expression of pro-inflammatory genes, including interleukin-1β (IL-1β) and inducible nitric oxide synthase, promoting cell survival in these environments[80]. Furthermore, inflammation is also linked to succinate through the activation of the NOD-like receptor protein 3 (NLRP3) inflammasome. This multiprotein complex is essential for innate immune responses and, once activated, it triggers the activation of caspase-1, which then processes and matures pro-inflammatory cytokines, including IL-1β and interleukin-18 (IL-18)[81]. It is well-known that succinate enhances **ROS production**, which is pivotal in facilitating the assembly and activation of the NLPR3 inflammasome, thereby amplifying the inflammatory response[7,81,82].

Beyond its role in inflammation, succinate plays a crucial role in modulating gene expression through **epigenetic mechanisms** by inhibiting α-KG-dependent dioxygenases, such as Jumonji C-domain-containing histone demethylases and the ten-eleven translocation family of DNA demethylases[83]. These enzymes rely on α-KG as a co-substrate and are competitively inhibited by the accumulation of succinate. As a result, this inhibition alters histone and DNA methylation patterns, which subsequently affects gene expression and cellular function[84].

Succinate is also implicated in additional regulatory pathways, including protein post-translational modifications (PTMs), such as **succinylation.** PTMs influence the biological mechanisms of human diseases by modulating cellular pathophysiology and expanding the genetic code[85]. In recent years, PTMs such as propionylation, glutarylation, acetylation and succinylation, have gained significant research attention[86,87]. Among these, succinylation has been identified as a critical regulator of metabolic pathways across different species[85,87–89]. This modification involves the transfer of a succinyl group from succinyl-CoA to the ε-amino group of lysine residues in target proteins, altering their chemical properties and significantly impacting various cellular processes and pathways[90]. Remarkably, it also plays a crucial role in regulating energy metabolism[91] and nuclear function[92]. The transfer of the succinyl group can occur through enzymatic and non-enzymatic pathways. Enzymatic succinylation is facilitated by succinyltransferases, a conserved family of enzymes found across different species, which transfer succinyl groups from succinyl-CoA to lysine residues on target proteins with precision[93,94]. Conversely, non-enzymatic succinylation can regulate protein succinylation in the cytoplasm, potentially influenced by the activity of cytoplasmic Sirtuin 5 (SIRT5). SIRT5, primarily a mitochondrial enzyme, acts as a desuccinylase to remove succinyl groups from proteins, thereby reversing succinylation[95]. This dual mechanism of enzymatic and

non-enzymatic regulation underscores the complexity of succinylation in cellular processes and metabolic pathways, impacting protein function and potentially contributing to disease mechanisms.

Aberrant succinylation patterns and dysregulation of its associated enzymes, such as SIRT5, have been linked to various diseases, including metabolic disorders, and neurodegenerative diseases[85,86,96–99]. An imbalance in protein succinylation has been linked to adverse impacts on cellular metabolism by altering both enzyme kinetics and substrate binding, thereby disturbing the metabolic balance within cells[100].

In essence, the exploration of intracellular succinate reveals its significant contributions to cellular signaling and metabolism. Beyond its established role as a metabolic intermediate, succinate emerges as a signaling molecule, exerting diverse functions within cells and the extracellular environment[61].

1.3. SUCCINATE TRANSPORT TO THE EXTRACELLULAR SPACE

In addition to its intracellular roles, cytosolic succinate, when accumulated to significant levels within the cell, can also be transported into the extracellular space. This process is facilitated by specific plasma membrane transporters. Among those that have been characterized are the organic anion/dicarboxylate transporters (OATs) and the monocarboxylate transporters (MCTs). These transporters are essential for maintaining cellular metabolic balance, allowing for the controlled release of succinate into the surrounding environment[71,101].

The OATs, which are part of the SLC22 family, play a pivotal role in transporting small endogenous metabolites, drugs, and toxins, particularly relevant in the renal and hepatic systems[102]. They operate as exchangers, facilitating the import of organic anions into the cells while simultaneously exporting metabolic byproducts back into the circulation. Several OAT subtypes have been discovered and functionally analyzed, revealing considerable variations in terms of substrate specificity, distribution across different tissues, and regulatory mechanisms[103]. Among these, OAT1, OAT2, OAT3, OAT5, and OAT10 have been specifically recognized for their ability to exchange organic anions with succinate[101,104].

The MTCs represent a diverse group within the SLC16 family, encompassing a total of 14 distinct members. This family is characterized by its ability to facilitate the transport of monocarboxylates across cell membranes, a process linked with proton transport[105]. Specifically, MCT1 has been identified as capable of transporting succinate in its protonated monocarboxylate form, indicating its potential role in succinate metabolism and signaling. This study have also explored the role of succinate in skeletal muscle physiology and discovered that both human and mouse muscles release succinate during exercise through an MCT1 dependent mechanism, which is notably sensitive to pH fluctuations[71].

Additionally, the extracellular succinate can be reabsorbed through the action of sodium-dependent dicarboxylate transporters. The SLC13 family of Na^+-dependent transport proteins play a crucial role in the cellular uptake of succinate. Specifically, the sodium-dependent dicarboxylate cotransporter 1 (NaDC1, encoded by *SLC13A2*) is notably expressed in key organs such as the kidney and intestine[105], where it functions to reabsorb TCA intermediates from both the renal tubular filtrate and digested food. The reabsorption of succinate by the kidneys is believed to play a significant role in the regulation of blood pressure[106]. Another member of this family, NaDC3, encoded by *SLC13A3*, exhibits a wider distribution across different tissues and a higher substrate affinity compared to NaDC1. Intriguingly, variations in the *SLC13A3* gene are linked to the development of T2DM through an unknown mechanism[107]. Succinate can also be transported by the Na^+/citrate cotransporter (NaCT), encoded by *SLC13A5*, primarily found in the liver and brain, although with lower affinity[105].

This bidirectional transport mechanisms ensures that succinate levels are finely regulated, reflecting the dynamic interplay between metabolic processes within the cell and the extracellular space. The regulation of circulating succinate levels depends on a variety of interconnected processes, including its release and uptake. Succinate clearance can occur through cellular scavenging, as demonstrated by Peruzzotti-Jametti and colleagues in neuronal stem cells[108], and through uptake for utilization, as explored by Mills and collaborators in brown AT (BAT) thermogenesis[109].

Despite these insights, the specific mechanisms that control the release and regulation of succinate are still mostly unknown, underscoring the importance of further studies to determine the factors influencing extracellular succinate levels.

1.4. CIRCULATING SUCCINATE IN HEALTH AND DISEASE

1.4.1. CIRCULATING SUCCINATE IN HEALTH

As previously mentioned, for many years, elevated circulating levels of succinate have been linked to various chronic inflammatory pathologies (see next section for more detailed information). However, recent insights challenge this assumption, revealing that extracellular succinate levels exhibit dynamic responses to various physiological stimuli and conditions[3]. For instance, succinate transiently increases in response to acute physiological adaptations such as exercise[110], food ingestion[111], and cold exposure[109] (**Figure 5**). This new perspective emphasizes that succinate serves not just as a metabolic marker in disease but also as a signaling molecule that actively responds to physiological challenges, suggesting its pivotal role in modulating broader metabolic adaptations.

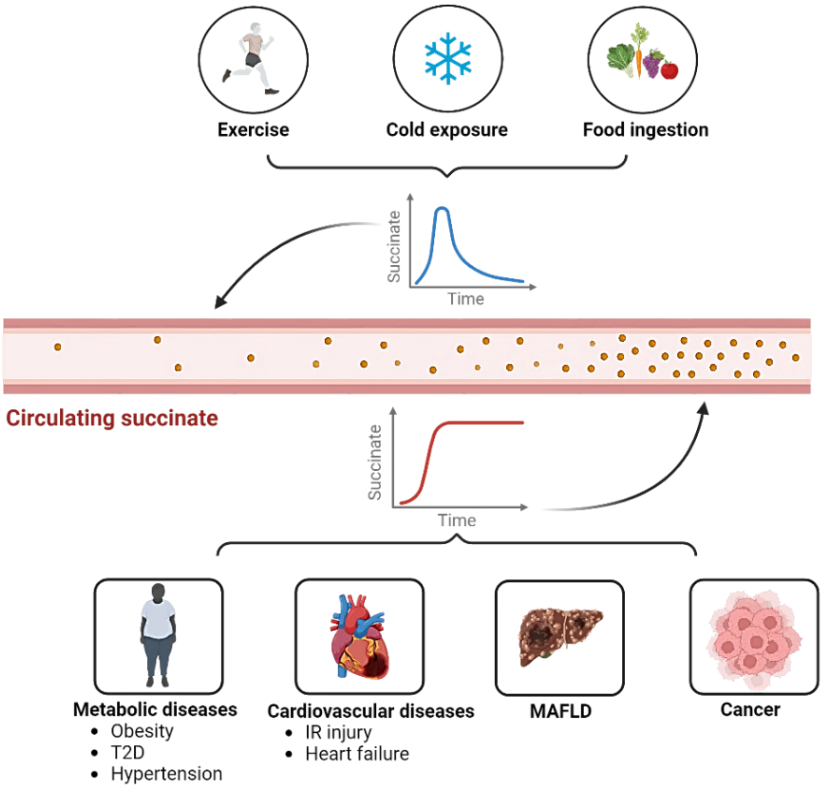

Figure 5. Circulating succinate in physiological and pathological conditions. Image from Biorender.

During **exercise**, the body demand for ATP increases exponentially, leading to an upsurge in metabolic processes. Within this context, the TCA cycle is one of the critical pathways through which energy production is enhanced to meet this increased demand. Succinate, a key player in this cycle, contributes to the generation of ATP upon oxidation, leading to the transient accumulation of succinate in the extracellular space during anaerobic exercise[110]. Recent studies have unveiled that extracellular succinate acts as a metabolic signal that stimulates angiogenesis and innervation in skeletal muscle, thereby leading to an increase in oxygen supply and blood flow and playing a crucial role in muscle remodeling. In addition, it has been shown that skeletal muscle selectively secrete succinate to control muscle remodeling during exercise via pH-dependent secretion, underscoring the significant role of circulating succinate in exercise physiology and adaptation[71].

Similarly, **food intake** also affects circulating levels of succinate. Our group recently described that plasma succinate levels are modulated postprandially, varying significantly depending on the metabolic status of the subject and on glucose detection by the gastrointestinal tract. The typical response of circulating succinate to food intake is diminished in patients with morbid obesity and T2DM. Nevertheless, this succinate response is reactivated after weight loss through bariatric surgery, highlighting its critical role in metabolic regulation[111]. Another study highlighted a succinate response similar

to our findings, transitioning between fasting and postprandial states[112]. Furthermore, recent data from our research group demonstrated a notable increase in circulating succinate levels following post-glucose administration, particularly prominent among individuals with prediabetes. This increased succinate response related to nutrition is strongly correlated with enhanced insulin secretion, suggesting that succinate may play a role in compensating for the hyperinsulinemic response commonly observed in prediabetes. Nonetheless, this dietary influence on succinate is disrupted as the disease progresses in patients with severe obesity and T2DM[25].

Cold exposure represents another condition that stimulates a transient increase in extracellular succinate levels, which serves as a signal for the activation of thermogenesis in BAT. This adaptative thermogenic response is crucial for maintaining body temperature in cold conditions by converting stored energy into heat. Succinate accumulation is regulated by the newfound ability of brown adipocytes to capture succinate. This rapid uptake of extracellular succinate and its oxidation by SDH are crucial for activating thermogenesis[109]. Furthermore, a more recent study suggests that succinate serves as a promoter of beige adipogenesis in white adipocyte progenitors[113]. Consequently, dietary supplements of succinate have been proposed to boost energy expenditure and prevent diet-induced obesity[109,113]. However, dietary succinate may not be effective in reversing the adverse metabolic effects of obesity once it has been established[114].

1.4.2. CIRCULATING SUCCINATE IN PATHOLOGY

A persistent elevation of extracellular succinate has been linked to various disorders ranging from metabolic syndromes to chronic inflammatory diseases, including obesity[13,14], diabetes[15,16], hypertension[115], retinal complications[116], gastrointestinal disorders[117], cardiovascular diseases (CVD)[17,118], fatty liver diseases[119–121], rheumatoid arthritis[7], and some cancers[31,69]. This elevation of succinate extends beyond a mere metabolic imbalance. Instead, it takes on a dual role, not only contributing to the metabolic dysregulation observed in these disorders but also actively influencing the inflammatory response, thereby disrupting its physiological function[3]. The increase in circulating succinate has garnered attention in recent years due to its potential implications in the development and progression of metabolic diseases.

In the context of metabolic disorders, particularly in the case of **T2DM** and **obesity**, there is a well-documented evidence of elevated circulating succinate levels. The intricate relationship between these conditions often complicates the differentiation of their individual metabolic impacts. Initial studies in mice indicated increased succinate levels in obesity and T2DM, but these findings were not consistently replicated in human subjects with T2DM[115]. However, subsequent research confirmed that elevated fasting succinate levels are present in diabetic patients with hyperglycemia compared to those

with normal glucose levels[15]. Our recent findings further validate that plasma succinate concentrations are elevated in individuals with obesity, including those with T2DM, and are associated with adverse metabolic markers such as insulin resistance (IR), glucose levels, HbA1c, and triglycerides. Notably, the body mass index (BMI) and glucose levels were identified as the key determinants of succinate levels[37]. Furthermore, we also found that weight loss surgery led to a reduction in succinate levels, and preoperative succinate levels were predictive of diabetes remission following bariatric surgery[111,122]. These observations underscore succinate as a promising biomarker for metabolic disturbances. Furthermore, as previously highlighted in section 1.4.1, we also have demonstrated that dietary succinate modulation is effective in healthy individuals but ineffective in T2DM and severe obesity, and it does not counteract the effects of long-term obesity[25].

In terms of **gestational diabetes mellitus** (GDM), there is also a significant rise in succinate levels preceding delivery, particularly among women undergoing insulin treatment, suggesting that it may be linked to the administration of insulin or the severity of GDM[123]. Additionally, studies have reported increased succinate levels within the placenta, further emphasizing the association between succinate and GDM[16].

Research underscores an association between abnormal succinate levels and diabetes-related complications[61]. Notably, individuals with diabetic complications exhibit elevated succinate levels compared to those with well-controlled T2DM[124]. Within this realm, higher succinate concentrations have been identified in individuals with progressive **diabetic nephropathy**[125] and **diabetic retinopathy**, particularly in cases of retinal vascular dysfunction and neurodegeneration[126]. Furthermore, **MAFLD** is a pathological state arising from the accumulation of fat in the liver, resulting in diverse complications such as liver failure, cirrhosis, and even hepatic cancer. MAFLD, affecting approximately 25% of the global population, is associated with IR, obesity, and T2DM, with prevalence escalating to 50-70% in individuals with diabetes[127]. The function of succinate in the progression of MAFLD is currently under research, especially considering the identification of elevated blood succinate levels in those individuals with this condition[128]. Remarkably, recent clinical data analyses have unveiled the promising potential of succinate as a non-invasive biomarker for detecting fatty liver[28].

Moreover, given the high expression of succinate receptor SUCNR1 in renal tissues[129], recent investigations have explored the potential for elevated circulating succinate to cause **kidney damage** and elucidate the underlying molecular mechanisms. Research has demonstrated that increased succinate levels can lead to specific interstitial fibrosis within the kidney, which exacerbates renal damage and accelerates the progression of chronic kidney disease[130]. Notably, studies have indicated that succinate induces apoptosis in proximal tubular cells via SUCNR1 activation[131].

Considering **cardiovascular diseases**, our research group identified a notable association between elevated succinate levels in plasma and an increased risk of CVD in

young population. Moreover, those with elevated succinate levels displayed a distinctive pro-inflammatory omega-6 signature pattern[118]. Additionally, recent studies have revealed critical insights into the role of succinate in cardiac pathophysiology. Cardiomyocyte hypertrophy is known to be a prevalent cause of ischemic heart disease and can lead to myocardial infarction, which exacerbates ischemia. Despite extensive research, many aspects of this syndrome remain poorly understood[17]. One notable finding is that succinate accumulates in ischemic rabbit hearts, with its levels correlating with the degree and duration of myocardial ischemia[132]. Additionally, succinate concentrations have been observed to rise in the serum of patients with cardiac hypertrophy due to obstructive coronary artery diseases. This study suggests that succinate promotes cardiomyocyte hypertrophy by directly activating the SUCNR1 receptor[17].

Within the scope of **cancer** research, succinate has garnered significant attention as an oncometabolite due to its elevated levels in various tumours[63]. Oncometabolites are compounds that are abnormally accumulated and contribute to cancer development and progression. The role of succinate as an oncometabolite was initially identified in association with SDH mutations[133]. Hobert et al. were the first to identify a link between SDH mutations and increased circulating succinate[134], which has been observed in cancers such as renal cell carcinoma[135], gastrointestinal stromal tumors[136], and pheochromocytoma and paraganglioma[137]. SDH downregulation has also been linked to succinate accumulation and progression of several cancers, including colorectal cancer, where reduced SDH activity has been observed[138]. Furthermore, it has been established that TRAP-1, a mitochondrial chaperone overexpressed in many cancers, including prostate cancer, promotes tumour growth by inhibiting SDH, which contributes to succinate accumulation[139]. Research conducted by Wu and colleages provided experimental evidence demonstrating that tumor growth correlates with elevated serum succinate levels. They also reported that succinate levels are increased in patients with lung carcinoma, and this elevation is accompanied by enhanced cancer metastasis. This suggests that succinate not only serves as a metabolic biomarker for lung cancer but also plays an active role in cancer progression[140]. Additionally, our group has also contributed to this field by identifying elevated circulating succinate as a biomarker for human head and neck squamous carcinoma[141]. These findings suggest that succinate could be a valuable biomarker for diagnosing various types of tumors and understanding cancer metabolism.

Overall, circulating succinate has been implicated in various pathological conditions, revealing its significance in disease processes. Understanding the role of circulating succinate in pathology may offer insights into disease mechanisms and potential therapeutic interventions.

1.5. THE SUCCINATE RECEPTOR

In 2001, the gene for G-protein-coupled receptor 91 (GPR91) was discovered on human chromosome 3q24-3q25 using an expressed sequence tag data mining strategy. This discovery was part of a study that identified and analyzed five new members of this receptor superfamily, including GPR84, GPR86, GPR87, GPR90, and GPR91, revealing a cluster of related receptors likely evolved from a common ancestor[142]. In 2004, succinate was recognized as the natural ligand for GPR91, which had previously been classified as an orphan receptor, leading to its renaming as SUCNR1[4]. This significant advance enhanced our understanding of succinate signaling, showing that succinate, through its interaction with SUCNR1, acts as a signaling molecule influencing various cellular and physiological processes. This receptor is widely distributed among various cell types and tissues, revealing high expression in the kidney[129], but also in other tissues such as AT[26], heart[143], liver[119], retina[21], and immune cells[56]. This diverse expression pattern highlights the multifunctional nature of SUCNR1 and its importance in maintaining various physiological processes across different organ systems.

SUCNR1 is primarily localized to the plasma membrane, which enables SUCNR1 to act as a sensor for extracellular succinate levels, initiating crucial downstream signaling pathways in response to metabolic changes. However, we cannot exclude the possibility of SUCNR1 being present in other cellular structures, similar to what has been described for other GPCRs[144]. Indeed, recent studies have identified SUCNR1 in the endoplasmic reticulum (ER), where it has been shown to be functional[145]. This dual localization suggests that SUCNR1 may have additional roles within intracellular compartments, contributing to its regulatory functions in cellular metabolism and signaling.

Given the growing recognition of SUCNR1 role in various inflammatory diseases and pathophysiological processes[3,146], it is crucial to investigate its signaling pathways and metabolic functions in greater detail. Compared to other GPCRs, information on SUCNR1 signaling is relatively limited. This section will explore the characteristics and functions of the GPCR family, transitioning to the specific signal transduction pathways mediated by SUCNR1.

1.5.1. SUCCINATE RECEPTOR STRUCTURE AND LIGANDS

SUCNR1 is a member of the GPCRs family, which represents the largest assembly of proteins engaged in signal transduction across biological membranes within the human genome.[4] Most databases indicate that the human *SUCNR1* gene encodes a protein comprising 334 amino acids. However, an intriguing analysis within this sequence uncovered a methionine residue at position 5, which is suggested by the Kozak sequence to be the actual start site, resulting in a receptor that is 330 amino acids long[142].

The SUCNR1 sequence exhibits significant homology among humans, rats, and mice, although there is a notable difference in the C-terminus, which is shorter by 12 amino acids in rodents. The precise impact of this variation on receptor signaling remains largely unexplored. However, it is noteworthy that succinate exhibits a slightly decreased potency on the receptors of rat and mice compared to those of humans[4].

An extensive understanding of the structure of SUCNR1 will play a pivotal role in the advancement of potent small-molecule modulators. Minimal information exists about the receptor three-dimensional structure. Recently, numerous crystallographic datasets have emerged, showcasing class A GPCRs interacting with various ligands[147]. Despite the absence of SUCNR1 crystallization, insights into its structure can be hypothesized through comparison with closely related proteins[148]. Through recent developments in crystallography, researchers have managed to crystallize two representative purinergic receptors, $P2Y_1$ and $P2Y_{12}$, facilitating insightful interpretations regarding the structure of SUCNR1[149,150]. SUCNR1, akin to other GPCRs, exhibits a typical extracellular structure characterized by transmembrane domains with seven helices embedded in the cell membrane. These transmembrane helices, critical for signal transduction, are interconnected by three extracellular loops (ECLs) and three intracellular loops (ICLs). However, subtle structural variations are observed in these loops among members of distinct GPCR classes[151,152] (**Figure 6**).

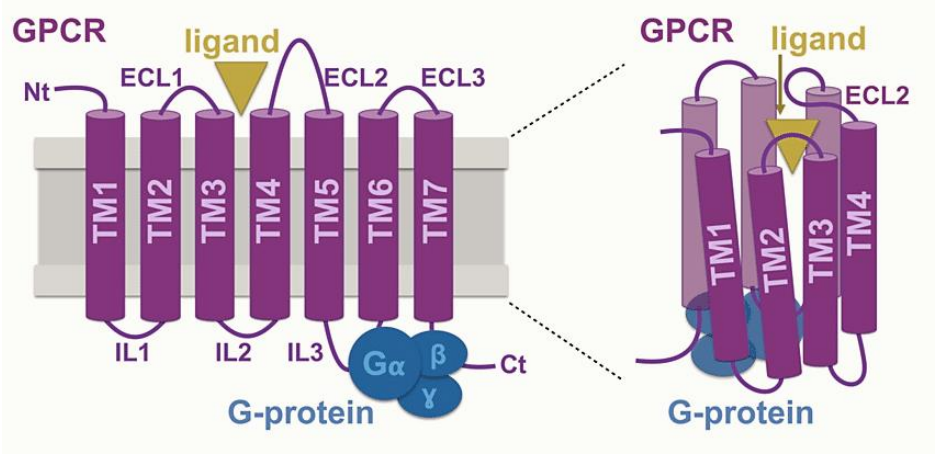

Figure 6. Schematic representation of the basic structure of GPCRs[153]

SUCNR1 possesses two N-glycosylation sites, located at N8 within the N-terminus and N168 within the second extracellular loop, yet the specific functions of these post-translational modifications remain elusive[142]. However, similar modifications have been extensively studied in certain members of the P2Y receptor family. For instance, N-linked glycosylation of $P2Y_{12}$ receptors plays a crucial role in signal transduction processes. In the case of SUCNR1, there is an additional phosphorylation site, specifically at S326 within the C-terminus, which could potentially play a significant role

in receptor internalization mechanisms[154]. Further research is warranted to elucidate the precise roles of these modifications in the functional regulation of SUCNR1.

As mentioned above, succinate is widely recognized as the primary ligand for SUCNR1, but some studies suggest that this receptor may also interact with other carboxylic acids, albeit at much lower affinities. For instance, compounds such as maleate and methylmalonate have been tested for their ability to activate SUCNR1; however, they exhibit significantly reduced binding affinities compared to succinate. The effective concentration for succinate action, with an EC50 value estimated between 20-50 μM, indicates that while these alternative ligands can theoretically engage the receptor, the concentrations required for meaningful physiological effects would be much higher, potentially diminishing their relevance in biological contexts[4]. Thus, it is currently recognized that SUCNR1 is primarily specific to succinate[4].

Recent research has led to the discovery of two potent synthetic SUCNR1 agonists: *cis*-epoxysuccinic acid (*c*ESA) and *cis*-cyclopropane-1,2-dicarboxylic acid (*c*CPDA). Among these, *c*ESA has been identified as the more potent agonist with 10-fold higher potency than succinate to activate the receptor. Both *c*ESA and *c*CPDA exhibit significant efficacy without interacting with SDH, thus allowing for targeted SUCNR1 studies without disrupting the TCA cycle[155].

Furthermore, the development of SUCNR1 antagonists have also been reported. Among the few SUCNR1 antagonists identified, NF-56-EJ40 is particularly recognized for its high-affinity binding to SUCNR1, making it a crucial agent in the study of SUCNR1-mediated signaling and its potential therapeutic implications[156,157].

1.5.2. SIGNAL MECHANISMS OF GPCRs

GPCRs play a crucial role in signal transduction across the cell membrane. Upon activation by their respective ligands, GPCRs undergo conformational changes that initiate downstream signaling cascades. This activation induces a conformational rearrangement in the receptor, promoting the recruitment of heterotrimeric G proteins, which are composed of three subunits: α, β, and γ[158]. In the inactive state, the α subunit is bound to a guanosine diphosphate (GDP), and the βγ dimer is associated with it. Upon GPCR activation, the G protein undergoes a conformational change, leading to the exchange of GDP for GTP on the α subunit. This results in the dissociation of the α subunit from the βγ dimer, allowing both subunits to interact with downstream effector molecules, initiating downstream signaling pathways that ultimately mediate cellular responses[152,159] (**Figure 7**).

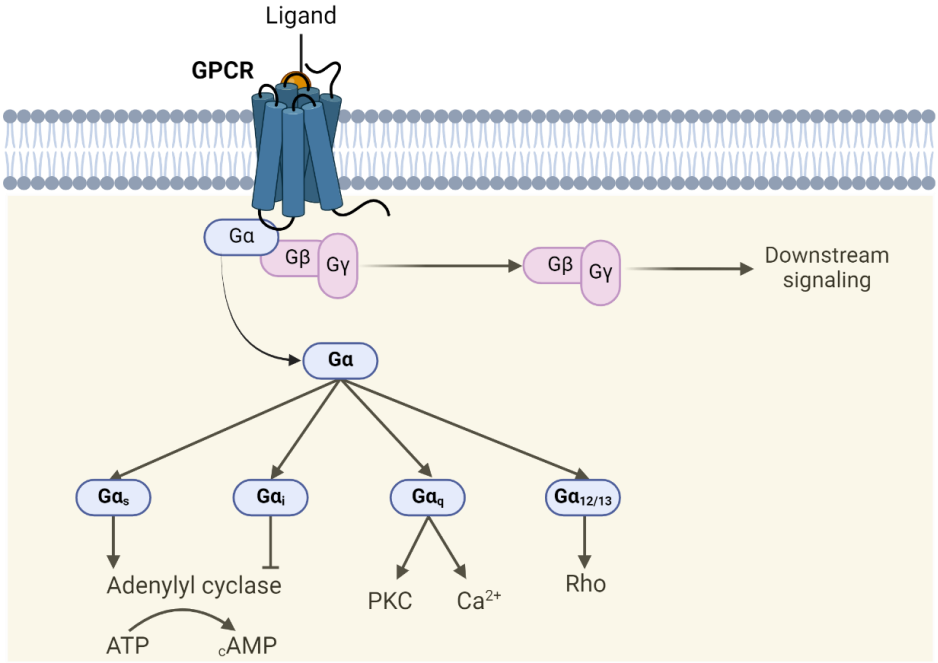

Figure 7. Signaling pathways triggered by the activation of GPCRs via Gα proteins. Image from Biorender.

Gα subunits, depending on their specific type bound to the receptor, modulate different effectors, while Gβγ is responsible for recruiting GPCR kinases (GRKs) to the membrane and governing various signaling pathways. There are four main families of Gα proteins, each coupling to distinct signaling pathways and mediating specific cellular responses. The $G\alpha_{i/o}$ family primarily inhibits adenylate cyclase (AC), leading to a decrease in cyclic AMP (cAMP) levels, thus regulating processes such as neurotransmission, hormone signaling, and immune responses. Conversely, the $G\alpha_s$ family stimulates AC activity, resulting in an increase in cAMP levels and subsequent activation of protein kinase A (PKA), which regulates various cellular functions including metabolism, gene transcription, and ion channel activity. $G\alpha_{q/11}$ proteins induce the release of calcium ions (Ca^{2+}) from intracellular stores and the activation of protein kinase C (PKC) , thereby modulating processes such as cell signaling, muscle contraction, and secretion. Lastly, the $G\alpha_{12/13}$ family activates Rho Family GTPases, inducing changes in cytoskeletal organization and cell shape[151,152,159].

In order to regulate signaling duration, many GPCRs undergo a process involving desensitization, becoming less responsive to continuous stimulation, followed by sequestration, where receptors are internalized into intracellular compartments such as endosomes[4]. GPCR desensitization often involves the action of GRKs, which phosphorylate the receptors at specific intracellular sites, particularly the C-terminal tail, promoting the recruitment of β-arrestins, a family of adapter proteins to the receptor complex[160] (**Figure 8**).

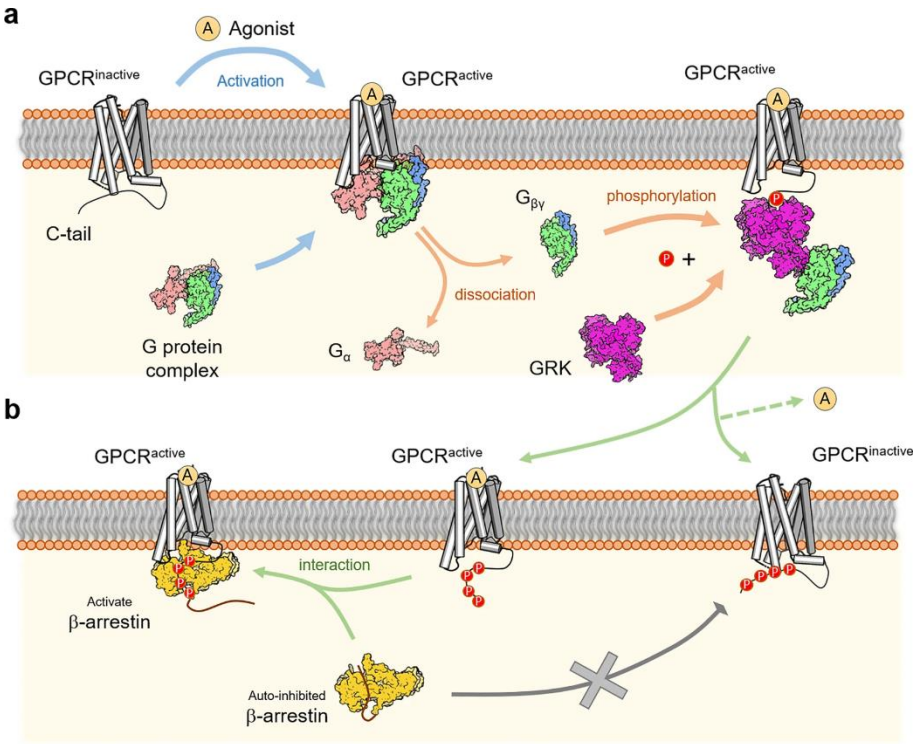

Figure 8. Schematic illustration of the activation of GPCRs and signaling events stimulated by agonists[161].

These β-arrestins play a crucial role in GPCR internalization by facilitating the recruitment of clathrin-coated pits, which then mediate the receptor endocytosis from the plasma membrane, where they can undergo dephosphorylation and can be recycled back to the plasma membrane or targeted for lysosomal degradation, removing the receptor altogether[162]. Additionally, β-arrestins may also participate in further signaling events, forming a bridge between the GPCRs, and downstream signaling molecules. Nevertheless, there are exceptions where GPCRs exhibit internalization independently of arrestins[163].

While many GPCRs follow known desensitization and internalization pathways, SUCNR1 exhibits context-dependent behavior, varying by cell type and environment. This underscores the importance of studying SUCNR1 in diverse cellular contexts. The exploration of GPCR mechanisms paves the way for the next section, focusing on SUCNR1-specific signaling pathways.

1.5.3. SIGNALING PATHWAYS MEDIATED BY SUCNR1

The signaling pathway activated by succinate binding to SUCNR1 has received increasing interest in recent years. SUCNR1 interacts with various Gα proteins, and the specific G-proteins involved can differ depending on the cell type. This variability results in distinct signaling pathways and cellular responses, which can lead to a range of physiological and pathological effects across different tissues[3].

In the **kidneys**, SUCNR1 is prominently expressed in the vascular lumen of the juxtaglomerular apparatus (JGA) and renal tubules[129]. This receptor has been shown to couple with $G\alpha_q$ proteins, activating the renin-angiotensin system, which leads to an increase in blood pressure[19,20]. For instance, studies in Madin-Darby canine kidney (MDCK) cells, have demonstrated that SUCNR1 signaling induces intracellular Ca^{2+} mobilization, transient phosphorylation of extracellular signal-regulated kinase (ERK)1/2, as well as cyclooxygenase-2 (COX-2), leading to the synthesis and release of prostaglandin E_2 (PGE_2), a key vasodilator and paracrine mediator of renin release[18,19]. Additionally, SUCNR1 is located in the luminal membrane of tubular cells, where succinate stimulation can induce the release of arachidonic acid and prostaglandins[18]. Given that succinate is filtered and reabsorbed in the renal system, it is hypothesized that SUCNR1 modulates these processes, playing a crucial role in nephron succinate handling[103]. Furthermore, recent studies have shown that succinate induces tubular epithelial cell apoptosis via SUCNR1 signaling by activating ERK1/2 pathway[131], suggesting that succinate acts as a risk factor and contributes to renal injury.

Notably, in **cardiomyocytes**, succinate has been shown to enhance global Ca^{2+} transients and modulate cell viability, effects that are mediated $G\alpha_q$ proteins[143]. Furthermore, recent findings indicate that SUCNR1 activation by succinate contributes to cardiac hypertrophy and promotes the phosphorylation of ERK1/2. Also, these authors have found that succinate increased intracellular Ca^{2+} transients, confirming previous data[143], which are essential for activating calcium/calmodulin dependent protein kinase IIδ (CaMKIIδ) and subsequently histone deacetylase 5[17]. Interestingly, in cardiomyocytes, succinate induces an increase in cAMP levels, which in turn activates PKA, suggesting the possibility of SUCNR1 coupling with $G\alpha_s$ proteins[17]. Additionally, succinate has been demonstrated to activate the phosphoinositide 3-kinase (PI3K)/Akt or protein kinase B (PKB) signaling pathway[164], which is another pathway also implicated in cardiac hypertrophy[165].

In **hepatic stellate cells** (HSCs), succinate does not inhibit cAMP production or increase Ca^{2+} in quiescent cells but accelerates activation of ischemic HSCs by upregulating α-smooth muscle actin (α-SMA), indicating early hepatic stress detection. SUCNR1 expression decreases rapidly upon HSC activation, suggesting its role in early liver damage response, potentially contributing to fibrosis[119,166]. Additionally, research has

shown that increasing brown and beige adipocytes in mice can mitigate SUCNR1-dependent liver inflammation, regulating immune cell infiltration and systemic glucose intolerance[120]. Also, our recent findings indicate that in **hepatocytes**, SUCNR1 activation influences hepatic metabolism during MAFLD progression by reducing lipogenesis, promoting glycogenesis, and protecting against lipid accumulation and glycogen depletion, partly through the activation of AMPKα and PKAc signaling pathways[28].

Within the **pancreas**, it is widely recognized that various GPCR-mediated mechanisms cooperate in β cells to modulate insulin secretion[167]. Recent findings from our group indicate that SUCNR1 in human β cells enhances insulin release in response to elevated glucose levels[25], mirroring the effects of incretins such as glucagon-like peptide 1 (GLP-1) and glucose-dependent insulinotropic polypeptide (GIP)[168]. Investigating the intracellular signaling mechanisms behind this insulin-stimulating action, we discovered that the activation of SUCNR1 engages a $G\alpha_q$- and PKC-dependent pathway, which is essential for the potentiation of insulin secretion[25]. Although some prior studies have posited that the increases in intracellular calcium concentration ($[Ca^{2+}]$) observed upon SUCNR1 activation, which we also observed in β cells, are mediated by $G\alpha_i$ and βγ subunit-induced phospholipase C (PLC)- β activation[169,170], recent research has clarified that $G\alpha_q$ signaling is crucial for the PKC- and $[Ca^{2+}]$-dependent responses linked to SUCNR1 activation, particularly in immune cells[171,172]. Moreover, other GPCRs, such as GPR40, which is activated by free fatty acids (FFAs), have also been shown to use signaling pathways involving $G\alpha_q$, PKC, and $[Ca^{2+}]$ to stimulate insulin secretion[173,174]. This underscores a broader trend in GPCR-mediated insulinotropic effects, highlighting the complexity of the signaling networks involved in glucose-induced insulin release.

Moreover, SUCNR1 is abundantly expressed in **adipocytes**[13], yet its primary recognized function in this tissue is the inhibition of lipolysis. This inhibition is particularly relevant in the context of obesity, where dysregulated lipolysis contributes to excess fat accumulation[13,26,27]. In white adipocytes, SUCNR1 activation by succinate regulates lipolysis through $G\alpha_i$ proteins, which subsequently reduces cAMP levels[26]. Further investigation into SUCNR1 roles in AT may reveal additional functions that could be targeted for obesity treatments. This thesis explores the detailed mechanisms of SUCNR1 signaling in AT, with the goal of elucidating its overall impact on metabolic regulation.

SUCNR1 signaling also plays a critical role in maintaining **retinal health**, particularly in regulating angiogenesis and vascular development. In diabetic rat retinas, the knockdown of SUCNR1 disrupts the activation of ERK1/2 and COX-2, resulting in lower levels of key angiogenic factors such as PGE_2 and vascular endothelial growth factor (VEGF)[175]. Furthermore, retinal ganglion cells exhibit an increase in VEGF production in response to succinate, which is essential for blood vessel formation[21]. Recent research has

demonstrated that SUCNR1 is also localized in the ER in these cells, and that this localization is crucial for its angiogenic regulatory role[145].

Human umbilical vein endothelial cells (HUVECS), widely used in vascular biology studies, demonstrate SUCNR1-mediated activation of the mitogen-activated protein kinases (MAPK) pathway. In HUVECs, this signaling primarily involves $G\alpha_i$ proteins, which inhibit adenylate cyclase, reducing cAMP levels, suggesting a significant role in regulating vascular responses and endothelial function[16].

The succinate-SUCNR1 axis is also essential for the growth of **hematopoietic progenitor cells** (HPCs). SUCNR1 is expressed in CD34+ bone marrow progenitor cells, erythroid and megakaryocyte cultures, and the TF-1 erythroleukemic cell line. It was found that succinate promotes proliferation in these cells via $G\alpha_i$ signaling and also involving the activation of the ERK/MAPK pathway and inositol phosphate accumulation. Additionally, succinate was shown to prevent serum deprivation-induced cell death in TF-1 cells and increase hemoglobin, platelet, and neutrophil levels in a mouse model of chemotherapy-induced myelosuppression. These findings underscore the significant role of SUCNR1 signaling in HPC development and survival[176].

Human platelets also express SUCNR1 and play a crucial role in regulating their function and aggregation. Upon activation by succinate, SUCNR1 signaling triggers a decrease in intracellular cAMP levels via $G\alpha_i$ proteins. Furthermore, the role of $G\beta\gamma$-mediated signaling is highlighted by the strong activation of PI3K, which results in the phosphorylation of Akt/PKB, further emphasizing the importance of this pathway in platelet physiology[177].

Overall, the diverse intracellular signaling pathways triggered by SUCNR1 activation (summarized in **Table 1**) highlight the diverse roles succinate can play as a hormone. SUCNR1 ability to modulate various cellular processes through different Gα-protein couplings underscores the complexity of succinate signaling, shedding light on its multifaceted physiological effects.

Table 1. SUCNR1 signaling pathways in various cell sub-types.

Tissue	Cell types	Signaling pathways and effectors	Pathophysiological effect
Kidney	Kidney and macula densa cells[19]	$G\alpha_q$, P38 and ERK1/2. Renin release via COX-2 and PGE_2[19]	Hypertension, diabetic nephropathy, and renal complications[18,19]
	MDCK cells[18]	$G\alpha_q$, ERK1/2. PGE_2.[19]	Hypertension[19]
Heart	Cardiomyocytes	$G\alpha_q$ and PKA dependent pathway[143]	Cell viability and cardiac hypertrophy[143]
Liver	Hepatic stellate cells	α-SMA[119,166]	Hepatic fibrosis[119,166]
Pancreas	Pancreatic β cells	$G\alpha_q$ and PKCpathway[25]	Insulin release in response to elevated glucose levels[25].
Adipose tissue	Adipocytes	$G\alpha_i$ proteins, ↓cAMP[26]	Inhibition of lipolysis[26]
Retina	Retinal ganglion neurons[21,129]	VEGF/cell proliferation via COX-2 and PGE_2[21,22,129]	Diabetic retinopathy[22]
Endothelial tissue	HUVECs	$G\alpha_i$ proteins[16]	Vascular responses and endothelial function[16].
Bone marrow	Hematopoietic progenitor cells (erythroid and megakaryocytes TF-1)	$G\alpha_i$ and ERK1/2[176]	Stimulation of immunity, protection from apoptosis[176]
Blood	Immature dendritic cells	$G\alpha_q$, Ca^{2+} and ERK1/2. TNFα, IL-1β and cytokines[56]. iMODCs migration[56].	Enhancement of immunity[56]
	Platelets	$G\alpha_i$ proteins, ↓ cAMP Bγ proteins, PI3K/Akt[177]	Potentiation of platelet aggregation[177]
	Monocytes T and B	↑ TNFα and interferon-γ (IFN-γ)[56]	Immunity[56]

1.5.4. SUCCINATE/SUCNR1 SIGNALING IN INFLAMMATION

Over the years, considerable research has been dedicated to understanding the link between SUCNR1 and inflammation. SUCNR1 is present in various immune cells, including macrophages, DCs and some T-cell subsets. This broad distribution highlights its crucial role in modulating immune responses[56,178,179]. Although intracellular succinate is recognized as a crucial pro-inflammatory signal, its extracellular presence not only enhances pro-inflammatory responses but can also have anti-inflammatory effects under specific conditions[180].

Interestingly, despite proinflammatory macrophages release succinate, SUCNR1 is predominantly expressed in anti-inflammatory or pro-resolving macrophages M2[14,181]. Initially, it was observed that activating SUCNR1 enhances IL-1β secretion through $G\alpha_i$ in interferon-primed macrophages[5]. However, a subsequent study found that *Sucnr1*-deficient mouse peritoneal exudate macrophages exhibit a cytokine profile akin to control cells[15]. We recently indicated that myeloid-specific KO of SUCNR1 correlates with increased inflammation and impaired glucose tolerance, suggesting that succinate, as a marker of metabolic stress, primarily exerts an anti-inflammatory effect through SUCNR1 on M2 macrophages. Intriguingly, the effects of *Sucnr1* deficiency on AT macrophages (ATMs) vary based on their location and inflammatory state. Particularly, *Sucnr1*-deficient ATMs from subcutaneous fat exhibit a proinflammatory phenotype, while those from visceral fat, typically proinflammatory, display reduced inflammation[14]. Consistent with this, in a study by Peruzzotti-Jametti and colleages, it was demonstrated that succinate triggers an anti-inflammatory response in neural stem cells (NSCs) through SUCNR1 signaling. This activation results in the release of PGE_2, which regulates various cell types within the inflammatory microenvironment[108].

These findings underscore the intricate nature of modulating the succinate/SUCNR1 axis in macrophages, with effects varying depending on the context. However, we have suggested that succinate, like other dual-role cytokines such as interleukin 6 (IL-6)[182], is generated during inflammation to booster the acute response while also serving as a feedback signal to promote pro-resolving macrophages via SUCNR1, thus regulating inflammation[3] (**Figure 9A**).

DCs, vital for antigen presentation and adaptive immune regulation, show high SUCNR1 expression in their immature monocyte-derived DCs (iMoDCs) state, which decreases upon maturation[56]. Extracellular succinate binding to SUCNR1 induces Ca_i^{2+} mobilization and ERK1/2 phosphorylation, a process that promotes DC maturation and IL-1β secretion, thereby enhancing the inflammatory response to pathogens (**Figure 9B**). Succinate also enhances the migratory and T-cell activating capabilities of DCs in an antigen-specific manner. Notably, these succinate-induced effects are diminished in the absence of SUCNR1, as demonstrated in KO studies[56].

Moreover, succinate influences T-cell function both indirectly through its effects on DCs and directly within inflammatory microenvironments. Studies have shown that succinate can suppress degranulation and cytokine release in $CD4^+$ and $CD8^+$ T cells, notably reducing the production of interferon-γ (IFN- γ)[183]. Additionally, the inhibition of SDH during T-cell activation markedly reduces the expression of activation markers, inflammatory cytokine production, and cell proliferation[184]. Research on experimental autoimmune uveitis in mice revealed that succinate boosts the presence of T helper (Th) 1 and Th17 cells. This effect, driven by the succinate/SUCNR1 axis, results in higher production of IFN-γ[185] (**Figure 9C**). These observations emphasize the significant influence of SDH and succinate on the adaptive immune response.

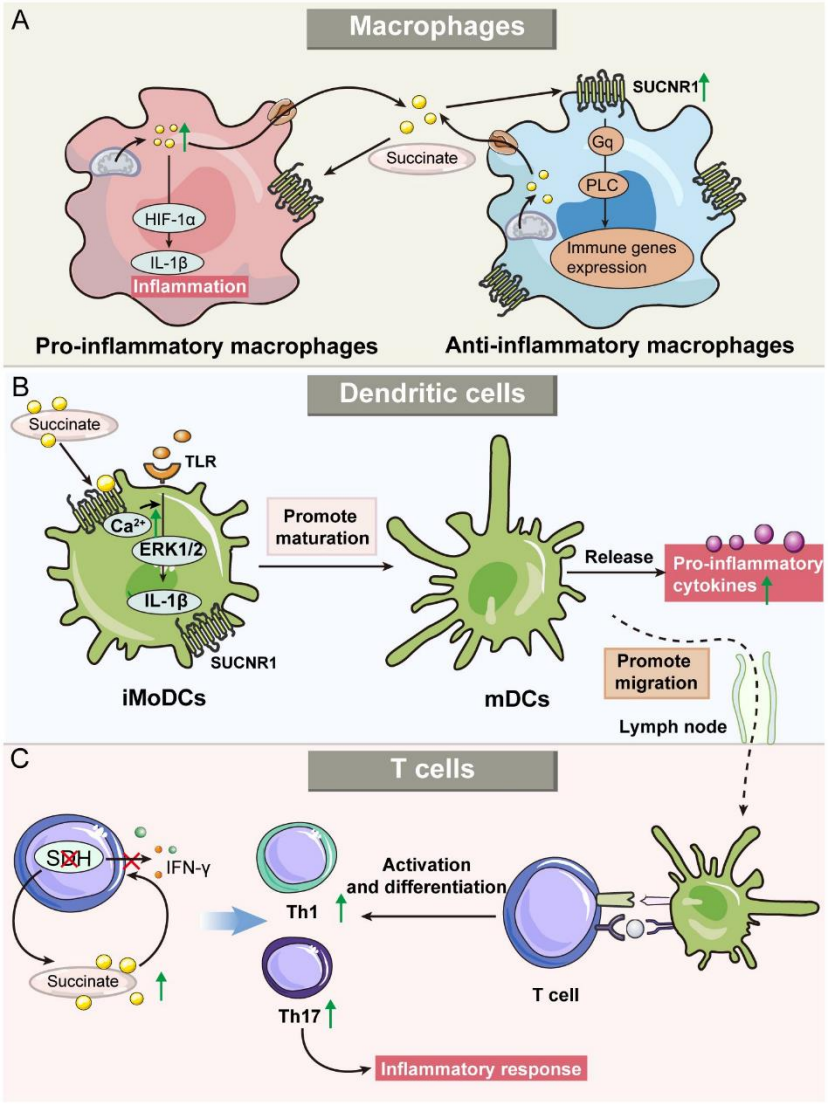

Figure 9. Roles of SUCNR1 signaling in immune cells, including macrophages, DCs, and T cells[35].

Because disruptions in the immune system play a role in metabolic disorders, it is understandable that SUCNR1 is implicated in the development of obesity. Numerous studies have highlighted the close connection between excessive nutrient intake and immune system activation within metabolic tissues, which is directly linked to IR and T2DM[186]. Together, these findings underscore the importance of succinate/SUCNR1 axis in pathological contexts and open new avenues for clinical use in patients with a range of inflammation-related conditions, such as obesity or diabetes.

1.5.5. METABOLIC FUNCTIONS ASCRIBED TO SUCNR1 SIGNALING

As discussed, SUCNR1 studies were largely focused within inflammatory-related conditions[5,56,187], especially those linked with chronic hypersuccinemia[8,37,115,118]. However, the recently reported transient increase in extracellular succinate induced by physiological stimulus, previously outlined in section 1.4.1, reflected additional metabolic activity for succinate, suggesting its potential as a hormone-like metabolite[3].

In a revolutionary study, McCreath and colleagues demonstrated for the first time that the absence of SUCNR1, previously known for its role in immune response, has a significant impact on metabolic processes. Using a transgenic mouse model with whole-body *Sucnr1* deletion, they found that SUCNR1 regulates adipose mass and glucose homeostasis. The study highlighted the complex effects of whole-body *Sucnr1* KO: beneficial metabolic impacts on a standard diet versus detrimental outcomes like weight gain and hyperglycemia on a HFD. This dichotomy emphasizes the need for further research to understand its precise role in different tissues and cell-specific scenarios[13]. Since SUCNR1 is widely expressed across metabolically active tissues[26] and energy homeostasis requires multi-tissue crosstalk, discerning the specific function of extracellular succinate as a signaling molecule requires targeted genetic methodologies focusing on particular cell types implicated in SUCNR1 signaling.

As detailed earlier, SUCNR1 is highly expressed in **WAT** and purified adipocytes. The first function ascribed to SUCNR1 in WAT was the inhibition of lipolysis[26]. Studies have demonstrated that succinate inhibits lipolysis in a pertussis toxin-dependent mechanism, suggesting that the antilipolytic effects of succinate are mediated by SUCNR1. This observation was confirmed in mice with a global deficiency in *Sucnr1*[13,26]. It is well-established that the lipolytic activity of WAT is minimal in the post-prandial state due to the antilipolytic action of insulin[188], and recent studies have shown an increase in circulating succinate levels during the fasted-to-fed transition, which is consistent with its antilipolytic role[111]. Interestingly, new insights have shed light on the critical role of mDIC transporter, which facilitates the exchange of succinate across the inner mitochondrial membrane, in regulating adipocyte lipolysis and protecting the liver, helping to reduce damage associated with obesity-related conditions. This suggests that

the mDIC/succinate/SUCNR1 pathway could be a promising therapeutic target for addressing metabolic disorders such as obesity and MAFLD[27].

While SUCNR1 is abundantly expressed in WAT, its expression in **BAT** is minimal[13]. Nevertheless, succinate functions as an intracellular signaling molecule that regulates BAT physiology due to its thermogenic properties. Research has shown that succinate significantly accumulates in thermogenic AT during cold exposure, independently of the adrenergic signaling pathways typically associated with thermogenesis. This accumulation enhances thermogenic respiration in brown adipocytes by promoting succinate oxidation via SDH, leading to the production of ROS that activate uncoupling protein 1 (UCP1), a crucial protein in the thermogenesis process that is exclusively expressed in brown and beige adipocytes[189]. Additionally, increasing circulating succinate pharmacologically enhances thermogenesis, offering protective effects against diet-induced obesity and improving glucose tolerance[109]. Recent studies conducted by the same authors have identified an endocrine pathway regulated by UCP1 that counteracts liver inflammation and pathology, independent of its effects on obesity. Their findings demonstrate that the presence and activity of UCP1-expressing adipocytes are crucial for the capacity of BAT to clear and metabolize circulating succinate. Furthermore, increasing brown and beige adipocyte content in mice mitigates liver inflammation and pathology by preventing chronic activation of SUCNR1, which otherwise affects HSC and macrophage populations in the liver. Importantly, the UCP1/succinate/SUCNR1 axis is essential for controlling liver inflammation and systemic glucose intolerance in an obesogenic environment. Therefore, the therapeutic potential of brown and beige adipocytes, as well as UCP1, extends beyond their role in thermogenesis and can be utilized to combat liver diseases and SUCNR1-mediated liver inflammation[120].

The role of succinate/SUCNR1 axis in the **gastrointestinal tract** is debated due to conflicting evidence regarding the expression of SUCNR1 in the intestine. While systemic analysis in mice suggests *Sucnr1* expression in both large and small intestines[190], other studies propose exclusive expression in intestinal tuft cells, which potentially sense succinate from pathogens, activating mucosal type 2 immunity. Moreover, *Sucnr1*-expressing tuft cells detects dietary succinate, prompting cell expansion and increased type 2 cytokines. Thus, succinate/SUCNR1 signaling in tuft cells monitors microbial metabolism in the intestinal lumen[187,191].

Many years ago, researchers discovered that succinate is released by skeletal muscle into the circulation during exercise[110,192]. However, it took 50 years to uncover the crucial role of succinate/SUCNR1 axis in regulating **skeletal muscle** remodeling and mitochondrial biogenesis[193]. Interestingly, prolonged succinate administration improved mice endurance exercise by inducing a transformation in skeletal muscle fiber-type[194]. The same researchers also found that acute succinate administration elevates oxidative phosphorylation and boosts the explosive strength of skeletal muscle, a process dependent on SUNR1[195]. Additionally, recent studies revealed that muscle releases

succinate during exercise through an MCT-1-dependent process, which is sensitive to fluctuations in pH. These findings suggest that succinate is essential for skeletal muscle adaptation to exercise training through paracrine signaling, where SUCNR1 expressed on non-myocellular stomal cells, rather than on mouse skeletal muscle cells, plays a pivotal role[71]. This study shows that SUCNR1 is absent in skeletal muscle cells[71]; however, this remains controversial as other researchers have observed that SUCNR1 mRNA and protein levels were expressed around the skeletal muscle fibers[196]. However, the specific cell types that respond to succinate and the direction of their signaling are still not well understood. Recent research has claimed that SUCNR1 is absent in muscle fibers but is present in macrophages within skeletal muscle. Utilizing single-cell RNA sequencing and RNAscope, researchers discovered high SUCNR1 levels in M2-polarized macrophages, which are involved in the anti-inflammatory response. Upon stimulation with selective agonists, these macrophages activated Gq- and Gi- coupled signaling pathways, while primary human skeletal muscle cells showed no response to SUCNR1 agonists. Thus, and according to these data, the role of SUCNR1 in skeletal muscle adaptation to exercise is likely mediated through paracrine mechanisms involving M2-like macrophages within the muscle[197].

Our group has significantly contributed to the understanding that the succinate/SUCNR1 axis also plays a significant role in the **pancreas**, particularly in the regulation of insulin secretion[167]. Previous research had shown that mice lacking *Sucnr1* globally and fed a HFD exhibit impaired insulin secretion and glucose intolerance without substantial alterations in body weight and β-cell mass, suggesting a potential role of SUCNR1 in governing β-cell function[13]. Accordingly, our recent investigations have shown that SUCNR1 is expressed in β-cells and its levels increase during hyperglycemia in both mice and humans. Mice with a β-cell-specific deletion of *Sucnr1* displayed impaired glucose tolerance and insulin secretion under a HFD, underscoring the importance of SUCNR1 in maintaining insulin secretion in the context of diet-induced IR. Additionally, individuals with impaired glucose tolerance demonstrated an enhanced succinate response, which correlated with increased insulin secretion during glucose challenge tests. These findings confirm that the succinate/SUCNR1 axis is activated by elevated glucose levels and contributes to insulin secretion regulation, particularly relevant for managing hyperinsulinemia in prediabetes conditions[25].

In conclusion, the succinate/SUCNR1 axis plays crucial roles in a range of metabolic processes. Despite its relative low expression in certain tissues, the involvement of SUCNR1 in these essential physiological functions underscores its potential as a therapeutic target for a variety of disorders. Nonetheless, it is important to recognize that many aspects of SUCNR1 function in metabolic regulation remain unexplored.

2. ADIPOSE TISSUE

AT is now recognized to be a multifunctional organ that not only serves as an energy storage site but also functions as an insulator, a protector of internal organs, and a critical endocrine organ regulator of energy balance. It is composed of a diverse array of cells, where **mature adipocytes** are the most abundant cell type, alongside a variety of other cells such as mesenchymal stem cells (MSCs), pre-adipocytes, fibroblasts, endothelial cells, macrophages, vascular smooth muscle cells, leukocytes, T-cells, and erythrocytes[198], which constitutes the stromal vascular fraction (SVF). These cells create a complex communication network essential for regulating the functions and activities of AT reservoirs[199]. As the obesity epidemic grows, our understanding of AT and adipocytes has grown considerably. Recent discoveries have shown how AT contributes to normal physiology and obesity, highlighting the importance of studying adipocyte biology in the global rise of metabolic diseases[200].

In mammals, there are two primary types of AT, WAT and BAT, each with distinct physiological functions and regulatory mechanisms that contribute to the body overall metabolic health[201]. Over the past few decades, the perception of WAT has shifted from being a mere fat storage site to an active participant that adapts to nutrient and energy changes, contributing to hormonal signaling and energy balance[202,203]. The discovery of thermogenic and lipid-combusting BAT in adult humans 15 years ago has further transformed our perception of energy regulation, suggesting new therapeutic strategies for obesity and metabolic disorders[204]. Understanding these distinct types of AT is crucial for developing targeted interventions to improve metabolic health[200]

This chapter will detail the different types, anatomical locations, composition and physiological roles of AT depots, along with an analysis of their secretory capabilities and metabolic implications.

2.1. ADIPOCYTES

2.1.1. FUNCTIONS AND TYPES

The earliest function attributed to adipocytes, the primary cellular component of AT, was the storage of energy as triglycerides (TGs). It was not until the mid-1980s that researchers discovered that AT also has secretory functions and produces adipocyte-specific proteins[200]. Despite the limited understanding of the functions of AT secretory products, their discovery highlighted adipocytes and AT as significant sources of various proteins, including endocrine hormones. One of the most crucial discoveries was leptin, an adipocyte-derived hormone with broader roles (detailed in section 2.5.1.2) but primarily known for signaling to the brain to control body weight[203].

In addition, adipocytes are highly responsive to insulin and play a crucial role in regulating blood glucose levels. Insulin stimulates glucose uptake in adipocytes and modulates lipid metabolism by promoting TGs accumulation and reducing their breakdown, thereby limiting the release of FFAs into the circulation[200]. The significance of these three adipocyte functions -lipid storage, secretory activity, and insulin sensitivity- is highlighted by evidence showing that disruption in any of these roles leads to substantial systemic effects in both mice and humans. These disruptions can contribute to various metabolic diseases associated with obesity[205]. Moreover, adipocytes are also crucial for maintaining body temperature through a mechanism known as non-shivering thermogenesis. This process allows for the dissipation of energy in the form of heat, which is particularly important in response to cold exposure[206].

They are classified into three distinct types -white, brown, and beige adipocytes- each differing in their histological structure, molecular characteristics, and functions in both mice and humans[207] (**Figure 10**).

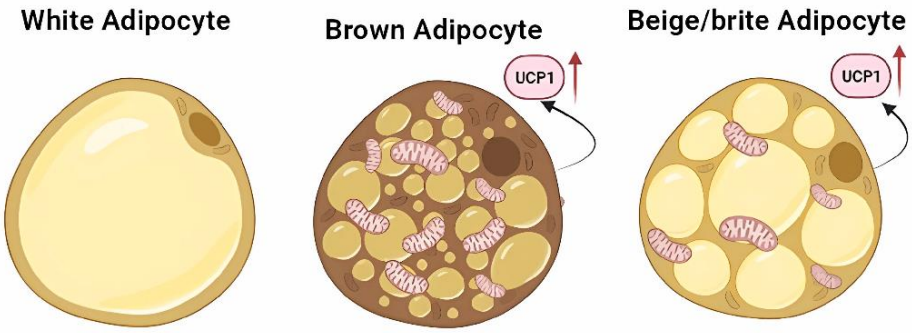

Figure 10. Morphological aspects of white, brown, and beige adipocytes[208].

Brown adipocytes are found in the BAT depot, whereas both white and beige adipocytes are present in WAT depots[209]. WAT has been shown to exhibit different types of adipocytes, extending beyond the thermogenic beige cells that appear in response to cold exposure, but the underlying mechanisms and implications of this diversity remain unclear. Current research has largely focused on a few adipose depots and specific conditions, necessitating broader studies to enhance our understanding of adipocyte heterogeneity. Although single-cell analyses have provided fundamental data, they often lack detailed metabolic insights[210]. To advance our knowledge, it is essential to employ epigenomic techniques and multi-omics approaches to provide a clearer understanding of adipocyte diversity and its metabolic roles[211].

White adipocytes are the most abundant type, and they are characterized by a spherical shape with variable size determined by the dimensions of the single lipid droplet housed within. This lipid droplet, predominantly consisting of TGs, constitutes over 90% of the cell volume. Mitochondria within white adipocytes are thin, elongated, and variable in

quantity. In situations where energy intake exceeds demand, white adipocytes store the excess nutrients as TGs. In contrast, when energy is scarce, they provide nutrients to other tissues via lipolysis[212]. In addition to their role in energy storage, white adipocytes exhibit endocrine properties, with WAT secreting various hormones including adiponectin, leptin, and resistin, among others. Furthermore, in pathological conditions such as obesity, white adipocytes can also produce cytokines such as tumor necrosis factor-alpha (TNF-α) or IL-6. These molecules play crucial roles in the regulation of systemic metabolism, IR, and inflammation[213].

In contrast, **brown adipocytes** store TGs in multiple small vacuoles, exhibiting a typical polygonal shape with varying diameters. Brown adipocytes are characterized by abundant mitochondria that present a large, spherical structure filled with laminar cristae. Due to its elevated oxygen demand, BAT contains more capillaries compared to WAT. Moreover, BAT exhibits a denser nerve supply in contrast to WAT. The brown color of BAT results from its elevated mitochondrial density and increased vascularization[214]. Brown adipocytes are essential for maintaining body temperature through non-shivering thermogenesis, utilizing the brown adipocyte-specific protein UCP1[215], also known as thermogenin. UCP1 is a protein located on the inner mitochondrial membrane that uncouples substrate oxidation from ATP synthesis, leading to the dissipation of excess energy as heat[216].

Upon cold exposure or activation of β-adrenergic receptors, a third type of adipocyte, known as brown-in-white (brite) or **beige adipocyte**, emerges within WAT in both rodents and humans, and is involved in cold-induced thermogenesis. This phenomenon, named "browning of WAT", involves the transformation of cells from a white adipocyte-like to a brown adipocyte-like phenotype[217]. Interestingly, beige/brite adipocytes have characteristics of both white and brown adipocytes. In the basal state, these cells present a lipid morphology characterized by large, singular droplets and the same gene expression patterns as the white adipocytes. However, in response to cold stimuli, beige/brite adipocytes adopt an "intermediate cell morphology" marked by multilocular lipid droplets surrounding larger ones, leading to the conversion into the multilocular/small lipid morphology distinctive of brown adipocytes[218]. Interestingly, the inducible browning mechanisms are reversible responses, and the former beige/brite adipocytes can be reverted to their original state as white adipocytes through a process known as "whitening"[219]. In terms of function, beige adipocytes are more akin to brown adipocytes than to white adipocytes, due to their capacity to convert chemical energy into heat in response to specific stimuli[220].

Detailed explanation of the functions of each AT will be examined in their respective sections, 2.2 and 2.3.

2.1.2. ORIGIN OF BROWN, WHITE AND BEIGE ADIPOCYTES

White, brown, and beige adipocytes originate from MSCs, adult stem cells first identified in bone marrow known for their multipotent capabilities, including the ability to differentiate into mature adipocytes, osteoblasts, chondroblasts, and myoblasts[199]. Bone marrow MSCs (BM-MSCs) have been broadly studied since 1960s for their therapeutic potential[221] and have been successfully isolated from various tissues throughout the body[222], including AT[223]. This tissue is especially valuable for its abundance of stem cells, which can differentiate into both adipogenic and myogenic cell types[199].

Adipose-derived stem cells (ASCs) were initially recognized as MSCs in AT in 2001, leading to significant research into the potential applications of AT in tissue engineering and regenerative medicine[224]. ASCs are present in any type of WAT, exerting a physiological role in AT by contributing to tissue homeostasis, cell renewal and spontaneous repair[225]. These ASCs share many characteristics with BM-MSCs, including their potential to differentiate into several tissue lineages, their ability to release adipogenic and angiogenic cytokines, and their immunomodulatory properties. The predominant value attributed to ASCs is linked to their ability to undergo differentiation into diverse mature lineages. These cells exhibit multi-lineage plasticity, and they can differentiate into cells from the mesoderm, endoderm, and ectoderm germ layers[226].

Under normal conditions, ASCs predominantly reside in perivascular locations and undergo differentiation into specific cell type in response to diverse signals[227]. These signals can be soluble factors in the cell culture medium or mechanical signals transmitted through matrix properties, and they can differentiate into numerous cell types, including adipocytes, chondrocytes, osteocytes, myocytes, neuronal cells, among others[224] (**Figure 11**).

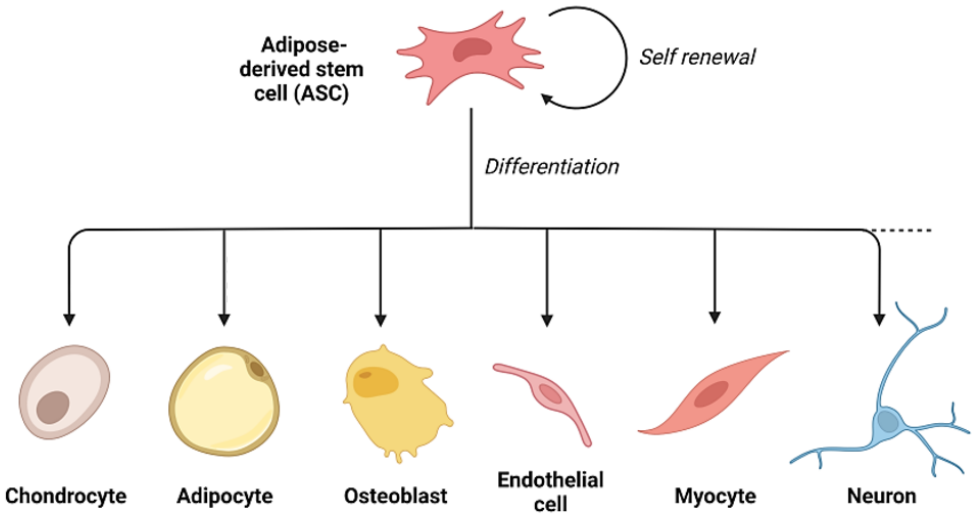

Figure 11. Differentiation potential of ASCs into different cell types. Image adapted[228].

Differentiation is a complex process marked by a regulation of lineage-specific transcription factors, such as peroxisome proliferator-activated receptor gamma (PPARγ) for adipogenic lineage[229], runt-related transcription factor 2 (RUNX2) for osteogenic lineage[230], or Sox9 for chondrogenic lineage[231].

White adipocytes, predominantly with an adipogenic lineage, mainly arise from myogenic transcription factor 5 negative ($Myf5^-$) progenitor cells[232]. The adipogenic lineage is driven by various factors, such as bone morphogenetic proteins (BMPs), transforming growth factor-β (TGF-β), fibroblast growth factor 1 and 2 (FGF1 and FGF2), insulin-like growth factor 1 (IGF-1), among others[233]. Additionally, T-cell factor 21, a distinct transcription factor in preadipocytes, promotes differentiation into the white adipocyte lineage and suppresses myogenic differentiation[234,235].

Specifically, white adipocyte differentiation begins with a phase called determination, where ASCs commits to adipocyte lineage, transforming into preadipocytes, unable to differentiate into any other cell type. In the subsequent phase, called adipogenesis, white preadipocytes differentiate into mature adipocytes, equipped for lipid transport and synthesis, insulin sensitivity, and adipokine secretion[236]. This process involves cell cycle arrest and the initiation of a transcriptional cascade, with PPAR-γ as the master regulator[237], along with C/EBPs proteins such as C/EBPβ, C/EBPγ, and C/EBPα[238], and sterol regulatory element binding protein 1c (SREBP1c)[239] (**Figure 12**).

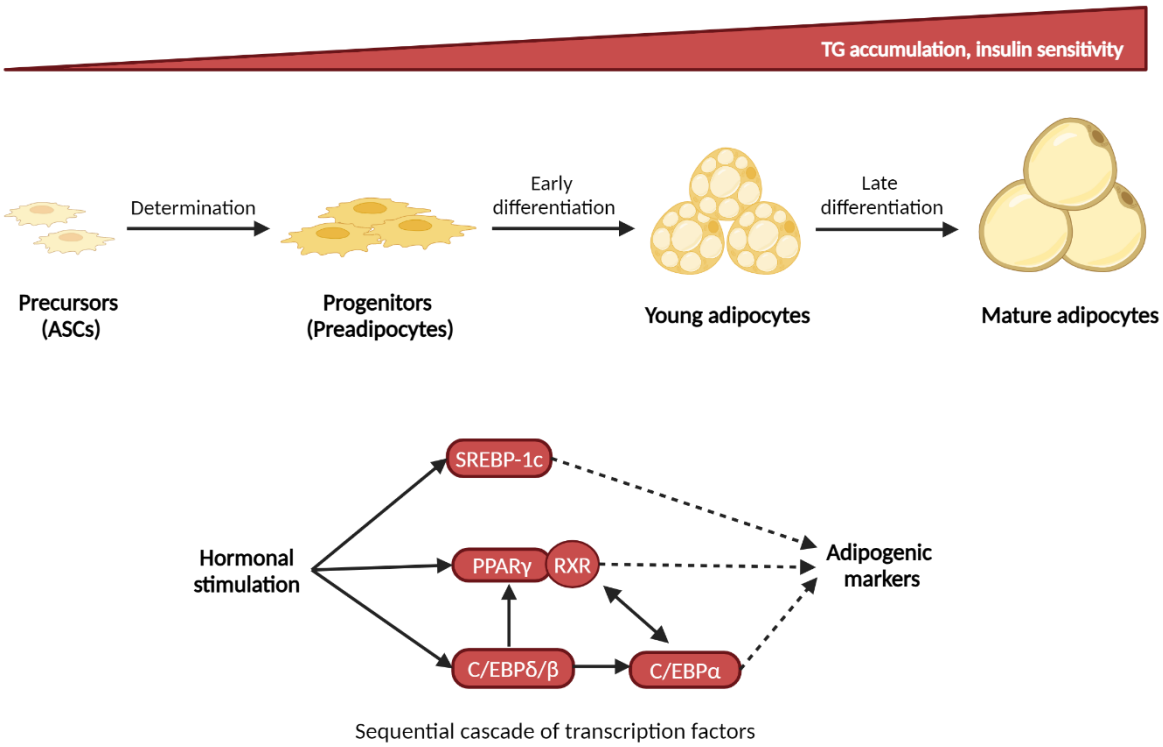

Figure 12. Schematic representation of the regulatory processes involved in adipogenesis from mesenchymal precursors. Image adapted[236].

Initially, it was believed that brown and white adipocytes originated from a common developmental pathway due to their shared lipid metabolism and gene expression profiles[240]. However, research has revealed that **brown adipocytes** and myocytes are both derived from a myogenic lineage, which is originated from myogenic transcription factor 5 positive ($Myf5^+$) progenitor cells[232] (**Figure 13**). The differentiation into brown preadipocytes is driven by BMP7[241], PR domain containing 16 (PRDM16)[242], and early B-cell transcription factor 2[243], which upregulate BAT-specific markers like PPARγ and C/EBPs in cooperation with PRDM16[238].

During the final differentiation stage, specific factors drive the conversion of preadipocytes into mature brown adipocytes[238]. BMP7 induces UCP1, promoting brown or beige lineages, while BMP4 enhances UCP1 levels in beige adipocytes. β-adrenergic signaling, along with PPARγ, peroxisome proliferator-activated receptor gamma coactivator 1α (PGC1α), and PRDM16, are crucial for the development and function of brown and beige adipocytes, with PGC1α playing a key role in BAT metabolism by enhancing fatty acid oxidation, mitochondrial biogenesis, and UCP1 activity in response to cold exposure.

The origin of **beige adipocytes** remains unclear, though research indicates they might originate from $Myf5^-$ progenitor cells or through transformation of pre-existing mature white adipocytes[209,244] (**Figure 13**). White adipocytes can differentiate into beige adipocytes when exposed to cold, β3-adrenergic agonists, PPARγ agonists, and other similar conditions[245].

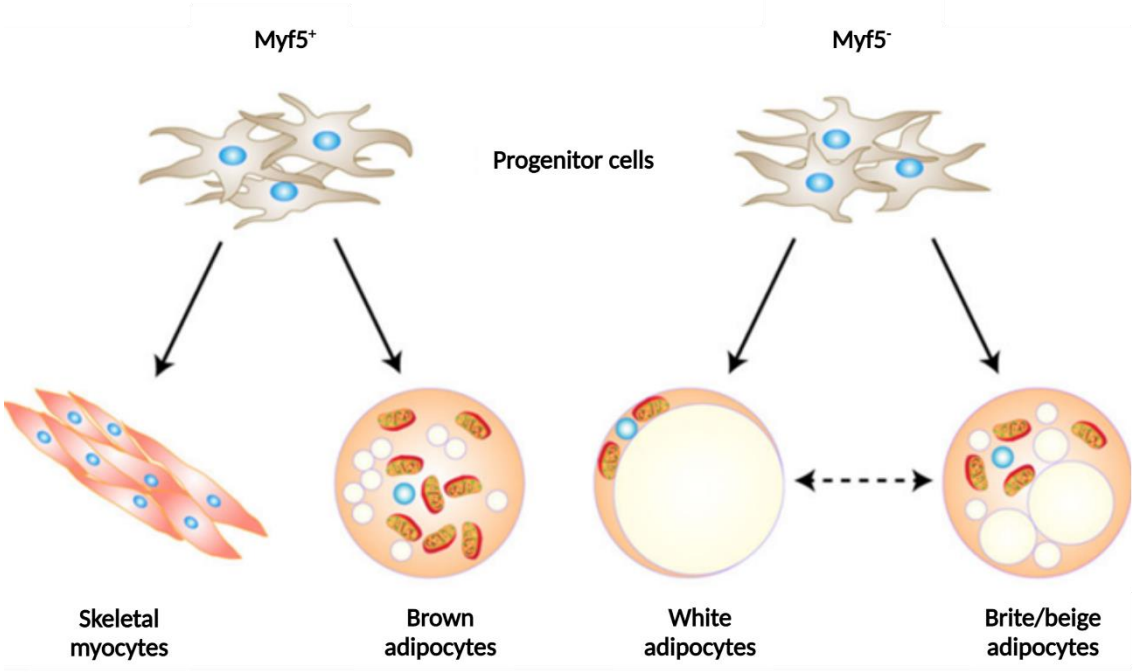

Figure 13. Origin of white, brown and beige adipocytes[246].

Understanding the origin of brown, white, and beige adipocytes is crucial for uncovering the mechanisms underlying AT function and its role in metabolic health. By studying these cell types, we can better comprehend how adipocyte lineage and plasticity influence energy balance, thermogenesis, and the development of metabolic disorders such as obesity and T2DM.

2.2. WHITE ADIPOSE TISSUE

2.2.1. FUNCTIONS

WAT is the predominant deposit of AT in human adults, representing 10-20% of body weight in healthy subjects[247]. As previously noted, the main function of WAT is to store energy in the form of TGs, which can be mobilized via lipolysis from fat stores to meet energy demands such as fasting and physical exercise[248]. The disruption of this balance, characterized by excessive lipid storage and decreased removal, leads to conditions like obesity, IR, and T2DM[249].

In addition to its role in lipid storage, WAT also has important endocrine roles by secreting adipokines and cytokines such as adiponectin, leptin, or TNFα, which contribute to the regulation of diverse metabolic processes[250]. Also, maintaining intracellular WAT lipid homeostasis is a fundamental factor influencing body weight and insulin sensitivity in both mice and humans. Because of their crucial function in regulating adipocyte function, both storage and release of lipids in WAT are physiologically under a precise hormonal control[251]. Moreover, the understanding of the diverse functions of WAT continues to evolve, with new evidence suggesting that it plays a crucial role as an immune organ in defending the body against infections[252].

The roles of WAT as an energy reservoir and an endocrine organ will be explored more thoroughly in section 2.4 and section 2.5 of this doctoral thesis.

2.2.2. DISTRIBUTION AND METABOLIC IMPLICATIONS

Generally, both in mice and humans, WAT depots can be divided into two significant anatomical regions: **subcutaneous WAT** (scWAT), positioned just beneath the skin, and **visceral WAT** (vWAT), located within the central body cavity. The scWAT is considered as the primary physiological location for lipid storage. In lean individuals, this depot usually constitutes the major portion, approximately 80%, of the entire body fat[253].

The location of scWAT depots can vary slightly between species. In mice, scWAT is primarily located in the posterior inguinal WAT (iWAT) depot and the anterior axillary region. In humans, scWAT is predominantly located in the abdominal region (abWAT), as well as in the femoral (thigh) and gluteal (buttock) regions, with a heightened presence in women[254].

Comparing visceral fat pads directly between species is less accurate. In mice, the most extensively studied is the peri-gonadal WAT (gWAT), also referred to as epididymal fat in males and periovarian fat in females, which dominates their central cavity. Mice also have retroperitoneal WAT (rWAT), as well as some mesenteric and omental WAT (oWAT)[255]. Therefore, the gWAT has remained the primary focus, and in rodent studies it is often referred to just as vWAT. Conversely, humans organize most of their vWAT into the oWAT, composed by mesenteric and retroperitoneal fat. Numerous studies have demonstrated that the accumulation of human oWAT is associated with metabolic disorders and elevated risk for developing comorbidities such as IR, dyslipidaemia, T2DM and CVD[256,257]. A comprehensive view of WAT and BAT distribution can be found in **Figure 16**, located in Section 2.3.2.

Subcutaneous and visceral WAT differ significantly in their endocrine function and metabolic impact. scWAT primarily secretes hormones such as leptin and adiponectin, which generally enhance insulin sensitivity and regulate appetite, contributing to better metabolic health. In contrast, vWAT, is characterized by higher concentrations of pro-inflammatory cytokines like TNF-α and IL-6, which are linked to increased inflammation and IR[258]. Additionally, lipolysis rates are typically higher in vWAT, leading to a greater release of FA into the bloodstream, which can adversely affect liver metabolism and increase the risk of metabolic disorders[259]. Therefore, while scWAT is associated with fewer health risks, excess vWAT is strongly correlated with a higher incidence of metabolic syndrome, CVD, and other health complications[260,261].

2.2.3. NON-ADIPOCYTE CELLULAR FRACTION

WAT depots are known for their heterogeneous cellular composition, with a significant cellular diversity beyond mature white adipocytes. Although the adipocyte fraction constitutes approximately 80% of the AT volume, the SVF is actually the predominant cellular component in terms of cell number[236]. Additionally, WAT can be surrounded by lymphoid structures or even infiltrated by them[262,263].

ATMs have been identified as the most abundant **immune cells** within this tissue and have been associated with obesity for more than a decade[264]. In simple terms, macrophages can be broadly categorized into two distinct populations: proinflammatory M1 macrophages, which are activated via classical pathways, and the anti-inflammatory M2 macrophages, which are activated through alternative pathways[265] (for a more detailed explanation of the M1 and M2 macrophage classification, refer to page 80). However, it is important to note that AT is home to a diverse array of immune cells beyond just macrophages[266]. The role of the immune system function within AT is multifaceted, extending beyond the regulation of inflammation. For example, the tissue remodeling during prolonged exposure to cold or adrenergic stimulation recruits specific innate immune cells, including M2 macrophages and eosinophils[267,268]. Moreover,

WAT also functions as a key immune reservoir, playing a significant role in the whole-body response against infections and hosting parasitic and viral pathogens[252].

Additionally, AT needs to be vascularized and its architecture also includes **endothelial cells** and **smooth muscle cells**. This vascular cells are located near the stem cell niche, providing endocrine signals that modulate adipocyte development[269]. Moreover, WAT also contains **preadipocytes**, which, together with **ASCs,** play a crucial role in renewing mature adipocytes during normal tissue turnover or in response to various stimuli. In humans, it is estimated that about 10% of the mature adipocyte population experiences turnover annually[270], and this process depends on the presence of preadipocytes within a specialized niche. In rodents, adipocyte turnover occurs much more rapidly, with up to 5% of adipocytes being replaced daily[271]. Furthermore, preadipocytes play a significant role as the primary source of specific secreted factors from AT, such as TNF-α[272].

Overall, AT is characterized by significant heterogeneity, not only at the cellular level but also across different tissue types. The functional heterogeneity across different types of AT further exemplifies its critical role in maintaining metabolic homeostasis and responding to pathological conditions. The cellular elements of AT are schematically detailed in **Figure 14**.

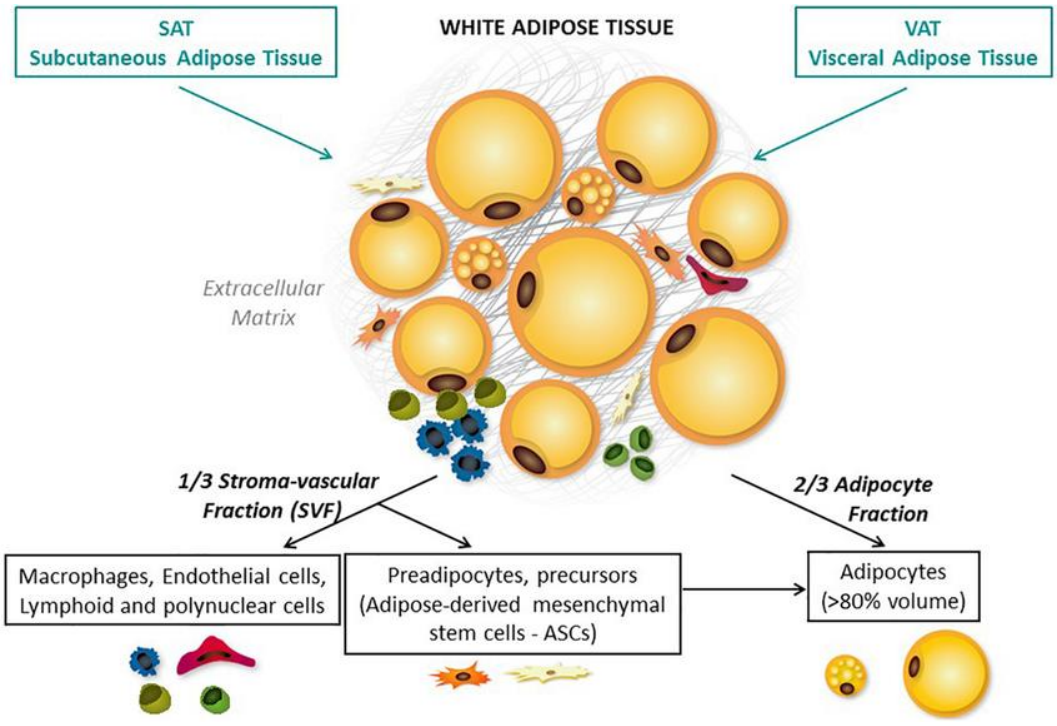

Figure 14. Schematic overview of the cellular components of the AT[143].

2.3. BROWN ADIPOSE TISSUE

As previously discussed, the body contains not only WAT but also BAT, which is uniquely specialized in thermogenesis—a process that generates heat to maintain body temperature and stores thermal energy[204]. This remarkable thermogenic property makes it a highly attractive target or therapies for obesity and cardiometabolic complications. However, the presence of BAT in humans was a subject of debate for many years. Initially identified in marmots[273], BAT was later recognized in newborn infants[274], and subsequently in human autopsies[275]. In 2003, the existence of metabolically active BAT in adults was confirmed [275,276]. A series of influential studies published in *The New England Journal of Medicine* in 2009 significantly advanced BAT research, both in humans and preclinical models[277–279]. The recognition of active BAT in adults has subsequently catalyzed a significant expansion in our understanding of the potential physiological and pathophysiological functions of this tissue.

Throughout this section, we will discuss in depth the functions of BAT, including its distribution in the body and cellular composition.

2.3.1. FUNCTIONS

BAT has a unique ability to generate heat via uncoupled oxidative phosphorylation. This **thermogenic potential**, especially prevalent in small mammals, allows them to survive in cold temperatures without the need for shivering[280]. As discussed, BAT is responsible for dissipating energy through heat production in response to cold exposure via non-shivering thermogenesis by uncoupling the mitochondrial electron transport chain, mediated by the specific expression of UCP1[216].

The classical model of BAT thermogenesis in response to cold exposure or food intake centers on the UCP1 and begins with a sympathetic nervous system (SNS) activation and subsequent norepinephrine (NA) release. This neurotransmitter binds to the β3-adrenergic receptor (β3-AR), which initiates a cascade that involves cAMP-PKA signaling, promoting glucose uptake and lipolysis of intracellular TGs[277]. Additionally, stimulation of thyroxine receptor, which is a nuclear receptor that binds to thyroid hormones, amplifies the sympathetic activity, further facilitating the utilization of FA and glucose in the electron transport chain. These substrates contribute to the activation of UCP1, which uncouples the mitochondrial respiratory chain from ATP synthesis, creating an alternative pathway for proton glow that generates heat[281] (**Figure 15**).

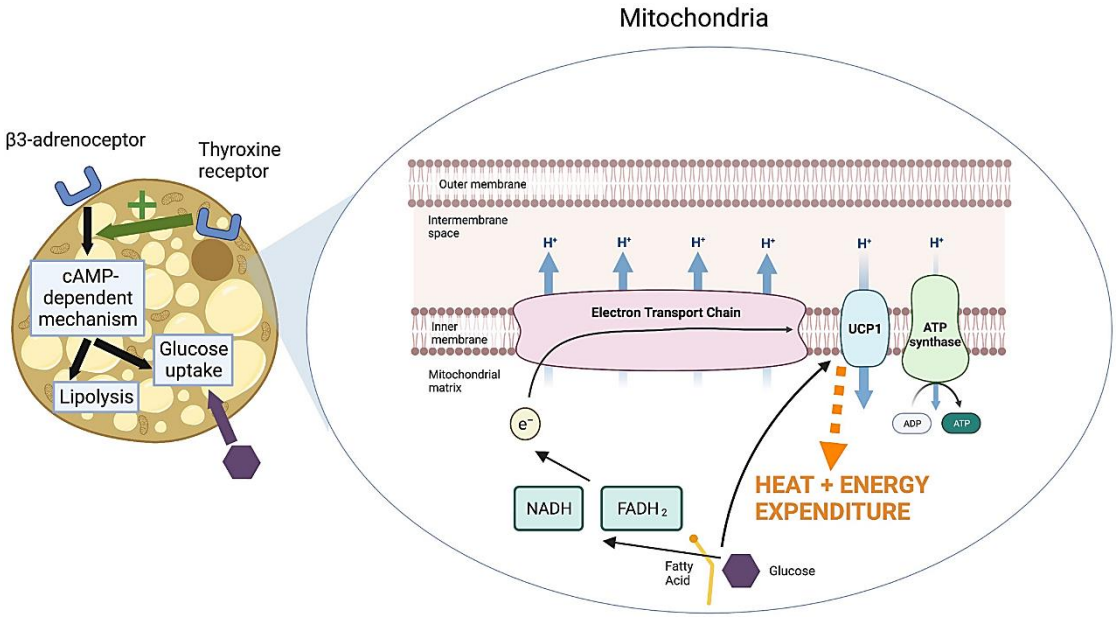

Figure 15. Thermogenic mechanisms within the mitochondria of BAT[282].

There are numerous molecules and elements involved in BAT activation. For example, it is well-established that BAT sympathetic activity[283] and heat production[284–286] are activated by leptin, an adipocyte-derived hormone which plays a key role in the regulation of energy balance and is linked to food intake[287]. Accordingly, chronic leptin administration can stimulate thermogenesis in BAT by enhancing both sympathetic innervation and activation, particularly in leptin-deficient *ob/ob* mice[288]. Conversely, adiponectin, another adipocyte-derived hormone, inhibits UCP1 expression and consequently reduces BAT thermogenesis in mice[289]. Furthermore, exposure to cold strongly elevates the levels of branches-chain amino acids (BCAAs) within mitochondria. BCAAs, which include leucine, isoleucine, and valine, are essential amino acids crucial for energy production during exercise. When exposed to cold temperatures, BCAAs undergo oxidation, providing an important source of energy and contributing to the activation of UCP1 in BAT[290].

Moreover, key regulatory proteins, such as calsyntenin-3β found in the endoplasmic reticulum, further facilitate this process by inducing the secretion of calcium-binding protein B, which stimulates the growth of sympathetic nerve fibers in BAT, thereby increasing its thermogenic capacity[291]. Pharmacological interventions also play a significant role in enhancing BAT activity. For instance, mirabegron, a β3-AR agonist, has been shown to enhance glucose uptake in BAT, contributing to improved whole-body glucose homeostasis and increase energy expenditure in humans[292,293].

Current research has underscored the potential role of certain small molecules found in fruits and vegetables in promoting WAT browning, BAT activation, and combating obesity. Long-term intake of specific plant extracts, such as capsaicin[294] and ephedrine[295], can directly stimulate brown fat activity, leading to increased energy expenditure and achieving weight managment[295]. Altogether, these insights highlight the multifaceted mechanisms that regulate BAT thermogenesis, from hormonal and amino acid interactions to key proteins and pharmacological agents, offering potential therapeutic avenues for enhancing metabolic health.

Notably, while UCP1 has traditionally viewed as the primary mechanism for thermogenesis in BAT, recent research has expanded our understanding by introducing alternative models that challenge the UCP1-centric view. These models highlight UCP1-independent mechanisms, such as creatine-driven substrate cycling and futile calcium cycling in the ER, as additional pathways that contribute to thermogenic energy expenditure in BAT[296–298].

In addition to its role in heat production, BAT has also been found to function as an **endocrine organ**, secreting several endocrine mediators, called batokines, that provide systemic metabolic advantages. This has been clearly shown in experimental models where BAT transplantation led to beneficial metabolic outcomes[299].

In conclusion, the thermogenic and endocrine properties of BAT present promising opportunities for therapeutic interventions aimed at improving metabolic health. Understanding the regulatory mechanisms of BAT, including its response to hormonal signals, dietary components, and pharmacological agents, can lead to innovative strategies to combat obesity and related metabolic disorders.

2.3.2. DISTRIBUTION

In rodents, BAT is found abundantly in specific regions, including the interscapular, subscapular, axillary, perirenal and periaortic areas, referred to as classic depots[300].

In humans, BAT is present in the cervical, supraclavicular, paravertebral, mediastinal, and perirenal regions, and its recognition typically requires stimulation, such as cold exposure[279]. Although these are the main sites for brown adipocytes, BAT can also be present in other scattered locations and within WAT[301]. BAT is developed and differentiated prior to birth to ensure newborns can maintain their body heat in cold environments[302,303]. Previously, it was thought that BAT disappeared postnatally, but it is now recognized that this tissue can be activated and remains relevant even in adult humans[279,301,304] (**Figure 16**).

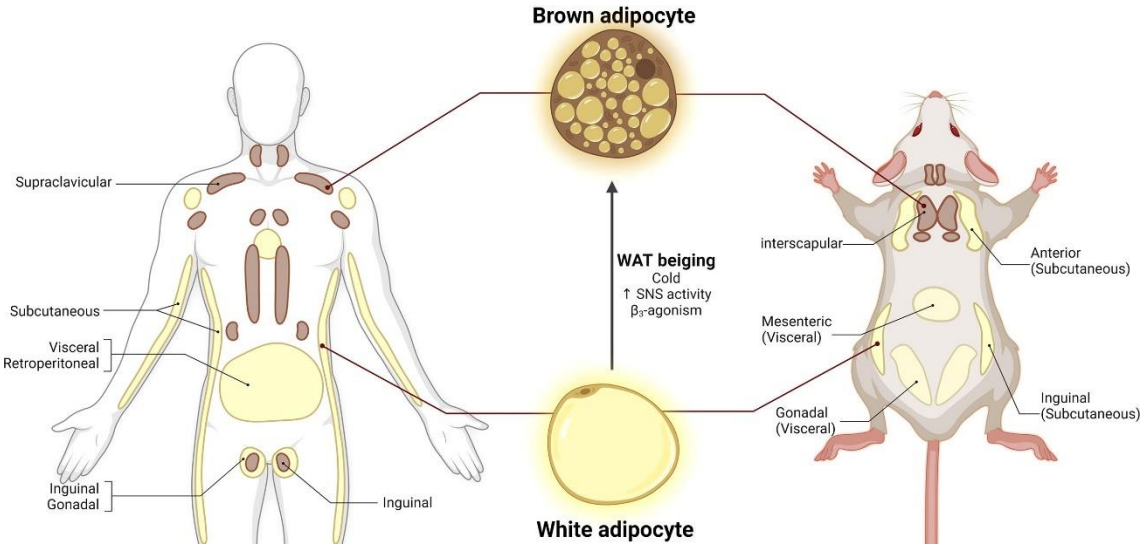

Figure 16. WAT and BAT distribution in humans and mice[305].

2.3.3. CELLULAR COMPOSITION

Adipocytes are the main cellular component of BAT. In rodents, adipocytes found in BAT are characteristically brown, while in humans, their origin remains under debate and may include contributions from "beige" adipocytes[218,306]. As previously detailed in section 2.1.1, **brown adipocytes** are distinguished by their high mitochondrial content, contributing to the brown color of BAT. These mitochondria contain UCP1, which plays a pivotal role in BAT thermogenesis[281]. In addition to brown adipocytes, **beige adipocytes** are usually found in WAT depots and sometimes alongside brown cells in BAT tissue[307] . Beige adipocytes can undertake thermogenesis due to the presence of UCP1 in their mitochondria[306]. However, unlike brown adipocytes, which maintain high UCP1 levels naturally, beige adipocytes only express UCP1 in response to stimuli like cold exposure or β3-AR agonists[281]. Beige cells can also achieve thermogenesis through UCP1-independent mechanisms, such as ATP-dependent calcium cycling[308] or creatine cycling[309], as mentioned earlier.

BAT is highly vascularized, facilitating the extensive delivery of oxygen and substrates to its cells, which is essential for its thermogenic function. Moreover, it is extensively innervated by the SNS, which is essential for regulating BAT function. Additionally, BAT contains a significant number of **preadipocytes** capable of differentiating into brown adipocytes as needed[310–313].

Although the concentration of **immune cells** in BAT is less than in WAT, the presence of both innate and adaptive immune cells has been documented within BAT, including macrophages, monocytes, DCs, T cells, B cells, and mast cells. These immune cells seem to play a significant role in modulating the thermogenic activity of BAT[314,315].

While significant progress has been made in understanding the role of immune cells during adaptive thermogenesis, research has predominantly focused on the browning of scWAT depots. Consequently, the impact of eosinophils and other immune cells on the classical physiological functions of BAT has been relatively overlooked, often leading to the erroneous attribution of WAT browning-associated immune cell functions to BAT resident populations[316]. To advance our knowledge, it is imperative to clarify the specific roles and compositions of immune cells within BAT.

2.4. ADIPOSE TISSUE AS AN ENERGY STORAGE ORGAN

The role of AT in energy storage has been a fundamental focus of scientific research for decades. In this section of the doctoral thesis, we will explore further the mechanisms by which white adipocytes take up and store nutrients, the regulatory pathways involved in lipid metabolism, and how these processes are influenced by various internal and external factors.

Living organisms require energy from their environments to survive. Specifically, the physiological process of storing excess energy obtained during periods of food abundance becomes a key factor that enhances survival during times of food scarcity. Multicellular organisms have developed specialized cells or organs for the storage of excess nutrients in the form of lipids due to their higher caloric value compared to other nutrients[317]. Similarly, sharks and *Drosophila* store excess lipids in their liver and fat body, respectively[318,319]. In other organisms, the AT functions as a specialized reservoir of energy, especially in certain fishes and higher vertebrates[320]. Distributed throughout the body, this tissue can expand to store excess energy in the form of lipids, setting it apart from other organs and tissues[240].

The importance of AT in overall metabolism has been increasingly recognized, serving as the body fuel reservoir for energy storage and controlling lipid mobilization[321]. AT stores TGs in lipid droplets and releases FAs through the processes of lipogenesis and lipolysis, respectively. At a systemic level, feeding stimulates the lipogenic pathway, leading to the storage of TGs within AT. Conversely, fasting induces the activation of the lipolytic pathway, facilitating the breakdown of TGs and the release of FFAs from AT[322].

Lipogenesis is the process that involves the *de novo* FAs synthesis from acetyl-CoA and the biosynthesis of TGs. Adipocytes uptake lipids in the form of FFAs released from circulating TGs by the action of lipoprotein lipase, an enzyme secreted by adipocytes[322], which is transported to the adjacent capillary lumen to facilitate the hydrolysis of FFAs from circulating lipoproteins containing TGs originated in the small intestine or in the liver[323,324]. Adipocytes also take up glucose, which provides acetyl-CoA as a substrate for the initiation of *de novo* FAs synthesis and induces the expression of acetyl-CoA carboxylase (ACC), the rate-limiting enzyme in lipogenesis. Additionally, glucose

stimulates the release of pancreatic insulin which promotes lipogenesis[206]. As a result, insulin stimulates glucose uptake within adipocytes, activates glycolytic and lipogenic enzymes, and induces the expression of the lipogenic gene SREBP1c, that controls the genes required for synthesizing cholesterol, FAs, TGs, and phospholipids[325].

In contrast, **lipolysis** is the catabolic pathway that breaks down stored TGs in adipocytes, releasing FFAs and glycerol[326]. The glycerol and FAs released from AT can be re-esterified within the adipocyte or transported through the bloodstream, infiltrating into other oxidative tissues, such as liver and muscle, contributing to lipid distribution and modulating the energy balance of the whole body[324]. Lipolysis is induced by fasting or when energy demand is high, such as exercise, and cold exposure, providing glycerol for hepatic gluconeogenesis in the liver and FFAs for oxidation in the muscle based on the energy requirements of peripheral organs[327].

During fasting, reduced levels of circulating insulin result in the suppression of lipogenesis, while catecholamines released by the SNS and the increased levels of circulating glucagon activate PKA and the subsequent lipolysis[328]. The increase in exercise intensity is linked to elevated levels of growth hormone, NA, adrenaline, and cortisol, with a concurrent decrease in insulin levels, contributing to an enhanced lipolytic response[329]. The lipolysis process involves lipases breaking down fats into individual FAs. The primary lipases involved in this process are adipocyte triglyceride lipase (ATGL), responsible for the conversion of TGs to diglycerides (DGs), and hormone-sensitive lipase (HSL), which then hydrolyzes DGs into monoglycerides (MGs)[330,331] (**Figure 17**).

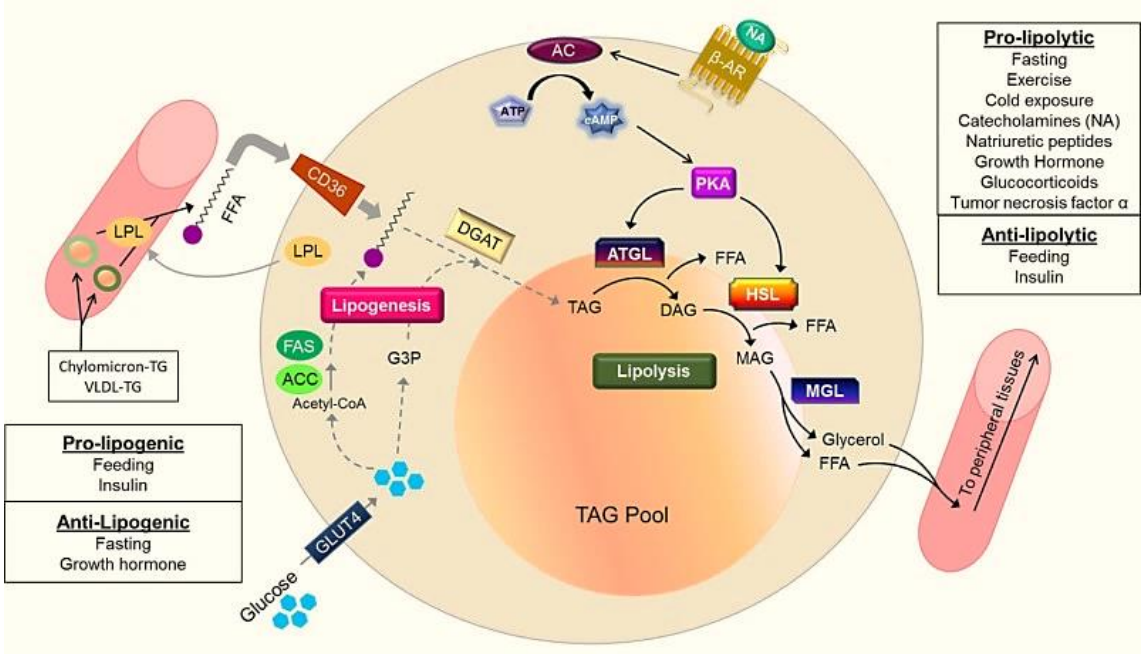

Figure 17. Lipid metabolism and mobilization controlled by AT[200].

An imbalance between lipolysis and lipogenesis can profoundly impact metabolic health. Excessive lipogenesis leads to TGs accumulation and obesity, while excessive lipolysis depletes fat reserves and raises FFAs, potentially leading to lipotoxicity and IR[332]. Thus, maintaining a balance between these processes is crucial for systemic metabolism. The ability of AT to adapt by storing and mobilizing energy efficiently is essential for survival and energy management[200].

2.5. ADIPOSE TISSUE AS AN ENDOCRINE ORGAN

As previously discussed, AT was traditionally considered a mere storage depot for excessive energy with limited significance. However, it is now recognized as an active endocrine organ with broader functions. In the past two decades, there has been a significant focus on understanding the substances derived from AT and their functions in the body[202,203,333]. This section will explore these substances, known as adipokines, and their impact on systemic metabolism and inflammation. These bioactive factors secreted from AT circulate through the bloodstream, relaying information to other metabolically organs[334,335]. Adipokines, which include cytokines, hormones, and peptides, play their biological roles in an autocrine, paracrine, or systemic manner and impact diverse physiological processes, including energy regulation, glucose metabolism, and immunity[336].

While this thesis primarily focuses on adipokines, particularly leptin, it is important to recognize that AT engages in inter-organ communication through the secretion of a diverse array of signaling molecules. These include, but are not limited to, signaling lipids, inflammatory mediators, and microRNAs (miRNAs) encapsulated in exosomes. This intricate network of signaling molecules underscores the complexity of AT function in maintaining metabolic homeostasis and coordinating systemic metabolic processes.

2.5.1. ADIPOKINES

The emergence of adipokines commenced with the discovery of leptin in 1994[203], succeeded by the cloning of adiponectin in 1995[337]. Subsequently, many other adipokines such as resistin, chemerin, apelin, visfatin, plasminogen activator inhibitor 1 (PAI1), TNFα, and IL-6 were identified[338]. Leptin and adiponectin are the primary adipokines released predominantly by adipocytes, playing a critical role for the regulation of energy homeostasis[339]. Furthermore, leptin is also produced or present in non-ATs, including the stomach, muscles, and intestines[340–343].

Although resistin was initially identified as adipocyte-specific hormone linking obesity and IR, accumulating evidence now indicates that it is also expressed in human mononuclear leukocytes, macrophages, and bone marrow cells[344]. Similar to resistin, chemerin was initially considered an adipocyte hormone involved in the regulation of adipocyte differentiation and lipolysis. However, it is also detected in other cell types,

such as endothelial cells[345,346]. Other adipokines, including apelin, visfatin, PAI1, TNFα, and IL6, are predominantly produced by immune cells residing in AT and endothelial cells[264,347–349]. Abundant evidence has demonstrated that disruptions in the synthesis, assembly, release, and signaling transmission of these adipokines are implicated in the development of obesity and its related complications[350].

AT is recognized as a crucial metabolic organ, essential in conjunction with the liver and skeletal muscle, for the proper maintenance of glucose homeostasis[351]. This interconnection emphasizes the importance of adipokines and other adipose-derived factors in systemic metabolic regulation.

In the upcoming section, we will focus on leptin as the central subject of this thesis, exploring its functions, regulatory mechanisms, and broader biological implications.

2.5.1.1. THE BIOLOGY OF LEPTIN

Leptin, a 16-kDa satiety hormone of 167 amino acids, is encoded by the *Lep* gene and plays a crucial role in regulating energy balance by suppressing hunger[352]. Beyond its role as a master regulator of energy balance, leptin also plays a crucial role in glucose homeostasis, neuroendocrine axes, memory, the autonomic nervous system, neural plasticity, and additional biological functions[353]. Leptin expression and circulating levels change in accordance with nutritional status, displaying a circadian pattern with higher values in the evening and early morning[354,355]. In concordance, leptin levels decrease during fasting or weight loss, and conversely, increase during feeding or in obese conditions[356].

Circulating leptin has the capability to cross the blood-brain barrier (BBB), and the leptin levels in the cerebral spinal fluid are also associated with BMI. Once released by AT, leptin send signals to the brain, providing information about the status of the body energy stores. In both rodents and humans, this leads to a decrease in food intake and a rise in energy expenditure to maintain the size of the body fat stores[352,357,358]. After leptin crossing the BBB, it binds to the hypothalamic leptin receptors[359], altering the function of various hypothalamic neurons and the expression of different neuropeptides, suppressing appetite-stimulating peptides (orexigenic) and stimulating appetite-suppressing peptides (anorexigenic). Among the orexigenic peptides regulated by leptin are neuropeptide Y (NPY), melanin concentrating hormone, agouti-related protein (AgRP), galanin, orexin, and galanin-like peptide (GALP). Likewise, leptin has an impact on the expression of anorexigenic peptides, including pro-opiomelanocortin (POMC), cocaine- and amphetamine-regulated transcript (CART), neurotensin, corticotropin-releasing hormone, and brain-derived neurotrophic factor[360–365].

Leptin exerts its effects by binding to its membrane receptor, which is expressed in multiple tissues. Among the different identified isoforms of leptin receptor (LepR)[366], only the long isoform (LepRb or Ob-Rb) encompasses all intracellular motifs required for the activation of intracellular signaling pathways. LepRb, predominantly expressed in the central nervous system (CNS), is crucial for leptin action. Therefore, this isoform is responsible for the major biological responses induced by leptin[367,368]. LepRb signals via an associated tyrosine kinase protein from the Janus kinase family (JAK) and the primary signaling pathway activated by leptin is the signal transducer and activator of transcription 3 (STAT3)[353]. Indeed, STAT3 phosphorylation subsequent to an acute leptin stimulus became a commonly used marker for identifying leptin-responsive cells[369], and also it is a widely method for evaluating leptin sensitivity[370,371].

So far, only a few metabolic and endocrine factors are known to be implicated in the regulation of leptin expression and release. Among them, the adrenergic system and cold exposure are involved in the reduction of leptin levels[372,373]. Specific hormones, such as growth hormone, androgens, or cortisol, are also associated with a reduction in leptin levels[374], while others, like insulin or estrogens, have the potential to increase it[375,376]. Furthermore, some proinflammatory cytokines can increase circulating leptin levels initially, followed by a long-term decrease[377] (**Figure 18**). However, no significant advances had been made in understanding how this hormone is produced in the AT.

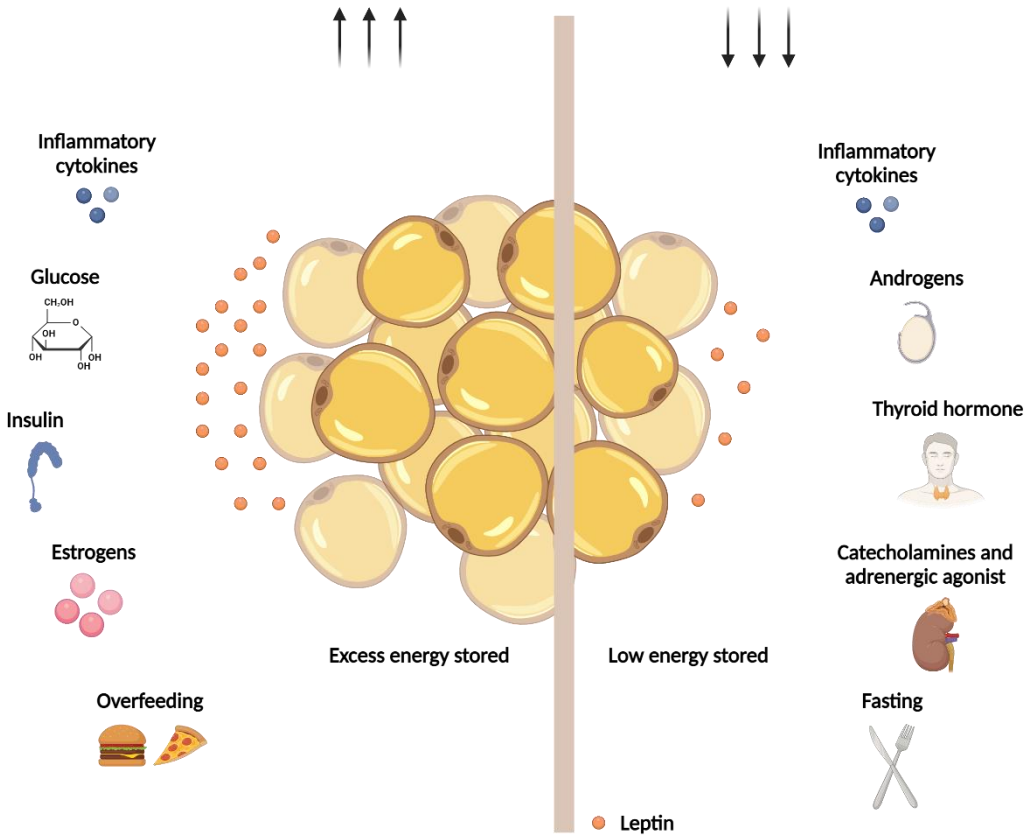

Figure 18. Factors implicated in circulating leptin levels[378].

2.5.1.2. LEPTIN ROLES IN PHYSIOLOGY AND PATHOLOGY

Initially recognized for its role in modulating food intake and energy balance, leptin has emerged as a multifaceted adipokine with a wide array of physiological functions. We will thoroughly explore the influence of leptin on bone remodeling[379], with a focus on both its direct and indirect effects on bone health. Nonetheless, it is essential to note that leptin also plays a pivotal role in numerous other biological processes[380].

Among its various functions, leptin significantly contributes to glucose metabolism by reducing blood glucose levels, particularly in instances of leptin or insulin deficiency[381]. In hematopoiesis, leptin promotes the expansion of HPCs[382]. The neuroprotective properties of leptin are well-documented, supporting brain function and offering protection against neurodegenerative diseases[383]. As a cytokine, leptin modulates both innate and adaptive immune responses, and is involved in autoimmune and inflammatory diseases[384]. In the context of reproductive physiology, leptin is involved in regulating key processes including menstruation, pregnancy, and lactation[385]. Moreover, leptin regulates the synthesis of thyroid hormones by modulating the hypothalamic-pituitary-thyroid axis[386]. Beyond these roles, leptin contributes to angiogenesis by stimulating endothelial cell proliferation[387], regulates blood pressure[388], elevates heart rate[389], and inhibits gastric emptying to promote satiety[390]. These diverse physiological roles underscore the broader significance of leptin beyond its initial function in energy homeostasis[380] (**Figure 19**).

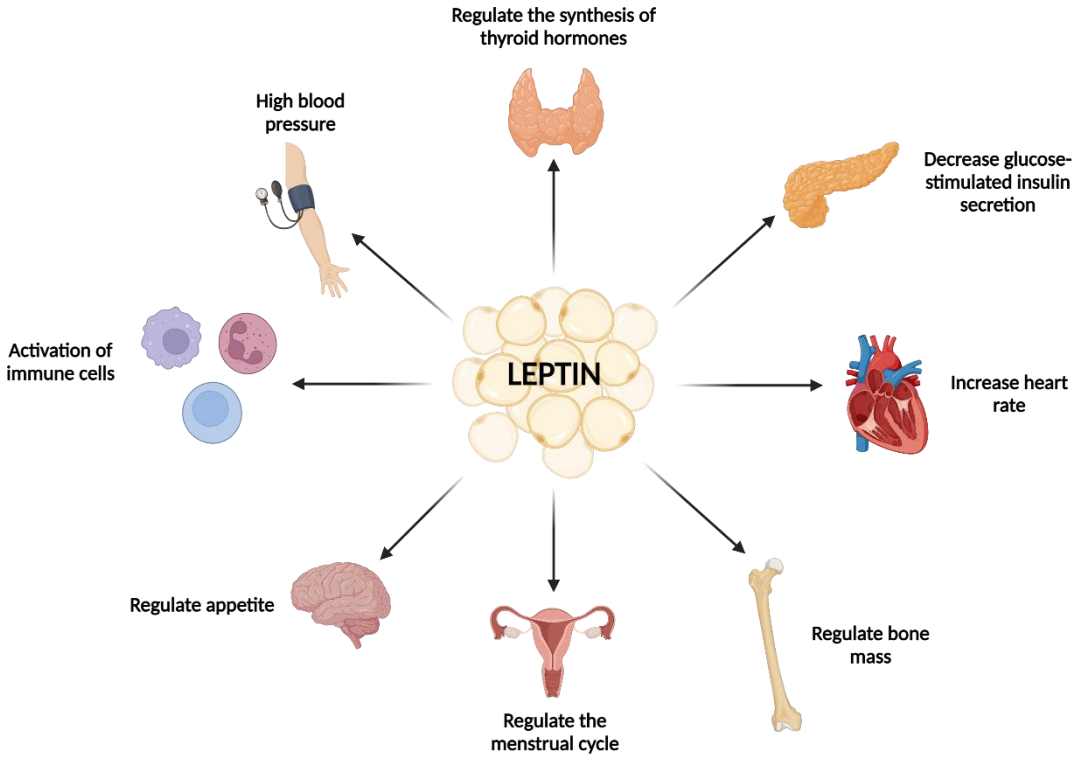

Figure 19. Illustrative overview of leptin major physiological functions[391].

2.5.1.3. LEPTIN AND REGULATION OF BONE METABOLISM

Although increasing data supports AT influence on bone mass, it remains difficult to define leptin impact on bone remodeling. The process of bone remodeling is a process that couples the breakdown of bone by osteoclasts (bone resorption) followed by its formation through osteoblasts (bone formation). The constant process of remodeling is necessary to respond the physical demands on bones and to regulate blood mineral homeostasis[386].

BM-MSCs are a group of heterogeneous cells capable of differentiating into multiple cell types, including osteoblasts, adipocytes, chondroblasts and myoblasts[393]. Given that adipocytes and osteoblasts both originate from the same precursors, the link between them has garnered attention, suggesting that AT play a role in bone homeostasis. Leptin is known to exhibit both positive and negative effects on bone mass depending on two signalling pathways[394]: one involves a direct stimulatory impact on bone growth when administered peripherally[395,396], and the other is an indirect approach trough a hypothalamic relay that inhibits bone formation through a hypothalamic pathway mediated downstream by the SNS[397,398] (**Figure 20**). Studies have demonstrated that through its effect on the SNS, leptin increases the expression of RANKL in osteoblast progenitor cells, thereby promoting bone resorption[399]. Consequently, leptin influences the bone remodeling process through the modulation of both osteoblasts and osteoclasts[400].

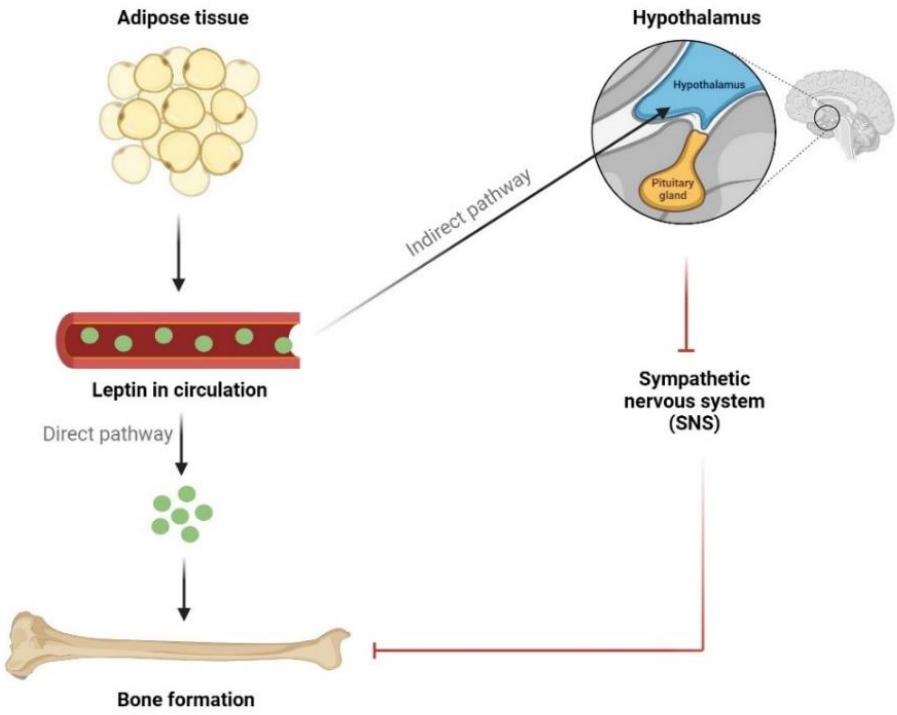

Figure 20. Signalling pathways involving leptin effects on bone mass. Image from Biorender.

In *vitro* studies predominantly suggest that leptin acts directly on osteoblasts and chondrocytes, which also express leptin receptors, to stimulate their proliferation and differentiation[401,402], while inhibiting adipogenic differentiation of BM-MSCs[403]. In contrast, there is also evidence suggesting leptin might be neutral or even lead to increased apoptosis in stromal cells[404]. Conversely, in *vivo* studies suggest that leptin suppresses bone formation acting through the CNS, independent of fat mass[398]. Indeed, obesity-related hyperleptinemia has been found to correlate with lower bone mass, even in the presence of leptin resistance[405,406].

2.5.2. OTHER ADIPOCYTE-DERIVED FACTORS

As discussed in section 2.5.1, AT produces several peptide hormones such as leptin and adiponectin, but also various signaling molecules and miRNAs packaged in exosomes[407]. These factors regulate several processes within AT[200] and can also influence systemic functions, influencing appetite, cognitive function, energy expenditure, insulin secretion and sensitivity, gluconeogenesis, cardiovascular health, and exercise capacity[408] (**Figure 21**).

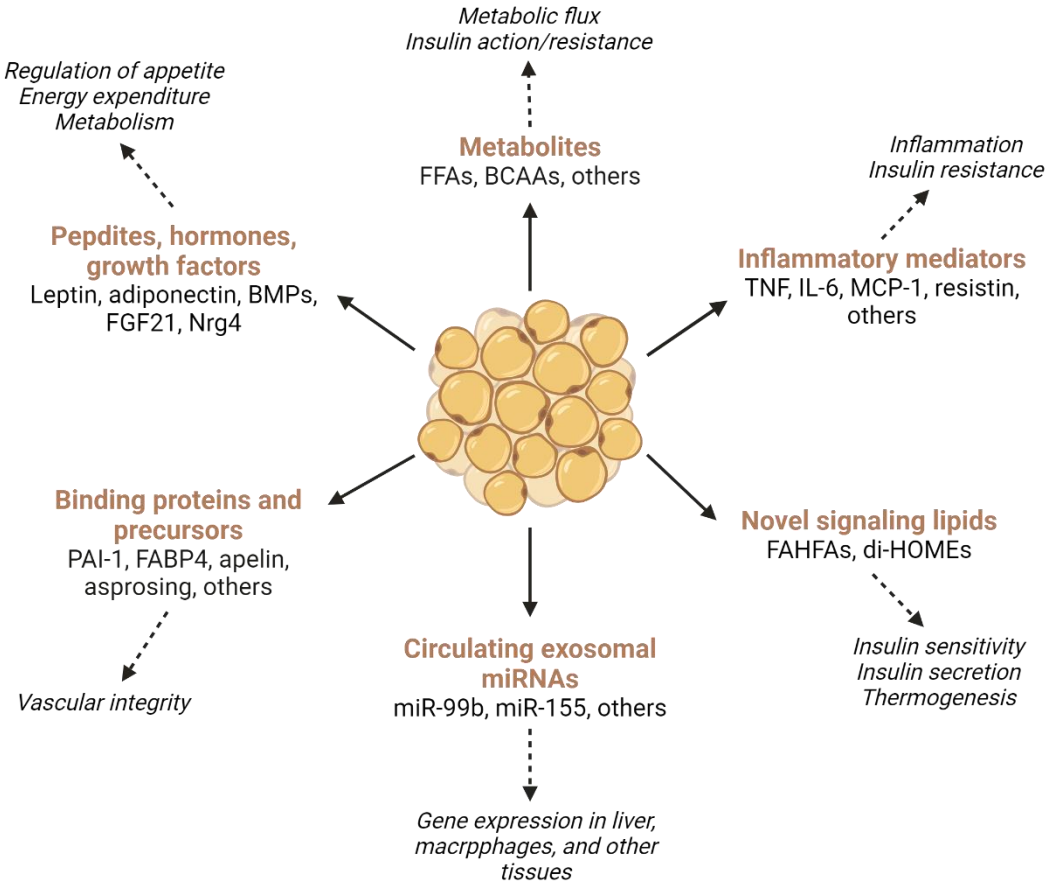

Figure 21. Illustration of adipose-derived secretory factors and their functions in inter-tissue communication. Image adapted[409].

Among peptide hormones, resistin is mainly produced by vWAT in mice and it is known to induce IR[410,411]. In humans, resistin is mostly secreted by macrophages, and its role in IR is less clearly defined[412]. Retinol-binding protein 4 (RBP4), also secreted by visceral adipocytes and the liver, can cause inflammation in AT, contributing to IR[413–415]. Other adipocyte-derived peptide hormones include apelin, with three active peptides that may influence cardiovascular function[338,348]; omentin, an insulin-sensitizing peptide from non-adipocyte cells in AT[416]; vaspin, a serine protease inhibitor that acts as an insulin sensitizer[416]; nesfatin-1, derived from nucleobinding-2, which enhances insulin secretion in response to glucose from β cells[417]; dipeptidyl peptidase-4 (DPP4), a peptidase degrading GLP-1[418]; and aprosin, a product of fibrillin-1 gene cleavage that promotes hepatic glucose release[419].

Moreover, AT also serves as a significant source of **various growth factors**, such as fibroblast growth factor 21 (FGF21), BMPs, TGF-β, and VEGFs[409]. BMP2 and BMP4 are known to facilitate white adipocyte differentiation[420], while BMP7 plays a crucial role in the development of brown adipocytes[421]. Additionally, AT is responsible for the synthesis of neurotrophic factors including nerve growth factor (NGF), neuregulin 4 (Nrg4), and semaphorins, which are essential for the proper innervation of BAT[409].

In pathological contexts such as obesity, it is well-known that AT undergoes remodeling, marked by the infiltration of macrophages that release numerous proinflammatory cytokines. Indeed, inflammation within AT is a hallmark of both T2DM and obesity. This inflammatory state is characterized by the secretion of various **inflammatory cytokines and proteins** from the alternative complement system, alongside the **infiltration of macrophages** into the AT[409]. Epidemiological studies link T2DM with elevated levels of inflammatory markers and mediators, such as C-reactive protein, IL-6, PAI-1, and TNF-α[422]. In the setting of obesity, elevated levels of monocyte chemoattractant protein-1 (MCP-1) within AT lead to increased infiltration of macrophages, which contribute to a proinflammatory environment by secreting various cytokines that exacerbate IR[423].

AT is a site of intense lipid flux due to its primary function in lipid metabolism and energy storage. However, AT also secretes **specialized signaling lipids** that facilitate communication with other tissues, such as branched fatty acid esters of hydroxyl fatty acids (FAHFAs) and dihydroxy fatty acids (diHOMEs), among others[409]. Studies indicate that FAHFAs are markedly elevated in mice overexpressing the glucose transporter Glut4 in their AT, and this increase is associated with improved metabolic outcomes[424]. Additionally, diHOMEs, which result from linoleic acid metabolism, is more abundant in BAT compared to WAT, and its levels in BAT and serum rise when humans and rodents are exposed to cold temperatures[425].

Furthermore, **exosomal miRNAs** have emerged as crucial signaling molecules in AT, contributing to the regulation of metabolic processes and inter-tissue communication[426]. miRNAs are small noncoding RNA sequences, about 22 nucleotides long, produced by all cell types, including adipocytes[427]. These miRNAs are integral to the differentiation and function of brown, beige, and white fat cells[428–430]. Moreover, the expression of miRNAs in AT varies between lean individuals and subjects with obesity with distinct correlations to BMI, glycemia, and IR[431].

Recent studies have highlighted AT as a major source of circulating miRNAs, particularly those in extracellular vesicles or exosomes[432]. These exosomal miRNAs act as novel adipocyte hormones, facilitating communication between AT and other tissues, such as the liver and muscles, to modulate miRNA translation and stability[432,433]. A notable example is miR-99b, which regulates the expression of FGF21 in the liver, thereby playing a role in metabolic homeostasis[432]. In the context of metabolic disorders, changes in the profiles of circulating miRNAs are significant. Individuals with obesity, T2DM, and metabolic syndrome exhibit altered levels of specific miRNAs, such as increased miR-122, miR-142-3p, miR-192, miR-222, and miR-378a, alongside decreased miR-138 and miR-221[434–436]. These alterations contribute to the pathogenesis of IR and other metabolic disturbances[432,437–440]. Adipocyte-derived exosomes also mediate inflammation in AT and the liver. Indeed, research has shown that mice injected with extracellular vesicles from the AT of obese mice develop elevated levels of inflammatory cytokines, including IL-6 and TNF-α, and display IR[441], and this inflammatory response is linked to miR-155[442].

Overall, the multifaceted secretory functions of AT emphasize its central role in metabolic health and disease. The interplay between these various secreted factors underscores the complexity of AT as an endocrine organ. Perturbations in these secretory pathways can lead to significant metabolic dysregulation, contributing to the pathophysiology of obesity, T2DM, and related metabolic disorders.

3. CIRCADIAN CLOCK

3.1. MAMMALIAN CIRCADIAN SYSTEM

In the intricate landscape of mammalian biology, there exists a phenomenon that governs our daily lives, influencing everything from the sleep-wake cycles to the metabolic functions. This phenomenon is known as the "circadian rhythm", a fundamental aspect of our physiology that regulates the timing of various biological processes within an approximate 24-hour cycle, which allow organisms to adapt to a fluctuating environment[443]. The term "circadian" originates from the Latin words "circa" (meaning "around") and "dies" (meaning "day"). Indeed, the circadian rhythm synchronizes our internal biological clock with the external environment, particularly the Earth rotation cycle. While humans are diurnal, meaning we are active during the day and rest at night, the circadian rhythm exerts its impact beyond mere sleep patterns, regulating a multitude of biological processes, including neuronal, endocrine, metabolic, and behavioral function[444]. This circadian rhythm is produced by endogenous clocks that oscillate even in the absence of external stimuli[445].

The mammalian circadian system comprises two primary components: the central clock situated in the suprachiasmatic nucleus (SCN) of the hypothalamus, which acts as a master clock and receive direct input from the retina, and peripheral clocks present in nearly every major tissue within the body[446,447]. To be beneficial for an organism, clocks must synchronize with each other and with the external environment. This synchronization is caused by external factors such as light signals, feeding cues and exercise, influencing the central circadian clock, and subsequently synchronizing the peripheral clocks[448]. These peripheral clocks govern tissue-specific activities, as evidenced by experiments conducted in controlled environments and the analysis of genetically modified mice lacking functional clocks in particular tissues or cell types. For instance, the hepatic clock regulates fasting glycemic control and glucose clearance[449], the pancreatic clock manages insulin release and its response to glucose[450], the adipose clock regulates the storage and release of lipids[451,452], and the skeletal muscle clock regulates glucose absorption and metabolism[453].

3.2. MOLECULAR BASIS OF CIRCADIAN RHYTHM

At the core of the molecular circadian clock in animals lies a mechanism known as the transcription-translation feedback loop. This intricate process involves a series of molecular interactions that regulate the expression of key genes responsible for maintaining the circadian rhythm[454].

The central structure of this model is a primary loop between two transcription factors, BMAL1[455] and the circadian locomotor output cycles kaput (CLOCK), which form a

heterodimeric partnership[456]. In particular, the transcription of *BMAL1* and *CLOCK* genes, as well as their related gene *NPAS2* (encoding the neuronal PAS domain-containing protein 2), mainly expressed in the forebrain, results in the formation of the BMAL1:CLOCK heterodimer in the cytoplasm, which undergoes translocation to the nucleus, where it binds to canonical Enhancer Boxes (E-Boxes) sequences containing either the canonical CACGTG sequence or non-canonical E-Boxed of genes regulated by the circadian clock. Across multiple target genes, BMAL1 and CLOCK additionally stimulate the expression of negative arm molecular clock elements, such as period (PER1, PER2, PER3) and cryptochrome (CRY1, CRY2). After combining in the cytoplasm, PER and CRY translocate into the nucleus, where they suppress the transcriptional activity of the BMAL1:CLOCK complex following translation and nuclear accumulation[457].

At the posttranscriptional level, PER and CRY protein stability is controlled by Skp1-Cullin-F-box protein (SCF) E3 ubiquitin ligase complexes, which encompass β-Transducin Repeat Containing E3 Ubiquitin Protein Ligase (β-TrCP) and F-Box and Leucine Rich Repeat Protein 3 (FBXL3). PER and CRY proteins are phosphorylated by casein kinase 1ε/δ (CK1ε/δ) and AMPK enzymes, respectively. This phosphorylation event promotes their polyubiquitination via β-TrCP and FBXL3, tagging them for degradation by the 26 S proteasome complex[458,459]. Reduction in PER and CRY protein levels removes the suppression of BMAL1:CLOCK activity, enabling the onset of a renewed cycle of oscillation[460] (**Figure 22**).

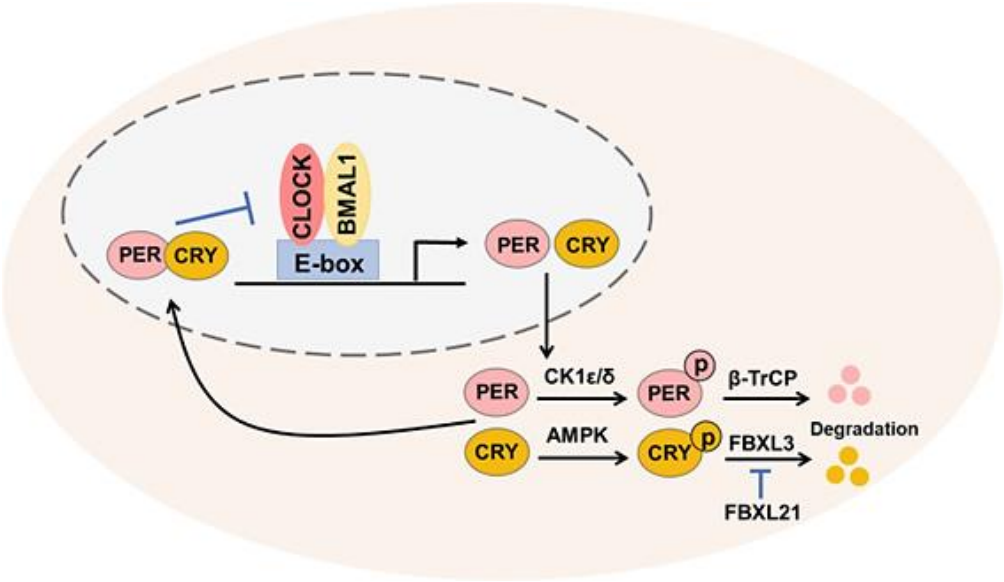

Figure 22. Structure of the molecular circadian clock[461].

Besides the central loop, additional pivotal regulators of the circadian clock, including nuclear receptors REV-ERBα and REV-ERBβ (referred to collectively as REV-ERBs), and the retinoic acid orphan receptor (RORα, RORβ, and RORγ), establish another feedback mechanism. Specifically, REV-ERBs function as inhibitors of BMAL1 transcription, whereas RORs enhance BMAL1 expression by binding to ROR Element (RORE) sites within the *BMAL1* gene promoter[462,463] (**Figure 23**).

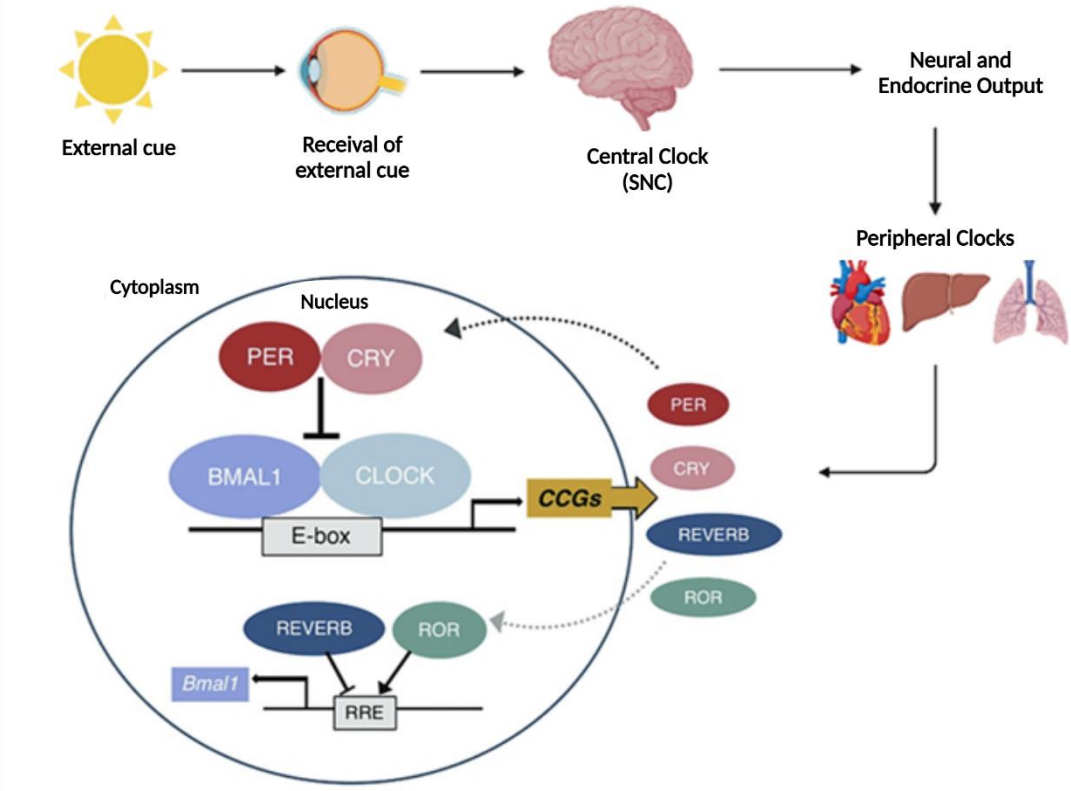

Figure 23. The mammalian molecular clock. Image adapted[464].

Additionally, the biological clock relies not only on transcriptional processes, but also on other mechanisms such as membrane depolarization, intracellular calcium flux, or the activation of cAMP signaling, which appear to play crucial roles in regulating the mammalian transcriptional clock[465].

However, it is not possible to oversimplify the processes underlying the molecular clock. Clock genes integrate a multitude of signals to create a unified output over the 24-hour cycle, preparing organisms for the different tasks associated with periods of light and darkness[466]. Interestingly, through an analysis of the transcriptome profile across major tissues and brain regions in primates, it was established that baboons manifest daily expression rhythms in more than 80% of protein-coding genes[467].

3.3. CIRCADIAN RHYTHMICITY WITHIN METABOLIC TISSUES

For many years, the SCN was considered the unique orchestrator of circadian rhythms. However, it is now evident that peripheral tissues also host their own internal clocks, which play a crucial role in regulating circadian physiology[468]. In experiments conducted in rodents, it has been observed that most tissues exhibit circadian rhythmicity that tends to diminish gradually in the absence of the SCN[469]. Interestingly, the rhythmicity in gene expression within tissues is typically unique, resulting in specific patterns of oscillations that vary over the circadian cycle. Furthermore, the brain also shows tissue-specific oscillations in gene expression, which can occur independently of SCN rhythmicity. This implies that different regions of the brain may have their own internal clocks, contributing to the complexity of circadian regulation within the CNS[470,471]. While some genes display tissue-specific rhythmicity, others, like *Per2*, demonstrate synchronicity across diverse tissues[472]. Moreover, recent discoveries have unveiled unexpected molecular players that link the circadian clock to specific metabolic tissues, including the liver, AT, pancreas, among others. These discoveries shed light on novel mechanisms by which circadian physiology may be intricately regulated in tissue-specific manners[473].

In the case of the **liver,** the peripheral clock plays a pivotal role in preserving liver homeostasis, including the regulation of energy metabolism, and controlling the expression of enzymes crucial for absorbing and metabolizing xenobiotics[474]. The liver expresses the most circadian genes[473], and in the last twenty years, research have focused on understanding the molecular pathways linking circadian clock genes with the regulation of liver functions. The rhythmicity of liver functions depends partially on the rhythmic patterns of food intake, which persist even in conditions of constant darkness. Intriguingly, even when the central clock is functional, more than 80% of genes in the liver exhibit rhythmic activity in response to food intake[475]. Disruption of the circadian clock accelerates the progression of liver diseases like fatty liver disease, cirrhosis, hepatitis, and liver cancer, and conversely, these disorders also disturb the function of the clock[474].

Apart from the hepatic clock, other metabolic tissues like **AT** also display rhythmic gene expression. Adipocytes have their own molecular clocks regulated by factors like C/EBPβ and the circadian protein REV-ERBα. These factors influence adipocyte proliferation by modulating the expression of genes involved in adipogenesis[476]. AT plays a vital role in metabolic homeostasis as it releases leptin and adiponectin in a circadian manner. Adiponectin levels decrease at night[477], impacting metabolism and body weight regulation, especially in conditions like obesity and T2DM[478]. The oscillation of adiponectin influences target tissues like muscle, affecting mitochondrial quantity and exercise capacity[479]. Recent studies show that adiponectin signaling, mediated by proteins like AMPK and sirtuin 1 (SIRT1), modulates muscle insulin sensitivity, highlighting its importance in metabolic health[480].

Leptin secretion from adipocytes also exhibits rhythmic oscillations in its release throughout the day, potentially influencing metabolic physiology. In humans, these fluctuations follow a pattern where plasma leptin levels peak during late night and early morning hours, inversely to adiponectin[468]. Limiting food intake to the resting phase reverses leptin circadian rhythm, while fasting completely disrupts the daily rhythm of leptin and reduces plasma leptin levels below baseline[481]. Thus, external cues related to food intake have been thought to be the primary factor controlling the daily fluctuations in leptin signaling. Nevertheless, recent research has shown that circadian disturbances can disrupt the daily oscillations of plasma leptin levels in both humans and animal models, even in the absence of changes in external food cues, potentially contributing to metabolic imbalances and obesity[482–484]. Furthermore, research shows that in AT, the BMAL1/CLOCK complex regulates leptin expression by controlling C/EBPα activity, driving diurnal oscillations of serum leptin. However, disrupting core clock components, like through experiencing jet lag, leads to leptin dysregulation. Indeed, chronic circadian disruption may induce leptin resistance in mice, potentially contributing to the global obesity pandemic[485].

The **pancreas** also hosts its own internal clock, which is crucial for insulin production and regulating blood glucose[450]. Specifically, elimination of *Clock* or *Bmal1* genes in pancreatic cells lowers glucose tolerance, disrupts insulin secretion, and alters islet cells size and proliferation. Interestingly, IR in mice with disrupted circadian rhythms can be fixed by restoring pancreatic cell function, even if obesity remains[486].

The **kidney**, essential for managing body fluids and minerals, operates under a circadian rhythm influenced by light and, to some degree, food intake, which helps it adapt swiftly to changes. However, the physiological consequences of disrupting this natural rhythm on kidney remain less understood[487].

In summary, these findings have unveiled a wide variety of molecular mechanisms between the circadian clock and specific metabolic tissues, revealing complex, tissue-specific regulatory processes.

4. OBESITY

4.1. EPIDEMIOLOGY OF OBESITY

Obesity is nowadays considered the pandemia of the 21st century and its rapidly increasing prevalence, coupled with related complications, constitutes one of the most serious healthcare challenges in our society[488].

The world health organization (WHO) defines overweight and obesity as a significant global public health challenge characterized by the abnormal or excessive fat accumulation that presents a risk to health. From 1975 to 2016 obesity substantially increased from 4% to just over 18% among children and adolescents aged from 5 to 19 years old[489].

BMI is the standard measure used for classifying overweight and obesity in adults and it is calculated by dividing an individual weight in kilograms by the square of their height in meters (kg/m^2). For adults, a BMI greater or equal to 25 is considered overweight, and greater or equal to 30 is considered obese[489]. Predictions indicate that by 2035, the global prevalence of overweight and obesity could impact more than 4 billion individuals, a significant increase from the over 2.6 billion recorded in 2020[490] (**Table 2**).

Table 2. Numbers of people and percentage of the population with overweight or obesity[488].

	2020	2025	2030	2035
Number with overweight or obesity (BMI≥25kg/m²) (millions)	2,603	3,041	3,507	4,005
Number with obesity (BMI ≥30kg/m²) (millions)	988	1,249	1,556	1,914
Proportion of the population with overweight or obesity (BMI ≥25kg/m²)	38%	42%	46%	51%
Proportion of the population with obesity (BMI ≥30kg/m²)	14%	17%	20%	24%

A diverse distribution of healthy weight and overweight is observed across all social classes, but obesity is more commonly found in the lower (middle) social class in contrast to the (upper) middle social class[491]. In the majority of populations, the prevalence of obesity in adults shows a tendency to be higher in women than in men; however, the magnitude of the difference between the sexes varies significantly from one country to another[492]. The disparities in overweight and obesity between genders are accentuated among women in developing countries, particularly in the Middle East and North Africa. Yet, in developed countries, there is a higher prevalence of overweight in men compared to women[493]. This intricate interaction between socioeconomic status, gender, and geographic location in shaping the dynamics of obesity and overweight, suggests the need for targeted approaches in addressing these global health challenges.

4.2. PATHOPHYSIOLOGY OF OBESITY

The pathophysiology of obesity involves a complex interplay of genetic, environmental, and behavioral factors. Obesity is a medical condition characterized by the excessive accumulation of AT, resulting from an imbalance between energy intake and energy expenditure. Factors such as genetic predisposition, unhealthy dietary patterns, sedentary lifestyle, and metabolic influences contribute to the development of obesity[494]. This condition arises when caloric consumption consistently exceeds the energy requirements of the body, leading to the storage of surplus energy as fat, predominantly in AT[495]. The increased adiposity observed in obesity is associated with various metabolic, inflammatory, immune, and mechanical alterations that contribute to tissue injury and the development of comorbidities associated with obesity[496] (**Figure 24**).

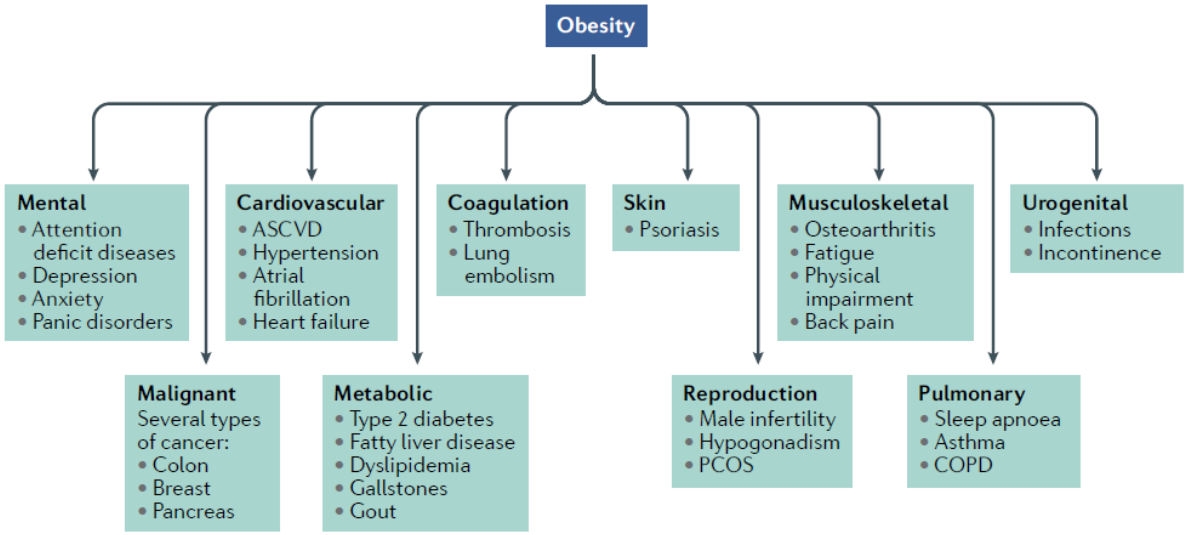

Figure 24. Obesity-associated metabolic disturbances[497].

In 2019, around five million premature deaths were attributed to an elevated BMI[490]. The primary cause of death associated with obesity was CVD, followed by chronic kidney disease, T2DM, and various types of cancer, which are the most common complications arising from obesity[498]. Furthermore, obesity affects mental health, quality of life, and both physical and sexual capacities[499]. Due to recent global circumstances, including the COVID-19 pandemic and an increase in food insecurity, global obesity rates are expected to continue to increase[500].

4.3. OBESITY, INSULIN RESISTANCE AND TYPE 2 DIABETES

Diabetes mellitus is a chronic, metabolic disease characterized by elevated levels of blood glucose, resulting in long-term damage to the heart, vasculature, eyes, kidneys, and nerves. The majority of diabetes cases, exceeding 90%, are classified as T2DM. This condition is characterized by IR, impaired insulin secretion from pancreatic islet β-cells,

and an inadequate compensatory insulin secretory response[501,502]. As the disease progresses, the ability of β-cells to secrete sufficient insulin diminishes, leading to a failure in maintaining glucose homeostasis and contributing to the development of hyperglycemia[503].

The correlation between obesity and T2DM has been established for many years. In fact, obesity is the most crucial factor for the development of T2DM, and this is further highlighted by the predictive factors of obesity, body fat distribution, and weight gain throughout adulthood in the context of diabetes[504,505]. The primary basis for this association is the role of obesity to induce IR, which is a pathological condition in which the cells of the body, particularly those in the liver, muscle, and AT, become less responsive to the action of insulin. This condition disrupts glucose uptake, triggering the pancreas to produce excess insulin, which leads to hyperinsulinemia[506]. Such dysfunction can contribute to a range of metabolic disturbances, including hyperglycemia, hypertension, dyslipidemia, elevated inflammatory markers, among others, all of which can progress to T2DM [507,508].

Although the association between obesity and T2DM is well-documented epidemiologically, the precise mechanism connecting these conditions remain unclear. One proposed explanation is the AT expandability hypothesis, which suggests that the crucial factor is not simply the presence of obesity, but rather the inability of AT to expand properly, connecting positive energy balance and T2DM[509,510]. AT has a finite capacity to accommodate excess fat, and when this capacity is surpassed, visceral fat and surplus lipids are stored in non-ATs, such as the liver and muscle, leading to the accumulation of harmful lipid intermediates like diacylglycerols (DAGs) and ceramides. These intermediates disrupt insulin signaling, impairing glucose uptake and contributing to elevated blood sugar levels[511]. Additionally, obesity triggers chronic low-grade inflammation, especially in visceral fat, where pro-inflammatory cytokines like TNF-α and IL-6 are released. These cytokines exacerbate systemic inflammation and further interfere with insulin action, worsening IR and increasing the risk of T2DM[512].

Developed and developing countries are both experiencing a significant increase in the prevalence of T2DM linked to obesity[513]. Consequently, obesity-induced diabetes is emerging as a global health-care problem, with the potential to escalate to pandemic levels by 2030. The projected incidence is expected to more than double of cases over just thirty years, increasing from 171 million in 2000 to 366 million in 2030[514].

4.4. OBESITY AND PHENOMENON OF LEPTIN RESISTANCE

As explained in Section 2.5.1, leptin, a hormone secreted by adipocytes, plays a crucial role in inducing satiety, reducing hunger, and promoting energy expenditure. Due to these functions, leptin was initially hailed as a potential breakthrough in the treatment of obesity. The early expectation was that administering leptin to individuals with obesity

could effectively reduce food intake and facilitate weight loss[515]. Despite this, the use of leptin therapies in the clinic has proven ineffective in managing obesity, predominantly due to the phenomenon of **leptin resistance**[516]. Contrary to initial beliefs, obesity is not characterized by leptin deficiency but rather by elevated leptin levels accompanied by both leptin resistance and impaired leptin signaling within the brain[517]. The concept of leptin "resistance" describes the incapacity of leptin, whether endogenous or pharmacologically administered, to decrease food intake and induce weight loss[518].

Leptin resistance is a multifaceted condition induced by multiple factors, including genetic mutations, autoregulation of leptin, and restricted tissue accessibility, among others[519]. Until recently, one of the primary mechanisms involves the disruption of leptin transport across the BBB. Excessively high leptin levels in the plasma can saturate leptin receptors, reducing the efficiency of leptin transport across the BBB, which leads to central leptin resistance[520,521]. Additionally, certain mutations in the *ob* gene can shorten the intracellular signaling domain of LepRb, impairing its ability to mediate leptin signaling. In such cases, the binding of leptin to LepRb fails to achieve its function, resulting in severe leptin resistance[522]. Another critical aspect involves impaired cellular signaling; neurons expressing LepR might not be sufficient sensitive to circulating leptin levels, which diminishes the efficacy of leptin binding. Furthermore, cells expressing LepR may have impaired signaling capabilities. Several factors and mechanisms underlying the development of leptin resistance are associated with disruptions in leptin cellular signaling[522].

Leptin resistance extends beyond the CNS to peripheral tissues, including skeletal muscle, AT, and the liver[523]. This peripheral leptin resistance contributes significantly to the overall pathophysiology of obesity. In individuals with obesity, the decreased sensitivity to leptin impairs the normal metabolic processes involved in lipid and glucose metabolism in AT, muscle and liver, as well as the gastrointestinal nutrient absorption, ultimately exacerbating the severity of obesity[524].

Restoring leptin sensitivity offers promising potential as a treatment for obesity. By addressing the root causes of leptin resistance—such as impaired receptor signaling, ER stress, and inflammation in the hypothalamus—therapies could help reestablish the critical role of leptin in regulating energy balance. However, leptin resistance is a complex condition, suggesting that a comprehensive approach may be necessary. For instance, studies by Scherer and colleagues have demonstrated that reducing leptin levels can markedly improve leptin sensitivity, thereby facilitating significant weight loss[516]. This suggests that partial leptin reduction could be an effective strategy for managing obesity and its related IR, underscoring the importance of combining targeted therapies with lifestyle changes to achieve lasting metabolic health improvements[525].

4.5. OBESITY AND CIRCADIAN RHYTHMS

Disruption of the circadian clock has been linked to various pathologies, and its connection to obesity is a key focus of current research[526,527]. Obesity is typically attributed to factors such as overeating, poor dietary habits, low physical activity, and chronic IR[528]. However, numerous studies indicate that circadian disruption -whether due to genetic of environmental influences such as nocturnal light exposure, sleep disorders, social jet lag, and late-night eating- significantly impacts lipid metabolism and accelerates the onset of obesity[529–532] (**Figure 25**).

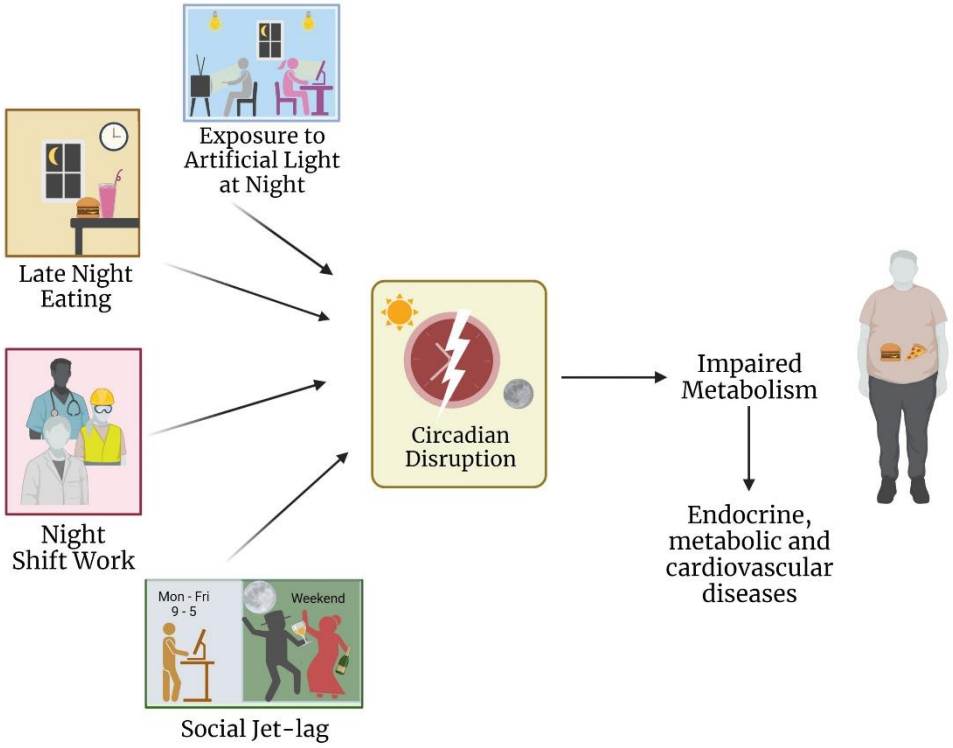

Figure 25. Role of circadian disruption in obesity development[533].

For instance, mice with mutations in the *Clock* gene or KO of the *Bmal1* gene show glucose intolerance, reduced insulin secretion, increased susceptibility to HFD feeding, hyperphagia, and subsequent weight gain[486,534,535]. Moreover, glucose metabolism and systemic glucose homeostasis are disrupted in models with tissue-specific *Bmal1* deficiency[449,536–538].

In humans, there is a notable alteration in the expression of circadian clock genes such as *Bmal1*, *Cry1*, *Cry2*, and *Per2* in individuals with obesity, with increased expression during the light phase and decreased expression during the dark phase[539]. This suggests that circadian clock gene expression and their downstream pathways are influenced by lipid metabolic disorders.

Further evidence of the link between the circadian clock and lipid metabolism is provided by environmental disruptions that lead to or exacerbate obesity. For instance, exposure to artificial light at night disrupts circadian rhythms and is associated with lipid metabolism disorders[540]. Regularly eating midnight snacks correlates with higher BMIs and increased obesity rates[531]. Additionally, getting less than 6-7 hours of sleep per night is linked to decreased leptin levels, increased IR, impaired glucose tolerance, and overeating[541]. Therefore, existing research suggests that both genetic and environmental disruptions to the circadian clock adversely affect lipid metabolism, raising the risk of obesity.

4.6. OBESITY-INDUCED CHANGES IN ADIPOSE TISSUE

The onset of obesity leads to a complex reorganization of AT, which expands to manage the excess caloric intake, significantly modifying its structure and cellular composition. This obesity-associated remodeling is commonly acknowledged to result in a systemic pro-inflammatory state, caused by the imbalanced secretion of adipocyte-derived adipokines[542].

In this section, we will explore the complex changes that obesity induces within the AT microenvironment. This encompasses AT expansion, the infiltration of different immune cells, the deterioration of vascular integrity and functionality, the emergence of AT fibrosis, and other critical transformations that collectively impact metabolic health.

4.6.1. ADIPOSE TISSUE EXPANSION

In obesity, there are two mechanisms by which adipose depots expand in response to an excessive caloric intake. Firstly, existing adipocytes increment the size, leading to a more hypertrophic tissue. Secondly, the differentiation of pre-adipocytes leads to the emergence of new adipocytes and a more hyperplastic AT[543].

It has been traditionally accepted that hyperplasia allows a "healthy" expansion of the AT, as it creates functional adipocytes from progenitor cells (adipogenesis), supporting an anti-inflammatory state and the formation of new vasculature. This process facilitates efficient energy storage and helps maintain metabolic health. Conversely, "unhealthy" AT expansion, commonly seen in obesity, involves adipocyte hypertrophy, where existing adipocytes enlarge, leading to cellular stress and a pro-inflammatory state. This detrimental form of expansion is associated with reduced angiogenesis, increased fibrosis, and hypoxia, which contribute to metabolic dysfunction and a host of related diseases[544] (**Figure 26**).

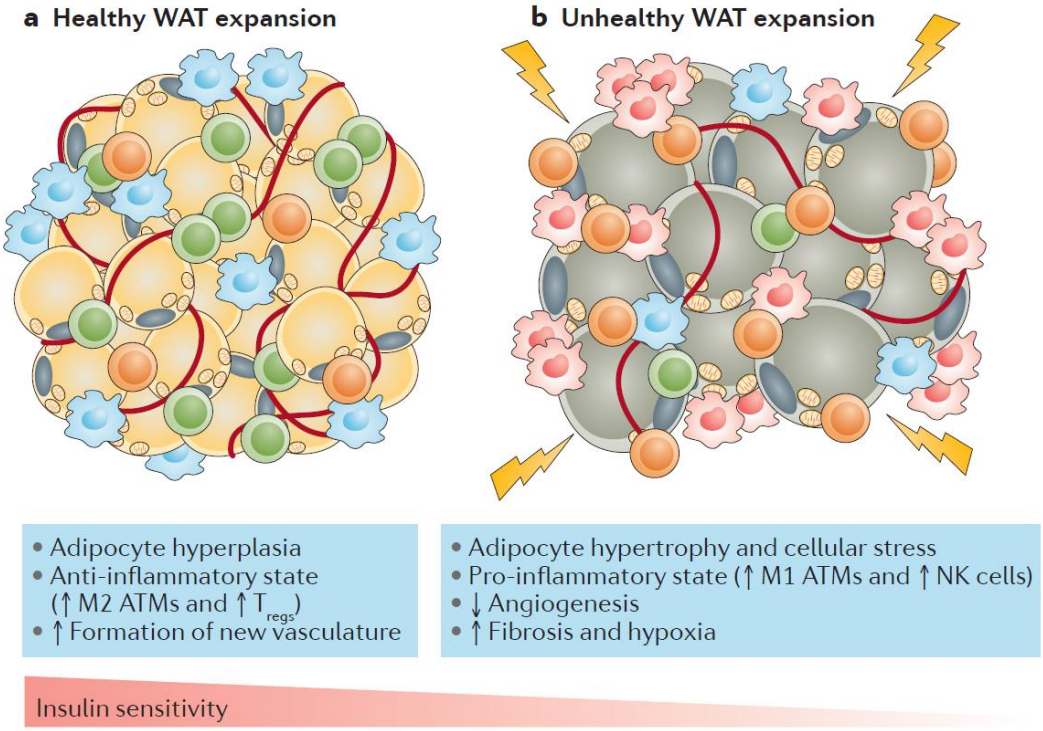

Figure 26. Healthy versus pathological expansion of WAT in obesity progression[545].

The location of WAT expansion plays a crucial role in metabolic health during obesity. Visceral fat is associated with a "**metabolically unhealthy**" state, leading to increased risk of IR, diabetes, and cardiovascular disorders. This type of fat expansion often results in hypertrophic adipocytes that are larger and more prone to inflammation and cellular stress[546]. In contrast, "**metabolically healthy**" expansion occurs primarily in subcutaneous fat. Here, excess lipids are stored in new adipocytes (hyperplasia), promoting better insulin sensitivity and overall metabolic health. Subcutaneous fat typically has smaller, more insulin-sensitive adipocytes and a more favorable vascular and inflammatory profile, which helps mitigate metabolic disturbances[545,547]. Thus, the site of WAT expansion significantly influences the risk of metabolic diseases in obesity.

4.6.2. IMMUNE CELL INFILTRATION

Regardless of the process of AT expansion, chronic excessive caloric intake typically results in adipocyte dysfunction and changes in the cellular composition of AT, where immune cells play a crucial role. Obese AT is characterized by chronic, low-grade inflammation, notable for containing almost every immune cell type, as observed in mice. Obesity increases the numbers of T and B cells, macrophages, neutrophils, and mast cells, particularly in vWAT. In contrast, the number of eosinophils and certain T cell types, like Th2 and Treg cells, remain unchanged or decrease. Macrophages are the most prevalent immune cells within AT of individuals with obesity, and their recruitment and proliferation in response to a high-calorie intake typically lead to inflammation in AT and

IR[548]. Additionally, the phenotype of ATMs differs significantly between obese and lean organisms. In lean individuals, ATMs express genes associated with a M2-like phenotype, which is anti-inflammatory. Conversely, in individuals with obesity, ATMs express genes linked to a M1-like phenotype, which is pro-inflammatory[265].

The M1/M2 classification system is simplified representation of macrophage activation states. In reality, macrophages exist on a spectrum between M1 and M2 phenotypes and can exhibit mixed characteristics. Despite its limitations, the M1/M2-like dichotomy is useful for understanding ATMs biology[549,550]. Stimulation with Th1-type cytokines, such as IFN-γ, triggers a M1 phenotype in macrophages, leading to increased production of pro-inflammatory cytokines such as TNF-α. These M1 macrophages are typically linked to inflammation and tissue damage. In contrast, stimulation with Th2-type cytokines, such as IL-4 and IL-13, results in M2 macrophages. These cells produce anti-inflammatory cytokines, like IL-10, and are involved in wound healing, angiogenesis, and resolving inflammation. M1-like macrophages are believed to promote IR, while M2-like macrophages help protect against obesity-induced AT inflammation and IR[551]. Obesity not only changes the number and phenotype of macrophages but also their distribution within AT. In lean individuals, ATMs are dispersed throughout the tissue. However, in individuals with obesity, they gather in structures known as "crown-like" structures (CLS)[552,553]. These CLS are clusters of lipid-scavenging macrophages that encircle dead adipocytes and are associated with AT dysfunction. The presence of CLS is corelated with AT inflammation and IR in patients with metabolic syndrome[552,554].

Besides macrophages, other myeloid cells such as neutrophils and mast cells play roles in AT dysfunction in obesity. Neutrophils quickly accumulate in AT following HFD feeding and encourage further macrophage recruitment and AT inflammation[555,556]. Similarly, mast cells gather in obese AT, and research on mast-cell deficient mice indicates that these cells contribute to obesity-associated metabolic dysfunction[557].

The **figure 27** illustrates the contrasting inflammatory profiles of AT in lean versus obese states. In essence, in lean individuals, AT maintains a balanced, anti-inflammatory environment conducive to metabolic health. Conversely, in obesity, AT shifts to a pro-inflammatory state characterized by increased cytokines and immune cell infiltration, which contributes to metabolic dysfunction and related complications.

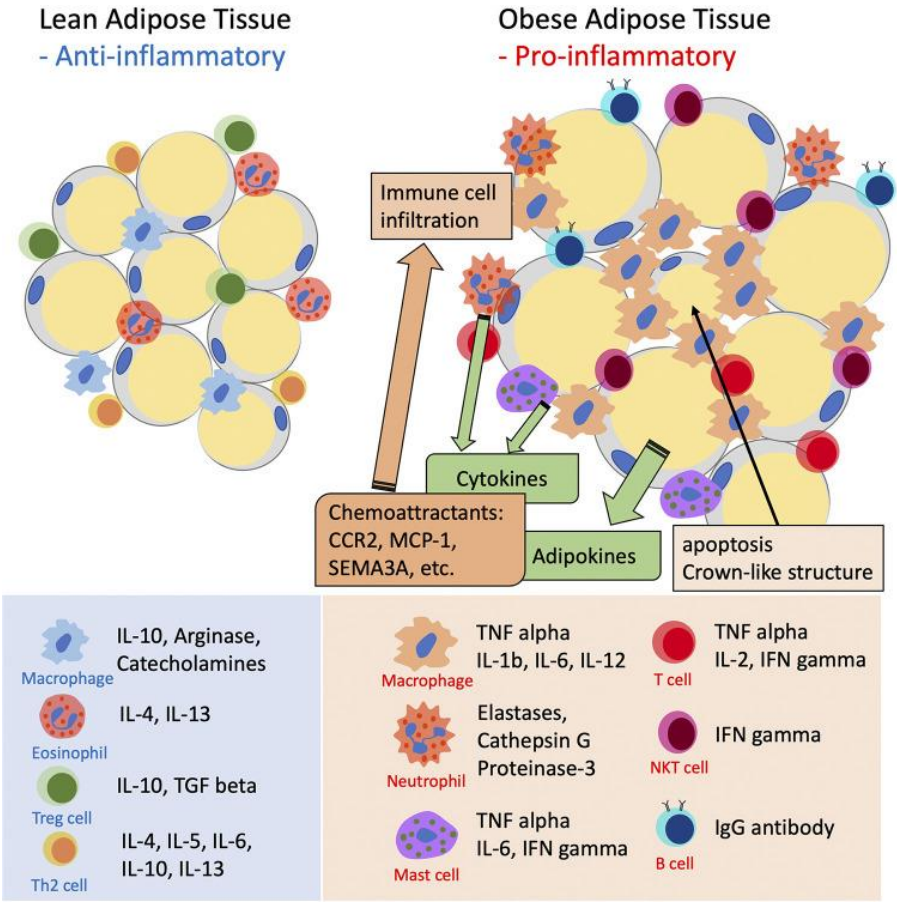

Figure 27. Visual representation of inflammatory differences in lean and obese AT[558].

4.6.3. IMPAIRED VASCULAR STRUCTURE AND FUNCTION

Extensive research in both human and animal models has revealed that obesity significantly disrupts the vascular architecture of AT, a condition known as capillary rarefaction. This phenomenon is increasingly recognized as a key factor in metabolic dysfunction associated with obesity. Reduced capillarization in AT caused by obesity limits the effective delivery of nutrients and oxygen to adipocytes, which can impair their function and exacerbate IR[559–561].

Recent studies utilizing genetically modified mice have shed light on the crucial role of AT vascularization in obesity-related metabolic disturbances. For example, mice engineered to overexpress VEGF-A specifically in adipocytes exhibit enhanced angiogenesis within their AT. This increased in blood vessel formation mitigates some adverse metabolic outcomes of diet-induced obesity, such as IR and hepatic steatosis[562,563]. Conversely, targeted deletion of VEGF-A in adipocytes results in reduced vascularization, which exacerbates AT inflammation and leads to systemic metabolic dysfunction. These findings underscore the critical role of AT vascular health in modulating obesity impact on metabolism[564,565].

In addition to the reduction in capillary density, obesity also triggers endothelial cell activation in AT. This activation results in increased expression of adhesion molecules, including P-selectin, E-selectin, and intercellular adhesion molecule 1 (ICAM-1). Elevated levels of these adhesion molecules enhance the recruitment and infiltration of immune cells, particularly macrophages, into AT[566]. Experimental evidence demonstrates that blocking ICAM-1 with specific antibodies can effectively prevent macrophage infiltration, highlighting the pathological interaction between AT and the vascular endothelium[567].

Moreover, human studies have shown that inflammatory cytokines overproduced in obese AT can impair the vasoregulatory functions and anti-atherogenic properties of the local microvasculature as well as systemic vessels. This impairment leads to dysfunction in blood vessel regulation and contributes to overall vascular health deterioration[554,568].

4.6.4. ADIPOSE TISSUE FIBROSIS

Within the AT, adipocytes are embedded in an extracellular matrix (ECM) that not only offers structural support but also plays a role in cell signaling. Upon the onset of obesity, excessive ECM accumulation occurs due to the hyperactivation of myofibroblasts, which are specialized cells that both produce and contract ECM components, contributing to AT fibrosis and associated metabolic disruptions in mice[569]. AT fibrosis in obesity is driven by complex interplay of factors, including changes in adipocyte behavior. Normally, adipocytes adapt to fluctuations in nutrient availability by expanding or contracting, which helps mitigate lipotoxic damage to peripheral organs. However, in the context of chronic obesity, this response becomes dysfunctional, and adipocytes undergo abnormal hypertrophy, leading to excessive accumulation of ECM components[570]. This process is activated by unresolved chronic inflammation, sustained hypoxia, and increased numbers of myofibroblasts[571–573]. Consequently, the resultant fibrosis hampers the expansion and contraction of AT, ultimately initiating the development of various diseases[570].

Recent studies uncovered specific factors that contribute to AT fibrosis in the context of obesity. Notably, one key factor is endotrophin, a byproduct of collagen VI -a crucial component of the ECM-secreted by adipocytes. It has been shown to promote both fibrosis within AT and systemic metabolic dysfunction[574]. Additionally, platelet-derived growth factor receptor α (PDGFRα) signaling plays a crucial role by inhibiting the differentiation of AT progenitors into adipocytes, instead driving the formation of profibrotic cells, which contribute to the worsening of AT fibrosis[575].

4.7. ECTOPIC FAT ACCUMULATION

Ectopic fat deposition refers to the accumulation of TGs in tissues that are not typically involved in significant fat storage, such as the liver, skeletal muscle, heart, and pancreas.

These tissues, which normally contain minimal fat, can become sites of pathological lipid accumulation when the body AT storage capacity is overwhelmed[576]. This excessive lipid accumulation in non-AT is often a consequence of the body inability to effectively store and manage surplus fat within the primary fat depots, such as scWAT. The AT expandability hypothesis, previously discussed in section 4.3, suggests that the limited expansion of scWAT may cause vWAT and ectopic lipid deposition in these non-adipose organs, leading to adverse metabolic outcomes[577,578] as outlined in **figure 28**.

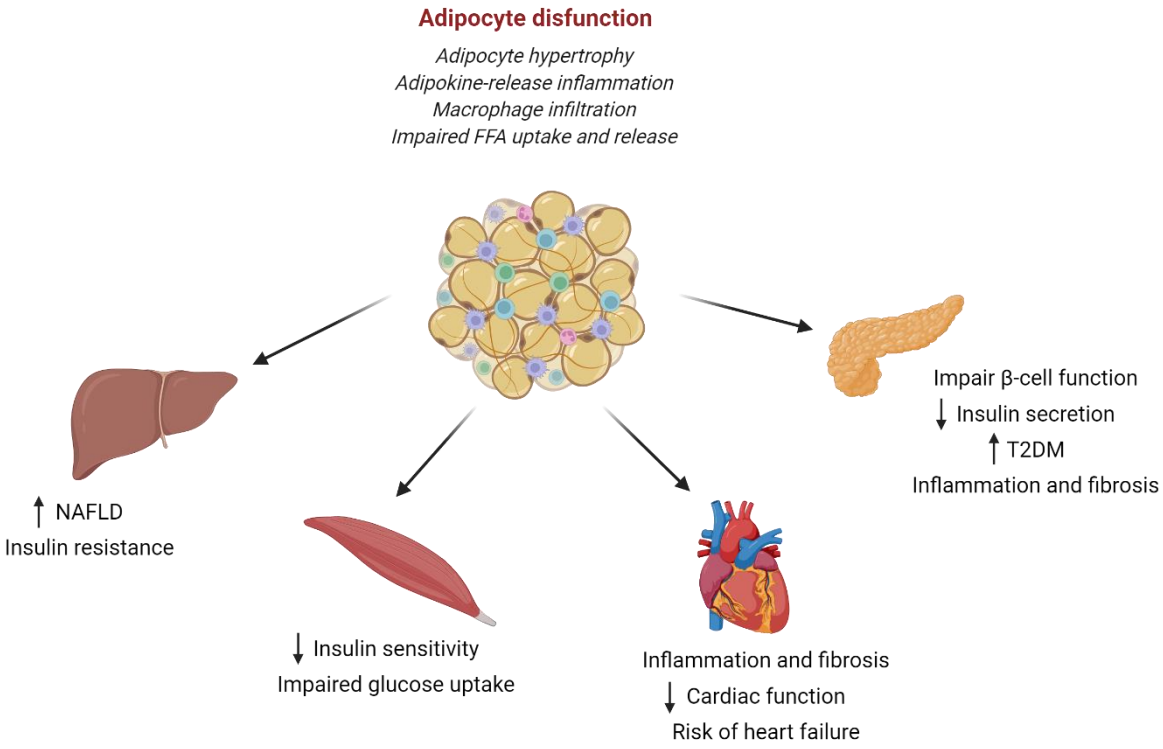

Figure 28. Adipocyte disfunction and ectopic fat deposition in non-adipose organs. Image from Biorender.

In the **liver**, ectopic fat accumulation is a critical factor in the development of hepatic steatosis, which is closely associated with the onset of MAFLD[579]. When the liver ability to manage lipid overload is compromised, excess lipids are stored as lipid droplets within liver cells. This excessive accumulation disrupts normal hepatic function, potentially interfering with insulin signaling and leading to IR. Research has identified multiple mechanisms involved in the development of IR in the liver[579]. As noted earlier in section 4.3, one of the substantial factors, is the intracellular accumulation of harmful lipid intermediates such as DAG and ceramides, which arise from elevated FFAs levels in circulating plasma[580,581]. These intermediates interfere with insulin signaling pathways by activating PKC, which impairs the phosphorylation of insulin receptor substrates and decreases insulin sensitivity. This results in IR, contributing to further hepatic glucose production and exacerbating systemic hyperglycemia[582]. Chronic inflammation, driven by

the accumulation of toxic lipid intermediates, also exacerbates liver dysfunction and can progress to more severe conditions such as non-alcoholic steatohepatitis (NASH) and cirrhosis[583,584].

Ectopic fat accumulation in **skeletal muscle** is associated with decreased insulin sensitivity and impaired glucose uptake. Excessive fat deposits within muscle fibers disrupt the normal metabolic processes, leading to IR[585]. Similar to the liver, this is due to several factors, including the accumulation of toxic lipid intermediates such as DAG and ceramides[586]. The presence of ectopic fat also contributes to chronic low-grade inflammation within the muscle, which further exacerbates IR and impairs muscle function[587]. This can lead to reduced physical performance, increased fatigue, and a higher risk of metabolic syndrome[588,589].

Ectopic fat accumulation in the **heart**, particularly within the myocardium and around the coronary arteries, can lead to several cardiovascular complications[590]. Excessive fat deposits in the heart tissue can contribute to inflammation and fibrosis, impairing cardiac function and increasing the risk of heart failure[591]. Additionally, the presence of ectopic fat in the coronary arteries can promote atherosclerosis, which narrows the arteries and reduces blood flow to the heart muscle[592], and this can lead to coronary artery disease[593]. The metabolic dysfunction associated with ectopic fat accumulation also affects endothelial function, further increasing cardiovascular risk[594].

In the **pancreas**, ectopic fat deposition impacts both the pancreatic islets and the exocrine pancreas. Within the islets, excess lipid accumulation can impair β-cell function and reduce insulin secretion. This dysfunction is linked to the development of T2DM, as the pancreas struggles to produce sufficient insulin in response to elevated blood glucose levels[595]. Additionally, ectopic fat in the pancreas contributes to inflammation and fibrosis of the pancreatic tissue, which can further compromise insulin production and exacerbate metabolic disturbances[596]. As well, intra-pancreatic fat deposition not only disrupts β-cell function but also impacts α-cells. Recent studies have indicated that this fat accumulation is associated with elevated postprandial levels of circulating glucagon, which is secreted by α-cells[597]. Increased glucagon levels can counteract the effects of insulin, worsening hyperglycemia and contributing to the overall metabolic imbalance seen in conditions like T2DM[598]. Furthermore, the presence of excess lipids can also interfere with the synthesis and secretion of digestive enzymes, affecting overall pancreatic function[599].

Ectopic fat accumulation is not limited to the more commonly discussed organs, and it can also occur in a variety of other tissues, such as kidneys, particularly in the renal sinus, leading to increased risk for hypertension and chronic kidney disease[600]; the bone marrow, potentially influencing hematopoiesis and bone metabolism[601], and in the lungs, where it may contribute to respiratory dysfunction[602]. Therefore, preventing the

accumulation of fat in tissues is crucial for maintaining metabolic health and reducing the risk of associated diseases, such as IR, T2DM, and cardiovascular disorders.

4.8. OBESITY TREATMENTS

Significant progress has been made in the last 50 years in the management of diseases associated with excess body weight, including hypertension, adult-onset diabetes, and elevated cholesterol[497], among others.

Given the intricate processes involved in the pathophysiology and the significant impact on health, obesity has begun to be categorized as a chronic disease rather than simply a risk factor. Recognizing obesity as a chronic, degenerative condition contributes to destigmatizing the idea that obesity is the product of poor self-discipline[603,604]. This provides a framework that facilitates the establishment of obesity management programs by healthcare providers and insurance companies, supports scientific and clinical research, and pushes pharmaceutical companies to create body weight management strategies[605].

Since lifestyle and behavioral interventions show moderate effectiveness, it is recommended to enhance obesity treatment approaches by incorporating pharmacological and/or surgical interventions. **Bariatric surgery** represents the most successful approach to lose weight, which reduces mortality from cancer or CVD by 23% and 30%, respectively[606]. Advancements in laparoscopic techniques contribute to a reduction in hospitalization time and bariatric surgery increases overall life expectancy by up to 3 years, accompanied by notable and long-lasting improvements in blood pressure, glucose levels, and lipid metabolism[607].

Successful weight loss exceeding 15% carries substantial benefits, preventing T2DM, facilitating its remission, and improving cardiometabolic risk factors. Additionally, it extends its positive impact to mitigating obesity-related complications, including hyperlipidemia, hypertension, obstructive sleep apnea, MAFLD, and cancer. For years, such degree of weight loss could be achieved only with bariatric surgery. With a better understanding of obesity pathophysiology, new treatment approaches have emerged, promising enhanced effectiveness in weight reduction[608].

Developing anti-obesity medication (AOM) has proven to be exceptionally complicated, facing both technical and societal obstacles. Historically, there has been a series of failures in AOM post-regulatory approval. Most of these cases are associated with adverse cardiovascular effects, elevated risk of suicidal behavior, or an increased potential for drug dependence and abuse. Consequently, certain drugs are suggested only for short-term consumption, due to their additive potential[609,610].

Until recently, long-term drug treatment to achieve normal body weight with adequate tolerability and safety has remained an extremely difficult challenge[611]. However, recent

clinical trials involve advanced therapeutic candidates, such as GLP-1 receptor agonists (**GLP-1RA**), which are approved for diabetes management. These drugs have shown promising results due to their beneficial effects on glucose metabolism, its weight-loss potential, and the cardioprotective properties, generating optimism that innovative, drug-based approaches to managing obesity may be possible. Several GLP-1RAs have been approved by the US Food and Drug Administration (FDA) for weight management, including liraglutide for adult and adolescent obesity[612], and semaglutide for chronic weight management in adults with obesity or overweight and associated conditions like high blood pressure or T2DM. Importantly, these treatments are recommended to be combined with a reduced-calorie diet and increased physical activity. Semaglutide produces an average weight loss close to 15%, offering notable advantages in managing obesity-related complications[613].

Meanwhile, documented evidence demonstrates a weight reduction exceeding 20% using the dual GIP/GLP-1RA tirzepatide in people with obesity[614]. Other AOMs exhibit potential to increase the diversity of treatment options and could be accessible to us in the near future[615].

As previously discussed in this doctoral thesis, the discovery of the leptin gene and its role in obesity has led to the development of **leptin therapy**. However, leptin resistance that occurs in obesity make it an unsuitable target for treating diet-induced or externally derived obesity, which explains the absence of such drugs on the market[616]. In general obesity, plasma leptin levels are already elevated, indicating leptin resistance, and thus exogenous leptin administration has little to no effect on reducing food intake[617].

However, leptin plays a crucial role in cases of congenital and genetic leptin deficiencies, which lead to obesity through internal mechanisms. The absence of leptin is a key factor in congenital or acquired generalized lipodystrophy, making leptin an effective drug target in these specific conditions[618]. Although leptin therapy is not FDA-approved for general obesity management[617], it has been successful in treating rare familial obesity cases caused by congenital leptin deficiency, significantly reducing hyperphagia. Metreleptin, a leptin replacement therapy, was FDA-approved in 2014 as an adjunct to diet specifically for treating patients with generalized lipodystrophy[619].

In conclusion, the landscape of obesity treatments is diverse, encompassing lifestyle modifications, pharmacotherapy, surgical interventions, and emerging therapies targeting the complex pathophysiology of obesity. Future research offers the potential for developing more effective and personalized treatments, underscoring the importance of a multidisciplinary approach in combating this global health challenge.

In summary, the multifactorial nature of obesity makes personalized medicine essential for effective treatment. Tailoring interventions, such as selecting appropriate medications—like GLP-1RA for appetite regulation or agents targeting fat absorption—can enhance treatment outcomes. Personalized approaches also extend to lifestyle

modifications, with customized diet plans—whether low-carb, low-fat, or Mediterranean—designed to fit individual metabolic needs. Recent dietary strategies, including meal timing and intermittent fasting, further optimize weight management. Additionally, personalized exercise regimens aligned with individual capabilities and preferences can improve adherence and long-term success. This holistic approach, integrating tailored pharmacological and lifestyle interventions, is key to managing obesity effectively.

HYPOTHESIS AND OBJECTIVES

BACKGROUND

Traditionally, peripheral SUCNR1 was thought to be inactive in healthy tissues, becoming active only under pathological states characterized by chronic high concentrations of succinate[3]. However, transient increases in circulating succinate have been observed in normal physiological situations, such as the shift from a fasted to fed state, as recently demonstrated by our research group[111].

Despite being highly expressed in adipocytes, the unique recognized function of SUCNR1 in WAT is the inhibition of lipolysis. This anti-lipolytic action of the succinate/SUCNR1 axis could explain the lean phenotype of the whole-body *Sucnr1*-KO mice under standard diet, observed in previous studies[13]. Nevertheless, inconsistent results were observed in these mice in the context of obesity[13,15]. To better characterize the specific functions of a gene in a specific tissue, the use of cell-specific KO strategies is crucial. In this context, this doctoral thesis explores the role of succinate/SUCNR1 axis in AT physiology by generating mice lacking *Sucnr1* specifically in adipocytes.

HYPOTHESIS

The central **hypothesis of this thesis** posits that the succinate/SUCNR1 axis functions as a novel metabolic sensor in adipocytes, playing a crucial role in maintaining energy homeostasis. Specifically, we propose that this axis is an integral component of the metabolite-sensing machinery that enables adipocytes to coordinate metabolic responses following nutrient intake. Beyond its role in lipid metabolism, we hypothesize that succinate acts as a signaling molecule via its receptor SUCNR1 in WAT, regulating the endocrine function of adipocytes, thereby impacting overall metabolic homeostasis.

OBJECTIVES

This doctoral thesis aims to uncover the physiological and pathological relevance of the succinate/SUCNR1 axis in AT biology, with a specific focus on how it governs leptin production and contributes to metabolic homeostasis.

The **specific objectives** are:

1. Investigate the physiological role of the succinate/SUCNR1 axis in adipocytes.
2. Examine the contribution of SUCNR1 to obesity development.
3. Elucidate the molecular mechanisms and identify the downstream mediators by which SUCNR1 influences adipocyte function.

EXPERIMENTAL DESIGN

To achieve the objectives of this research, a comprehensive experimental approach has been implemented, integrating *in vivo*, *in vitro*, and human data validation methods. A transgenic mouse model with targeted deletion of the *Sucnr1* gene in adipocytes (Ad-*Sucnr1* KO) has been generated. This model enables the exploration of SUCNR1 regulatory role in adipocyte physiology and its impact on obesity. Extensive metabolic profiling of Ad-*Sucnr1* KO mice under both standard and high-fat dietary conditions has been conducted to assess the effects of *Sucnr1* deficiency on AT function and obesity development. In parallel, *in vitro* experiments using adipocyte cell lines have been performed to examine the effects of SUCNR1 activation on cellular behavior and metabolic processes. These experiments have identified the signaling pathways activated by SUCNR1, focusing on downstream mediators that modulate gene expression, metabolic pathways, and cellular responses. To translate preclinical findings into a clinical context, the succinate/SUCNR1 axis has been also evaluated in the context of human obesity. This includes characterizing SUCNR1 expression in AT samples from individuals with obesity and correlating it with metabolic dysfunction. The comparison and validation of these findings with preclinical data ensure the relevance of the succinate/SUCNR1 axis in human metabolic health.

The research conducted for this doctoral thesis has been performed in the Diabetes and Associated Metabolic Diseases (DIAMET) Research Group at the Institut d'Investigació Sanitària Pere Virgili, with funding provided by an FPI fellowship (PRE2019-090360) granted by the Spanish Ministry of Education. Additionally, as part of my doctoral studies, I performed a three-month research stay at the Lunenfeld-Tanenbaum Research Institute, affiliated with Mount Sinai Hospital, located in Toronto. This opportunity was made possible through a grant received from the Mobility Program of Doctorate Biomedicine URV 2023.

MATERIALS AND METHODS

1. EXPERIMENTAL MODELS AND SUBJECT INFORMMATION

1.1. HUMAN COHORTS

For this study, recruitment of subjects was conducted at two hospitals: the University Hospital Joan XXIII and the Hospital de Santa Tecla, both located in Tarragona, Spain. Each participant voluntarily provided informed consent prior to participation. The ethical integrity and approval of the study were reviewed by the ethics and research committees at the respective hospitals, with the approvals documented under references CEIm 177/2018, granted on November 29, 2018, and CEIm 41p/2015, granted on August 31, 2015, consistent with the Declaration of Helsinki standards.

Biological samples were collected from the subjects, specifically plasma, scWAT, and vWAT. These samples were obtained from age- and gender-matched donors who were undergoing non-acute surgical procedures, such as hernia repairs or cholecystectomies, which were scheduled as part of routine surgical practices. Further, the classification of donors was carried out based on their BMI, aligning with the WHO classification standards. Individuals with a BMI of 25 kg/m^2 or less were categorized as lean, while those with a BMI of 30 kg/m^2 or higher were classified as individuals with obesity. Detailed anthropometric and biochemical data from the study cohort are summarized in **Annex Table 1.**

1.2. MICE STUDIES

All animal studies were conducted under the supervision and approval of the Rovira i Virgili University Animal Welfare and Ethics Committee (project reference number 10970). All animal procedures followed the guidelines set by the European Union Directive 86/609/EEC and recommendation 2007/526/EC for the protection of animals used in experiments and scientific studies, in compliance with Spanish Law 1201/2005.

All mice were housed under controlled conditions of 12-hour light/dark cycles and a constant temperature of 22°C at the animal facility of the Faculty of Medicine and Health Science of Rovira i Virgili University. Dietary conditions were also controlled, with mice having *ad libitum* access to either a normal chow diet (NCD) containing 3.1% fat, provided by SAFE diets, or a HFD comprising 60% fat, supplied by Research Diets, beginning at the age of 8 weeks, and continued until the time of sacrifice. The weight of male mice was monitored weekly and prior to any experimental procedure.

At the end of the study, animals were fasted overnight, which involves removing food for approximately 12 to 16 hours, from late afternoon until the following morning, to stabilize metabolic conditions for analysis. Subsequently, animals were euthanized via cervical dislocation, and blood and various tissues were harvested and immediately

frozen in liquid nitrogen for gene and protein expression analysis or fixed in 4% paraformaldehyde (PFA) for histological studies.

1.2.1. ADIPOCYTE-CELL SPECIFIC *SUCNR1* KO MICE

1.2.1.1. GENERATION

To further investigate the role of the *Sucnr1* gene in adipocytes, we used the Cre-loxP system, a prominent method in mouse genetic research, to generate mice with a specific deletion of *Sucnr1* in adipocytes. This system originates from bacteriophage P1 and enables controlled genetic modifications within a live organism. It comprises the Cre recombinase enzyme, which recognizes and interacts with loxP sites -specific short DNA sequences. A gene surrounded by these loxP sites is described as "floxed" (notated as "fl"), meaning it can be specifically targeted and modified by the Cre enzyme.

To specifically target genetic modifications within adipocytes and avoid unintended alterations in other cell types, we integrated the Cre-loxP system, coupled with a promoter active exclusively in adipocytes. This method of targeted gene manipulation ensures that any genetic modifications are confined to adipocytes, thereby minimizing off-target effects, and enabling precise studies on the function of *Sucnr1* gene within this specific cell type.

Our approach to selectively inactivate the *Sucnr1* gene in murine adipocytes involved a strategic breeding protocol. We crossed mice possessing a floxed *Sucnr1* allele (characterized by the presence of two loxP sites flanking exon 23) with transgenic mice expressing Cre recombinase under the adiponectin promoter, known as AdipoQ-Cre. These AdipoQ-Cre transgenic mice were kindly provided by G. Sabio from the Centro Nacional de Investigaciones Cardiovasculares (CNIC) in Madrid, Spain. This approach resulted in the creation of *Sucnr1*$^{fl/fl}$ AdipoQ-Cre$^{+/-}$ mice, hereafter referred to as Ad-*Sucnr1* KO mice. In these mice, the Cre recombinase is selectively active in adipocytes, which leads to the targeted inactivation of the *Sucnr1* gene specifically in adipocytes.

As a control group, we used Cre-negative *Sucnr1*$^{fl/fl}$ mice (*Sucnr1*$^{fl/fl}$ AdipoQ-Cre$^{-/-}$), also referred as *Sucnr1*$^{fl/fl}$ mice. These control mice carry the floxed *Sucnr1* allele but do not express the Cre recombinase, thereby maintaining an intact and active *Sucnr1* gene (**Figure 29**).

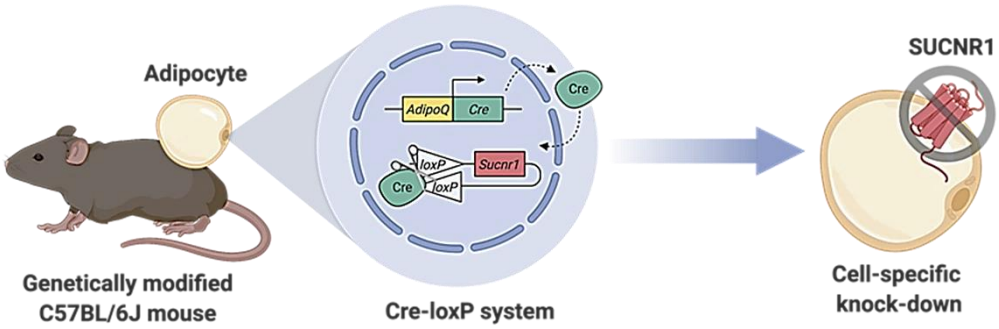

Figure 29. Generation of a cell-specific KO mouse to study of *Sucnr1* in adipocytes. Image from Biorender.

In this research, all mice were consistently bred from a C57BL/6 genetic background. This homogeneity is vital as it minimizes genetic variability, thus ensuring that any observed differences in the study are due to the experimental variables rather than genetic differences. This approach not only facilitated the simultaneous generation of both control and Ad-*Sucnr1* KO mice within the same litter but also allowed for direct comparisons. By breeding the mice this way, we could isolate and examine the specific effects of *Sucnr1* gene function in adipocytes while controlling for potential variability caused by differences in litter conditions.

1.2.1.2. GENOTYPING

The genetic modifications were verified using polymerase chain reaction (PCR) genotyping, an essential technique in transgenic mouse studies for identifying specific alleles and confirming recombination events. This method involved PCR amplification of targeted genomic regions to differentiate between the floxed *Sucnr1* gene and the Cre recombinase driven by the adiponectin promoter, also known as AdipoQ. The PCR products, varying size based on the alleles present, provided a clear basis for categorizing each mouse accurately.

For genotyping, mouse blood was lysed using a specific protocol that employed the DreamTaq Green DNA Polymerase kit (Thermo Fisher Scientific, Rockford, IL). Specifically, 5 µL of blood from the tail vein was collected and mixed with 10 µL of a lysis solution for blood (Sigma-Aldrich, St Louis, MO), causing the mixture to darken within 2-3 minutes. After 5 minutes, 90 µL of a neutralization solution for blood (Sigma-Aldrich) was added, and the samples were stored at 4 °C.

The PCR amplification for each gene and sample involved preparing a 20 µL PCR reaction mixture, which consists of 19 µL of PCR master mix including Dream Taq Buffer, Taq DNA polymerase, deoxyribonucleotide triphosphates (dNTPs), and forward and reverse primers for the loxP-*Sucnr1* allele, as well as for the AdipoQ^{+} or AdipoQ^{Cre}

alleles. Additionally, 1 µL of the genotyping sample was used as the DNA template, and nuclease-free water was added, as specified in **Table 3**, to complete the reaction setup.

Table 3. PCR Mastermix Preparation for Use in Genotyping.

Reagent	Final concentration	Volume per sample
10X DreamTaq green buffer	1X	2 µL
dNTPs 2mM	0.2 Mm	2 µL
Forward primer	0.3 µM	0.6 µL
Reverse primer	0.3 µM	0.6 µL
Taq DNA polymerase	62.5 $Mu \cdot \mu L^{-1}$	0.25 µL
Nuclease-free H_20	-	13.55 µL
DNA template (sample)	-	1 µL
Total	-	20 µL

The PCR reactions were conducted in a thermal cycler (Thermo Fisher Scientific), starting with an initial denaturation step at 95°C for 5 minutes. This was followed by 35 cycles, each consisting of a denaturation phase at 95°C for 30 seconds, an annealing phase at 58°C for 30 seconds, and an extension phase at 72°C for 1 minute. A final extension phase was then performed at 72°C for 10 minutes to ensure the complete synthesis of all PCR products.

For the electrophoresis step of the genotyping protocol, a 1.5% agarose gel was prepared by dissolving 1.5 grams of agarose in 100 mL of 1X Tris-acetate-ethylenediaminetetraacetic acid (EDTA) buffer (TAE), which consists of 40 mM Tris base, 20 mM acetic acid, and 1 mM EDTA. During the gel preparation, 6 µL of SYBR Safe DNA-binding dye (Thermo Fisher Scientific) was added per 100 mL of gel solution to enable visualization of DNA under UV light. The prepared gel was then loaded with 10 µL of the PCR product alongside 7 µL of a 50 ng/µL 100 bp DNA ladder (Thermo Fisher Scientific) and run at 100 V for approximately 30-45 minutes to separate the DNA by size.

After running, the gel was visualized under UV light using an iBright CL1000 Imaging System (Thermo Fisher Scientific). This visualization process allowed for the identification of specific band sizes correlating to different alleles: a 500-bp product indicated the presence of the loxP-targeted allele, while a 700-bp product confirmed the presence of the AdipoQ-Cre allele.

Precise execution of this genotyping protocol is crucial as it ensures the accuracy and reliability of genetic data, which is essential for the effective management and monitoring of transgenic mouse colonies.

1.2.2. OTHER MOUSE MODELS

WT C57BL/6 mice were supplied by Charles River Laboratories (Barcelona, Spain). Upon their arrival at the animal facility, these mice were carefully moved from their shipping containers to their prepared housing units. This carefully handling is crucial as it minimizes stress, which can affect their health and the validity of experimental results and reduces the risk of physical injury.

Global *Sucnr1* KO mice, generously provided by K. McCreath, are genetically modified mice in which the *Sucnr1* gene has been completely inactivated or "knocked out" throughout the whole body. These mice serve as valuable models for exploring the comprehensive physiological and pathological functions of this receptor. By comparing these *Sucnr1* KO mice to their WT mice counterparts, researchers can explore the specific impacts resulting from the absence of *Sucnr1*-mediated signaling.

B6.129-*Arntl*^{tm1Bra}/J KO heterozygous mice, hereafter referred to as *Bmal1* KO mice, were obtained from The Jackson Laboratory (Bar Harbor, ME), and C57BL/6J WT mice were used as control animals for comparative analyses. The KO status and the corresponding reduction in *Bmal1* expression levels were verified through quantitative real-time PCR (qPCR). In liver tissue, *Bmal1* expression was significantly reduced in *Bmal1* KO mice compared to WT controls (0.55 ± 0.03 vs. 1.00 ± 0.11, respectively; p=0.002). Similarly, in rWAT, *Bmal1* expression was lower in *Bmal1* KO mice compared to WT controls (0.65 ± 0.03 vs. 1.00 ± 0.09, respectively; p=0.005).

1.3. MOUSE AT EXPLANTS

Mouse WAT was freshly isolated from at least three mice for each set of experiments. Each sample of WAT was meticulously cleaned using phosphate buffered saline (PBS; Hyclone, GE Healthcare Life Sciences, Logan, UT) containing 1% antibiotic/antimycotic (Ab/Am) solution (Hyclone) and combined into a pooled sample for consistent analysis.

For the leptin secretion experiments, 0.2 g of the tissues were placed in 1 mL of Dulbecco Modified Eagle Medium/Nutrient Mixture F-12 (DMEM/F12; Gibco, Life Technologies Limited, Paisley, UK) for 24 h under controlled conditions at 37°C with a 5% CO_2. Following incubation, the supernatants were carefully collected and stored at -20°C pending further biochemical analysis. For protein studies, 0.8 g of WAT were cultured in 24-well plates with Krebs-Ringer bicarbonate HEPES (KRBH) buffer containing 120 mM NaCl, 5 mM KCl, 2 mM $CaCl_2$, 1 mM $MgCl_2$, 25 mM $NaHCO_3$, and 5.5 mM HEPES, and supplemented with 0.1% bovine serum albumin (BSA, Sigma-

Aldrich). After a 2-hour incubation period, the samples were treated either with 100 µM *c*ESA (TCI chemicals, Tokyo, Japan) or 400 mM succinic acid (Sigma-Aldrich) for 10 minutes. Similarly, for examining gene expression, 0.8 g of tissue were cultured in 24-well plates containing KRBH buffer supplemented with 0.1% BSA for 2 hours and treated with 400 mM succinic acid for 6 hours.

To conclude this section, it is noteworthy that our work has led to the development and publication of a comprehensive protocol in the STAR protocols journal by Cell Press. This protocol, entitled "Protocol for the *in vitro* isolation and culture of mature adipocytes and white adipose tissue explants from humans and mice", meticulously details the procedures for the isolation and culture of mature adipocytes, which will be outlined in the following section, and WAT explants from adult mice and humans. It has been successfully utilized with various types of WATs, in both lean and diet-induced obese mice, as well as in a variety of genetically modified mouse models. For further information, the complete protocol is included in this doctoral thesis in the Results Section as "Study 2". This protocol serves as a valuable resource for researchers interested in replicating or expanding upon our work.

1.4. PRIMARY mASCS AND MATURE ADIPOCYTES

WAT was collected from Ad-*Sucnr1* KO and *Sucnr1*$^{fl/fl}$ mice, weighed, and pooled into groups based on WAT location and genotype of mice. The harvested tissues were then minced, rinsed with PBS to remove cellular debris, and treated with a solution containing 0.2% collagenase (Sigma-Aldrich) in PBS and 1% BSA for 1 hour at 37°C with gentle agitation to facilitate effective digestion of WAT. After digestion, the tissue was centrifuged at 300 g for 10 minutes, facilitating the separation of mature adipocytes, which float to the top, from the SVF, which settles at the bottom (**Figure 30**).

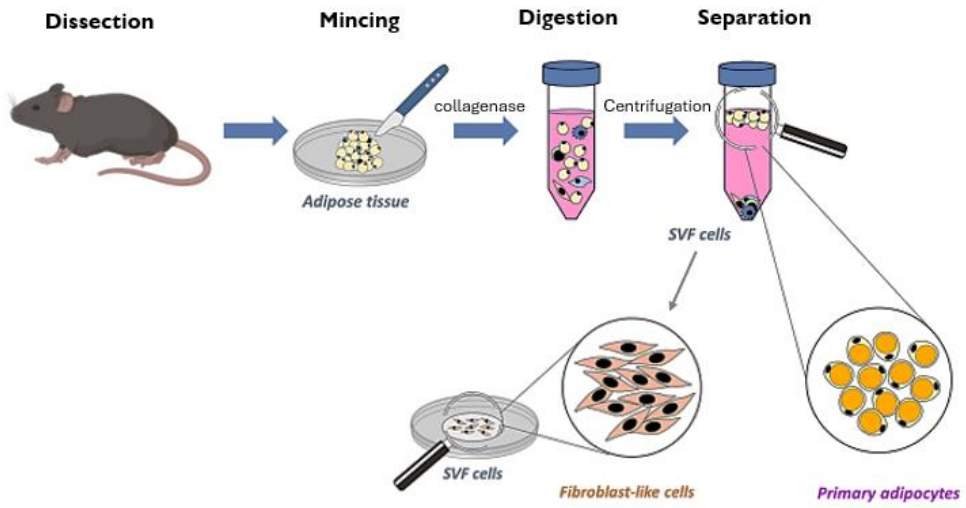

Figure 30. Isolation of mouse mature adipocytes and SVF[620].

The top layer, which held mature adipocytes, was gently moved and subjected to further centrifugation at 300 g for 5 minutes. Isolated adipocytes were then cultured in 12-well plates containing DMEM/F12 medium supplemented with 10% fetal bovine serum (FBS, Hyclone) for 24 hours at 37°C and 5% CO_2. Subsequently, adipocytes were treated with 400 mM succinic acid for 6 hours. Simultaneously, the SVF pellet was resuspended in DMEM/F12 medium enriched with 10% FBS and 1% Ab/Am solution. Mouse ASCs (mASCs) derived from SVF were cultured at 37°C with 5% CO_2. The medium was refreshed 24 hours post-seeding to remove non-adherent cells. All experimental analyses were conducted on cells at passage three.

As mentioned in the previous section, we have published a protocol on the isolation and culture of mature adipocytes in the STAR Protocols journal. This publication provides a more detailed description of each step in the procedure and is included in this doctoral thesis in the Results Section as "Study 2".

1.5. ISOLATION AND CULTURE OF PRIMARY MOUSE BM-MSCS

Tibias and femurs were carefully extracted from mice under sterile conditions and cleaned using PBS. To access the bone marrow, both ends of each bone were cleanly cut, exposing the marrow cavity, and a 20-G needle attached to a syringe was then used to flush out the bone-marrow contents into a collection tube (**Figure 31**).

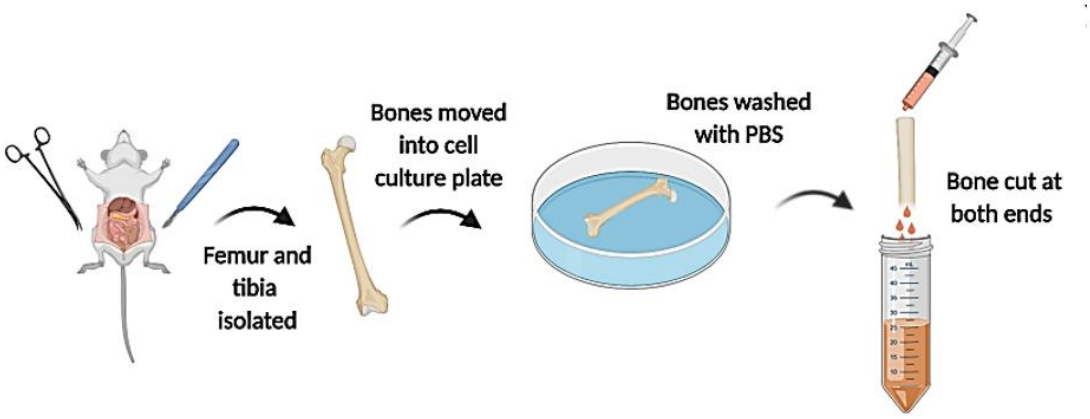

Figure 31. Primary isolation of bone marrow from mice[621]

The harvested bone marrow was centrifuged to concentrate the cells into a pellet, which was subsequently resuspended and cultured in DMEM-High Glucose (Hyclone) supplemented with 15% FBS and 1% Ab/Am in a humified cell incubator set at 37°C with 5% CO_2.

Within 24 hours post-plating, non-adherent cells, which mainly consist of hematopoietic cells and other non-MSC elements, were removed by changing the medium. The medium was refreshed every 2 to 3 days until BM-MSCs reached confluence. Once confluent, the cells were either passaged for further expansion or used for experimental analysis.

1.6. PRIMARY HUMAN ASCS

1.6.1. ISOLATION

Human ASCs (hASCs) were isolated following the established protocol as described[622] from scWAT biopsies obtained from a cohort of four female donors, divided into two groups based on their BMI: lean (n=2, BMI 20.3 ± 0.7 kg/m^2) and obese (n=2, BMI 32.9 ± 0.7 kg/m^2). Briefly, scWAT samples were thoroughly rinsed with PBS and then subjected to enzymatic dissociation using a digestion solution containing 0.1% collagenase and 1% BSA in PBS at 37°C with gentle agitation for 1 hour to effectively dissociate the adipose cells. Following digestion, the samples were centrifuged at 300 g for 5 minutes at 4°C to separate the SVF, which contains hASCs, from the mature adipocytes.

Subsequently, the SVF was resuspended and cultured in DMEM/F12 supplemented with 10% FBS and 1% Ab/Am solution before being frozen. Cells were cryopreserved and stored at the Pere Virgili Health Research Institute BioBank (PT17/0015/0029), which is listed at the National Register of Biobanks under registration number #C.0003609.

1.6.2. DIFFERENTIATION INTO MATURE ADIPOCYTES

The differentiation of hASCs into mature white adipocytes was executed according to a well-established method[623]. Upon reaching confluence, differentiation was induced using a specialized medium composed of DMEM/F12, DMEM-High Glucose, 10% FBS, and 1% Ab/Am, enhanced with differentiation-promoting agents including 1 mM dexamethasone, 33 mM biotin, 17 mM calcium pantothenate, 500 mM 3-isobutyl-1-methylxanthine (IBMX), 100 nM insulin, and 5 mM rosiglitazone (all sourced from Sigma-Aldrich). After 4 days of differentiation, the medium was refreshed every two days until day 14 of differentiation with DMEM/F12, DMEM-High Glucose medium only containing dexamethasone, biotin, and calcium pantothenate.

Upon completion of the differentiation process, cells underwent a 2-hour serum deprivation with FBS-free medium containing 0.2% BSA, followed by treatment with either 400 mM succinic acid or 100 µM *c*ESA to assess cellular responses to metabolic stimuli.

1.7. 3T3-L1 CELL LINE

1.7.1. CELL CULTURE CONDITIONS

Mouse embryonic 3T3-L1 preadipose cells (CL-173™; ATCC, Manassas, VA) were cultured under specific conditions in DMEM-High Glucose medium enriched with 10% FBS and 1% Ab/Am solution within a humified cell culture incubator at 37°C with 5% CO_2.

1.7.2. DIFFERENTIATION

Upon reaching confluence, 3T3-L1 cells were subjected to a specific differentiation protocol to induce adipogenesis. During the initial 2 days of differentiation, cells were maintained in their growth medium, which was supplemented with specific differentiation agents. These included 0.25 mM dexamethasone to stimulate the adipogenic process, 0.5 mM IBMX to elevate intracellular cAMP levels, 5 µg/mL insulin to promote glucose uptake, and 1 µM rosiglitazone to activate PPARγ.

Following the initial differentiation phase, cells were further incubated for an additional 2 days in growth medium supplemented with 5 µg/mL insulin and 1 µM rosiglitazone, supporting maturation and functional development of the newly formed adipocytes. After the maturation phase, the culture medium was reverted to the original growth medium without differentiation supplements for the rest of the culture period. This step was crucial for stabilizing the differentiated state of the adipocytes, ensuring their viability and functionality. The entire process and resultant morphological changes in the cells were documented and analyzed to confirm successful adipogenesis, as illustrated in **Figure 32**.

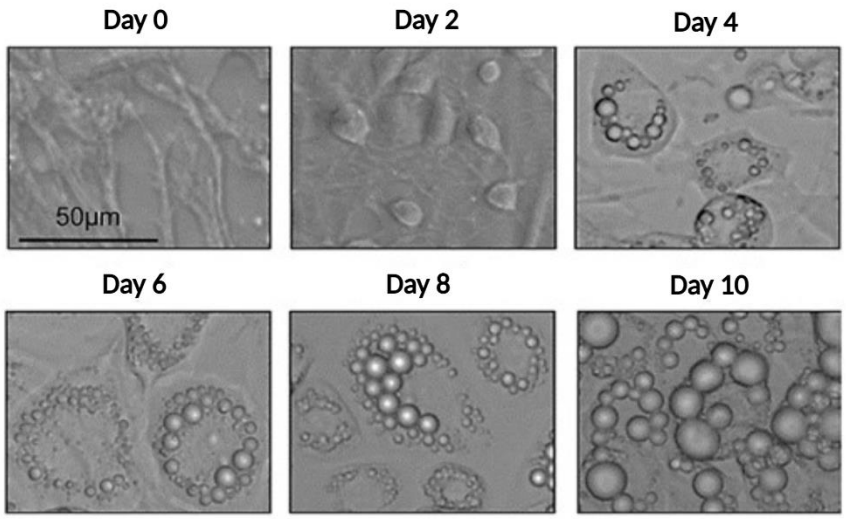

Figure 32. 3T3-L1 adipocyte differentiation. Phase contrast images from induction (day 0) to ten days post-induction[624].

1.7.3. EXPERIMENTAL CONDITIONS

On day 9 or 10 of the adipocyte differentiation protocol, cells underwent a 2-hour resting period in FBS-free medium containing 0.2% BSA. Following the resting phase, cells were exposed to various treatments with either succinic acid, cESA, or 5-aminoimidazole-4-carboxamide ribonucleotide (AICAR; Sigma-Aldrich), a well-known activator of AMPK.

In specific experiments designed to investigate the role of kinases in cellular signaling, cells were pre-treated with kinase inhibitors prior to the application of the main treatment compounds. The inhibitors used were SP600125 (JNK inhibitor), SB202190 (p38 MAPK inhibitor) (both from MedChemExpress, Monmouth Junction, NJ), and compound C (AMPK inhibitor; Calbiochem, San Diego, CA). Each inhibitor was applied to the cells for 30 minutes to effectively inhibit target kinases, thereby allowing for the investigation of phosphorylation events in subsequent treatments.

1.8. HEK 293 CELL LINE

Human embryonic kidney 293 (HEK 293) cells were sourced from the ATCC catalogued under the identifier CRL-1573™. This cell line is widely recognized for its robust growth and transfection efficiency, making it suitable for a variety of biochemical and genetic studies.

HEK 293 cells were cultured in DMEM-High Glucose supplemented with 10% FBS and 1% Ab/Am in a humified incubator set at 37°C and 5% CO_2.

2. METHOD DETAILS

2.1. INDIRECT CALORIMETRY

Indirect calorimetry experiments were conducted using a 16-chamber TSE Phenomaster monitoring system (TSE Systems GmbH, Bad Homburg, Germany), adhering to a standardized protocol[625]. This system allows for precise monitoring of metabolic parameters under controlled conditions.

Prior to data collection, each mouse was individually housed in a designated chamber within the measurement setup. An acclimatization period of 3 days was provided in the measuring room to allow the mice to adjust to the environment, minimizing stress-induced variations in metabolic data. Following this period, continuous monitoring of oxygen consumption and CO_2 production was carried out from 48 to 72 hours.

The collected data on gas exchange were used to calculate key metabolic indicators. The Respiratory Exchange Ratio (RER) was determined using the formula $RER = VCO_2/VO_2$, which provides insights into the substrates being utilized for metabolism. Energy Expenditure (EE) was calculated based on the formula $EE = (3.185 + 1.232 * RER) * VO_2$, allowing an assessment of the total energy burned by the animals. These calculations are critical for understanding the metabolic dynamics and overall energy balance of the subjects under study.

2.2. LOCOMOTOR ACTIVITY AND FOOD INTAKE

In conjunction with the indirect calorimetry experiments, the locomotor activity of the mice was continuously monitored to assess their physical movements and overall activity levels. This was achieved using an infrared grid system, which consisted of photocell beams strategically placed to detect and record the horizontal movements of the mice as they moved freely within their individual cages. Alongside monitoring locomotor activity, the intake of food and water by the mice was also tracked. Each cage was equipped with sensors that automatically recorded the amount of food and water consumed. These sensors ensured accurate and continuous measurement of intake, providing valuable data on the feeding behavior of the mice. Both food and water were made available *ad libitum*, ensuring that the mice had unrestricted access unless specific experimental conditions required otherwise.

2.3. QUANTITATIVE MAGNETIC RESONANCE IMAGING

Quantitative Magnetic Resonance Imaging (qMRI) is an advanced imaging technique utilized to measure and analyze various body composition parameters such as fat mass, muscle volume, and other vital metrics.

2.3.1. FAT MASS

Prior to imaging, mice were anesthetized using a 1.5–2% isoflurane-oxygen mixture to ensure immobility and reduce stress during the procedure. The qMRI scans were performed using a high-resolution 7.0T Bruker Biospect system with a 16 cm bore diameter, equipped with a 40-mm quadrature coil and a 90-mm gradient coil insert capable of reaching a maximum intensity of 360 G/cm (Bruker Medical GmbH, Ettlingen, Germany).

During the qMRI procedure, the physiological state of the mice, including body temperature and respiratory rate, was closely monitored. Temperature was measured using a rectal probe, while respiratory rate was tracked with a gating system specifically designed for small animals (SA Instruments, INC., Stony Brook, NY). For imaging, T2-weighted spin echo images were captured using a technique known as rapid acquisition with relaxation enhancement (RARE) sequence. This approach allows for high-quality imaging in both axial and coronal planes.

In the axial scans, two image sets captured consecutively for each animal: one with the fat suppression module activated and one without. In the coronal scans, images highlighting fat tissue were obtained using a frequency-selective radiofrequency pulse set at high-field offset of 1000–1100 Hertz relative to the water signal, effectively isolating the signal from fat protons.

The imaging parameters were set to include a repetition time of 3200 milliseconds, an echo time of 44 milliseconds, and two averages to enhance image clarity. The images were generated using a 256 x 256 matrix within a field of view of 50 x 50 mm. The protocol included acquiring 14 slices in axial orientation and 36 slices in coronal orientation, each slice being 1.5 mm thick without any spacing between slices. The acquired images were analyzed using NIH ImageJ software. For each mouse, the volume of fat was measured and then converted to grams assuming AT density of 0.9 g/mL[626]. Fat mass was then reported as a percentage of the overall weight of the animal.

2.3.2. *IN VIVO* PROTON MAGNETIC RESONANCE SPECTROSCOPY

In vivo proton magnetic resonance spectroscopy (1H-MRS) is a sophisticated non-invasive imaging technique used to investigate the chemical composition of tissues by analyzing the magnetic properties of hydrogen protons. In this study, 1H-MRS was performed using a non-localized single pulse sequence. This approach was selected to avoid water signal suppression, thereby enhancing the visibility of all spectral components within the tissue.

The spectroscopic data were collected with a resolution of 2018 data points across a spectral width of 7.5 Kilohertz. This high resolution facilitated precise and detailed spectral analysis, critical for accurate quantification and comparison of biochemical

components. The primary focus was on the intensity of water and fat signals within the biological samples.

The intensities of these signals were analyzed using Mnova software (Mestrelab Research, Santiago de Compostela, Spain), allowing for the quantification of the relative concentrations of fat and water within each sample, providing valuable data on tissue composition and changes therein.

2.3.3. MUSCLE VOLUME

qMRI was employed to measure muscle volume, utilizing the same equipment and initial procedures as previously detailed. For this specific analysis, T2-weighted spin echo images were captured using RARE sequence, applied in both axial and coronal planes.

The imaging sequence was carefully calibrated with a repetition time of 3000 milliseconds, an echo time of 11.57 milliseconds, and a RARE factor of 8 to optimize image quality. The protocol included an average of 12 acquisitions per sequence, with a field of view of 2.5 cm to focus on the muscle area. The acquisition matrix was set at 256 x 256, achieving an in-plane resolution of approximately 97 x 97 mm^2. To ensure detailed cross-sectional analysis, the slice thickness was maintained at 1 mm with no gaps between slices.

Images specifically targeting the hind limbs were analyzed using ImageJ software (NIH) across five consecutive slices, and the measurements from both limbs were combined to produce a single value per mouse. In axial slides, imaging commenced dorsally just beyond the slice displaying the full length of the tibia. For coronal slices, imaging started three slices proximal to the distal end of the tibial plateau. Within each slice, manual tracing of regions of interest (ROIs) was performed for each projection, with exclusion of segments that showed hyperintense or hypointense signals, which typically indicate the presence of fat and bone, respectively, to ensure accuracy in muscle tissue delineation.

2.4. METABOLIC TOLERANCE TESTS

2.4.1. GLUCOSE TOLERANCE TEST

Glucose tolerance test (GTT) is a critical diagnostic tool used to assess the ability of mice to regulate their blood glucose levels, providing insights into their metabolic health and glucose metabolism efficiency. The procedure began with a 6-hour fasting period to stabilize the glucose levels in the mice. Subsequently, a glucose solution was administered through an intraperitoneal (i.p.) injection at a dose of 2 g/kg body weight. This method allows for the rapid absorption of glucose into the bloodstream.

Blood glucose levels were then obtained from tail vein blood samples at specific intervals of 0, 15-, 30-, 60-, and 120-minutes post-injection, using a handheld glucometer (Accu-Chek glucose reader; Roche, Mannheim, Germany). Rapid decreases in glucose levels post-injection indicate effective glucose regulation, while slower decreases may point to IR or impaired pancreatic function.

2.4.2. INSULIN TOLERANCE TEST

Insulin tolerance test (ITT) evaluates the efficacy of glucose regulation in response to administered insulin, serving as an important measure of insulin sensitivity. For this test, mice underwent a shorter fasting period of 3 hours, considering that prolonged fasting can itself influence insulin sensitivity.

After fasting, mice received an i.p. injection of insulin dosed at 0.75 U/kg body weight, tailored to significantly lower blood glucose levels without inducing hypoglycemia. Glucose levels were subsequently monitored using the same procedure and equipment as the GTT. This test is particularly relevant for identifying decreased insulin sensitivity, a common feature of various metabolic disorders such as T2DM and obesity.

2.5. EFFECT OF ORAL SUCCINATE ON CIRCULATING LEPTIN

Ad-*Sucnr1* KO mice and their control counterparts, *Sucnr1*$^{fl/fl}$ mice, were subjected to an experimental procedure designed to assess the metabolic response to oral succinate administration on leptin levels in the blood. Both groups of mice were fasted overnight prior to an oral administration via gavage of 500 mg/kg of disodium succinate (Sigma-Aldrich).

Blood samples were collected from the tail vein at different intervals to monitor changes in leptin levels over time. Sampling occurred immediately prior to the administration (0 hours) and subsequently at 2-, 4-, and 6-hours post-gavage. Collected blood samples were centrifuged at 2000 g for 5 minutes at 4°C to separate the plasma, which was then used for leptin analysis.

2.6. *IN VIVO* LIPOLYSIS INHIBITION

The primary focus of this experiment was to explore the effects of the ATGL inhibitor (ATGLi) on lipolysis in live mice. The experimental setup included two groups of mice; one group consisted of 8-week-old mice fed NCD, and the other group included 14-week-old mice that had been on a HFD for 8 weeks.

Mice in both groups received daily administrations of 200 µmol/kg of ATGLi (Cayman Chemical, Ann Arbor, MI) via oral gavage for a duration of 2 weeks. For the control group, corn oil (Sigma-Aldrich) was used as the vehicle. Throughout the two-week treatment period, several parameters including body weight and food intake were

monitored daily. At the conclusion of the treatment period, mice were fasted overnight, killed via cervical dislocation, and various tissues were collected for subsequent biochemical and histological analysis.

2.7. CHRONIC LEPTIN TREATMENT

This part of the study aimed to explore the long-term metabolic effects of leptin in 8-week-old Ad-*Sucnr1* KO mice fed NCD. The treated group was administered with 0.5 mg/kg leptin (Sigma-Aldrich). This dose was delivered i.p. twice daily at structured times: once at 8:00 am and again at 7:00 pm, continuing for a period of 4 weeks. The control group received an equivalent volume of PBS, serving as the vehicle.

Daily monitoring of body weight and food intake was conducted for both groups prior to each injection to compare their metabolic responses to the treatment. To accurately evaluate the effects of leptin on metabolism independently of caloric intake, control mice were pair-fed to the leptin-treated group, meaning that the control mice were given the same amount of food as consumed by the leptin-treated mice the previous day, ensuring that any differences in metabolic outcomes could be attributed to the physiological actions of leptin rather than differences in food intake. At the end of the treatment, all mice were fasted overnight, killed by cervical dislocation, and various tissues were collected for further analysis.

2.8. FEEDING STUDIES AND LEPTIN SENSITIVITY TESTS

This detailed study incorporates various experimental approaches to assess the physiological and molecular responses associated with dietary transitions and leptin sensitivity in mice.

To assess gene expression changes during the transition from fasted to a fed state, mice were initially subjected to a 24-hour fasting period. Subsequently, the cohort was divided into two groups: one group was sacrificed immediately after fasting to serve as the baseline, while the other group was allowed to refeed for 12 hours before being sacrificed.

Parallel to gene expression studies, protein levels were examined through western blot analysis to capture rapid postprandial changes. After the same 24-hour fasting period, mice were housed individually and acclimated for 3 days. Post fasting, they were divided into two groups; one was sacrificed immediately, and the other was refed for a brief period of 20 minutes before sacrifice.

For leptin sensitivity tests, mice were first habituated with handling and sham injections to minimize stress. Following an overnight fast, mice received an i.p. injection of 3 mg/kg of recombinant mouse leptin (R&D Systems) or PBS as a control. After 1 hour, mice

were sacrificed, and their hypothalamus was immediately harvested and frozen for subsequent analysis.

Additionally, the impact of leptin on body weight and food intake was evaluated in both Ad-*Sucnr1* KO and *Sucnr1*$^{fl/fl}$ mice. These mice were administered twice daily i.p. injections of 0.5 mg/kg leptin or PBS for 4 days with injections timed at 8:00 am and 7:00 pm. Body weight and food intake were recorded daily prior to the injections to monitor the effects of leptin over this period.

2.9. MICROCOMPUTED TOMOGRAPHY

Microcomputed tomography (microCT) was employed to evaluate the structural integrity and composition of tibias from mice subjected to different dietary conditions. This non-invasive imaging technique is pivotal for assessing bone architecture, providing essential data for understanding the impact of dietary influences on bone health.

The study utilized tibias from two group of mice: one group comprised 22-week-old mice fed NCD, and the other included 21-week-old mice that had been on a HFD for 13 weeks. To prepare for imaging, each tibia was removed and cleaned of any adhering soft tissue. Following dissection, tibias were fixed in 4% PFA (Sigma-Aldrich) for 24 hours at 4°C. The bones were subsequently placed in PBS at 4°C for another 24 hours, and then preserved in 20% sodium azide solution (Thermo Fisher Scientific) diluted in PBS at 4°C until the time of analysis. High-resolution tibial images were captured using a microCT scanner (SkyScan 1272, Brucker microCT, Kontich, Belgium), which complies with the American Society of Bone and Mineral Research standards. During the scanning process, samples were exposed to 70 kV and 10 W (143 µA) for 2700 milliseconds, using a 1-mm aluminum filter for an 11 µm voxel size. Two-dimensional images were acquired throughout a complete 180° rotation of each sample.

The collected images were reconstructed using NRecon software and analyzed with a CT-Analyzer (SkyScan). For trabecular bone analysis, manual ROIs were identified starting 0.6 mm from the growth plate and extending 2 mm towards the diaphysis, which refers to the mid-section of a long bone. For cortical bone, the analysis focused on a 3-mm section starting from the bifurcation of the fibula. During reconstruction, a Gaussian noise filter was applied to enhance image quality, and manual thresholds were set at 15 for trabecular and 50 for cortical evaluations.

2.10. *EX VIVO* LIPOLYSIS DETERMINATION

For the analysis of lipolysis, mouse eWAT tissues weighing 0.8 g, were cultured in 24-well plates. The tissue explants were immersed in KRBH buffer supplemented with 0.1% FFA-free-BSA to support and mimic physiological conditions. Lipolysis was chemically induced in eWAT explants by the addition of 1 µM of isoproterenol (Sigma-Aldrich), a

β-adrenergic agonist known to stimulate lipolytic activity in adipocytes by mimicking adrenaline action. Additionally, tissue explants were treated with 100 µM *c*ESA for 3 hours to explore its effects on the lipolysis process. Lipolysis was assessed by measuring the amount of glycerol released into the culture medium, which serves as a direct indicator of TG breakdown. Glycerol release was quantified using the Free Glycerol Reagent (Sigma-Aldrich).

2.11. BROWN ADIPOCYTE DIFFERENTIATION OF mASCS

2.11.1. CULTURE AND DIFFERENTIATION

mASCs were cultured in 6-well plates and subjected to a differentiation protocol to promote their development into brown adipocytes. The differentiation medium used for this process consisted of DMEM/F12 supplemented with 10% FBS, 15 mM HEPES, 1 nM insulin, 100 mM IBMX, 1 mM dexamethasone, and 3 mM rosiglitazone. After 4 days of culture, the medium was replaced to one without insulin to reduce the promotion of adipogenic factors, and this medium was maintained until day 10 of differentiation.

2.11.2. LIPID ACCUMULATION ASSESSMENT AND IMAGING

To evaluate lipid accumulation, a critical indicator of adipocyte differentiation, the differentiated cells were fixed using 4% PFA for 15 minutes. Following fixation, cells were thoroughly rinsed with distilled water to remove any residual fixative. Lipid droplets within the cells were stained with Oil Red O (Sigma-Aldrich) for 45 minutes, which specifically binds to neutral lipids, thus visually highlighting these components under microscopy.

The Oil Red O-stained lipid vesicles were visualized using a high-resolution light microscope equipped with a Zeiss AxioCam MRM (Zeiss, Germany). Digital images were captured and managed using ZEN Digital Imaging for Light Microscopy v3.1 software (blue edition; Zeiss). To quantify the staining, Oil Red O was subsequently eluted from the stained cells using isopropanol for 5 minutes, and the optical density (O.D.) of the eluate was measured at a wavelength of 540 nm using a spectrophotometer.

2.12. OSTEOBLAST DIFFERENTIATION OF BM-MSCS

2.12.1. CULTURE AND DIFFERENTIATION

BM-MSCs were plated in 12-well plates and cultured under conditions designed to promote osteoblast differentiation. The culture medium used was DMEM-High Glucose, which was supplemented with osteogenesis-promoting factors including 10 mM β-glycerol phosphate for matrix mineralization, 100 mM dexamethasone to stimulate

osteoblastic differentiation, and 0.5 mM L-ascorbic acid to support collagen synthesis (all sourced from Sigma-Aldrich). This medium was maintained for a period of 2 weeks.

2.12.2. STAINING PROCEDURE AND IMAGING

Post-differentiation, cells were fixed using 4% PFA and subsequently rinsed with distilled water. For the detection of mineral deposits indicative of osteoblast activity, the fixed cells were stained with 1% Alizarin Red S staining solution (pH 4.1; Sigma-Aldrich) at room temperature (RT) for 45 minutes. Alizarin Red S specifically binds to calcium ions in the mineralized matrix, thereby marking areas of bone formation. Following staining, cells were thoroughly rinsed with distilled water to wash away any non-specifically bound dye.

The degree of mineralization was visually assessed using a light microscope equipped with a Zeiss AxioCam MRM. Images were captured and processed using ZEN Digital Imaging for Light Microscopy v3.1 software (blue edition). For quantitative analysis, Alizarin Red S was eluted from the stained cells using 10% hexadecylpyridinium chloride (Sigma-Aldrich), a cationic surfactant that solubilizes the bound stain. The O.D. of the resulting solution was measured at a wavelength of 540 nm to quantify the extent of mineralization, providing a direct measure of osteoblast differentiation efficiency.

2.13. CELL FRACTIONATION ASSAY

Differentiated and treated 3T3-L1 adipocytes were prepared for fractionation to isolate nuclear components for further analysis. The cells were disrupted using a lysis buffer containing 20 mM Tris-HCl, 2 mM EDTA, 2 mM EGTA, 1 mM phenylmethylsulfonyl fluoride, 10 mM 2-mercaptoethanol, and protease inhibitors including 10 mg/L aprotinin, and 10 mg/mL leupeptin.

The adipocytes were mechanically disrupted using a Dounce homogenizer, a method chosen for its effectiveness in breaking down cell membranes while preserving the integrity of cellular organelles, particularly nuclei. Following homogenization, total cell lysates were centrifuged at 200 g for 10 minutes, which allows for the separation of heavier components, primarily nuclei, from the rest of the cell debris and supernatant containing cytoplasmic contents. The resulting pellet, which contains the nuclei, was carefully collected from the bottom of the tubes, ensuring minimal contamination from other cellular fractions. The isolated nuclear pellets were then processed to analyze protein expression by western blot.

2.14. BIOCHEMICAL PARAMETERS

2.14.1. ENZYMATIC QUANTIFICATION OF PLASMA LIPIDS

To assess the levels of plasma TGs and non-esterified FAs, enzymatic assays were conducted using commercial kits specifically designed for compatibility with the COBAS 6000 autoanalyzer (Roche Diagnostics, Rotkreuz, Switzerland). This method allows for precise and automated analysis of lipid profiles.

2.14.2. LEPTIN MEASUREMENT

Leptin levels in both plasma and cell-conditioned media were determined using Leptin Quantikine ELISA kits suitable for mouse and human samples (R&D Systems). The use of ELISA provides a quantitative measure of leptin concentrations, which is essential for studies exploring metabolic and hormonal responses.

2.14.3. DETERMINATION OF SUCCINATE LEVELS

For the quantification of succinate in human plasma, samples were initially processed by filtration through a 10-kDa filter. Following filtration, succinate levels were measured using a fluorometric Succinate Assay Kit (Sigma-Aldrich), which involves a fluorescence-based detection method according to the guidelines provided by the manufacturer.

In addition, the accumulation of succinate in AT was quantified in 20 mg of eWAT tissue. This analysis was performed using a Succinate Colorimetric Assay Kit (Sigma-Aldrich), which provides a colorimetric readout proportional to the succinate concentration.

2.15. GENE EXPRESSION ANALYSIS

Gene expression analysis is a fundamental technique in molecular biology that provides insights into gene regulation and cellular function by quantifying mRNA levels. This analysis is crucial for exploring the dynamic changes in gene activity under various physiological and experimental conditions.

The first and critical step in gene expression analysis involves the extraction of RNA from biological samples. The integrity and purity of RNA are vital for the reliability of gene expression data. Total RNA was isolated from various tissues and cells using TRIzol Reagent (Invitrogen, Carlsbad, CA), a solution known for its efficiency in cell lysis and RNA preservation due to its ribonuclease (RNase) inhibitory properties that prevent RNA degradation during the extraction process.

2.15.1. TOTAL RNA EXTRACTION AND QUANTIFICATION

Tissue samples were processed by homogenization in 1 mL of TRIzol reagent, while cell samples underwent lysis directly in 500 µL of TRIzol. Following a brief incubation at RT, chloroform (Sigma-Aldrich) was added to facilitate phase separation. After vigorous mixing and centrifugation, the RNA-containing aqueous phase was carefully transferred to a new tube and precipitated with isopropanol. Ethanol washes were then performed to remove impurities, and the RNA pellet was air-dried briefly. Subsequently, the dried RNA pellet was dissolved in 20-50 µL of RNase-free water, adjusting the volume based on RNA quantity and desired concentration. The resuspended RNA was heated at 55°C for optimal solubility before quality assessment or storage at -80°C for long-term preservation.

The concentration and quality of the extracted RNA were determined using the µDrop Plate and the Varioskan LUX spectrophotometer (Thermo Fisher Scientific), a crucial step to ensure the integrity of RNA for further molecular analyses. Concentration measurements were assessed based on the O.D. measured at 260 nm, while the purity of RNA samples was evaluated by calculating the O.D. ratio at 260 nm and 280 nm (A260/A280). This ratio is a critical measure of RNA purity, particularly in assessing protein contamination, which absorb light at 280 nm due to the presence of aromatic amino acids. A ratio between 1.8 and 2.0 is typically indicative of high RNA purity, suggesting minimal protein contamination.

Additionally, the A260/A230 ratio was calculated to identify any residual contaminants, such as guanidine isothiocyanate, which can interfere with subsequent RNA applications. Ratios above 2.0 generally indicate that the RNA is relatively free from such contaminants.

2.15.2. cDNA SYNTHESIS AND qPCR

For the transcription of RNA into complementary DNA (cDNA), the High-Capacity cDNA Reverse Transcription kit (Applied Biosystems, Carlsbad, CA) was utilized. This kit is designed to efficiently convert a wide range or RNA concentrations into cDNA. Following cDNA synthesis, qPCR was performed to quantify gene expression levels. The qPCR analysis was conducted using TaqMan Fast Advanced Master Mix and TaqMan Gene Expression Assays (Applied Biosystems) on a 7900HT Fast Real-Time PCR System (Applied Biosystems). The specific assays used for each gene of interest are listed in **Anex Table 2**. The thermal cycling conditions for the qPCR were set as follows: an initial hold at 50°C for 2 minutes, a second hold at 95°C for 1 minute for polymerase activation, followed by 40 cycles of denaturation at 95°C for 1 second and annealing/extension at 60°C for 20 seconds, allowing for amplification of the target cDNA.

To ensure the accuracy and reliability of the qPCR data, gene expression results were normalized to housekeeping genes. For mouse samples, the Beta-2 microglobulin (*B2m*) gene was used as the reference gene, while for human samples, ribosomal RNA (rRNA) 18S5 gene served this role. These housekeeping genes were chosen for their stable expression across the experimental conditions, providing a consistent baseline for comparative analysis.

2.15.3. DATA ANALYSIS AND INTERPRETATION

Post-qPCR, data were processed using the SDS software (Thermo Fisher Scientific). This software accurately determines the Ct values for both the target gene and the housekeeping gene used as a reference. The Ct value is a critical measurement that indicates the point at which the amount of amplified cDNA reaches a detectable level.

For quantifying relative mRNA expression levels, the comparative $2^{-\Delta\Delta Ct}$ method was employed, where ΔCt indicates the target and housekeeping gene difference, and ΔΔCt compares control and test sample ΔCt values. Gene expression fold changes were then calculated using the formula $2^{-\Delta\Delta Ct}$, normalized to the housekeeping gene, reflecting relative expression changes between test and control conditions.

To enhance data interpretability and facilitate easier visualization of gene expression differences across samples, results are often converted into a logarithmic scale, specifically $\log_2$ of the fold change values. This transformation simplifies the presentation, with positive $\log_2$ values indicating an upregulation and negative values indicating a downregulation of the target gene expression relative to the control. This logarithmic approach is particularly useful for visualizing and comparing the magnitude of gene expression changes across different experimental conditions.

2.16. TRANSCRIPTOME ANALYSIS BY RNA SEQUENCING

2.16.1. SAMPLE COLLECTION AND LIBRARY PREPARATION

Transcriptome profiling by RNA sequencing was performed on vWAT from both *Sucnr1*$^{fl/fl}$ and Ad-*Sucnr1* KO mice, with five replicates from each group. RNA was extracted from tissues using TRIzol reagent, followed by purification and DNase treatment using the RNeasy Mini Kit (Qiagen, Hilden, Germany) to ensure removal of any contaminating DNA that could interfere with subsequent analysis. Sequencing was conducted at the Centro Nacional de Análisis Genómico (CNAG-CRG, Barcelona, Spain)

RNA libraries were prepared utilizing the TruSeq Stranded Total RNA Library Prep Kit (Human/Mouse/Rat, 96 samples, Illumina, San Diego, CA), with a specific process to remove rRNA using Ribo-Zero beads to enrich for mRNA and other non-rRNA species. Subsequent purification steps included Sera Mag and RNAClean XP beads (GE

Healthcare/Thermo, Chicago, IL) to ensure high purity of the RNA sample. Post rRNA removal, the RNA was fragmented using divalent cations at elevated temperatures, and random hexamers were used for priming the RNA for first-strand cDNA synthesis using reverse transcriptase Superscript II (Invitrogen). Following first-strand synthesis, the RNA template was replaced by a second strand cDNA, incorporating deoxyuridine triphosphate instead of deoxythymidine triphosphate, facilitated by DNA Polymerase I and RNase H.

To prepare the cDNA fragments for sequencing, each fragment was modified by adding a single adenine base to its 3´blunt end, a step known as "A-tailing". This modification prevents the fragments from joining together erroneously during the next step, which is the attachment of adapters. The adapters are designed with a thymine nucleotide at their 3´ends, creating a complementary overhand that matches the adenine base on the cDNA. This specific matching facilitates the correct ligation and ensures a low occurrence of chimeric sequences, which are hybrid sequences that can interfere with sequencing outcomes. After this "A-tailing", where the adenine base is added to the cDNA, a multiple indexing adapter is ligated to the ends of the double-stranded cDNA. Finally, PCR selectively enriched DNA fragments with adapters on both ends, enhancing the DNA amount in the library using a specific PCR Primer Cocktail.

The final libraries were assessed with Bioanalyzer DNA 1000 or Fragment Analyzer (Agilent, Santa Clara, CA) to check quantity and size distribution, and quantified by qPCR using the KAPA Library Quantification Kit KK4835 (Roche, Basel, Switzerland) before sequencing.

2.16.2. SEQUENCING AND DATA ANALYSIS

Sequencing achieved at least 60 million reads per sample on the Illumina NextSeq2000 platform, with sequences processed into single FASTQ files per sample. Quality checks were conducted with FastQC (version 0.11.9; BaseSpace Labs, Illumina) to identify any issues like inappropriate guanine-cytosine content.

The reads were aligned to the *Mus musculus* genome (GRCm38.p6) using STAR software and gene mapping was done using feature Counts from Rsubread (version 2.8.2). All data were uploaded to the Gene Expression Omnibus database.

2.17.PROTEIN LEVELS ANALYSIS BY WESTERN BLOT

2.17.1. PROTEIN EXTRACTION

Total protein extraction from cells and tissues were processed and lysed using the mammalian protein extraction reagent (M-PER; Thermo Scientific), which is specifically formulated with a mild detergent base, making it highly effective for cell lysis without compromising the integrity of the proteins extracted.

To prevent protein degradation during the extraction process, a combination of protease and phosphatase inhibitor cocktails (Thermo Fisher Scientific), was added to the M-PER reagent. These inhibitors are crucial for maintaining the native state of proteins by inhibiting enzymatic activities that could otherwise alter of degrade the protein structures. The protein extracts obtained using this protocol are compatible with a variety of biochemical assays, including western blot and ELISA.

Total Protein Extraction Protocol

1. The protein lysis buffer was prepared by combining 98% M-PER, 1% protease inhibitor cocktail, and 1% phosphatase inhibitor cocktail. This mixture was kept on ice throughout the procedure to control enzymatic activity that could potentially degrade the proteins.
2. The processing is different depending on the type of sample:
   - 2.1. **For attached cells:** The culture medium was removed, and cells were washed twice with ice-cold PBS. Then, an appropriate volume of M-PER lysis buffer (ranging from 20 to 100 µL, depending on cell density and container size) was added. Cells were then detached using a cell scraper and the cell lysate was transferred to a microcentrifuge tube.
   - 2.2. **For tissues:** Fresh or frozen tissue samples were weighed and minced using a sterile scalpel. For each 100 mg of tissue, 1 mL of M-PER lysis buffer was added. The tissue was then thoroughly homogenized by pipetting up and down to ensure effective lysis.
3. Lysates were incubated on ice for 15 minutes to ensure complete lysis and centrifuged at 14,000 g for 15 minutes at 4°C to separate the cell debris from the protein-rich supernatant.
4. The clear supernatant, containing the extracted proteins, was carefully transferred to new microcentrifuge tubes. To preserve the integrity of the proteins, the lysates were stored at -80°C. It is crucial to minimize freeze-thaw cycles to prevent protein degradation.

2.17.2. PROTEIN QUANTIFICATION

Protein levels were determined using the bicinchoninic acid (BCA) Protein Assay Kit (Thermo Fisher Scientific). Samples were diluted to concentrations ranging from 1:5 to 1:20, ensuring a final volume of 10 µL within each well of a 96-well plate. The BCA working solution was prepared following the detailed instructions provided by the manufacturer, and the plate was then incubated at 37°C for 30 minutes to allow the color development to reach completion.

Subsequently, the O.D. for each well was measured at 562 nm using the Varioskan LUX spectrophotometer. A standard curve was constructed by plotting the absorbance values of the BCA standards against their respective known protein concentrations. Using the standard curve, the protein concentration of each sample was calculated by interpolating their absorbance values.

2.17.3. WESTERN BLOTTING

Western blotting is a fundamental technique widely utilized in molecular biology for the detection and quantification of specific proteins within complex biological samples. This technique first separates proteins by size through gel electrophoresis. After separation, these proteins are transferred from the gel to a membrane, where they are specifically identified using antibodies that bind to the target protein. This method is crucial for analyzing protein levels in various biological contexts, providing detailed insights into protein expression and function.

In this study, a series of polyclonal and monoclonal antibodies were used to target various phosphorylated proteins. **Table 4** and **table 5** provide the detailed list of these antibodies.

Table 4. List of Monoclonal Antibodies

Antibody	Host Species	Dilution	Supplier
Phospho (p)-AMPKα (Thr172)	Rabbit	1:1000	Cell Signaling Technology
p-IGF-I Receptor β (Tyr1135/1136)/Insulin Receptor β (Tyr1150/1151) (19H7)	Rabbit	1:1000	Cell Signaling Technology
p38 MAPK (Thr180/Tyr182)	Rabbit	1:1000	Cell Signaling Technology
p-STAT3 (Tyr705)	Rabbit	1:1000	Cell Signaling Technology
β-Actin	Mouse	1:1000	Sigma-Aldrich
Lamin A/C	Mouse	1:1000	Santa Cruz Biotechnology

Table 5. List of Polyclonal Antibodies

Antibody	Host Species	Dilution	Supplier
p-AKT (Ser473)	Rabbit	1:1000	Cell Signaling Technology
p-AKT (Thr308)	Rabbit	1:1000	Cell Signaling Technology
p-C/EBPα (Ser21)	Rabbit	1:1000	Cell Signaling Technology
p-GSK3α/β (Ser21/9)	Rabbit	1:1000	Cell Signaling Technology
p-p44/42 MAPK (Erk1/2) (Thr202/Tyr204)	Rabbit	1:1000	Cell Signaling Technology
p-SAPK/JNK (Thr183/Tyr185)	Rabbit	1:1000	Cell Signaling Technology
p-BMAL1 (Ser42)	Rabbit	1:1000	Cell Signaling Technology
BMAL1	Rabbit	1:1000	Abcam

The methods section below outlines the specific western blotting protocol employed in this thesis.

Western Blotting Protocol

1. **Protein sample preparation and electrophoresis**:
   - **1.1.** Protein samples were prepared by mixing 10-20 µg of protein lysate with 5X Laemmli Sample Buffer (Bio-Rad, Hercules, CA) and 2-mercaptoethanol (Sigma-Aldrich), diluted to achieve a final concentration of 1X.
   - **1.2.** Samples were heated at 95°C for 5 minutes in a heating block to ensure complete denaturation of proteins. Post-heating, samples were briefly centrifuged to collect any condensation.
   - **1.3.** Using the Mini-PROTEAN Tetra Cell Casting Modules (Bio-Rad), the resolving gel was prepared at 10% concentration, covered with isopropanol to level the surface, and allowed to polymerize. Once set, the isopropanol was removed, and the gel was rinsed with 1X Tris/Glycine/SDS electrophoresis running buffer (Bio-Rad)
   - **1.4.** A stacking gel was added above the resolving gel, and the comb was inserted to create wells. The assembled gels were then placed in the Mini-PROTEAN Electrophoresis Cell (Bio-Rad). Protein samples and a pre-

stained protein ladder (Thermo Fisher Scientific) were loaded into the wells.

1.5. Electrophoresis was conducted at 70 V until the protein bands began to separate, then the voltage was increased to 120 V until the dye front reached the bottom of the gel.

2. **Protein transfer**:

2.1. Concurrently, the transfer buffer (25 mM Tris, 192 mM glycine, 20% methanol, pH 8.3) was prepared and chilled on ice.

2.2. After electrophoresis, the gel apparatus was disassembled, and the gel was carefully removed.

2.3. A Immobilon-P polyvinylidene fluoride (PVDF) membrane (Merck Millipore, Burlington, MA) was activated by immersing in methanol for one minute, rinsed, and then kept wet in the transfer buffer.

2.4. The Trans-Blot Turbo Transfer System (Bio-Rad) was set up as instructed, and the gel along with the PVDF membrane were placed in a transfer sandwich and immersed in the chilled buffer.

2.5. Protein transfer was conducted at 100 V for 1.5 hours, with the setup maintained on ice to ensure cooling, facilitating protein migration from the gel into the membrane.

3. **Blocking and primary antibody incubation**:

3.1. Post-transfer, the membrane was blocked using 5% non-fat dry milk in Tris-buffered saline with Tween 20 (TBS-T) for 1 hour at RT to minimize non-specific binding.

3.2. The membrane was incubated with the primary antibody, which was diluted in the blocking solution at a typical ratio of about 1:1000, based on prior experiments. This incubation usually took place overnight at 4°C, however, the duration of incubation can vary depending on the specific antibody used.

4. **Secondary antibody binding**:

4.1. The membrane underwent three consecutive washes, each lasting 10 minutes, with TBS-T to eliminate unattached primary antibodies.

4.2. Subsequently, the membrane was incubated with an HRP-conjugated secondary, which was specific to the host species of the primary antibody. This antibody was diluted 1:2000 in TBS-T for 1 hour at RT with gentle agitation.

4.3. Following secondary antibody incubation, the membrane was washed three times for 10 minutes each with TBS-T.

5. **Detection and imaging**:
   - **5.1.** The membrane was coated evenly with a chemiluminescent substrate (Pierce ECL or SuperSignal West Femto, Thermo Fisher Scientific), prepared following the instructions provided by the manufacturer.
   - **5.2.** The emitted light was captured using an iBright CL1000 Imaging System (Thermo Fisher Scientific), where the brightness level reflected the quantity of the target protein.
   - **5.3.** The intensity of the bands was analyzed for protein quantification using iBright Analysis Software (Thermo Fisher Scientific) or similar image analysis software.
   - **5.4.** If necessary, the membrane was stripped of antibodies using Restore PLUS western blot Stripping Buffer (Thermo Fisher Scientific) and re-probed.

2.18. HISTOLOGICAL ANALYSIS METHODS FOR MOUSE TISSUE

2.18.1. HEMATOXYLIN AND EOSIN STAINING

Mouse tissue samples were processed for histological examination. Initially, tissue samples were dehydrated, embedded in paraffin, and subsequently sectioned into 5-µm thick slices. These sections were then subjected to deparaffinization and rehydration through a graded series of alcohols to water. Following rehydration, sections were stained using Harris hematoxylin (StatLab Medical Products, McKinney, TX) to highlight the cell nuclei, followed by counterstaining with eosin (Sigma-Aldrich) which stains the cytoplasmic components and connective tissue. This dual staining provides a clear differentiation of tissue structures and cellular details, essential for general histopathological evaluation.

2.18.2. UCP1 IMMUNOHISTOCHEMISTRY

For the detection of UCP1, tissue sections were deparaffinized and rehydrated through a series of xylene and alcohol washes. Subsequently, antigen retrieval was performed on the sections by heating in a solution containing 10 mM Tris, 1 mM EDTA, and 0.05% Tween-20 (Sigma-Aldrich) for 10 minutes. Sections were then treated with 1% hydrogen peroxide to block endogenous peroxidase activity. To reduce non-specific antibody binding, the tissue was incubated in a blocking solution comprising 0.2% gelatin (Sigma-Aldrich), 2% BSA, and 2% FBS in PBS at RT for 30 minutes. Sections were incubated with a primary antibody against UCP1 (1:500, Abcam) overnight at 4°C in a humidity-controlled chamber. This was followed by an incubation with a secondary anti-rabbit antibody (1:250, Amersham ECL, GE Healthcare) for 1 hour, and then with Vectastain ABC (Vector Laboratories, Burlingame, CA) for an additional hour.

Finally, the slides were stained with 3,3'-diaminobenzidine peroxidase substrate (Vector Laboratories) for 4 minutes, and nuclei were counterstained with Mayer hematoxylin for 1.5 minutes. Visualization and image capturing were conducted using a Leica DM4 B microscope and Leica software, with adipocyte size measured using the Adiposoft plug-in of ImageJ software.

2.18.3. BONE HISTOLOGY

Bone samples were first fixed in 4% PFA for 24 hours at 4°C and subsequently decalcified in 14% EDTA (pH 7.4) over a period of 6 weeks to ensure complete mineral removal without damaging the tissue structure. After decalcification, samples were embedded in paraffin, and sections of 5-µm thickness were cut. These sections were stained with hematoxylin and eosin (H&E) to assess general bone morphology and cell distribution, including osteocytes and osteoblasts.

For the identification of osteoclasts, sections underwent tartrate-resistant acid phosphatase (TRAP) staining. After deparaffinization and rehydration, slides were treated with naphthol AS-BI phosphate (Sigma-Aldrich) for 1 hour at 37°C and developed using pararosaniline hydrochloride (Sigma-Aldrich) for 3 minutes. Non-reactive tissue areas were counterstained with a 0.02% fast green solution (Sigma-Aldrich) for 45 seconds to enhance contrast. Cell counts and morphological assessments were conducted using a Nikon Eclipse E800 Microscope (Nikon, Tokyo, Japan).

2.19. LUCIFERASE REPORTER ASSAY

2.19.1. TRANSFECTION AND TREATMENT

HEK 293 cells were cultured at a density of 10^5 cells/cm^2. For the assay, cells were co-transfected with 10 ng of pBMAL-LUC plasmid (generously provided by S. Yamazaki at UT Southwestern Medical Center and K. Eckel-Mahan at the University of Texas) and pCMV6 human SUCNR1 (GFP-tagged; Origene, Rockville, MD). Transfections were performed using 0.15 mL of Lipofectamine 3000 reagent (Invitrogen) following the protocol recommended by the manufacturer. Twenty-four hours following transfection, cells were treated with SR1078 (Calbiochem), a selective agonist for the ROR-related orphan receptors a/g (RORa/RORg), which are known to activate BMAL1 expression. At 43 hours post-transfection, the cell culture medium was replaced with FBS-free medium containing 0.2% BSA to induce a state of serum deprivation. Subsequently, cells were treated with 100 µM *c*ESA to further analyze the response under these conditions.

2.19.2. LUCIFERASE ASSAY AND LUMINESCENCE MEASUREMENT

Forty-eight hours after transfection, luciferase activity within the samples was quantified using the Nano-Glo Dual-Luciferase Reporter Assay System (Promega, Madison, WI), in accordance with the instructions provided by the manufacturer. The resulting luminescence was measured with a Varioskan Luc plate reader (Thermo Fisher Scientific) in a white 96-well plate. For control measurements, the pGL3-Basic plasmid (Promega), which lacks a promoter, was transfected into cells to determine the basal luciferase expression level (designated as Luc). Additionally, cells were co-transfected with the pNL1.1.PGK[Nluc/PGK] vector (Promega) to facilitate the normalization of the results based on transfection efficiency. Each construct and treatment condition were tested in three independent transfection experiments to validate the reproducibility and reliability of the findings.

3. QUANTIFICATION AND STATISTICAL ANALYSIS

3.1. STATISTICAL ANALYSIS METHODOLOGY

To assess the normality of data distribution, Shapiro-Wilk tests were performed. For datasets adhering to a Gaussian distribution, comparisons between two groups were made using an unpaired two-tailed t-test, while comparisons involving multiple groups against a control group were conducted using one-way ANOVA followed by Dunnett post-test. For data not following a Gaussian distribution, the non-parametric Mann-Whitney two-tailed test was employed for comparing two groups, and the Kruskal-Wallis test with Dunn multiple comparisons test was utilized for assessing multiple groups against a control.

In analysis involving time-course data, such as body weight changes, GTT, ITT, two-way ANOVA was applied. All statistical analysis were performed using GraphPad Prism 8 software for Windows. Statistical significance was set at a p-value of less than 0.05.

3.2. DATA PRESENTATION TECHNIQUES

In the presentation of data, various graphical formats were employed including box-and-whisker plots, where the median was represented by the center line, the upper and lower quartiles by the box limits and the range from minimum to maximum by the whiskers; time-course graphs, which depicted data as mean ± standard error mean (SEM); and violin plots, showcasing the median and quartile lines.

3.3. REGRESSION AND MODEL FITTING

For variables dependent on mass, such as energy expenditure and food intake, a Generalized Linear Model was used to explore significant interactions between genotype and body weight, following the guidelines proposed by Mina and colleges[627]. This analysis was conducted using R software v4.2.0[628]. If no significant interaction was detected, analysis of covariance (ANCOVA) was carried out without the interaction term, with body weight as a covariate. In cases where a significant genotype effect was observed without a corresponding body weight effect, the analysis was simplified to a one-way ANOVA. Non-mass-dependent measurements like the RER were analyzed using one-way ANOVA.

3.4. STATISTICAL ANALYSIS FOR CLINICAL DATA

Clinical data were analyzed to explore associations between quantitative variables using Spearman correlation coefficients. Multiple linear regression analyses, incorporating stepwise forward selection procedures, were used to identify independent factors

associated with variables like leptin gene expression. These regression analyses were facilitated by IBM SPSS Statistics software (v27.0).

3.5. RNA SEQUENCING AND BIOINFORMATICS ANALYSIS

RNA sequencing data management and visualization were conducted using R software v4.1.2. Principal component analysis was performed using the limma package[629] (version 3.50.1) to address potential technical batch effects. Normalization and differential expression analyses were executed using the DESeq2 package[630] (version 1.34.0), with p-values adjusted for the Benjamini-Hochberg procedure to control for false discovery rates (fold change>1.25, adjusted $p<0.05$). Pathway enrichment analysis was conducted using rotation gene set tests/Gene Ser Analysis (ROAST-GSA, version 1.03.2), which integrates statistical inference techniques from limma rotations in ROAST and the re-standarized MaxMean statistic from GSA into a single hybrid methodology. Gene annotations were based on the Kyoto Encyclopedia of Genes and Genomes (KEGG) pathways using the org.Hs.eg.db Bioconductor R package. Adjusted p-values <0.25 were considered significant for pathway enrichments.

RESULTS

STUDY 1

Title: SUCNR1 signaling in adipocytes controls energy metabolism by modulating circadian clock and leptin expression.

Authors: **Villanueva-Carmona T**, Cedó L, Madeira A, Ceperuelo-Mallafré V, Rodríguez-Peña MM, Núñez-Roa C, Maymó-Masip E, Repollés-de-Dalmau M, Badia J, Keiran N, Mirasierra M, Pimenta-Lopes C, Sabadell-Basallote J, Bosch R, Caubet L, Escolà-Gil JC, Fernández-Real JM, Vilarrasa N, Ventura F, Vallejo M, Vendrell J, Fernández-Veledo S.

Journal: Cell Metabolism

Impact factor: 27.7

Citation: Villanueva-Carmona T, Cedó L, Madeira A, et al. SUCNR1 signaling in adipocytes controls energy metabolism by modulating circadian clock and leptin expression. *Cell Metab*. 2023;35(4):601-619.e10. doi:10.1016/j.cmet.2023.03.004

The study was highlighted in Nature Reviews Endocrinology under the title "Succinate Signalling Regulates Leptin Production in Adipocytes". *Nat Rev Endocrinol*. 2023;19(6):314. doi:10.1038/s41574-023-00838-z (Impact Factor: 47.6), emphasizing the significance of the findings within the scientific community. Furthermore, this work led to the development and publication of a comprehensive protocol entitled "Protocol for the *in vitro* isolation and culture of mature adipocytes and white adipose tissue explants from humans and mice", which is included as "Study 2" in this doctoral thesis.

STUDY 2

Title: Protocol for the *in vitro* isolation and culture of mature adipocytes and white adipose tissue explants from humans and mice

Authors: **Villanueva-Carmona T**, Cedó L, Núñez-Roa C, Maymó-Masip E, Vendrell J, Fernández-Veledo S.

Journal: STAR Protocols

Impact factor: 1.3

Citation: Villanueva-Carmona T, Cedó L, Núñez-Roa C, Maymó-Masip E, Vendrell J, Fernández-Veledo S. Protocol for the *in vitro* isolation and culture of mature adipocytes and white adipose tissue explants from humans and mice. *STAR Protoc*. 2023;4(4):102693. doi:10.1016/j.xpro.2023.102693

STUDY 1

SUCNR1 signaling in adipocytes controls energy metabolism by modulating circadian clock and leptin expression.

Villanueva-Carmona T, Cedó L, Madeira A, Ceperuelo-Mallafré V, Rodríguez-Peña MM, Núñez-Roa C, Maymó-Masip E, Repollés-de-Dalmau M, Badia J, Keiran N, Mirasierra M, Pimenta-Lopes C, Sabadell-Basallote J, Bosch R, Caubet L, Escolà-Gil JC, Fernández-Real JM, Vilarrasa N, Ventura F, Vallejo M, Vendrell J, Fernández-Veledo S.

ABSTRACT

AT plays a key role in regulating energy balance by secreting leptin. However, the factors influencing leptin production are not well understood. Our research indicates that succinate, traditionally known for its role in immune response and lipolysis, regulates leptin expression through its receptor SUCNR1. Deleting *Sucnr1* specifically in adipocytes affects metabolic health depending on the nutritional state. *Sucnr1* deficiency in adipocytes disrupts leptin response to feeding, while oral succinate mimics nutrient-induced leptin changes via SUCNR1. Activation of SUCNR1 modulates leptin expression through the circadian clock and involves the AMPK/JNK-C/EBPα pathway. Despite its anti-lipolytic role in obesity, SUCNR1 also regulates leptin signaling, contributing to a metabolically favorable phenotype in mice with adipocyte-specific *Sucnr1* KO under normal diet conditions. In humans, obesity-related hyperleptinemia is associated with overexpression of SUCNR1 in adipocytes, making it a primary predictor of leptin levels in AT. Our findings identify the succinate/SUCNR1 axis as a critical pathway for nutrient-related leptin dynamics and overall energy homeostasis.

UNIVERSITAT ROVIRA I VIRGILI
Metabolic Impact of the Succinate/SUCNR1 Axis in Adipocytes: Insights into Circadian and Leptin Regulation
TERESA VILLANUEVA CARMONA

Article

Cell Metabolism

SUCNR1 signaling in adipocytes controls energy metabolism by modulating circadian clock and leptin expression

Graphical abstract

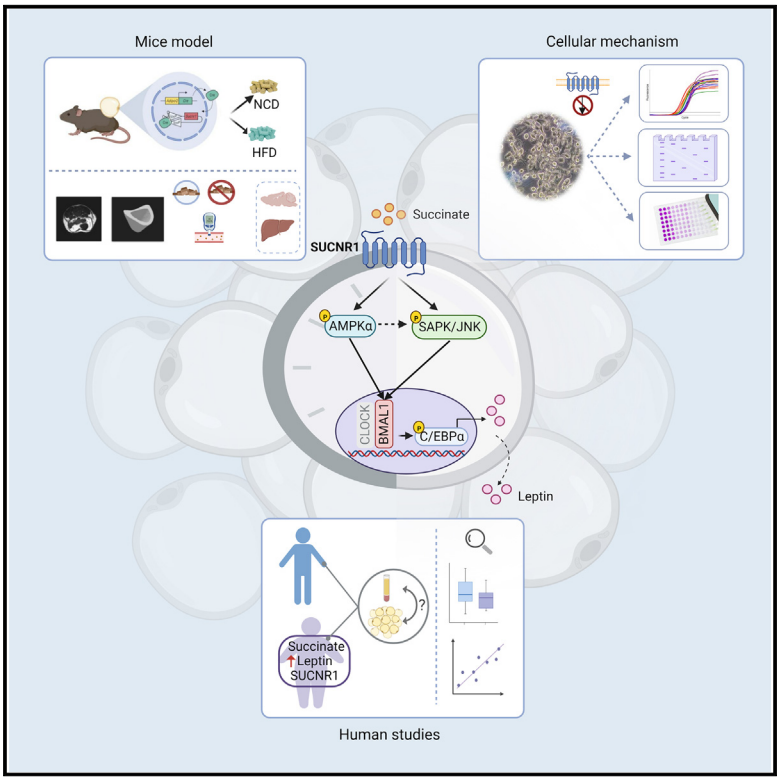

Authors

Teresa Villanueva-Carmona, Lídia Cedó, Ana Madeira, ..., Mario Vallejo, Joan Vendrell, Sonia Fernández-Veledo

Correspondence

sonia.fernandez@iispv.cat

In brief

Villanueva-Carmona et al. describe a new function for the succinate/SUCNR1 axis in controlling leptin expression in adipocytes via a mechanism involving the circadian clock. This system is overactivated in obesity, which might contribute to obesity-related hyperleptinemia.

Highlights

- Extracellular succinate in adipocytes controls circadian clock and leptin via SUCNR1
- SUCNR1 modulates leptin via AMPK/JNK-BMAL1-C/EBPα-dependent signaling
- The metabolic impact of SUCNR1 deficiency in adipocytes is dependent on nutritional status
- Hyperleptinemia in human obesity is related to overactive succinate/SUCNR1 signaling

Villanueva-Carmona et al., 2023, Cell Metabolism *35*, 601–619
April 4, 2023 © 2023 Elsevier Inc.
https://doi.org/10.1016/j.cmet.2023.03.004

CellPress

UNIVERSITAT ROVIRA I VIRGILI
Metabolic Impact of the Succinate/SUCNR1 Axis in Adipocytes: Insights into Circadian and Leptin Regulation
TERESA VILLANUEVA CARMONA

Cell Metabolism

CellPress

Article

SUCNR1 signaling in adipocytes controls energy metabolism by modulating circadian clock and leptin expression

Teresa Villanueva-Carmona,[1,2,15] Lídia Cedó,[1,2,15] Ana Madeira,[1,2] Victòria Ceperuelo-Mallafré,[1,2,3] M.-Mar Rodríguez-Peña,[1,2] Catalina Núñez-Roa,[1,2] Elsa Maymó- Masip,[1,2] Maria Repollés-de-Dalmau,[1,2,3] Joan Badia,[4] Noelia Keiran,[1,2] Mercedes Mirasierra,[2,5] Carolina Pimenta-Lopes,[6] Joan Sabadell-Basallote,[1,2] Ramón Bosch,[7] Laura Caubet,[8] Joan Carles Escolà- Gil,[2,9,10] José-Manuel Fernández-Real,[11,12,13] Nuria Vilarrasa,[2,14] Francesc Ventura,[6] Mario Vallejo,[2,5] Joan Vendrell,[1,2,3,16] and Sonia Fernández-Veledo[1,2,16,17,*]

[1]Department of Endocrinology and Nutrition, Research Unit, Institut d'Investigació Sanitària Pere Virgili (IISPV), Hospital Universitari de Tarragona Joan XXIII, Tarragona 43005, Spain
[2]CIBER de Diabetes y Enfermedades Metabólicas Asociadas (CIBERDEM), Instituto de Salud Carlos III, Madrid 28029, Spain
[3]Department of Medicine and Surgery, Universitat Rovira i Virgili (URV), Reus 43201, Spain
[4]Institut d'Oncologia de la Catalunya Sud, Hospital Universitari Sant Joan de Reus, IISPV, Reus 43204, Spain
[5]Instituto de Investigaciones Biomédicas Alberto Sols, Consejo Superior de Investigaciones Científicas/Universidad Autónoma de Madrid (CSIC/UAM), Madrid 28029, Spain
[6]Departament de Ciències Fisiològiques, Universitat de Barcelona, IDIBELL, Hospitalet de Llobregat, Barcelona 08907, Spain
[7]Department of Pathology, Oncological Pathology and Bioinformatics Research Group, Hospital de Tortosa Verge de la Cinta, IISPV, Tortosa 43500, Spain
[8]General and Digestive Surgery Service, Hospital Sant Pau i Santa Tecla, Institut d'Investigació Sanitària Pere Virgili, Tarragona 43003, Spain
[9]Institut d'Investigacions Biomèdiques (IIB) Sant Pau, Barcelona 08041, Spain
[10]Departament de Bioquímica i Biologia Molecular, Universitat Autònoma de Barcelona, Cerdanyola del Vallès, Barcelona 08193, Spain
[11]Department of Diabetes, Endocrinology and Nutrition, Institut d'Investigació Biomèdica de Girona (IdIBGi), Salt 17190, Spain
[12]CIBER Fisiopatología de la Obesidad y Nutrición (CB06/03/010), Instituto de Salud Carlos III, Madrid 28029, Spain
[13]Department of Medical Sciences, School of Medicine, University of Girona, Girona 17004, Spain
[14]Department of Endocrinology and Nutrition, Hospital Universitari Bellvitge – IDIBELL, Hospitalet de Llobregat, Barcelona 08907, Spain
[15]These authors contributed equally
[16]Senior author
[17]Lead contact
*Correspondence: sonia.fernandez@iispv.cat
https://doi.org/10.1016/j.cmet.2023.03.004

SUMMARY

Adipose tissue modulates energy homeostasis by secreting leptin, but little is known about the factors governing leptin production. We show that succinate, long perceived as a mediator of immune response and lipolysis, controls leptin expression via its receptor SUCNR1. Adipocyte-specific deletion of *Sucnr1* influences metabolic health according to nutritional status. Adipocyte *Sucnr1* deficiency impairs leptin response to feeding, whereas oral succinate mimics nutrient-related leptin dynamics via SUCNR1. SUCNR1 activation controls leptin expression via the circadian clock in an AMPK/JNK-C/EBPα-dependent manner. Although the anti-lipolytic role of SUCNR1 prevails in obesity, its function as a regulator of leptin signaling contributes to the metabolically favorable phenotype in adipocyte-specific *Sucnr1* knockout mice under standard dietary conditions. Obesity-associated hyperleptinemia in humans is linked to SUCNR1 overexpression in adipocytes, which emerges as the major predictor of adipose tissue leptin expression. Our study establishes the succinate/SUCNR1 axis as a metabolite-sensing pathway mediating nutrient-related leptin dynamics to control whole-body homeostasis.

INTRODUCTION

The concept of "signaling metabolites" in the control of metabolic homeostasis is gaining traction. The Krebs cycle substrate succinate, a pleiotropic metabolite that acts akin to hormones and cytokines through succinate receptor 1 (SUCNR1), is one example of this new class of metabolites.[1,2] SUCNR1 has a broad expression in tissues and is highly abundant in white adipose tissue (WAT).[3,4] It was generally assumed that SUCNR1 is functionally inactive in healthy tissues, and for many years, SUCNR1 was investigated mainly in inflammatory-related conditions,[5–8] particularly in those associated with chronic

UNIVERSITAT ROVIRA I VIRGILI
Metabolic Impact of the Succinate/SUCNR1 Axis in Adipocytes: Insights into Circadian and Leptin Regulation
TERESA VILLANUEVA CARMONA

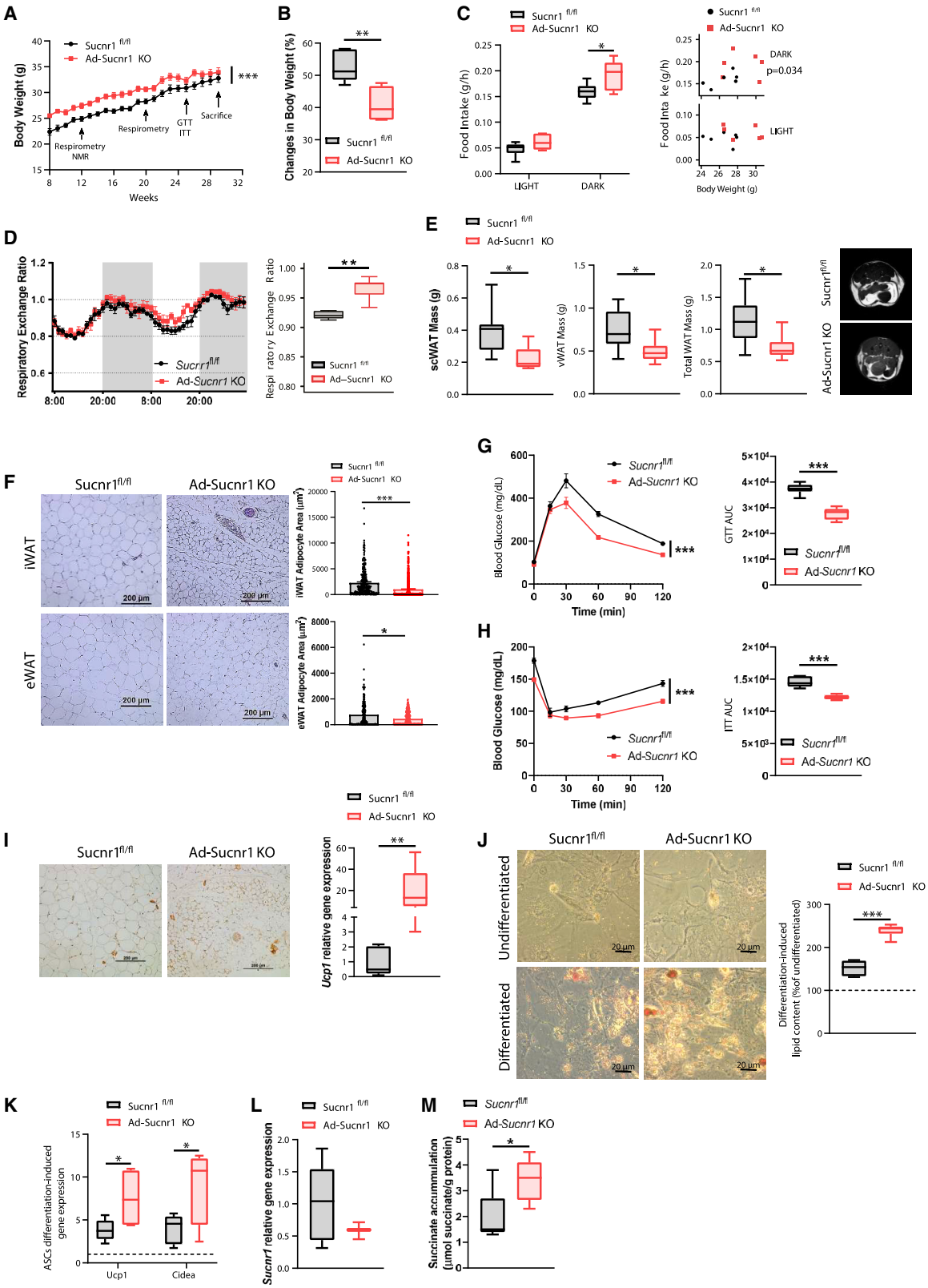

(legend on next page)

UNIVERSITAT ROVIRA I VIRGILI
Metabolic Impact of the Succinate/SUCNR1 Axis in Adipocytes: Insights into Circadian and Leptin Regulation
TERESA VILLANUEVA CARMONA

CellPress

hypersuccinemia.[9–12] Recent studies, however, have described that extracellular succinate transiently increases in response to physiological stimuli including exercise,[13] cold exposure,[14] or food ingestion, as we recently reported.[15] Succinate thus emerges as a reporter of both tissue stress and metabolism, opening up the possibility of its involvement in other metabolic functions as a hormone-like metabolite.[1] Indeed, "succinate sensing" by SUCNR1 may constitute part of the metabolite-sensing machinery governing energy homeostasis.

Adipose tissue is central in the regulation of whole-body energy homeostasis. WAT functions both as a key energy reservoir and an endocrine organ by producing an array of secreted factors that act centrally and peripherally to control metabolic activity.[16] Chief among these factors is leptin, which controls adipose tissue mass by regulating food intake through signaling in the central nervous system (CNS).[17,18] Circulating levels of leptin are proportional to fat stores[19,20] and increase after feeding.[21] The discovery of leptin in 1994 led to a paradigm shift in our conception of adipose tissue, but how adipocytes regulate leptin production remains enigmatic. Many studies have attempted to elucidate leptin action in both peripheral and CNS tissues[17,22] and understand leptin resistance in obesity.[23,24] So far, only a few factors have been described as regulators of leptin expression and secretion, including insulin,[25–27] glucocorticoids,[26–28] and catecholamines.[26,29,30]

Although SUCNR1 is highly expressed in adipocytes,[3] thus far, the only function ascribed to it in this tissue is the inhibition of lipolysis, which is important in obesity.[3,4,31] As with other G protein-coupled receptors (GPCRs), SUCNR1 transmits signals through multiple pathways in a cell-specific manner[32]; however, our knowledge of the signaling properties of this receptor is limited. SUCNR1 engagement in white adipocytes has been associated with the $G\alpha_i$-cAMP signaling transduction pathway,[4] and the anti-lipolytic action of the succinate/SUCNR1 axis could provide a good explanation for the moderate lean phenotype observed in whole-body *Sucnr1*-knockout (KO) mice under standard dietary conditions.[3] However, discrepant results have been reported in *Sucnr1*-KO mice fed obesogenic diets.[3,33] Given that energy homeostasis requires multi-tissue crosstalk, the use of cell-specific KO approaches is invaluable to decipher tissue-specific gene functions. This strategy has led to a better understanding of the key role of the succinate/SUCNR1 axis in macrophage immune response in obesity.[34]

Here, we investigated the contribution of the succinate/SUCNR1 axis to adipose tissue physiology by generating mice lacking *Sucnr1* specifically in adipocytes. Metabolic phenotyping of these mice under standard dietary conditions and after diet-induced obesity, coupled with *in vitro* and human studies, demonstrates that the succinate/SUCNR1 axis is a novel regulator of leptin production in adipocytes. Our study supports the novel concept that SUCNR1 is a key metabolic sensor in energy homeostasis.

RESULTS

Conditional adipocyte deletion of *Sucnr1* reduces adipose mass and improves systemic metabolic health

We selectively inactivated *Sucnr1* in murine adipocytes. Mice carrying the floxed *Sucnr1* allele containing two *loxP* sites flanking exon 2[3] were bred with transgenic mice expressing Cre recombinase driven by the adipocyte-specific *Adipoq* promoter, generating *Sucnr1*$^{fl/fl}$ *Adipoq*-Cre$^{+/-}$ mice (hereafter referred to as Ad-*Sucnr1* KO mice). Cre-negative *Sucnr1*$^{fl/fl}$ mice (*Sucnr1*$^{fl/fl}$ *Adipoq*-Cre$^{-/-}$) served as controls (referred to as *Sucnr1*$^{fl/fl}$ mice) (Figures S1A and S1B). Ad-*Sucnr1* KO mice were born at a normal Mendelian ratio and were viable, and no gross morphological differences were observed between genotypes. As expected, *Sucnr1* expression was negligible in all the examined fat depots of Ad-*Sucnr1* KO mice when compared with *Sucnr1*$^{fl/fl}$ mice, whereas no changes were observed in other tissues such as the liver and spleen (Figure S1C). *Sucnr1* expression in *Sucnr1*$^{fl/fl}$ mice was lower in brown adipose tissue (BAT) than that in WAT (Figure S1D).

Body weight was higher in 8-week-old Ad-*Sucnr1* KO mice than in age-matched *Sucnr1*$^{fl/fl}$ littermates on a normal chow diet (NCD), but these differences disappeared at 30 weeks of age (Figures 1A and 1B), suggesting that Ad-*Sucnr1* KO mice show resistance to age-related body weight gain. Indirect calorimetry analysis at 12 weeks of age revealed similar energy expenditure (EE) between genotypes (Figure S2A); however, Ad-*Sucnr1* KO mice had a significantly higher food intake during the dark (active) phase, which was independent of body weight (Figure 1C) and a significantly higher respiratory exchange ratio

Figure 1. Conditional adipocyte deletion of *Sucnr1* reduces adipose mass and improves systemic metabolic health

(A) Body weight progression in Ad-*Sucnr1* KO and *Sucnr1*$^{fl/fl}$ mice fed NCD for 29 weeks (n = 14 *Sucnr1*$^{fl/fl}$; n = 12 Ad-*Sucnr1* KO).

(B) Changes in body weight (n = 6 mice/group).

(C) Food intake during light and dark hours (left) and regression-based plot of food intake with body weight as a covariate (right) (genotype p = 0.034 in dark) (n = 6/group).

(D) RER (left: time course; and right: average/mouse) at week 12 of life (p = 0.003) (n = 6/group).

(E) qMRI quantification of scWAT, vWAT, and total WAT mass, and representative qMRI images of fat (n = 8 *Sucnr1*$^{fl/fl}$; n = 6 Ad-*Sucnr1* KO) at week 12 of life.

(F) Representative H&E-stained images of iWAT and eWAT, and quantification of adipocyte area (scale bars, 200 μm).

(G) Glucose tolerance test (GTT) and its respective area under the curve (AUC) at week 25 of life (n = 6 mice/group).

(H) Insulin tolerance test (ITT) and its respective AUC at week 25 of life (n = 6 mice/group).

(I) Representative images of UCP1 immunohistochemistry, and *Ucp1* relative gene expression in iWAT (n = 5/group) (scale bars, 200 μm).

(J) Representative oil-red O-stained images of mouse adipose tissue stem cells (mASCs) undifferentiated and differentiated to brown adipocytes, and quantification of differentiation-induced lipid accumulation (n = 6 *Sucnr1*$^{fl/fl}$; n = 9 Ad-*Sucnr1* KO) (scale bars, 20 μm).

(K) Fold change of *Ucp1* and *Cidea* expression in mASCs differentiated to brown adipocytes (n = 6 *Sucnr1*$^{fl/fl}$; n = 4 Ad-*Sucnr1* KO).

(L) *Sucnr1* expression in mASCs (n = 5 *Sucnr1*$^{fl/fl}$; n = 3 Ad-*Sucnr1* KO).

(M) Succinate accumulation in eWAT explants (n = 7 *Sucnr1*$^{fl/fl}$; n = 5 Ad-*Sucnr1* KO). Data are presented as box and whiskers plots showing median, first, and third quartiles and maximum and minimum values; or as mean ± SEM; *p < 0.05, **p < 0.01; ***p < 0.001 (unpaired t test or Mann-Whitney test in box and whiskers plots, two-way ANOVA in A, G, and H, one-way ANOVA in C and D).

UNIVERSITAT ROVIRA I VIRGILI
Metabolic Impact of the Succinate/SUCNR1 Axis in Adipocytes: Insights into Circadian and Leptin Regulation
TERESA VILLANUEVA CARMONA

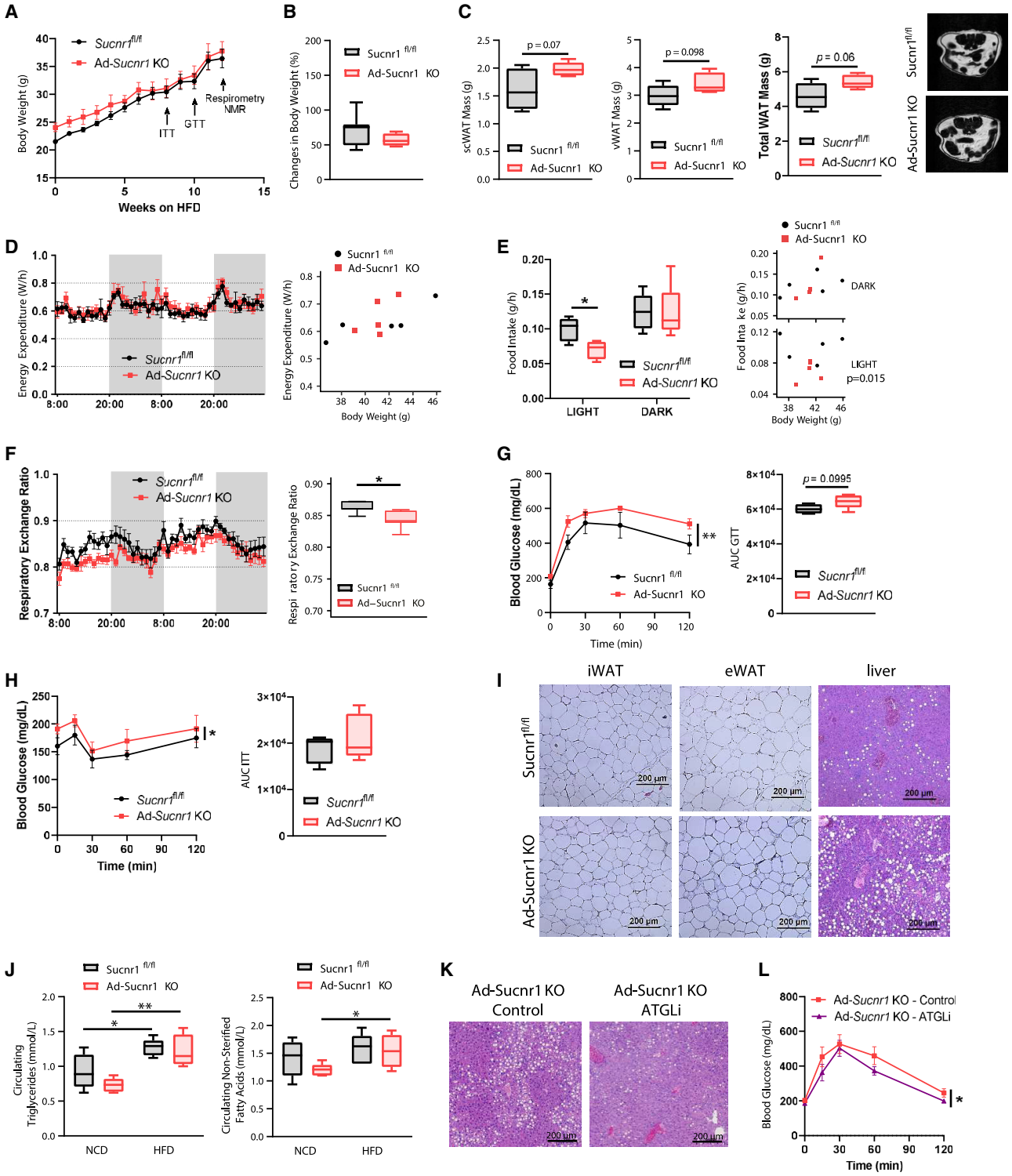

Figure 2. Mice with conditional adipocyte deletion of *Sucnr1* develop hepatic steatosis and glucose intolerance on a high-fat diet

(A and B) (A) Body weight progression and (B) body weight gain in Ad-*Sucnr1* KO and *Sucnr1*$^{fl/fl}$ mice fed HFD for 12 weeks, starting at 8 weeks of age (n = 11 *Sucnr1*$^{fl/fl}$; n = 4 Ad-*Sucnr1* KO).

(C) qMRI quantification of scWAT, vWAT, and total WAT mass, and representative qMRI images of fat after 12 weeks of HFD feeding (n = 5/group).

(D–F) (D) EE (left) and regression-based plot of EE with body weight as covariate (right) (weight p = 0.034 and genotype p = 0.437); (E) food intake during light and dark hours (left) and regression-based plot of food intake with body weight as a covariate (right) (genotype p = 0.015 in light), and (F) RER (left: time course; and right: average/mouse) (p = 0.048) after 12 weeks of HFD feeding (n = 5/group).

(legend continued on next page)

UNIVERSITAT ROVIRA I VIRGILI
Metabolic Impact of the Succinate/SUCNR1 Axis in Adipocytes: Insights into Circadian and Leptin Regulation
TERESA VILLANUEVA CARMONA

(RER) (Figure 1D). No differences were observed in locomotor activity between genotypes (data not shown). Similar results were obtained at 20 weeks of age (Figures S2B–S2D). Body composition analysis by quantitative magnetic resonance imaging (qMRI) at 12 weeks of age showed that the total amount of subcutaneous WAT (scWAT) and visceral WAT (vWAT) fat was significantly lower in Ad-*Sucnr1* KO mice than that in *Sucnr1*$^{fl/fl}$ mice (Figure 1E), whereas muscle mass was similar (Figure S2E). The lower adiposity in Ad-*Sucnr1* KO mice was also evident at 29 weeks of age (Figure S2F). In line with this, the histology of adipose tissue revealed a significantly smaller adipocyte area of inguinal WAT (iWAT) and epididymal WAT (eWAT) in Ad-*Sucnr1* KO mice (Figure 1F). No overt histological differences were noted between genotypes in other metabolic tissues (Figure S2G). Consistent with the adipose tissue phenotype, glucose tolerance (Figure 1G) and insulin sensitivity (Figure 1H) were significantly better in Ad-*Sucnr1* KO mice than those in *Sucnr1*$^{fl/fl}$ mice.

Although the lower fat mass in *Ad-Sucnr1* KO mice could be explained by the known anti-lipolytic function of SUCNR1[3,4] (Figure S2H), long-term inhibition of lipolysis *in vivo* with atglistatin (ATGLi, a specific inhibitor of adipose triglyceride lipase) had no significant impact on body weight gain as expected[35] (Ad-*Sucnr1* KO-control = 9.07% ± 4.98% vs. Ad-*Sucnr1* KO-ATGLi = 5.22% ± 3.08%). There were no substantial changes in adipocyte size (only a small increase was detected in iWAT, Figure S2I) and glucose tolerance (Figure S2J) in *Ad-Sucnr1* KO mice on NCD. This agrees with previous findings demonstrating that general GPCR-mediated lipolysis is not perturbed in global *Sucnr1* KO mice under steady-state conditions[3] and points to alternative mechanisms underlying the metabolically favorable phenotype of Ad-*Sucnr1* KO mice.

The reduced adipose mass in Ad-*Sucnr1* KO mice was associated with a marked increase in the expression of the BAT activation marker uncoupling protein 1 (UCP1) in WAT (Figure 1I) but not in BAT (Figure S2K). It was previously reported that the differentiation ability of adipocyte precursors to white adipocytes was unaffected by global *Sucnr1* deletion.[3] We found that adipose-derived stem cells from Ad-*Sucnr1* KO mice displayed a more robust brown adipocyte differentiation capacity than equivalent cells from control mice, as revealed by the higher expression of browning-related genes (Figures 1J and 1K). This was not related to the differences in *Sucnr1* expression in adipocyte precursors (Figure 1L). Induction of WAT browning correlated with the accumulation of succinate, which has been previously described as a thermogenic and browning agent,[14,36] in *ex vivo* adipocyte explants from *Sucnr1*-deficient WAT (Figure 1M). Overall, these results demonstrate that conditional *Sucnr1* deletion in adipocytes reduces adiposity (but not body weight) and improves glucose homeostasis by a mechanism that could be dependent on WAT browning.

Mice with conditional adipocyte deletion of *Sucnr1* develop hepatic steatosis and glucose intolerance on an HFD

Obesity induces elevated adipose tissue *SUCNR1* expression in both mice and humans.[34] To examine the role of adipocyte *Sucnr1* in the context of overnutrition, mice were placed on a high-fat diet (HFD) for 12 weeks. Contrary to the results on NCD, body weight gain (Figures 2A and 2B) was similar between genotypes after this period. Analysis of the fat mass revealed the opposite phenotype to that seen on NCD, with a trend for greater fat mass in Ad-*Sucnr1* KO mice than that in *Sucnr1*$^{fl/fl}$ mice (Figure 2C). Comparative analyses of energy parameters revealed a similar EE (Figure 2D), but a lower food intake during the light phase (Figure 2E) and a lower RER (Figure 2F) in Ad-*Sucnr1* KO mice. The change in fuel preference toward lipids is in agreement with the evident glucose intolerance (Figure 2G) and insulin resistance (Figure 2H) in the absence of significant changes in adipose tissue morphology (Figure 2I). Furthermore, HFD-induced hepatic steatosis was more severe in Ad-*Sucnr1* KO mice (Figure 2I). This might explain why no differences were detected in plasma triglycerides and non-esterified fatty acids between genotypes (Figure 2J) despite the known negative control of lipolysis by SUCNR1.[3,4] Indeed, the inhibition of lipolysis with ATGLi for 2 weeks ameliorated the HFD-induced hepatic steatosis in Ad-*Sucnr1* KO mice (Figure 2K), which was accompanied by improved glucose tolerance (Figure 2L). Collectively, the data indicate that in response to overnutrition, mice with adipocyte-specific deletion of *Sucnr1* have ectopic fat deposition in the liver and glucose homeostasis disturbances. The opposite metabolic phenotype of Ad-*Sucnr1* KO mice during the nutritional challenge seems to be mostly dependent on the anti-lipolytic effect of SUCNR1.

Mice with conditional adipocyte deletion of *Sucnr1* develop a bone mass phenotype

To better understand the greater body weight of young Ad-*Sucnr1* KO mice despite the lower fat mass (and similar skeletal muscle mass), we assessed whether *Sucnr1* loss in adipocytes might indirectly impact skeletal mass, which accounts for ~5% of total body weight in mice.[37] Microcomputed tomography analysis of tibias showed that the adipocyte deletion of *Sucnr1* changed the cortical bone mass. The cortical bone volume was significantly higher in Ad-*Sucnr1* KO mice than that in *Sucnr1*$^{fl/fl}$ mice, concomitant with a significant increase in cortical thickness and bone perimeter around the midshaft (Figure 3A). The trabecular bone architecture of the same mice was

(G) GTT and its respective AUC after 10 weeks of HFD feeding (n = 5/group).
(H) ITT and its respective AUC after 8 weeks of HFD feeding (n = 5/group).
(I) Representative H&E-stained images of iWAT, eWAT, and liver (scale bars, 200 μm).
(J) Circulating levels of triglycerides and non-esterified fatty acids (n = 8 *Sucnr1*$^{fl/fl}$ and n = 6 Ad-*Sucnr1* KO fed NCD; n = 5 *Sucnr1*$^{fl/fl}$ and n = 4 Ad-*Sucnr1* KO fed HFD).
(K and L) (K) Liver H&E staining (scale bars, 200 μm) and (L) GTT in Ad-*Sucnr1* KO mice fed HFD for 8 weeks and treated with ATGLi or vehicle (corn oil) for 2 weeks (n = 3 vehicle- and n = 4 ATGLi-treated mice). Data are presented as box and whiskers plots showing median, first, and third quartiles and maximum and minimum values, or as mean ± SEM; *$p < 0.05$; **$p < 0.01$ (unpaired t test or Mann-Whitney test in bar graphs; two-way ANOVA in A, G, H, and L; ANCOVA in D; and one-way ANOVA in E and F).

UNIVERSITAT ROVIRA I VIRGILI
Metabolic Impact of the Succinate/SUCNR1 Axis in Adipocytes: Insights into Circadian and Leptin Regulation
TERESA VILLANUEVA CARMONA

unchanged (Figure 3B), but the tibial length was significantly longer in Ad-*Sucnr1* KO mice (Figure 3C). Comparable numbers of osteoclasts (Ocls) per bone surface were observed between genotypes (Figure 3D), but hematoxylin and eosin (H&E) staining of the tibiae sections revealed a significantly higher number of osteocytes (Ocys) per bone area in the cortical bone of Ad-*Sucnr1* KO mice, together with a greater number of osteoblasts (OBs) in the bone surfaces of both cortical and trabecular bones (Figure 3E). Similar to adipocytes, OBs derive from mesenchymal stem cells (MSCs).[38] Analysis of the OB differentiation potential of bone-marrow-MSCs failed to reveal significant differences between genotypes (Figure S3A). Changes to the bone phenotype were less evident in mice on HFD (Figures S3B and S3C), and the increases in bone volume, cortical thickness, trabecular number, and the number of Ocys were not significant. Altogether, these findings point to a potential indirect effect of the adipocyte-specific deletion of *Sucnr1* on postnatal growth and bone development, which might explain the initial body weight differences between genotypes.

Mice with conditional adipocyte deletion of *Sucnr1* have disturbances in leptin expression

Mice with global loss of *Sucnr1* on NCD have low fasting levels of some adipokines,[3] suggesting a possible endocrine role for SUCNR1 in adipocytes. Given the metabolic phenotype of Ad-*Sucnr1* KO mice in terms of food intake and fat and bone mass, we investigated leptin as a master regulator of these biological processes. Strikingly, the circulating leptin response to refeeding was substantially weaker in global *Sucnr1* KO than that in wild-type (WT) mice (Figure 4A). This was also evident in Ad-*Sucnr1* KO mice (Figure 4B). In addition, the postnatal leptin surge that occurs physiologically in mice[39] (10-day leptin = 16.12 ± 2.35 ng/mL vs. 21-day leptin = 2.83 ± 0.57 ng/mL, *Sucnr1*$^{fl/fl}$ mice) was affected by *Sucnr1* deficiency, as Ad-*Sucnr1* KO mice showed a trend for a decrease in the 10-day leptin level (Figure 4C). Consistent with this, *Lep* gene expression in WAT (Figure 4D) and serum leptin levels (Figure 4E) were significantly lower in adult Ad-*Sucnr1* KO mice than those in *Sucnr1*$^{fl/fl}$ mice, which might explain the hyperphagia in Ad-*Sucnr1* KO mice on NCD (Figure 1C). Furthermore, Ad-*Sucnr1* KO mice displayed a disturbance in the natural regulation of appetite-related neuropeptides during the fasting-feeding transition, particularly those associated with orexigenic signaling (*Npy* and *Agrp*) (Figure 4F). In line with this, feed-induced signal transducer and activator of transcription 3 (STAT3) phosphorylation (a surrogate marker of leptin signaling) was diminished in the hypothalamus of Ad-*Sucnr1* KO mice (Figures 4G and S4A), which was not associated with changes in leptin sensitivity (Figures 4H and 4I).

Circulating levels of leptin are proportional to body fat mass.[19,20] No differences were observed in leptin levels between Ad-*Sucnr1* KO and control mice on HFD (*Sucnr1*$^{fl/fl}$ = 65.4 ± 8.1 ng/mL vs. Ad-*Sucnr1* KO = 64.3 ± 5.2 ng/mL), despite the trend for greater fat mass in the former (Figure 2C). Notably, the positive correlation between fat mass and leptin levels in *Sucnr1*$^{fl/fl}$ mice fed NCD or HFD ($r = 0.932$, $p = 0.006$; $r = 0.995$, $p = 0.0004$, respectively) was lost in Ad-*Sucnr1* KO mice ($r = 0.476$, $p = 0.417$; $r = 0.183$, $p = 0.768$, respectively), which supports our observations linking SUCNR1 to leptin.

We confirmed that the lower leptin levels found under standard dietary conditions were the consequence of *Sucnr1* deficiency and not an indirect effect of the lower fat mass in Ad-*Sucnr1* KO mice. Basal leptin release was lower in Ad-*Sucnr1* KO WAT *ex vivo* explants than in controls (Figure 4J). Of note, exogenous succinate enhanced *Lep* gene expression in *Sucnr1*$^{fl/fl}$ adipocytes but not in adipocytes from Ad-*Sucnr1* KO mice (Figure 4K). The expression of typical adipogenic markers (e.g., *Pparg*, *Fasn*, and *Slc2a4*) was comparable between adipocytes from both genotypes (Figure 4L), indicating that the nonresponse of Ad-*Sucnr1* KO adipocytes was a consequence of *Sucnr1* deficiency, rather than a defect in differentiation. Finally, oral administration of succinate provoked a significant increase in plasma leptin levels in *Sucnr1*$^{fl/fl}$ mice but not in Ad-*Sucnr1* KO mice (Figure 4M), confirming a role for the succinate/SUCNR1 axis in leptin regulation.

To investigate whether the low leptin levels are related to the metabolically favorable phenotype of Ad-*Sucnr1* KO mice under NCD, we performed a 4-week leptin intervention. Leptin replacement therapy increased adipocyte size (Figure 4N) and impaired glucose tolerance (Figure 4O) in Ad-*Sucnr1* KO mice. This suggests that the low leptin levels observed in Ad-*Sucnr1* KO mice on NCD, together with the induction of WAT browning (Figure 1I), are likely both associated with the reduction in adiposity of Ad-*Sucnr1* KO mice.

Succinate/SUCNR1 signaling controls leptin expression in an AMPK/JNK/C/EBPα-dependent manner

To question how succinate/SUCNR1 signaling controls leptin expression, we first evaluated the effect of SUCNR1 activation on leptin expression in murine 3T3-L1 adipocytes. Similar to our findings in *Sucnr1*$^{fl/fl}$ adipocytes (Figure 4K), exposure to succinic acid significantly increased *Lep* expression in 3T3-L1 adipocytes (Figure 5A), an effect that was mimicked by the SUCNR1 agonist *cis*-epoxysuccinic acid (cESA) (Figure 5B). We confirmed this in human adipocytes, finding also a positive effect of extracellular succinic acid on leptin release (Figure 5C). No significant upregulation of adiponectin gene expression was observed (Figure S5A). SUCNR1 engagement in adipocytes induced c-Jun N-terminal kinase (JNK) and p38 mitogen-activated protein kinase (MAPK) phosphorylation in a dose- and time-dependent manner (Figure 5D). Notably, we also found that SUCNR1 activation triggered AMP-activated protein kinase (AMPK) phosphorylation/activation at Thr172, which is concomitant with a blockade of activating Ser473 phosphorylation of AKT and its downstream target glycogen synthase kinase 3 (GSK-3).[40] Accordingly, the activation of AMPK with 5-aminoimidazole-4-carboxamide ribonucleotide (AICAR) induced leptin expression in 3T3-L1 adipocytes (Figure 5E), similar to the activation of SUCNR1 (Figure 5A). Of note, cESA-induced AMPK activation was blunted in *ex vivo* WAT explants from Ad-*Sucnr1* KO mice (Figures 5F and S4B). The treatment of 3T3-L1 cells with succinic acid increased insulin sensitivity (Figure 5G), which is in agreement with the beneficial effects reported for AMPK on glucose homeostasis.[41] To define the intracellular signaling pathways underlying leptin regulation by SUCNR1, we blocked these signaling cascades with specific chemical inhibitors. Inhibitions of JNK (with SP600125) and AMPK (with compound C [CC]), but not p38 MAPK (with SB202190), completely blocked succinic acid-induced *Lep*

UNIVERSITAT ROVIRA I VIRGILI
Metabolic Impact of the Succinate/SUCNR1 Axis in Adipocytes: Insights into Circadian and Leptin Regulation
TERESA VILLANUEVA CARMONA

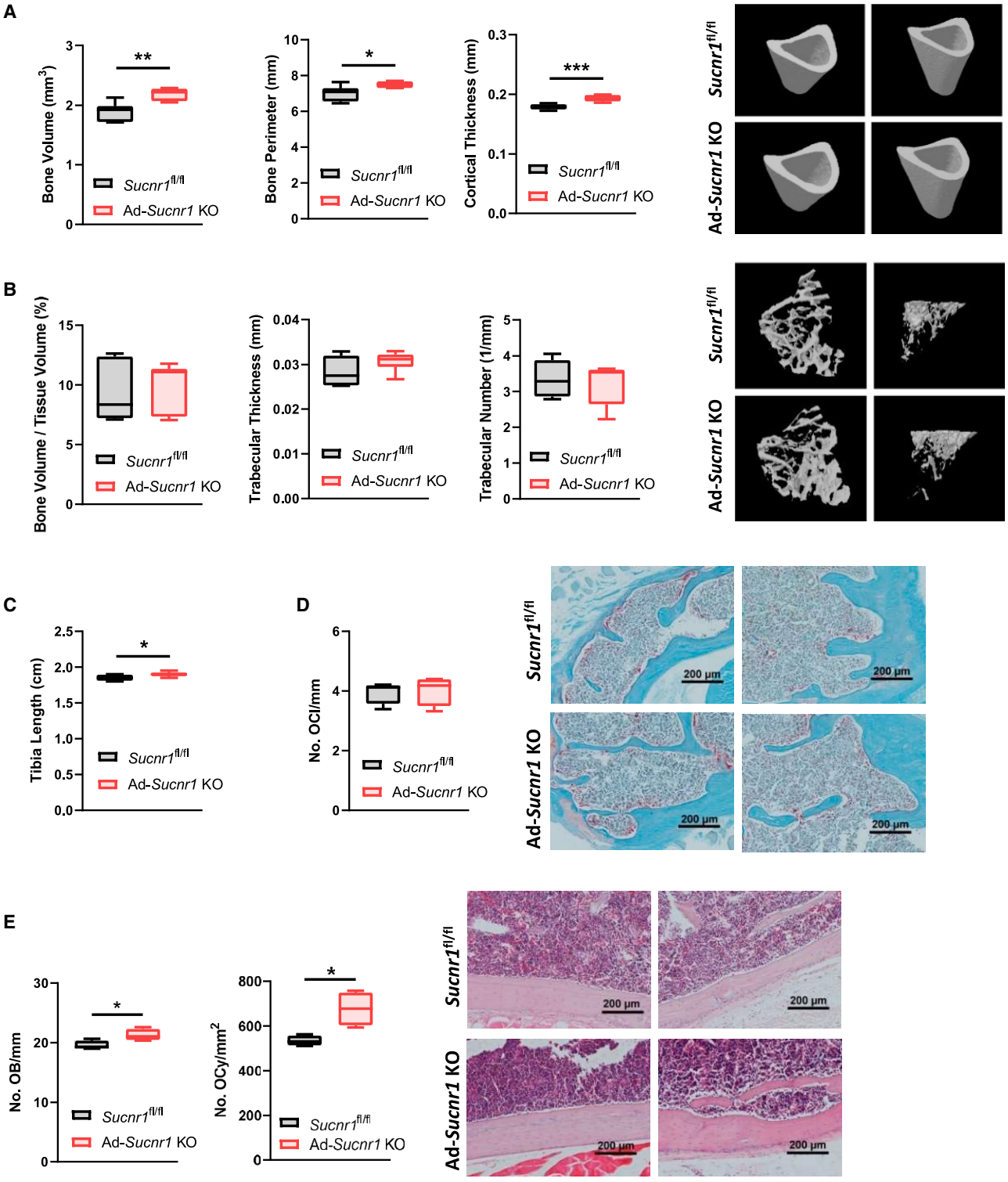

Figure 3. Mice with conditional adipocyte deletion of *Sucnr1* develop a bone mass phenotype

(A and B) Microcomputed tomography analysis and representative images of (A) cortical and (B) trabecular tibia (n = 7–8 *Sucnr1*$^{fl/fl}$ and n = 6 Ad-*Sucnr1* KO).

(C) Tibia length (n = 8 *Sucnr1*$^{fl/fl}$ and n = 6 Ad-*Sucnr1* KO).

(D) Quantification of the number of osteoclasts (Ocls) and representative images of tartrate-resistant acid phosphatase (TRAP) staining (n = 4/group) (scale bars, 200 µm).

(E) Quantification of the number of osteoblasts (OBs) and osteocytes (Ocys), and representative images of H&E staining (n = 4/group) (scale bars, 200 µm). Data are presented as box and whisker plots showing median, first, and third quartiles and maximum and minimum values; *p < 0.05, **p < 0.01; ***p < 0.001 (unpaired t test or Mann-Whitney test).

UNIVERSITAT ROVIRA I VIRGILI
Metabolic Impact of the Succinate/SUCNR1 Axis in Adipocytes: Insights into Circadian and Leptin Regulation
TERESA VILLANUEVA CARMONA

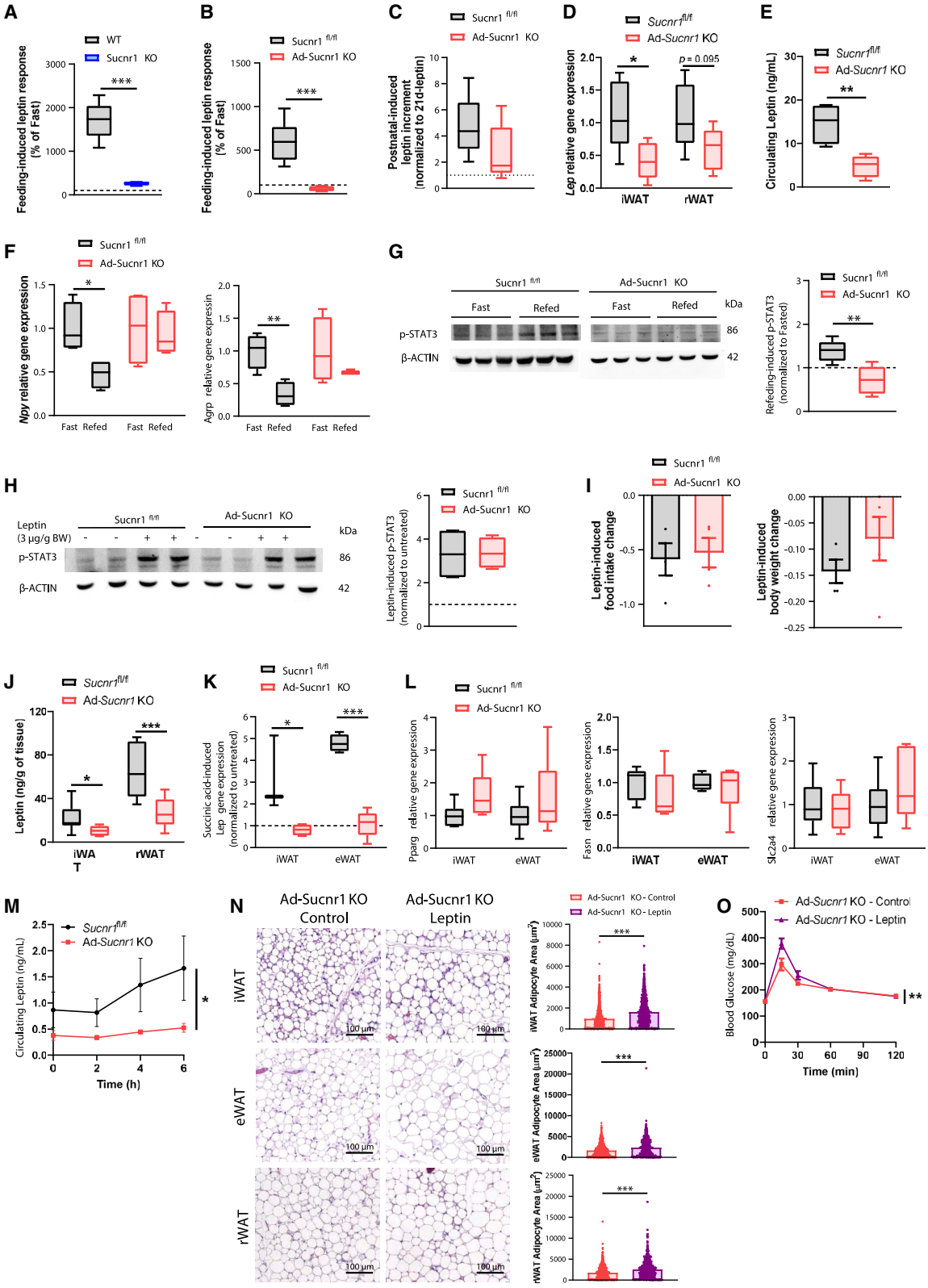

Figure 4. Mice with conditional adipocyte deletion of *Sucnr1* have disturbances in leptin expression

(A and B) Feeding-induced circulating leptin response in (A) WT (n = 5) and global *Sucnr1* KO mice (n = 4); and in (B) Ad-*Sucnr1* KO (n = 6) and *Sucnr1*$^{fl/fl}$ (n = 5) mice.

(legend continued on next page)

UNIVERSITAT ROVIRA I VIRGILI
Metabolic Impact of the Succinate/SUCNR1 Axis in Adipocytes: Insights into Circadian and Leptin Regulation
TERESA VILLANUEVA CARMONA

expression (Figure 5H). These effects were not observed for adiponectin expression (Figure S5B). In addition, the inhibition of AMPK with CC blocked JNK phosphorylation induced by *c*ESA (Figure 5I). By contrast, the inhibition of JNK with SP600125 had no effect on the *c*ESA-mediated activation of AMPK (Figure 5I), suggesting that AMPK is upstream of JNK in the signaling cascade. The treatment of 3T3-L1 cells with *c*ESA also induced CCAAT enhancer binding protein alpha (C/EBPα) phosphorylation (involved in leptin gene expression[42,43]), which was blocked by AMPK and JNK inhibitors (Figures 5I and 5J). Overall, these results suggest that succinate/SUCNR1 signaling controls leptin gene expression via the AMPK/JNK/C/EBPα axis.

SUCNR1 activation regulates the peripheral clock in adipose tissue

We profiled the transcription state of eWAT from Ad-*Sucnr1* KO and control mice. Gene set enrichment analysis indicated that the most significant change resulting from the loss of *Sucnr1* was the circadian rhythm (Figure 6A). Differential gene expression analysis provided a deeper insight into the misalignment of the circadian rhythm (Figures 6B and 6C; Table S1). Of the 103 genes differentially expressed in eWAT of Ad-*Sucnr1* KO and control mice (65 upregulated and 38 downregulated; fold change >1.25, adjusted $p < 0.05$; Table S1), 11 are key regulators of circadian rhythm. Ten of these genes were significantly upregulated in Ad-*Sucnr1* KO mice, whereas the core circadian gene encoding the brain and muscle aryl hydrocarbon receptor nuclear translocator-like protein 1 (*Bmal1*) was significantly downregulated.

Given that leptin secretion is controlled by the adipocyte circadian clock,[44–46] we evaluated the effect of SUCNR1 activation on the expression of core-clock genes using 3T3-L1 adipocytes (Figure 6D). Exposure to succinic acid significantly increased the positive circadian clock gene *Bmal1* and downregulated the negative clock genes (period [*Per*] 1, *Per2*, and *Per3*) and retinoic acid receptor-related orphan receptor alpha (*Rora*). Luciferase (LUC) reporter analysis in SUCNR1-overexpressing human embryonic kidney (HEK) 293 cells transiently transfected with a BMAL-LUC reporter confirmed that activated SUCNR1 enhanced the transcription of the *BMAL1* promoter (Figure 6E). Similar to leptin, *Bmal1* expression was also induced by AMPK activation (Figure 6F). The pharmacological inhibition of AMPK (and JNK) blocked succinic acid regulation of the clock gene expression (Figure 6G), comparable with their effects on *Lep* expression (Figure 5H). We confirmed at the protein level that BMAL1 upregulation induced by SUCNR1 activation was dependent on AMPK and JNK activation (Figure 6H). SUCNR1 activation also increases the presence of nuclear BMAL1 (total and Ser42-phosphorylated form), which is known to modulate *BMAL1* transcriptional activity[47] (Figure 6I). Notably, the upregulation of *Lep* expression by succinate in *ex vivo* WAT explants was blocked in those from mice with a heterozygous *Bmal1* deletion (Figure 6J), an effect that was not related to changes in *Sucnr1* expression (Figure 6K) or to the differences in succinate-induced AMPK activation (Figures 6L and S4C). By contrast, *Bmal1*-deficient WAT explants showed a blunted response to succinate-induced C/EBPα phosphorylation, which is in agreement with previous results demonstrating that BMAL1/CLOCK stimulates C/EBPα-mediated leptin transcription.[44] Overall, our data point to the succinate/SUCNR1 axis as a critical regulator of the circadian clock in adipose tissue that impacts leptin expression.

Leptin regulation by succinate/SUCNR1 signaling is disturbed in obesity

A paradoxical hallmark of obesity is hyperleptinemia, which is sufficient to promote resistance to its anorexigenic effects.[48] We previously demonstrated that circulating succinate[10] and *SUCNR1* in adipocytes[34] are elevated in human obesity. In line with this, mature adipocytes differentiated from adipocyte precursors of subjects with obesity released more leptin in response to SUCNR1 activation than did adipocytes from their lean counterparts (Figure 7A). To explore the link between leptin and the succinate/SUCNR1 axis in human obesity, we measured the circulating levels of leptin and succinate in a cohort of 56 subjects classified according to body mass index (BMI) (clinical and laboratory data are summarized in Table S2). As expected, circulating succinate and leptin levels were significantly higher in subjects with obesity (Table S2) and positively correlated with BMI in the bivariate analysis (Figure S6). We then measured *LEP* and *SUCNR1* expressions in scWAT and vWAT depots from the same subjects. In line with the obesity-related hyperleptinemia, *LEP* expression was significantly higher in scWAT of subjects with obesity, with a nearly significant increase in *SUCNR1* expression (Figure 7B). A trend toward increased *LEP* and *SUCNR1* expressions was also observed in visceral fat depots (Figure 7C), which is consistent with our previous study.[34] Circulating leptin positively correlated with *LEP* expression in scWAT

(C) Circulating leptin increase at 10 days normalized to 21-day leptin levels (n = 5 *Sucnr1*$^{fl/fl}$ and n = 6 Ad-*Sucnr1* KO).
(D) *Lep* expression in iWAT and retroperitoneal WAT (rWAT) (n = 5 mice/group).
(E) Circulating levels of leptin in 29-week-old mice (n = 5 mice/group).
(F) *Npy* and *Agrp* expressions in hypothalamus in fasted and refed states (n = 4 mice/group).
(G and H) Representative immunoblot images of p-STAT3 in hypothalamus, and densitometry analysis from Ad-*Sucnr1* KO and *Sucnr1*$^{fl/fl}$ mice (G) in fasted and refed states (n = 6), or (H) treated with leptin (n = 4). β-actin was used as a loading control.
(I) Food intake (n = 4/group) and body weight change (n = 4 *Sucnr1*$^{fl/fl}$ and n = 5 Ad-*Sucnr1* KO) induced by 4-day leptin treatment.
(J) Leptin secretion by iWAT and rWAT explants (n = 11 *Sucnr1*$^{fl/fl}$ and n = 7–9 Ad-*Sucnr1* KO).
(K) Fold change of *Lep* expression in primary adipocytes isolated from iWAT and eWAT and treated with succinic acid (n = 3–5 animals/group).
(L) *Pparg*, *Fasn*, and *Slc2a4* expressions in mature adipocytes isolated from iWAT and eWAT (n = 6–7 mice/group).
(M) Circulating leptin levels after an oral administration of sodium succinate (n = 6 *Sucnr1*$^{fl/fl}$ and n = 4 Ad-*Sucnr1* KO).
(N and O) (N) Representative H&E staining of WAT, and quantification of adipocyte area (scale bars, 100 μm); and (O) GTT in Ad-*Sucnr1* KO mice treated with leptin or vehicle for 4 weeks (n = 4 vehicle- and n = 5 leptin-treated mice). Data are presented as box and whiskers plots showing median, first, and third quartiles and maximum and minimum values, or as mean ± SEM; *$p < 0.05$; **$p < 0.01$; ***$p < 0.001$ (unpaired t tests or Mann-Whitney tests in bar graphs and two-way ANOVA in time-course graphs).

UNIVERSITAT ROVIRA I VIRGILI
Metabolic Impact of the Succinate/SUCNR1 Axis in Adipocytes: Insights into Circadian and Leptin Regulation
TERESA VILLANUEVA CARMONA

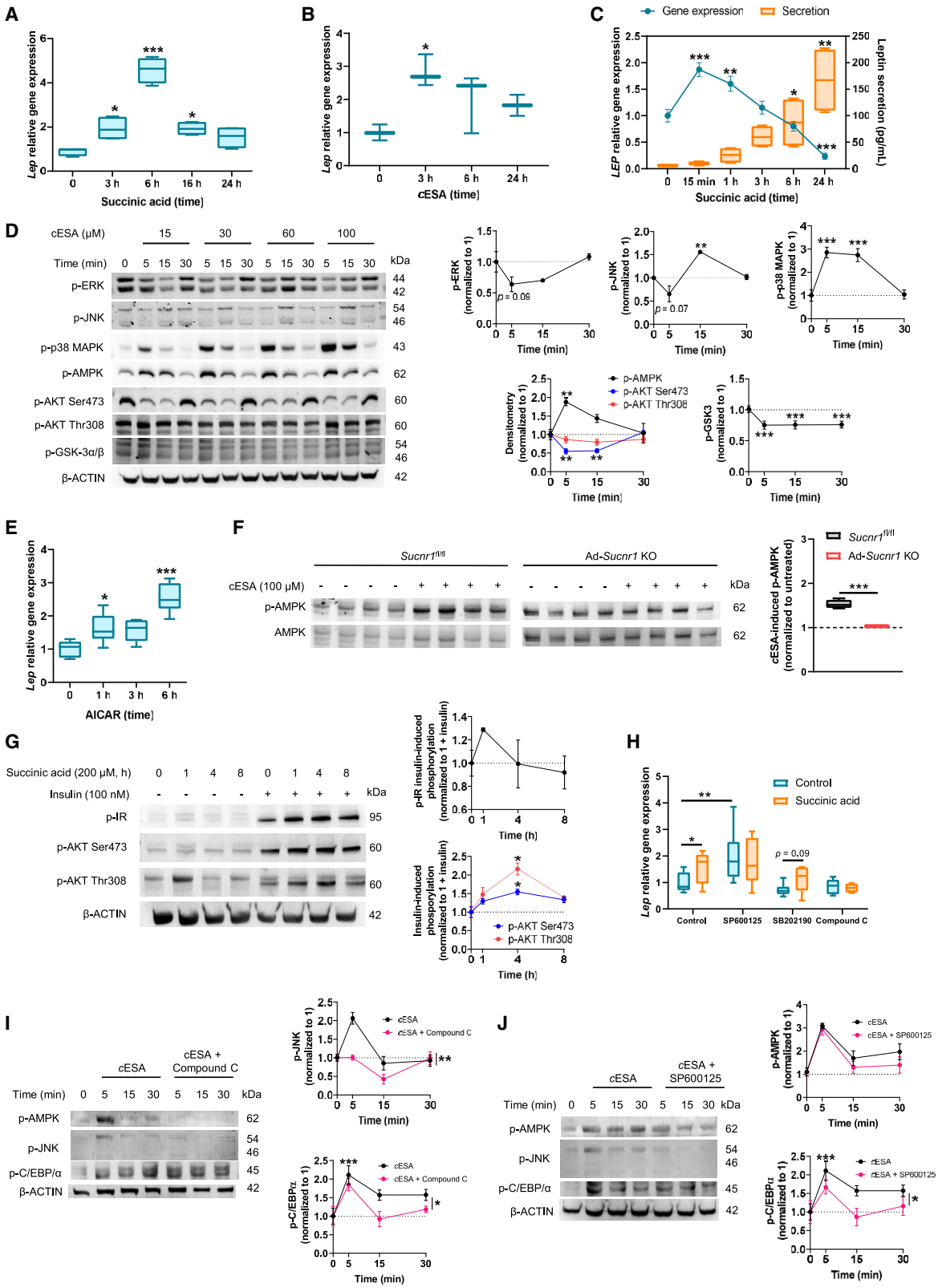

Figure 5. Succinate/SUCNR1 signaling controls leptin expression in an AMPK/JNK/C/EBPα-dependent manner

(A and B) *Lep* expression in differentiated 3T3.L1 cells treated with (A) succinic acid or (B) cESA.

(C) Leptin gene expression and secretion in adipocytes differentiated from human ASCs (hASCs) and treated with succinic acid.

(legend continued on next page)

UNIVERSITAT ROVIRA I VIRGILI
Metabolic Impact of the Succinate/SUCNR1 Axis in Adipocytes: Insights into Circadian and Leptin Regulation
TERESA VILLANUEVA CARMONA

(Figure 7D), which in turn correlated with circulating succinate (Figure 7D). Bivariate analysis also revealed that *LEP* expression correlated with *SUCNR1* expression in both scWAT and vWAT (Figure 7D). Finally, obesity was associated with an overall increase in the expression of several core-clock genes, and this was particularly pronounced in vWAT (Figure 7E). Only *CLOCK* expression in scWAT positively correlated with circulating leptin (Figure 7F).

We next constructed multiple regression analysis models including the significant bivariate correlations for each dependent variable (Figure S6), adjusting for age and sex. The best model showed that the main predictors of circulating leptin were *LEP* expression in scWAT (b = 2.261, beta = 0.286, $p < 0.05$), sex (b = 17.841, beta = 0.584, $p < 0.001$), and BMI (b = 0.831, beta = 0.359, $p < 0.05$) (Table S3). Notably, *SUCNR1* expression emerged as an independent factor associated with *LEP* expression in scWAT (b = 0.434, beta = 0.450, $p < 0.01$) (Table S4) and vWAT (b = 0.277, beta = 0.470, $p < 0.01$) (Table S5). These data show that obesity-associated hyperleptinemia is linked to elevated circulating levels of succinate and *SUCNR1* expression in adipose tissue, supporting the overactivation of this circuit in an obesity context.

DISCUSSION

We show that loss of succinate/SUCNR1 signaling in adipocytes inversely impacts WAT mass and glucose homeostasis according to nutritional status, a phenotype similar to that observed in global *Sucnr1* KO mice.[3] Although previous studies have ascribed this phenotype to the anti-lipolytic effects of SUCNR1 and "unrestrained lipolysis,"[3,31] our present analysis identifies a new additional function for succinate/SUCNR1 in adipocytes in regulating circadian clock and leptin expression, which also contributes to the regulation of energy homeostasis. Of note, we identify the precise contribution of succinate to the dichotomous effects of *Sucnr1* deficiency: the poor metabolic phenotype of Ad-*Sucnr1* KO mice during the nutritional challenge is mostly contingent on the anti-lipolytic effect of SUCNR1, in agreement with a previous report,[31] whereas its function as a regulator of leptin prevails in standard dietary states.

SUCNR1 is predominantly expressed in WAT and is highly abundant in purified adipocytes.[3,4] SUCNR1 has been suggested as a regulator of energy homeostasis through its participation in the breakdown of stored triglycerides in fat.[4] Consistent with an anti-lipolytic role, the disruption of *Sucnr1* specifically in adipocytes leads to lower WAT mass. However, the decrease in adiposity was not reflected by ectopic triglyceride storage but instead correlated with improved glucose tolerance and a preference for carbohydrates as fuel.[49,50] Notably, neither global[3] nor adipocyte-specific KO mice present with elevated serum lipids, as observed in other models of unrepressed lipolysis.[51–53] Indeed, the inhibition of lipolysis had no effect on fat mass or glucose tolerance, suggesting that it is not the main driver of the metabolically favorable phenotype in NCD. Rather, the specific deletion of *Sucnr1* in adipocytes induced WAT browning, which is known to be associated with reduced weight gain and glucose tolerance.[54,55] The white-to-brown phenotypic switch is linked to the higher brown adipocyte differentiation capacity of adipocyte precursors, likely favored by the local accumulation of succinate, which has been recently identified as a thermogenic activator[14] and browning agent.[36]

These aforementioned mechanisms seem not to operate in response to overnutrition, where the impact of the global loss of *Sucnr1* is more complex and contentious.[3,33] We found that HFD-feeding of Ad-*Sucnr1* KO mice increased fat deposition in the liver, which was accompanied by glucose intolerance, as previously observed in global *Sucnr1* KO mice.[3] A similar study did not observe the same phenotype,[33] most likely because of the different mouse models or the different diets/periods used, stressing the need for tissue-specific KO models to precisely capture the effects of *Sucnr1* deficiency in individual cell types. Our study confirms that the function of SUCNR1 as an anti-lipolytic effector in adipocytes is dominant in the context of overnutrition, which is in line with a recent report demonstrating that modulation of succinate export from the mitochondria mimics the metabolic phenotype of our model in an obesity setting.[31]

Beyond its role as a regulator of lipolysis, adipocyte-specific deletion of *Sucnr1* revealed an unexpected phenotype in terms of bone mass, which might partly underlie the higher body weight of Ad-*Sucnr1* KO mice. The inverse relationship between WAT and bone mass has been observed in other models of gene-specific deletion in adipocytes.[56–58] Perturbations in MSCs commonly cause this phenotype,[56–59] but this does not seem to be the case in our model. Adipocyte deletion of *Sucnr1* results in lower levels of circulating leptin, which is a relevant factor in the regulation of bone mass.[60,61] Although *in vitro* research suggests leptin as a positive regulator of chondrocytes and OBs,[62,63] many other experimental and clinical studies indicate that it is a major negative regulator of bone mass accrual by a central hypothalamic mechanism, independent of fat mass.[64,65] Indeed, obesity-related hyperleptinemia has been linked to decreased bone mass, even in the presence of leptin resistance.[66–68] We observed hypoleptinemia and an impaired leptin response to feeding in Ad-*Sucnr1* KO mice, which was

(D) Representative immunoblot images of phosphorylated kinases in 3T3-L1 adipocytes treated with cESA, and densitometry analysis of cESA (100 μM)-induced phosphorylation. β-actin was used as a loading control.
(E) *Lep* expression in differentiated 3T3-L1 cells treated with AICAR (n = 5–6).
(F) Representative immunoblot images and densitometry analysis of p-AMPK in WAT explants from Ad-*Sucnr1* KO and *Sucnr1*$^{fl/fl}$ mice treated with cESA. Total AMPK was used as a loading control.
(G) Representative immunoblot images of phosphorylated kinases in 3T3.L1 adipocytes treated with succinic acid and insulin. Densitometry analysis normalized to the control treated with insulin. β-actin was used as a loading control.
(H) *Lep* expression in differentiated 3T3-L1 cells treated with inhibitors and succinic acid (n = 6–9).
(I and J) Representative immunoblot images of phosphorylated kinases in 3T3-L1 adipocytes treated with compound C or SP600125, and cESA and densitometry analysis. β-actin was used as a loading control. Data are presented as box and whisker plots showing median, first, and third quartiles and maximum and minimum values or as mean ± SEM. Unless indicated, n = 2–4 independent samples. *$p < 0.05$; **$p < 0.01$; ***$p < 0.001$ vs. time 0 or control (one-way or two-way ANOVA when comparing more than two groups vs. control or unpaired t tests or Mann-Whitney tests when comparing two groups).

UNIVERSITAT ROVIRA I VIRGILI
Metabolic Impact of the Succinate/SUCNR1 Axis in Adipocytes: Insights into Circadian and Leptin Regulation
TERESA VILLANUEVA CARMONA

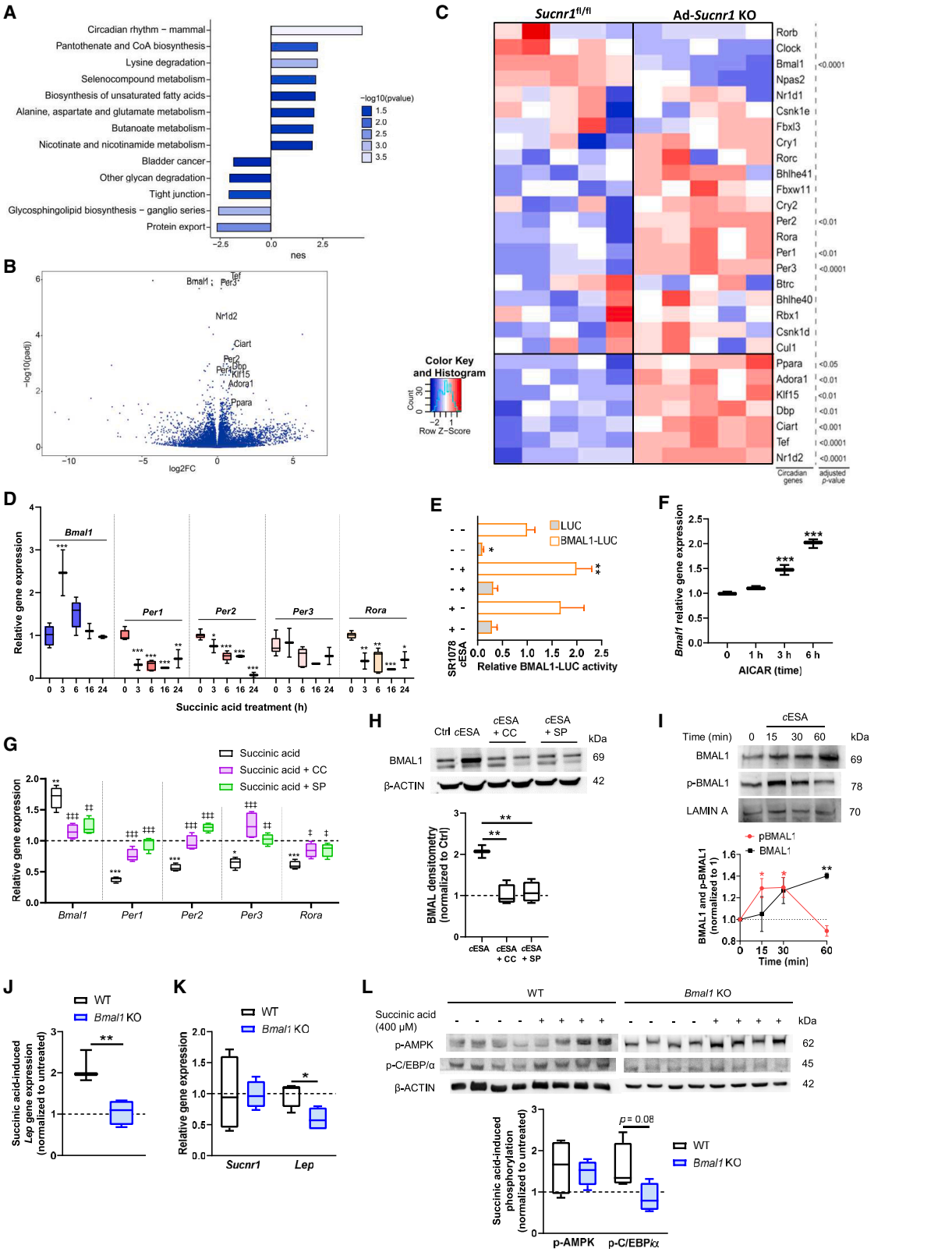

(legend on next page)

UNIVERSITAT ROVIRA I VIRGILI
Metabolic Impact of the Succinate/SUCNR1 Axis in Adipocytes: Insights into Circadian and Leptin Regulation
TERESA VILLANUEVA CARMONA

CellPress

mirrored by a disturbance in the hypothalamic response during the fasting-to-fed transition. Therefore, the cortical phenotype found in young Ad-*Sucnr1* KO mice supports leptin as a negative regulator of bone mass at the central level, which could be particularly relevant during postnatal bone development.

Our data point to succinate as a hormone-like metabolite with a key role in regulating leptin production, which is a novel physiological and molecular mechanism. SUCNR1 also emerges as a novel regulator of the circadian clock in adipose tissue, which is consistent with data from Kettner and colleagues who show that leptin expression, which exhibits diurnal variation in both humans and rodents,[69,70] is under the control of an adipose tissue peripheral clock in a CLOCK-BMAL1-C/EPB/α-dependent manner.[44] *Sucnr1* deletion disturbs the expression profile of core-clock genes, in accordance with a disruption in feeding behavior in mice fed NCD or HFD. Although no data exist on the circadian rhythmicity of circulating succinate, it is regulated by food intake,[15,71] and the succinate levels in saliva are under circadian control.[72] Because peripheral tissues such as adipose tissue respond to changes in food cues and nutrient sensors independent of the central clock to regulate nutrient uptake and metabolism,[73–75] it is conceivable that succinate operates as an internal physiological signal to influence the circadian period in addition to regulating lipid metabolism.[3,31] Published circadian transcriptome datasets of adipose tissue have yielded conflicting results,[76–79] likely due to species-specific differences and operational difficulties. Interestingly, the study of the circadian transcriptome in human WAT under constant, routine protocols predicts circadian variations in the tricarboxylic acid cycle,[76] and analysis of *Sucnr1* gene expression profile in CircadiOmics[80] reveals a circadian profile in primates, particularly in baboons. Our study identifies a novel transduction pathway by which succinate via a SUCNR1-AMPK-JNK-dependent mechanism controls BMAL1-C/EBPα-mediated regulation of leptin.

It is possible that peripheral SUCNR1 is activated in healthy tissues to regulate metabolic homeostasis in response to food ingestion,[15] and changes in circulating succinate after feeding thus emerge as a novel regulator of leptin expression. MAPK signaling pathways have been previously shown to mediate some SUCNR1-dependent effects.[81] Unexpectedly, we found that SUCNR1 engagement in adipocytes also activates AMPK, a master regulator of energy metabolism that functions to rewire metabolism by reducing anabolic processes and increasing catabolism.[82] Indeed, fasting[83,84] and exercise[85] activate AMPK in adipose tissue. Nonetheless, and similar to what occurs in skeletal muscle,[86] AMPK activation in adipocytes enhances basal glucose uptake,[87,88] a process that is stimulated after food ingestion. Moreover, similar to insulin and succinate, AMPK activation in adipocytes inhibits lipolysis,[89,90] which suggests that its function in adipose tissue goes beyond activating catabolic processes. Indeed, AICAR, a direct activator of AMPK, upregulates the expression of adiponectin in human adipose tissue,[91,92] and both adiponectin[92,93] and leptin[94] can activate AMPK in adipocytes. Remarkably, there is also evidence that some of the metabolic effects of AMPK might be mediated through the regulation of the circadian clock.[95] Our results show an increase of BMAL1 expression by AMPK activation, which is in agreement with previous studies reporting that AMPK promotes BMAL1 expression by inducing the degradation of PER2[96] and destabilization of the core-clock protein CRY1.[97] Our evidence for SUCNR1 and AMPK as direct regulators of the circadian clock and leptin in adipocyte physiology is supported by human data showing that *SUCNR1* expression is an important determinant of leptin levels in adipose tissues.

Beyond its physiological relevance, our study in the context of obesity demonstrates that disturbances in the succinate/SUCNR1 axis are linked to obesity-related hyperleptinemia. We and others recently demonstrated that succinate is involved in the natural resolution of inflammation[34,98]; however, obesity is linked to perturbations in this system associated with high levels of circulating succinate but reduced expression of *Sucnr1* in adipose-tissue resident macrophages.[34] This would represent a novel mechanism behind the inability of people with obesity to

Figure 6. SUCNR1 activation regulates the peripheral clock in adipose tissue

(A–C) RNA-seq gene expression of eWAT from *Sucnr1*$^{fl/fl}$ and Ad-*Sucnr1* KO mice (n = 5/group).

(A) Bar plots showing normalized enrichment scores (nes) annotated according to the Kyoto Encyclopedia of Genes and Genomes (KEGG) pathways, distinguishing between downregulated and upregulated pathways (filtered by gene sets with $p < 0.05$).

(B) Volcano plots for differential gene expression. p values were adjusted for multiple comparisons using the Benjamini-Hochberg procedure. Circadian clock genes with adjusted $p < 0.05$ are labeled.

(C) Heatmap showing relative expression levels for genes in the circadian rhythm pathway annotated according to the KEGG pathway and manually annotated (at the bottom). p values were adjusted for multiple comparisons using the Benjamini-Hochberg procedure.

(D) Relative expression of circadian rhythm genes in differentiated 3T3-L1 cells treated with succinic acid (n = 2–6).

(E) Luciferase assay showing expression from BMAL1-LUC in SUCNR1-overexpressing HEK293 cells transfected with the BMAL1-LUC reporter and treated with *c*ESA and SR1078.

(F) *Bmal1* expression in differentiated 3T3-L1 cells treated with AICAR (n = 2–3).

(G) Succinic acid and compound C (CC) or SP600125 (SP)-induced relative expression of circadian rhythm genes in differentiated 3T3-L1 cells (n = 4).

(H) Representative immunoblot images of BMAL1 in 3T3-L1 cells treated with *c*ESA ± CC or SP and densitometry analysis. β-actin was used as a loading control (n = 2–4).

(I) Representative immunoblot images of p-BMAL1 and BMAL1 in the nuclear fraction of 3T3-L1 cells after treatment with *c*ESA and densitometry analysis. LAMIN A was used as a loading control (n = 3–9).

(J) *Lep* expression in iWAT explants from *Bmal1* KO and WT mice treated with succinic acid (n = 3–4).

(K) Basal gene expression in iWAT explants from *Bmal1* KO and WT mice (n = 4).

(L) Representative immunoblot images of phosphorylated kinases in iWAT explants from WT and *Bmal1* KO mice treated with succinic acid and densitometry analysis. β-actin was used as a loading control (n = 4). Data are presented as box and whiskers plots showing median, first, and third quartiles and maximum and minimum values or as mean ± SEM; *$p < 0.05$, **$p < 0.01$, and ***$p < 0.001$ vs. time 0 or control and ‡$p < 0.05$, ‡‡$p < 0.01$, and ‡‡‡$p < 0.001$ vs. succinic acid-treated cells in (F) (one-way ANOVA when comparing more than two groups vs. time 0 or control; or unpaired t tests when comparing two groups).

UNIVERSITAT ROVIRA I VIRGILI
Metabolic Impact of the Succinate/SUCNR1 Axis in Adipocytes: Insights into Circadian and Leptin Regulation
TERESA VILLANUEVA CARMONA

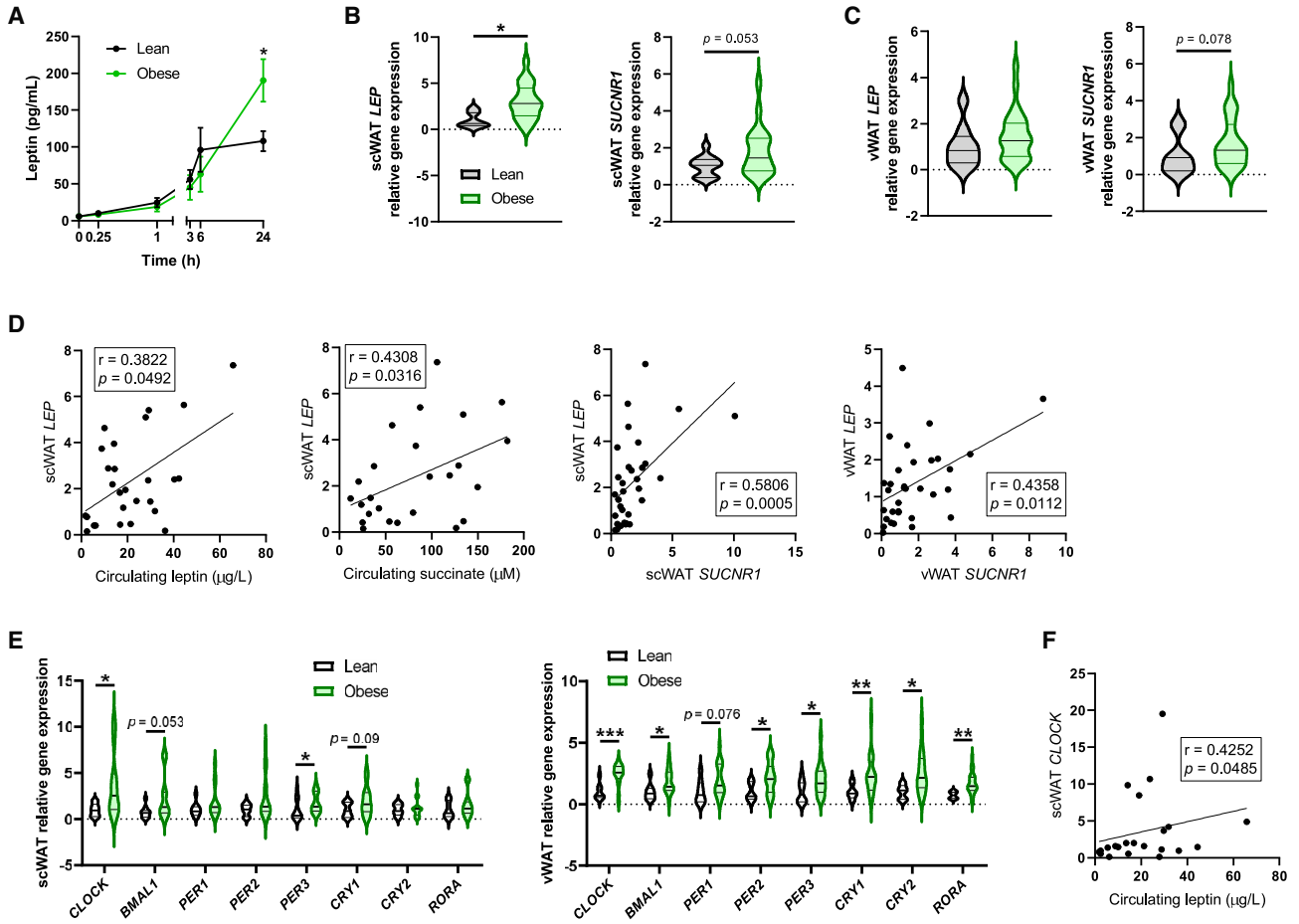

Figure 7. Leptin regulation by succinate/SUCNR1 signaling is disturbed in obesity

(A) Leptin secretion in adipocytes differentiated from lean or obese hASCs treated with *c*ESA (n = 4).

(B) *LEP* and *SUCNR1* expressions in scWAT (n = 12 lean and n = 20 obese subjects).

(C) *LEP* and *SUCNR1* expressions in vWAT (n = 9 lean and n = 24 obese subjects).

(D) Correlation between circulating leptin or succinate and scWAT *LEP* expression and between *SUCNR1* and *LEP* expressions in scWAT and vWAT.

(E) Relative gene expression of clock genes in scWAT and vWAT (n = 8 lean and n = 19 obese subjects).

(F) Correlation between circulating leptin and *CLOCK* expression in scWAT. Data are presented as mean ± SEM or as violin plots showing the frequency distribution of the data; *p < 0.05; **p < 0.01; ***p < 0.001 (two-way ANOVA vs. t = 0 in A; or unpaired t test or Mann-Whitney test for violin graphs). For (D) and (F), nonparametric Spearman's correlation analysis was used.

resolve uncontrolled inflammation. Conversely, "obese" adipocytes show higher expression of *SUCNR1* and are more sensitive to succinate-induced leptin release. Thus, we propose that obesity is associated with the hyperactivation of succinate/SUCNR1 signaling in adipocytes, which increases leptin production.

Overall, our study contributes toward the development of a holistic perspective of the succinate/SUCNR1 axis as part of the metabolite-sensing machinery that allows adipocytes to coordinate metabolic responses in response to nutrient intake. Thus, changes in circulating succinate during the fasted-to-fed transition might serve a physiological function not only in adipose tissue by regulating lipolysis but also in leptin via SUCNR1. Dysregulation of this system in obesity emerges as a novel causal mechanism of obesity-related hyperleptinemia. Further research is needed to provide a complete picture of succinate as a signal transducer of physiological functions and a potential regulator of the circadian clock. The possibility of SUCNR1 as a pharmacological target will require exhaustive investigation to understand the mechanics of the succinate/SUCNR1 axis in both health and disease.

Limitations of the study

Our study has some limitations. Experiments on animals were performed in the spirit of the reduce, reuse, and recycle approach (3Rs). A reduction strategy was used when the small sample sizes used for some experiments limited our ability to detect statistically significant differences for certain parameters but provide sufficient data to answer the research question. In addition, only male mice were used, as our initial experiments confirmed a similar phenotype in both sexes. BMAL1 activation by SUCNR1 was confirmed in a heterologous host (human SUCNR1-transfected HEK293 cells) rather than mature adipocytes (the most suitable cell model) due to their low transfection

UNIVERSITAT ROVIRA I VIRGILI
Metabolic Impact of the Succinate/SUCNR1 Axis in Adipocytes: Insights into Circadian and Leptin Regulation
TERESA VILLANUEVA CARMONA

efficiency. Finally, we acknowledge that to strengthen the translational relevance of our findings, the expression of clock genes in the human cohort would benefit from a temporal analysis to provide a more accurate perspective of the circadian dynamics in obesity.

STAR★METHODS

Detailed methods are provided in the online version of this paper and include the following:

- KEY RESOURCES TABLE
- RESOURCE AVAILABILITY
  - Lead contact
  - Materials availability
  - Data and code availability
- EXPERIMENTAL MODEL AND SUBJECT DETAILS
  - Human cohorts
  - Mouse lines
  - Mouse adipose tissue explants
  - Primary mASCs and mature adipocytes
  - Primary mouse BM-MSCs
  - Primary hASCs
  - 3T3-L1 cell line
  - HEK 293 cell line
- METHOD DETAILS
  - Indirect calorimetry
  - Locomotor activity and food intake
  - Quantitative Magnetic Resonance Imaging
  - Glucose and insulin tolerance tests
  - Effect of oral succinate on circulating leptin
  - *In vivo* lipolysis inhibition
  - Chronic leptin treatment
  - Feeding studies and leptin sensitivity tests
  - Microcomputed tomography
  - *Ex vivo* lipolysis determination
  - Brown adipocyte differentiation of mASCs
  - Osteoblast differentiation of BM-MSCs
  - Cell fractionation assay
  - Biochemical parameters
  - Gene-expression analysis
  - Transcriptome analysis by RNA sequencing
  - Western blotting
  - Histology
  - Luciferase reporter assay
- QUANTIFICATION AND STATISTICAL ANALYSIS

SUPPLEMENTAL INFORMATION

Supplemental information can be found online at https://doi.org/10.1016/j.cmet.2023.03.004.

ACKNOWLEDGMENTS

This study was supported by grants from the Spanish Ministry of Science and Innovation (MCIN)/AEI/10.13039/501100011033 (SAF2015-65019-R, RTI2018-093919-B-100, and PID2021-122480OB-I00 to S.F.-V.) and from the Instituto de Salud Carlos III (PI20/00095 to V.C.-M., and PI20/00338 to J.V.), all co-financed by the European Regional Development Fund (ERDF). This research was also supported by PID2020-119030RJ-I00 (to L. Cedó), PID2020-117640RB-I00 (to M.V.), and PID2020-117278GB-I00 (to F.V.) from MCIN/AEI/10.13039/501100011033. The project that gave rise to these results received funding from "La Caixa" Foundation under the grant agreement LCF/PR/HR20/52400013 (to S.F.-V.). N.V. is the recipient of grants "Ajuts per a projectes de recerca clínica de l'Hospital Universitari de Bellvitge (2011-PR143/11)" and the projects PI11/01960, PI14/01997, and PI17/01556 funded by the Instituto de Salud Carlos III and co-funded by "ERDF, A way to build Europe." T.V.-C. is a recipient of an FPI fellowship (PRE2019-090360), and V.C.-M. acknowledges support from the Ramón y Cajal program (RYC2019-02649-I), both from MCIN/AEI/10.13039/501100011033 and "European Social Fund (ESF) Investing in your future." M.R.-D.-D. is recipient of a Martí-Franquès Research Grant Programme (2021PMF-PIPF-2) from Universitat Rovira i Virgili. C.P.-L. is recipient of an FPU fellowship from the Spanish Ministry of Education. J.S.-B. is a recipient of a predoctoral contract for training in health research from the Instituto de Salud Carlos III, co-financed by the ESF (PFIS FI18/00151). S.F.-V. acknowledges support from the Miguel Servet tenure-track program (CP10/00438 and CPII16/00008) from the Fondo de Investigación Sanitaria, co-financed by the ERDF. The Spanish Biomedical Research Center in Diabetes and Associated Metabolic Disorders (CIBERDEM) (CB07708/0012) is an initiative or the Instituto de Salud Carlos III. We thank the Genomics Unit at the CRG for assistance with the sequencing, and the Biostatistics/Bioinformatics facility (IRB, Barcelona, Spain) for assistance with the data analysis. We particularly acknowledge the patients and the BioBank IISPV (PT17/0015/0029) integrated in the Spanish National Biobanks Network (registration number #C.0003609) for their collaboration. We thank G. Sabio (CNIC, Spain) for kindly providing the transgenic mice expressing Cre recombinase driven by the adipocyte-specific *Adipoq* promoter, and Kristin Mahan (University of Texas, USA) and Shin Yamazaki (UT Southwestern Medical Center, USA) for kindly providing the pGL3 BMAL-LUC construct. We thank Marc Claret (IDIBAPS, Barcelona), Sara Ramírez (IDIBAPS, Barcelona), and Aleix Ribas-Latre (University of Leipzig, Germany) for their scientific advice in some aspects of the research, and Kenneth McCreath for helpful comments on the manuscript.

AUTHOR CONTRIBUTIONS

Conceptualization, T.V.-C., L. Cedó, J.V., and S.F.-V.; methodology, T.V.-C., L, Cedó, A.M., M.-M.R.-P., C.N.-R., E.M.-M., M.R.-D.-D., N.K., J.S.-B., and R.B.; formal analysis, T.V.-C., L. Cedó, A.M., V.C.-M., and J.B.; investigation, T.V.-C., L. Cedó, A.M., M.M., C.P.-L., and J.C.E.-G.; resources, L. Caubet, J.-M.F.-R., and N.V.; writing – original draft, T.V.-C., L. Cedó, A.M., J.V., and S.F.-V.; writing – review & editing, M.V., F.V., J.V., and S.F.-V.; supervision, J.V. and S.F.-V.; funding acquisition, M.V., F.V., J.V., and S.F.-V.

DECLARATION OF INTERESTS

The authors declare no competing interests.

INCLUSION AND DIVERSITY

We worked to ensure gender balance in the recruitment of human subjects. We worked to ensure that the study questionnaires were prepared in an inclusive way. While citing references scientifically relevant for this work, we also actively worked to promote gender balance in our reference list.

Received: May 6, 2022
Revised: November 21, 2022
Accepted: March 3, 2023
Published: March 27, 2023

REFERENCES

1. Fernández-Veledo, S., Ceperuelo-Mallafré, V., and Vendrell, J. (2021). Rethinking succinate: an unexpected hormone-like metabolite in energy homeostasis. Trends Endocrinol. Metab. *32*, 680–692. https://doi.org/10.1016/j.tem.2021.06.003.
2. Tretter, L., Patocs, A., and Chinopoulos, C. (2016). Succinate, an intermediate in metabolism, signal transduction, ROS, hypoxia, and tumorigenesis. Biochim. Biophys. Acta *1857*, 1086–1101. https://doi.org/10.1016/j.bbabio.2016.03.012.

UNIVERSITAT ROVIRA I VIRGILI
Metabolic Impact of the Succinate/SUCNR1 Axis in Adipocytes: Insights into Circadian and Leptin Regulation
TERESA VILLANUEVA CARMONA

3. McCreath, K.J., Espada, S., Gálvez, B.G., Benito, M., de Molina, A., Sepúlveda, P., and Cervera, A.M. (2015). Targeted disruption of the SUCNR1 metabolic receptor leads to dichotomous effects on obesity. Diabetes *64*, 1154–1167. https://doi.org/10.2337/db14-0346.

4. Regard, J.B., Sato, I.T., and Coughlin, S.R. (2008). Anatomical profiling of G protein-coupled receptor expression. Cell *135*, 561–571. https://doi.org/10.1016/j.cell.2008.08.040.

5. Rubic, T., Lametschwandtner, G., Jost, S., Hinteregger, S., Kund, J., Carballido-Perrig, N., Schwärzler, C., Junt, T., Voshol, H., Meingassner, J.G., et al. (2008). Triggering the succinate receptor GPR91 on dendritic cells enhances immunity. Nat. Immunol. *9*, 1261–1269. https://doi.org/10.1038/ni.1657.

6. Lei, W., Ren, W., Ohmoto, M., Urban, J.F., Matsumoto, I., Margolskee, R.F., and Jiang, P. (2018). Activation of intestinal tuft cell-expressed Sucnr1 triggers type 2 immunity in the mouse small intestine. Proc. Natl. Acad. Sci. USA *115*, 5552–5557. https://doi.org/10.1073/pnas.1720758115.

7. Littlewood-Evans, A., Sarret, S., Apfel, V., Loesle, P., Dawson, J., Zhang, J., Muller, A., Tigani, B., Kneuer, R., Patel, S., et al. (2016). GPR91 senses extracellular succinate released from inflammatory macrophages and exacerbates rheumatoid arthritis. J. Exp. Med. *213*, 1655–1662. https://doi.org/10.1084/jem.20160061.

8. Peruzzotti-Jametti, L., Bernstock, J.D., Vicario, N., Costa, A.S.H., Kwok, C.K., Leonardi, T., Booty, L.M., Bicci, I., Balzarotti, B., Volpe, G., et al. (2018). Macrophage-derived extracellular succinate licenses neural stem cells to suppress chronic neuroinflammation. Cell Stem Cell *22*, 355–368.e13. https://doi.org/10.1016/j.stem.2018.01.020.

9. Sadagopan, N., Li, W., Roberds, S.L., Major, T., Preston, G.M., Yu, Y., and Tones, M.A. (2007). Circulating succinate is elevated in rodent models of hypertension and metabolic disease. Am. J. Hypertens. *20*, 1209–1215. https://doi.org/10.1016/j.amjhyper.2007.05.010.

10. Serena, C., Ceperuelo-Mallafré, V., Keiran, N., Queipo-Ortuño, M.I., Bernal, R., Gomez-Huelgas, R., Urpi-Sarda, M., Sabater, M., Pérez-Brocal, V., Andrés-Lacueva, C., et al. (2018). Elevated circulating levels of succinate in human obesity are linked to specific gut microbiota. ISME J. *12*, 1642–1657. https://doi.org/10.1038/s41396-018-0068-2.

11. Macias-Ceja, D.C., Ortiz-Masiá, D., Salvador, P., Gisbert-Ferrándiz, L., Hernández, C., Hausmann, M., Rogler, G., Esplugues, J.V., Hinojosa, J., Alós, R., et al. (2019). Succinate receptor mediates intestinal inflammation and fibrosis. Mucosal Immunol. *12*, 178–187. https://doi.org/10.1038/s41385-018-0087-3.

12. Osuna-Prieto, F.J., Martinez-Tellez, B., Ortiz-Alvarez, L., Di, X., Jurado-Fasoli, L., Xu, H., Ceperuelo-Mallafré, V., Núñez-Roa, C., Kohler, I., Segura-Carretero, A., et al. (2021). Elevated plasma succinate levels are linked to higher cardiovascular disease risk factors in young adults. Cardiovasc. Diabetol. *20*, 151. https://doi.org/10.1186/s12933-021-01333-3.

13. Reddy, A., Bozi, L.H.M., Yaghi, O.K., Mills, E.L., Xiao, H., Nicholson, H.E., Paschini, M., Paulo, J.A., Garrity, R., Laznik-Bogoslavski, D., et al. (2020). pH-gated succinate secretion regulates muscle remodeling in response to exercise. Cell *183*, 62–75.e17. https://doi.org/10.1016/j.cell.2020.08.039.

14. Mills, E.L., Pierce, K.A., Jedrychowski, M.P., Garrity, R., Winther, S., Vidoni, S., Yoneshiro, T., Spinelli, J.B., Lu, G.Z., Kazak, L., et al. (2018). Accumulation of succinate controls activation of adipose tissue thermogenesis. Nature *560*, 102–106. https://doi.org/10.1038/s41586-018-0353-2.

15. Astiarraga, B., Martínez, L., Ceperuelo-Mallafré, V., Llauradó, G., Terrón-Puig, M., Rodríguez, M.M., Casajoana, A., Pellitero, S., Megía, A., Vilarrasa, N., et al. (2020). Impaired succinate response to a mixed meal in obesity and Type 2 diabetes is normalized after metabolic surgery. Diabetes Care *43*, 2581–2587. https://doi.org/10.2337/dc20-0460.

16. Harvey, I., Boudreau, A., and Stephens, J.M. (2020). Adipose tissue in health and disease. Open Biol. *10*, 200291. https://doi.org/10.1098/rsob.200291.

17. Friedman, J.M. (2019). Leptin and the endocrine control of energy balance. Nat. Metab. *1*, 754–764. https://doi.org/10.1038/s42255-019-0095-y.

18. Picó, C., Palou, M., Pomar, C.A., Rodríguez, A.M., and Palou, A. (2022). Leptin as a key regulator of the adipose organ. Rev. Endocr. Metab. Disord. *23*, 13–30.

19. Levine, J.A., Eberhardt, N.L., and Jensen, M.D. (1999). Leptin responses to overfeeding: relationship with body fat and nonexercise activity thermogenesis. J. Clin. Endocrinol. Metab. *84*, 2751–2754. https://doi.org/10.1210/jcem.84.8.5910.

20. Jensen, M.D., Hensrud, D., O'Brien, P.C., and Nielsen, S. (1999). Collection and interpretation of plasma leptin concentration data in humans. Obes. Res. *7*, 241–245. https://doi.org/10.1002/j.1550-8528.1999.tb00402.x.

21. Elimam, A., and Marcus, C. (2002). Meal timing, fasting and glucocorticoids interplay in serum leptin concentrations and diurnal profile. Eur. J. Endocrinol. *147*, 181–188. https://doi.org/10.1530/eje.0.1470181.

22. Schneeberger, M., Gomis, R., and Claret, M. (2014). Hypothalamic and brainstem neuronal circuits controlling homeostatic energy balance. J. Endocrinol. *220*, T25–T46. https://doi.org/10.1530/JOE-13-0398.

23. Genchi, V.A., D'Oria, R., Palma, G., Caccioppoli, C., Cignarelli, A., Natalicchio, A., Laviola, L., Giorgino, F., and Perrini, S. (2021). Impaired leptin signalling in obesity: is leptin a new Thermolipokine? Int. J. Mol. Sci. *22*, 6445. https://doi.org/10.3390/ijms22126445.

24. Obradovic, M., Sudar-Milovanovic, E., Soskic, S., Essack, M., Arya, S., Stewart, A.J., Gojobori, T., and Isenovic, E.R. (2021). Leptin and obesity: role and clinical implication. Front. Endocrinol. *12*, 585887. https://doi.org/10.3389/fendo.2021.585887.

25. Zeigerer, A., Rodeheffer, M.S., McGraw, T.E., and Friedman, J.M. (2008). Insulin regulates leptin secretion from 3T3-L1 adipocytes by a PI 3 kinase independent mechanism. Exp. Cell Res. *314*, 2249–2256. https://doi.org/10.1016/j.yexcr.2008.04.003.

26. Lee, K.N., Jeong, I.C., Lee, S.J., Oh, S.H., and Cho, M.Y. (2001). Regulation of leptin gene expression by insulin and growth hormone in mouse adipocytes. Exp. Mol. Med. *33*, 234–239. https://doi.org/10.1038/emm.2001.38.

27. Lee, M.-J., Wang, Y., Ricci, M.R., Sullivan, S., Russell, C.D., and Fried, S.K. (2007). Acute and chronic regulation of leptin synthesis, storage, and secretion by insulin and dexamethasone in human adipose tissue. Am. J. Physiol. Endocrinol. Metab. *292*, E858–E864. https://doi.org/10.1152/ajpendo.00439.2006.

28. Jahng, J.W., Kim, N.Y., Ryu, V., Yoo, S.B., Kim, B.-T., Kang, D.-W., and Lee, J.-H. (2008). Dexamethasone reduces food intake, weight gain and the hypothalamic 5-HT concentration and increases plasma leptin in rats. Eur. J. Pharmacol. *581*, 64–70. https://doi.org/10.1016/j.ejphar.2007.11.029.

29. Keller, P., Keller, C., Steensberg, A., Robinson, L.E., and Pedersen, B.K. (2005). Leptin gene expression and systemic levels in healthy men: effect of exercise, carbohydrate, interleukin-6, and epinephrine. J. Appl. Physiol. (1985) *98*, 1805–1812. https://doi.org/10.1152/japplphysiol.00592.2004.

30. Carulli, L., Ferrari, S., Bertolini, M., Tagliafico, E., and Del Rio, G. (1999). Regulation of ob gene expression: evidence for epinephrine-induced suppression in human obesity. J. Clin. Endocrinol. Metab. *84*, 3309–3312. https://doi.org/10.1210/jcem.84.9.6007.

31. An, Y.A., Chen, S., Deng, Y., Wang, Z.V., Funcke, J.-B., Shah, M., Shan, B., Gordillo, R., Yoshino, J., Klein, S., et al. (2021). The mitochondrial dicarboxylate carrier prevents hepatic lipotoxicity by inhibiting white adipocyte lipolysis. J. Hepatol. *75*, 387–399. https://doi.org/10.1016/j.jhep.2021.03.006.

32. Gilissen, J., Jouret, F., Pirotte, B., and Hanson, J. (2016). Insight into SUCNR1 (GPR91) structure and function. Pharmacol. Ther. *159*, 56–65. https://doi.org/10.1016/j.pharmthera.2016.01.008.

UNIVERSITAT ROVIRA I VIRGILI
Metabolic Impact of the Succinate/SUCNR1 Axis in Adipocytes: Insights into Circadian and Leptin Regulation
TERESA VILLANUEVA CARMONA

33. van Diepen, J.A., Robben, J.H., Hooiveld, G.J., Carmone, C., Alsady, M., Boutens, L., Bekkenkamp-Grovenstein, M., Hijmans, A., Engelke, U.F.H., Wevers, R.A., et al. (2017). SUCNR1-mediated chemotaxis of macrophages aggravates obesity-induced inflammation and diabetes. Diabetologia *60*, 1304–1313. https://doi.org/10.1007/s00125-017-4261-z.

34. Keiran, N., Ceperuelo-Mallafré, V., Calvo, E., Hernández-Alvarez, M.I., Ejarque, M., Núñez-Roa, C., Horrillo, D., Maymó-Masip, E., Rodríguez, M.M., Fradera, R., et al. (2019). SUCNR1 controls an anti-inflammatory program in macrophages to regulate the metabolic response to obesity. Nat. Immunol. *20*, 581–592. https://doi.org/10.1038/s41590-019-0372-7.

35. Parajuli, N., Takahara, S., Matsumura, N., Kim, T.T., Ferdaoussi, M., Migglautsch, A.K., Zechner, R., Breinbauer, R., Kershaw, E.E., and Dyck, J.R.B. (2018). Atglistatin ameliorates functional decline in heart failure via adipocyte-specific inhibition of adipose triglyceride lipase. Am. J. Physiol. Heart Circ. Physiol. *315*, H879–H884. https://doi.org/10.1152/ajpheart.00308.2018.

36. Monfort-Ferré, D., Caro, A., Menacho, M., Martí, M., Espina, B., Boronat-Toscano, A., Nuñez-Roa, C., Seco, J., Bautista, M., Espín, E., et al. (2022). The gut microbiota metabolite succinate promotes adipose tissue browning in Crohn's disease. J. Crohns Colitis *16*, 1571–1583. https://doi.org/10.1093/ecco-jcc/jjac069.

37. Mazess, R.B., Peppler, W.W., and Gibbons, M. (1984). Total body composition by dual-photon (153Gd) absorptiometry. Am. J. Clin. Nutr. *40*, 834–839. https://doi.org/10.1093/ajcn/40.4.834.

38. Chen, Q., Shou, P., Zheng, C., Jiang, M., Cao, G., Yang, Q., Cao, J., Xie, N., Velletri, T., Zhang, X., et al. (2016). Fate decision of mesenchymal stem cells: adipocytes or osteoblasts? Cell Death Differ. *23*, 1128–1139. https://doi.org/10.1038/cdd.2015.168.

39. Skowronski, A.A., Shaulson, E.D., Leibel, R.L., and LeDuc, C.A. (2022). The postnatal leptin surge in mice is variable in both time and intensity and reflects nutritional status. Int. J. Obes. (Lond) *46*, 39–49. https://doi.org/10.1038/s41366-021-00957-5.

40. Ruvolo, P.P., Qiu, Y., Coombes, K.R., Zhang, N., Neeley, E.S., Ruvolo, V.R., Hail, N., Borthakur, G., Konopleva, M., Andreeff, M., et al. (2015). Phosphorylation of GSK3α/β correlates with activation of AKT and is prognostic for poor overall survival in acute myeloid leukemia patients. BBA Clin. *4*, 59–68. https://doi.org/10.1016/j.bbacli.2015.07.001.

41. Steinberg, G.R., and Carling, D. (2019). AMP-activated protein kinase: the current landscape for drug development. Nat. Rev. Drug Discov. *18*, 527–551. https://doi.org/10.1038/s41573-019-0019-2.

42. Hwang, C.S., Mandrup, S., MacDougald, O.A., Geiman, D.E., and Lane, M.D. (1996). Transcriptional activation of the mouse obese (ob) gene by CCAAT/enhancer binding protein alpha. Proc. Natl. Acad. Sci. USA *93*, 873–877. https://doi.org/10.1073/pnas.93.2.873.

43. Miller, S.G., De Vos, P., Guerre-Millo, M., Wong, K., Hermann, T., Staels, B., Briggs, M.R., and Auwerx, J. (1996). The adipocyte specific transcription factor C/EBPalpha modulates human ob gene expression. Proc. Natl. Acad. Sci. USA *93*, 5507–5511. https://doi.org/10.1073/pnas.93.11.5507.

44. Kettner, N.M., Mayo, S.A., Hua, J., Lee, C., Moore, D.D., and Fu, L. (2015). Circadian dysfunction induces leptin resistance in mice. Cell Metab. *22*, 448–459. https://doi.org/10.1016/j.cmet.2015.06.005.

45. Otway, D.T., Frost, G., and Johnston, J.D. (2009). Circadian rhythmicity in murine pre-adipocyte and adipocyte cells. Chronobiol. Int. *26*, 1340–1354. https://doi.org/10.3109/07420520903412368.

46. Shea, S.A., Hilton, M.F., Orlova, C., Ayers, R.T., and Mantzoros, C.S. (2005). Independent circadian and sleep/wake regulation of adipokines and glucose in humans. J. Clin. Endocrinol. Metab. *90*, 2537–2544. https://doi.org/10.1210/jc.2004-2232.

47. Lipton, J.O., Yuan, E.D., Boyle, L.M., Ebrahimi-Fakhari, D., Kwiatkowski, E., Nathan, A., Güttler, T., Davis, F., Asara, J.M., and Sahin, M. (2015). The circadian protein BMAL1 regulates translation in response to S6K1-mediated phosphorylation. Cell *161*, 1138–1151. https://doi.org/10.1016/j.cell.2015.04.002.

48. Knight, Z.A., Hannan, K.S., Greenberg, M.L., and Friedman, J.M. (2010). Hyperleptinemia is required for the development of leptin resistance. PloS One *5*, e11376. https://doi.org/10.1371/journal.pone.0011376.

49. Longo, K.A., Charoenthongtrakul, S., Giuliana, D.J., Govek, E.K., McDonagh, T., Qi, Y., DiStefano, P.S., and Geddes, B.J. (2008). Improved insulin sensitivity and metabolic flexibility in ghrelin receptor knockout mice. Regul. Pept. *150*, 55–61. https://doi.org/10.1016/j.regpep.2008.03.011.

50. Gilbertson, N.M., Eichner, N.Z.M., Francois, M., Gaitán, J.M., Heiston, E.M., Weltman, A., and Malin, S.K. (2018). Glucose tolerance is linked to postprandial fuel use independent of exercise dose. Med. Sci. Sports Exerc. *50*, 2058–2066. https://doi.org/10.1249/MSS.0000000000001667.

51. Ahmed, K., Tunaru, S., Tang, C., Müller, M., Gille, A., Sassmann, A., Hanson, J., and Offermanns, S. (2010). An autocrine lactate loop mediates insulin-dependent inhibition of lipolysis through GPR81. Cell Metab. *11*, 311–319. https://doi.org/10.1016/j.cmet.2010.02.012.

52. Zhang, G., Li, R., Li, W., Yang, S., Sun, Q., Yin, H., Wang, C., Hou, B., Wang, H., Yu, L., et al. (2021). Toll-like receptor 3 ablation prevented high-fat diet-induced obesity and metabolic disorder. J. Nutr. Biochem. *95*, 108761. https://doi.org/10.1016/j.jnutbio.2021.108761.

53. Tunaru, S., Kero, J., Schaub, A., Wufka, C., Blaukat, A., Pfeffer, K., and Offermanns, S. (2003). PUMA-G and HM74 are receptors for nicotinic acid and mediate its anti-lipolytic effect. Nat. Med. *9*, 352–355. https://doi.org/10.1038/nm824.

54. Bartelt, A., and Heeren, J. (2014). Adipose tissue browning and metabolic health. Nat. Rev. Endocrinol. *10*, 24–36. https://doi.org/10.1038/nrendo.2013.204.

55. Kazak, L., Chouchani, E.T., Lu, G.Z., Jedrychowski, M.P., Bare, C.J., Mina, A.I., Kumari, M., Zhang, S., Vuckovic, I., Laznik-Bogoslavski, D., et al. (2017). Genetic depletion of adipocyte creatine metabolism inhibits diet-induced thermogenesis and drives obesity. Cell Metab. *26*, 660–671.e3. https://doi.org/10.1016/j.cmet.2017.08.009.

56. Gao, H., Guo, Y., Yan, Q., Yang, W., Li, R., Lin, S., Bai, X., Liu, C., Chen, D., Cao, H., et al. (2019). Lipoatrophy and metabolic disturbance in mice with adipose-specific deletion of kindlin-2. JCI Insight *4*, 128405. https://doi.org/10.1172/jci.insight.128405.

57. Corsa, C.A.S., Walsh, C.M., Bagchi, D.P., Foss Freitas, M.C., Li, Z., Hardij, J., Granger, K., Mori, H., Schill, R.L., Lewis, K.T., et al. (2021). Adipocyte-specific deletion of Lamin A/C largely models human familial partial lipodystrophy Type 2. Diabetes *70*, 1970–1984. https://doi.org/10.2337/db20-1001.

58. Urs, S., Venkatesh, D., Tang, Y., Henderson, T., Yang, X., Friesel, R.E., Rosen, C.J., and Liaw, L. (2010). Sprouty1 is a critical regulatory switch of mesenchymal stem cell lineage allocation. FASEB J. *24*, 3264–3273. https://doi.org/10.1096/fj.10-155127.

59. Fazeli, P.K., Horowitz, M.C., MacDougald, O.A., Scheller, E.L., Rodeheffer, M.S., Rosen, C.J., and Klibanski, A. (2013). Marrow fat and bone–new perspectives. J. Clin. Endocrinol. Metab. *98*, 935–945. https://doi.org/10.1210/jc.2012-3634.

60. Upadhyay, J., Farr, O.M., and Mantzoros, C.S. (2015). The role of leptin in regulating bone metabolism. Metabolism *64*, 105–113. https://doi.org/10.1016/j.metabol.2014.10.021.

61. Reid, I.R., Baldock, P.A., and Cornish, J. (2018). Effects of leptin on the skeleton. Endocr. Rev. *39*, 938–959. https://doi.org/10.1210/er.2017-00226.

62. Kishida, Y., Hirao, M., Tamai, N., Nampei, A., Fujimoto, T., Nakase, T., Shimizu, N., Yoshikawa, H., and Myoui, A. (2005). Leptin regulates chondrocyte differentiation and matrix maturation during endochondral ossification. Bone *37*, 607–621. https://doi.org/10.1016/j.bone.2005.05.009.

63. Cheng, M., Li, T., Li, W., Chen, Y., Xu, W., and Xu, L. (2018). Leptin can promote mineralization and up-regulate RANKL mRNA expression in osteoblasts from adult female SD rats. Int. J. Clin. Exp. Pathol. *11*, 1610–1619.

UNIVERSITAT ROVIRA I VIRGILI
Metabolic Impact of the Succinate/SUCNR1 Axis in Adipocytes: Insights into Circadian and Leptin Regulation
TERESA VILLANUEVA CARMONA

64. Ducy, P., Amling, M., Takeda, S., Priemel, M., Schilling, A.F., Beil, F.T., Shen, J., Vinson, C., Rueger, J.M., and Karsenty, G. (2000). Leptin inhibits bone formation through a hypothalamic relay: a central control of bone mass. Cell *100*, 197–207. https://doi.org/10.1016/s0092-8674(00)81558-5.

65. Karsenty, G., and Khosla, S. (2022). The crosstalk between bone remodeling and energy metabolism: A translational perspective. Cell Metab. *34*, 805–817. https://doi.org/10.1016/j.cmet.2022.04.010.

66. Ealey, K.N., Fonseca, D., Archer, M.C., and Ward, W.E. (2006). Bone abnormalities in adolescent leptin-deficient mice. Regul. Pept. *136*, 9–13. https://doi.org/10.1016/j.regpep.2006.04.013.

67. Hamrick, M.W., Della-Fera, M.A., Choi, Y.-H., Pennington, C., Hartzell, D., and Baile, C.A. (2005). Leptin treatment induces loss of bone marrow adipocytes and increases bone formation in leptin-deficient ob/ob mice. J. Bone Miner. Res. *20*, 994–1001. https://doi.org/10.1359/JBMR.050103.

68. Hamrick, M.W., Pennington, C., Newton, D., Xie, D., and Isales, C. (2004). Leptin deficiency produces contrasting phenotypes in bones of the limb and spine. Bone *34*, 376–383. https://doi.org/10.1016/j.bone.2003.11.020.

69. Bodosi, B., Gardi, J., Hajdu, I., Szentirmai, E., Obal, F., and Krueger, J.M. (2004). Rhythms of ghrelin, leptin, and sleep in rats: effects of the normal diurnal cycle, restricted feeding, and sleep deprivation. Am. J. Physiol. Regul. Integr. Comp. Physiol. *287*, R1071–R1079. https://doi.org/10.1152/ajpregu.00294.2004.

70. Templeman, I., Smith, H.A., Walhin, J.P., Middleton, B., Gonzalez, J.T., Karagounis, L.G., Johnston, J.D., and Betts, J.A. (2021). Unacylated ghrelin, leptin, and appetite display diurnal rhythmicity in lean adults. J. Appl. Physiol. (1985) *130*, 1534–1543. https://doi.org/10.1152/japplphysiol.00920.2020.

71. Shrestha, A., Müllner, E., Poutanen, K., Mykkänen, H., and Moazzami, A.A. (2017). Metabolic changes in serum metabolome in response to a meal. Eur. J. Nutr. *56*, 671–681. https://doi.org/10.1007/s00394-015-1111-y.

72. Dallmann, R., Viola, A.U., Tarokh, L., Cajochen, C., and Brown, S.A. (2012). The human circadian metabolome. Proc. Natl. Acad. Sci. USA *109*, 2625–2629. https://doi.org/10.1073/pnas.1114410109.

73. Buijs, R., Salgado, R., Sabath, E., and Escobar, C. (2013). Peripheral circadian oscillators: time and food. Prog. Mol. Biol. Transl. Sci. *119*, 83–103. https://doi.org/10.1016/B978-0-12-396971-2.00004-X.

74. Challet, E. (2013). Circadian clocks, food intake, and metabolism. Prog. Mol. Biol. Transl. Sci. *119*, 105–135. https://doi.org/10.1016/B978-0-12-396971-2.00005-1.

75. Eckel-Mahan, K., and Sassone-Corsi, P. (2013). Metabolism and the circadian clock converge. Physiol. Rev. *93*, 107–135. https://doi.org/10.1152/physrev.00016.2012.

76. Christou, S., Wehrens, S.M.T., Isherwood, C., Möller-Levet, C.S., Wu, H., Revell, V.L., Bucca, G., Skene, D.J., Laing, E.E., Archer, S.N., et al. (2019). Circadian regulation in human white adipose tissue revealed by transcriptome and metabolic network analysis. Sci. Rep. *9*, 2641. https://doi.org/10.1038/s41598-019-39668-3.

77. Loboda, A., Kraft, W.K., Fine, B., Joseph, J., Nebozhyn, M., Zhang, C., He, Y., Yang, X., Wright, C., Morris, M., et al. (2009). Diurnal variation of the human adipose transcriptome and the link to metabolic disease. BMC Med. Genomics *2*, 7. https://doi.org/10.1186/1755-8794-2-7.

78. Stenvers, D.J., Jongejan, A., Atiqi, S., Vreijling, J.P., Limonard, E.J., Endert, E., Baas, F., Moerland, P.D., Fliers, E., Kalsbeek, A., et al. (2019). Diurnal rhythms in the white adipose tissue transcriptome are disturbed in obese individuals with type 2 diabetes compared with lean control individuals. Diabetologia *62*, 704–716. https://doi.org/10.1007/s00125-019-4813-5.

79. Zvonic, S., Ptitsyn, A.A., Conrad, S.A., Scott, L.K., Floyd, Z.E., Kilroy, G., Wu, X., Goh, B.C., Mynatt, R.L., and Gimble, J.M. (2006). Characterization of peripheral circadian clocks in adipose tissues. Diabetes *55*, 962–970. https://doi.org/10.2337/diabetes.55.04.06.db05-0873.

80. Ceglia, N., Liu, Y., Chen, S., Agostinelli, F., Eckel-Mahan, K., Sassone-Corsi, P., and Baldi, P. (2018). CircadiOmics: circadian omic web portal. Nucleic Acids Res. *46*, W157–W162. https://doi.org/10.1093/nar/gky441.

81. Hu, J., Li, T., Du, S., Chen, Y., Wang, S., Xiong, F., and Wu, Q. (2015). The MAPK signaling pathway mediates the GPR91-dependent release of VEGF from RGC-5 cells. Int. J. Mol. Med. *36*, 130–138. https://doi.org/10.3892/ijmm.2015.2195.

82. Trefts, E., and Shaw, R.J. (2021). AMPK: restoring metabolic homeostasis over space and time. Mol. Cell *81*, 3677–3690. https://doi.org/10.1016/j.molcel.2021.08.015.

83. Daval, M., Diot-Dupuy, F., Bazin, R., Hainault, I., Viollet, B., Vaulont, S., Hajduch, E., Ferré, P., and Foufelle, F. (2005). Anti-lipolytic action of AMP-activated protein kinase in rodent adipocytes. J. Biol. Chem. *280*, 25250–25257. https://doi.org/10.1074/jbc.M414222200.

84. Sponarova, J., Mustard, K.J., Horakova, O., Flachs, P., Rossmeisl, M., Brauner, P., Bardova, K., Thomason-Hughes, M., Braunerova, R., Janovska, P., et al. (2005). Involvement of AMP-activated protein kinase in fat depot-specific metabolic changes during starvation. FEBS Lett. *579*, 6105–6110. https://doi.org/10.1016/j.febslet.2005.09.078.

85. Park, H., Kaushik, V.K., Constant, S., Prentki, M., Przybytkowski, E., Ruderman, N.B., and Saha, A.K. (2002). Coordinate regulation of malonyl-CoA decarboxylase, sn-glycerol-3-phosphate acyltransferase, and acetyl-CoA carboxylase by AMP-activated protein kinase in rat tissues in response to exercise. J. Biol. Chem. *277*, 32571–32577. https://doi.org/10.1074/jbc.M201692200.

86. Musi, N., Hayashi, T., Fujii, N., Hirshman, M.F., Witters, L.A., and Goodyear, L.J. (2001). AMP-activated protein kinase activity and glucose uptake in rat skeletal muscle. Am. J. Physiol. Endocrinol. Metab. *280*, E677–E684. https://doi.org/10.1152/ajpendo.2001.280.5.E677.

87. Salt, I.P., Connell, J.M., and Gould, G.W. (2000). 5-aminoimidazole-4-carboxamide ribonucleoside (AICAR) inhibits insulin-stimulated glucose transport in 3T3-L1 adipocytes. Diabetes *49*, 1649–1656. https://doi.org/10.2337/diabetes.49.10.1649.

88. Sakoda, H., Ogihara, T., Anai, M., Fujishiro, M., Ono, H., Onishi, Y., Katagiri, H., Abe, M., Fukushima, Y., Shojima, N., et al. (2002). Activation of AMPK is essential for AICAR-induced glucose uptake by skeletal muscle but not adipocytes. Am. J. Physiol. Endocrinol. Metab. *282*, E1239–E1244. https://doi.org/10.1152/ajpendo.00455.2001.

89. Chuang, S.-J., Johanns, M., Pyr dit Ruys, S., Steinberg, G.R., Kemp, B.E., Viollet, B., and Rider, M.H. (2021). AMPK activation by SC4 inhibits noradrenaline-induced lipolysis and insulin-stimulated lipogenesis in white adipose tissue. Biochem. J. *478*, 3869–3889. https://doi.org/10.1042/BCJ20210411.

90. Szkudelski, T., and Szkudelska, K. (2017). Effects of AMPK activation on lipolysis in primary rat adipocytes: studies at different glucose concentrations. Arch. Physiol. Biochem. *123*, 43–49. https://doi.org/10.1080/13813455.2016.1227853.

91. Lihn, A.S., Jessen, N., Pedersen, S.B., Lund, S., and Richelsen, B. (2004). AICAR stimulates adiponectin and inhibits cytokines in adipose tissue. Biochem. Biophys. Res. Commun. *316*, 853–858. https://doi.org/10.1016/j.bbrc.2004.02.139.

92. Sell, H., Dietze-Schroeder, D., Eckardt, K., and Eckel, J. (2006). Cytokine secretion by human adipocytes is differentially regulated by adiponectin, AICAR, and troglitazone. Biochem. Biophys. Res. Commun. *343*, 700–706. https://doi.org/10.1016/j.bbrc.2006.03.010.

93. Wu, X., Motoshima, H., Mahadev, K., Stalker, T.J., Scalia, R., and Goldstein, B.J. (2003). Involvement of AMP-activated protein kinase in glucose uptake stimulated by the globular domain of adiponectin in primary rat adipocytes. Diabetes *52*, 1355–1363. https://doi.org/10.2337/diabetes.52.6.1355.

94. Orci, L., Cook, W.S., Ravazzola, M., Wang, M.-Y., Park, B.-H., Montesano, R., and Unger, R.H. (2004). Rapid transformation of white

UNIVERSITAT ROVIRA I VIRGILI
Metabolic Impact of the Succinate/SUCNR1 Axis in Adipocytes: Insights into Circadian and Leptin Regulation
TERESA VILLANUEVA CARMONA

adipocytes into fat-oxidizing machines. Proc. Natl. Acad. Sci. USA *101*, 2058–2063. https://doi.org/10.1073/pnas.0308258100.

95. Jordan, S.D., and Lamia, K.A. (2013). AMPK at the crossroads of circadian clocks and metabolism. Mol. Cell. Endocrinol. *366*, 163–169. https://doi.org/10.1016/j.mce.2012.06.017.
96. Um, J.H., Yang, S., Yamazaki, S., Kang, H., Viollet, B., Foretz, M., and Chung, J.H. (2007). Activation of 5′-AMP-activated kinase with diabetes drug metformin induces casein kinase Iepsilon (CKIepsilon)-dependent degradation of clock protein mPer2. J. Biol. Chem. *282*, 20794–20798. https://doi.org/10.1074/jbc.C700070200.
97. Lamia, K.A., Sachdeva, U.M., DiTacchio, L., Williams, E.C., Alvarez, J.G., Egan, D.F., Vasquez, D.S., Juguilon, H., Panda, S., Shaw, R.J., et al. (2009). AMPK regulates the circadian clock by cryptochrome phosphorylation and degradation. Science *326*, 437–440. https://doi.org/10.1126/science.1172156.
98. Trauelsen, M., Hiron, T.K., Lin, D., Petersen, J.E., Breton, B., Husted, A.S., Hjorth, S.A., Inoue, A., Frimurer, T.M., Bouvier, M., et al. (2021). Extracellular succinate hyperpolarizes M2 macrophages through SUCNR1/GPR91-mediated Gq signaling. Cell Rep. *35*, 109246. https://doi.org/10.1016/j.celrep.2021.109246.
99. Yeom, M., Pendergast, J.S., Ohmiya, Y., and Yamazaki, S. (2010). Circadian-independent cell mitosis in immortalized fibroblasts. Proc. Natl. Acad. Sci. USA *107*, 9665–9670. https://doi.org/10.1073/pnas.0914078107.
100. Dobin, A., Davis, C.A., Schlesinger, F., Drenkow, J., Zaleski, C., Jha, S., Batut, P., Chaisson, M., and Gingeras, T.R. (2013). STAR: ultrafast universal RNA-seq aligner. Bioinform. Oxf. Engl. *29*, 15–21. https://doi.org/10.1093/bioinformatics/bts635.
101. Liao, Y., Smyth, G.K., and Shi, W. (2019). The R package Rsubread is easier, faster, cheaper and better for alignment and quantification of RNA sequencing reads. Nucleic Acids Res. *47*, e47. https://doi.org/10.1093/nar/gkz114.
102. R Core Team (2022). R: A Language and Environment for Statistical Computing (R Foundation for Statistical Computing). https://www.R-project.org/.
103. Wickham, H. (2016). ggplot2: Elegant Graphics for Data Analysis (Springer-Verlag New York).
104. Ritchie, M.E., Phipson, B., Wu, D., Hu, Y., Law, C.W., Shi, W., and Smyth, G.K. (2015). limma powers differential expression analyses for RNA-sequencing and microarray studies. Nucleic Acids Res. *43*, e47. https://doi.org/10.1093/nar/gkv007.
105. Love, M.I., Huber, W., and Anders, S. (2014). Moderated estimation of fold change and dispersion for RNA-seq data with DESeq2. Genome Biol. *15*, 550. https://doi.org/10.1186/s13059-014-0550-8.
106. Wu, D., Lim, E., Vaillant, F., Asselin-Labat, M.L., Visvader, J.E., and Smyth, G.K. (2010). ROAST: rotation gene set tests for complex microarray experiments. Bioinform. Oxf. Engl. *26*, 2176–2182. https://doi.org/10.1093/bioinformatics/btq401.
107. Efron, B., and Tibshirani, R. (2007). On testing the significance of sets of genes. Ann. Appl. Stat. *1*, 107–129.
108. Carlson, M.. org.Hs.eg.db: Genome wide annotation for Human. R package version 2.14.0. https://bioconductor.org/packages/release/data/annotation/html/org.Hs.eg.db.html.
109. World Health Organization (2000). Obesity: preventing and managing the global epidemic. Report of a WHO consultation. 1–253. World Health Organ. Tech. Rep. Ser. *894*. i-xii.
110. Calvo, E., Keiran, N., Núñez-Roa, C., Maymó-Masip, E., Ejarque, M., Sabadell-Basallote, J., Del Mar Rodríguez-Peña, M., Ceperuelo-Mallafré, V., Seco, J., Benaiges, E., et al. (2021). Effects of stem cells from inducible brown adipose tissue on diet-induced obesity in mice. Sci. Rep. *11*, 13923. https://doi.org/10.1038/s41598-021-93224-6.
111. Pachón-Peña, G., Yu, G., Tucker, A., Wu, X., Vendrell, J., Bunnell, B.A., and Gimble, J.M. (2011). Stromal stem cells from adipose tissue and bone marrow of age-matched female donors display distinct immunophenotypic profiles. J. Cell. Physiol. *226*, 843–851. https://doi.org/10.1002/jcp.22408.
112. Del Río-Martín, A., Pérez-Taboada, I., Fernández-Pérez, A., Moratalla, R., de la Villa, P., and Vallejo, M. (2019). Hypomorphic expression of Pitx3 disrupts circadian clocks and prevents metabolic entrainment of energy expenditure. Cell Rep. *29*, 3678–3692.e4. https://doi.org/10.1016/j.celrep.2019.11.027.
113. Tang, H., Vasselli, J.R., Wu, E.X., Boozer, C.N., and Gallagher, D. (2002). High-resolution magnetic resonance imaging tracks changes in organ and tissue mass in obese and aging rats. Am. J. Physiol. Regul. Integr. Comp. Physiol. *282*, R890–R899. https://doi.org/10.1152/ajpregu.0527.2001.
114. Estañ, M.C., Fernández-Núñez, E., Zaki, M.S., Esteban, M.I., Donkervoort, S., Hawkins, C., Caparros-Martin, J.A., Saade, D., Hu, Y., Bolduc, V., et al. (2019). Recessive mutations in muscle-specific isoforms of FXR1 cause congenital multi-minicore myopathy. Nat. Commun. *10*, 797. https://doi.org/10.1038/s41467-019-08548-9.
115. Mina, A.I., LeClair, R.A., LeClair, K.B., Cohen, D.E., Lantier, L., and Banks, A.S. (2018). CalR: A web-based analysis tool for indirect calorimetry experiments. Cell Metab. *28*, 656–666.e1. https://doi.org/10.1016/j.cmet.2018.06.019.

UNIVERSITAT ROVIRA I VIRGILI
Metabolic Impact of the Succinate/SUCNR1 Axis in Adipocytes: Insights into Circadian and Leptin Regulation
TERESA VILLANUEVA CARMONA

STAR★METHODS

KEY RESOURCES TABLE

REAGENT or RESOURCE	SOURCE	IDENTIFIER
Antibodies		
Rabbit phospho-AKT (Ser473), polyclonal	Cell Signaling Technology	Cat.#4058S; RRID: AB_331168; Lot: #0030
Rabbit phospho-AKT (Thr308), polylclonal	Cell Signaling Technology	Cat.#9275S; RRID: AB_329828; Lot: #0021
Rabbit phospho-C/EBPα (Ser21), polyclonal	Cell Signaling Technology	Cat.#2841S; RRID: AB_2077882; Lot: #0002
Rabbit phospho-GSK3α/β (Ser21/9), polyclonal	Cell Signaling Technology	Cat.#9331; RRID: AB_329830; Lot: #0020
Rabbit phospho-p44/42 MAPK (Erk1/2) (Thr202/Tyr204), polyclonal	Cell Signaling Technology	Cat.#9101S; RRID: AB_331646; Lot: #0023
Rabbit phospho-SAPK/JNK (Thr183/Tyr185), polyclonal	Cell Signaling Technology	Cat.#9251S; RRID: AB_331659; Lot: #0026
Rabbit phospho-BMAL1 (Ser42) Antibody, polyclonal	Cell Signaling Technology	Cat.#13936; RRID: AB_2798348; Lot: #0001
Anti-BMAL1 antibody, from rabbit, polyclonal	Abcam	Cat.#ab93806; RRID: AB_10675117; Lot:#GR3368431-11
Phospho-AMPKα (Thr172) Rabbit mAb	Cell Signaling Technology	Cat.#2535S; RRID: AB_331250; Lot: #0021
Phosho-IGF-I Receptor β (Tyr1135/1136)/Insulin Receptor β (Tyr1150/1151) (19H7) Rabbit mAb	Cell Signaling Technology	Cat.#3024S; RRID: AB_331253; Lot: #0005
Phospho-p38 MAPK (Thr180/Tyr182) Rabbit mAb	Cell Signaling Technology	Cat.#4511P; RRID: AB_2139682; Lot: #0010
Phospho-Stat3 (Tyr705) (D3A7) XP Rabbit mAb	Cell Signaling Technology	Cat.#9145; RRID: AB_2491009; Lot: #0005
β-ACTIN, Mouse mAb	Sigma-Aldrich	Cat.#A1978; RRID: AB_476692; Lot: #055M4788V
Lamin A/C (N-18), from goat, polyclonal	Santa Cruz Biotechnology	Cat.#sc-6215, RRID:AB_648152, Lot: #F1713
Anti-UCP1 antibody, from rabbit, polyclonal	abcam	Cat.#ab10983; RRID: AB_2241462; Lot: #GR3315804-5
ECL™ anti-rabbit IgG, horseradish peroxidase (from donkey)	Amersham ECL (GE Healthcare)	Cat.#NA934V; Lot:#17572641
Biological Samples		
Human adipose tissue stem cells (hASCs)	IISPV Biobank (PT17/0015/0029)	N/A
Chemicals, Peptides, and Recombinant Proteins		
Phosphate buffered saline (PBS)	Hyclone (GE Healthcare Life Sciences)	Cat.#SH30028.02
Sodium Chloride (NaCl)	Panreac	Cat.#131659.1211; CAS ID: 7647-14-5
Potassium Chloride (KCl)	Panreac	Cat.#131494; CAS ID: 7440-09-7
Calcium Chloride ($CaCl_2$)	Fisher Chemical	Cat.#c/1500/53; CAS ID: 10043-52-4
Magnesium Chloride ($MgCl_2$)	Sigma-Aldrich	Cat.#M8266; CAS ID: 7786-30-3
Sodium bicarbonate ($NaHCO_3$)	Merck	Cat.#6329; CAS ID: 144-55-8
2-[4-(2-Hydroxyethyl)Piperazin-1-Yl] Ethanesulfonic Acid (HEPES)	Fisher Scientific	Cat.#BP310-1; CAS ID: 7365-45-9
Bovine Serum Albumin (BSA)	Sigma-Aldrich	Cat.#A7030; CAS ID: 9048-46-8
cis-epoxysuccinic acid	TCI Chemicals	Cat.#E0449; CAS ID: 16533-72-5
Succinic acid	Sigma-Aldrich	Cat.#S9512; CAS ID: 110-15-6
Disodium succinate	Sigma-Aldrich	Cat.#W327700; CAS ID: 150-90-3
Collagenase from *Clostridium histolyticum*	Sigma-Aldrich	Cat.#C0130; CAS ID: 9001-12-1
Dexamethasone	Sigma-Aldrich	Cat.#D2915; CAS ID: 50-02-2
Biotin	Sigma-Aldrich	Cat.#B4501; CAS ID: 58-85-5
Calcium pantothenate	Sigma-Aldrich	Cat.#C8721; CAS ID: 137-08-6
3-isobutyl-1-methylxanthine (IBMX)	Sigma-Aldrich	Cat.#I5879; CAS ID: 28822-58-4
Insulin from bovine pancreas	Sigma-Aldrich	Cat.#I1882; CAS ID: 11070-73-8

(*Continued on next page*)

UNIVERSITAT ROVIRA I VIRGILI
Metabolic Impact of the Succinate/SUCNR1 Axis in Adipocytes: Insights into Circadian and Leptin Regulation
TERESA VILLANUEVA CARMONA

Continued

REAGENT or RESOURCE	SOURCE	IDENTIFIER
Rosiglitazone	Sigma-Aldrich	Cat.#R2408; CAS ID: 122320-73-4
5-aminoimidazole-4-carboxamide ribonucleotide (AICAR)	Sigma-Aldrich	Cat.#A9978; CAS ID: 2627-69-2
SP600125	MedChemExpress	Cat.#HY-12041; CAS ID: 129-56-6
SB202190	MedChemExpress	Cat.#HY-10295; CAS ID: 152121-30-7
Compound C	Calbiochem	Cat.#171260; CAS ID: 866405-64-3
Atglistatin	Cayman Chemicals	Cat.#15284; CAS ID: 1469924-27-3
Corn oil	Sigma-Aldrich	Cat.#C8267; CAS ID: 8001-30-7
Leptin from mouse	Sigma-Aldrich	Cat.#L3772; CAS ID: 181030-10-4
rm-Leptin - recombinant mouse	R&D Systems	Cat.#498-OB
PFA 4%	Sigma-Aldrich	Cat.#1.00496.5000
Sodium azide	Thermo Scientific	Cat.#AC190380050; CAS ID: 26628-22-8
Isoproterenol	Sigma-Aldrich	Cat.#PHR2722; CAS ID: 51-30-9
Oil Red O	Sigma-Aldrich	Cat.#O0625; CAS ID: 1320-06-5
β-glycerolphosphate disodium salt	Sigma-Aldrich	Cat.#G9422; CAS ID: 154804-51-0
L-ascorbic acid	Sigma-Aldrich	Cat.#33034; CAS ID: 50-81-7
Alizarin red S	Sigma-Aldrich	Cat.#A5533; CAS ID: 130-22-3
Hexadecylpyridinium chloride	Sigma-Aldrich	Cat.#C9002; CAS ID: 6004-24-6
Tris-HCl	Fischer bioreagents	Cat.#BP153-500; CAS ID: 1185-53-1
Ethylenediaminetetraacetic acid (EDTA)	Sigma-Aldrich	Cat.#E6758; CAS ID: 60-00-4
Ethylene glycol-bis(2-aminoethylether)-*N,N,N′,N′*-tetraacetic acid (EGTA)	Sigma-Aldrich	Cat.#E3889; CAS ID: 67-42-5
2-mercaptoethanol	Sigma-Aldrich	Cat.#M3148; CAS ID: 60-24-2
Phenylmethylsulfonyl fluoride (PMSF)	Sigma-Aldrich	Cat.#P7626; CAS ID: 329-98-6
Aprotinin	Thermo Scientific	Cat.#78432; CAS ID: 9087-70-1
Leupeptin	Sigma-Aldrich	Cat.#L5793; CAS ID: 103476-89-7
TRIzol Reagent	Invitrogen	Cat.#15596018
RNAClean XP	Beckman Coulter	Cat.#A66514
Mammalian Protein Extraction Reagent (M-PER)	Thermo Scientific	Cat.#78501
Halt Phosphatase Inhibitor Cocktail 100x	Thermo Scientific	Cat.#78426
Halt Protease Inhibitor Cocktail 100x	Thermo Scientific	Cat.#78429
Harris Hematoxylin	StatLab Medical Products	Cat.#HXHHELT
Eosin	Sigma-Aldrich	Cat.#HT110216
Tween-20	Sigma-Aldrich	Cat.#P2287; CAS-ID: 9005-64-5
PERDROGEN 30% H_2O_2 (w/w)	Sigma-Aldrich	Cat.#31642; CAS ID: 7722-84-1
Gelatin, from cold water fish skin	Sigma-Aldrich	Cat.#G7765; CAS ID: 9000-70-8
Mayer's Hematoxylin	Sigma-Aldrich	Cat.#MHS32
Naphthol AS-BI phosphate	Sigma-Aldrich	Cat.#N2125; CAS ID: 1919-91-1
Pararosaniline hydrochloride	Sigma-Aldrich	Cat.#P3750; CAS ID: 569-61-9
Fast Green FCF	Sigma-Aldrich	Cat.#F7252; CAS ID: 2353-45-9
SR1078 (RORα/γ Agonist)	Sigma-Aldrich	Cat.#557352
Critical Commercial Assays		
Free Glycerol Reagent	Sigma-Aldrich	Cat.#F6428
Human Leptin Quantikine ELISA	R&D Systems	Cat.#DLP00
Quantikine ELISA Mouse/Rat Leptin	R&D Systems	Cat.#MOB00B
Succinate Assay Kit	Sigma-Aldrich	Cat.#CB04A13
Succinate Colorimetric Assay Kit	Sigma-Aldrich	Cat.#MAK184
High-Capacity cDNA Reverse Transcription kit with RNAse inhibitor	Applied Biosysems	Cat.#4374966
RNeasy Mini Kit	Qiagen	Cat.#74106

(*Continued on next page*)

UNIVERSITAT ROVIRA I VIRGILI
Metabolic Impact of the Succinate/SUCNR1 Axis in Adipocytes: Insights into Circadian and Leptin Regulation
TERESA VILLANUEVA CARMONA

Continued

REAGENT or RESOURCE	SOURCE	IDENTIFIER
TruSeq Stranded Total RNA Library Prep kit	Illumina	Cat.#20020597
Reverse transcriptase SuperScript II	Invitrogen	Cat.#10328062
KAPA Library Quantification Kit KK4835	Roche	Cat.#07960204001
Pierce BCA Protein Assay Kit	Thermo Scientific	Cat.#23225
Immobilon ECL Ultra Western HRP Substrate	Merck Millipore	Cat.#WBULS0500
Vectastain ABC	Vector Laboratories	Cat.#SK-4000
DAB peroxidase substrate kit	Vector Laboratories	Cat.#SK-4100
Nano-Glo® Dual-Luciferase® Reporter Assay System	Promega	Cat.#N1610
Deposited Data		
RNA sequencing data	Gene Expression Omnibus (GEO)	Accession number: GSE200749
Experimental Models: Cell Lines		
3T3-L1 cell line	ATCC	CL-173™; RRID: CVCL_0123
HEK 293 cell line	ATCC	CRL-1573™; RRID: CVCL_0045
Experimental Models: Organisms/Strains		
Adipoq-Cre mice	kindly provided by G.Sabio, CNIC, Madrid, Spain	N/A
Sucnr1$^{fl/fl}$ mice	Keiran et al.[34]	N/A
Sucnr1 KO mice	McCreath et al.[3]	N/A
C57BL/6 wild-type mice	Charles River	N/A
B6.129-*Arntl*^{tm1Bra}/J	The Jackson Laboratory	Strain: #009100; RRID: IMSR_JAX:009100
Oligonucleotides		
Taqman Gene Expression Assays	Applied Biosystems	See Table S6
Recombinant DNA		
pBMAL1-LUC	kindly provided by S. Yamazaki (UT Southwestern Medical Center) and K. Eckel-Mahan (University of Texas); Yeom et al.[99]	N/A
pCMV6-human SUCNR1 (GFP-tagged)	Origene	Cat.#RC205888
pGL3-Basic	Promega	Cat.#E1751
pNL1.1.PGK[Nluc/PGK]	Promega	Cat.#N1441
Software and Algorithms		
ImageJ software 1.53k	National Institutes of Health, USA	RRID: SCR_003070
Mnova software	Mestrelab Research	N/A
NRecon resontruction software	SkyScan	N/A
CT-Analyzer	SkyScan	N/A
ZEN Digital Imaging for Light Microscopy v 3.1 (blue edition)	Zeiss	RRID: SCR_013672
Bioanalyzer DNA 1000	Agilent	N/A
Fragment Analyzer Standard Sensitivity	Agilent	N/A
FastQC v0.11.9	BaseSpace Labs	RRID: SCR_014583
STAR software v 2.5.2	Dobin et al.[100]	RRID: SCR_004463
Rsubread package v 2.8.2	Liao et al.[101]	RRID: SCR_016945
iBright Analysis Software	Invitrogen	RRID: SCR_017632
Leica microsystems imaging software	Leica	N/A
Adiposoft plug-in (Image J)	Natrional Institutes of Health, USA	N/A
Nikon Eclipse E800 microscope	Nikon	RRID: SCR_020326
Graphpad Prism 8	Graphpad Software	RRID: SCR_002798

(*Continued on next page*)

UNIVERSITAT ROVIRA I VIRGILI
Metabolic Impact of the Succinate/SUCNR1 Axis in Adipocytes: Insights into Circadian and Leptin Regulation
TERESA VILLANUEVA CARMONA

CellPress

Continued

REAGENT or RESOURCE	SOURCE	IDENTIFIER
R software v4.2.0	R Core Team[102]	RRID: SCR_001905
ggplot2 R package v3.3.6	Wickham[103]	RRID: SCR_014601
ggpubr R package v0.4.0	N/A	RRID: SCR_021139
IBM SPSS Statistics v 27.0	IBM Corp	RRID: SCR_002865
R software v 4.1.2	R Core Team[102]	RRID: SCR_001905
limma package v 3.50.1	Ritchie et al.[104]	RRID: SCR_010943
R/Bioconductor package DESeq2 v 1.34.0	Love et al.[105]	RRID: SCR_015687
ROAST-GSA v 1.03.2	Wu et al.[106]; Efron and Tibshirani[107]	N/A
Bioconductor R package org.Hs.eg.db	Carlson[108]	RRID:SCR_006442
Other		
Normal control diet	SAFE diets	Cat.#A04
High-fat diet 60% fat	Research diets	Cat.#D12492
DMEM/F12 medium	Gibco (Life Technologies Limited)	Cat.#31330-038
DMEM-High glucose	Hyclone (GE Healthcare Life Sciences)	Cat.#SH30081.01
Fetal Bovine Serum (FBS)	Hyclone (GE Healthcare Life Sciences)	Cat.#SH30071.03
Antibiotic/antimycotic solution	Hyclone (GE Healthcare Life Sciences)	Cat.#SV30079.01
Immobilon-P PVDF membrane	Merck Millipore	Cat.#IPVH00010

RESOURCE AVAILABILITY

Lead contact

Further information and requests for resources and reagents should be directed to and will be fulfilled by the lead contact: Sonia Fernández-Veledo (sonia.fernandez@iispv.cat).

Materials availability

Mouse lines generated in this study are available from the lead contact upon request.

Data and code availability

- RNAseq data have been deposited in GEO and are publicly available as of the date of publication. Accession numbers are listed in the key resources table.
- This study did not generate new code.
- Any additional information required to reanalyze the data reported in this paper is available from the lead contact upon request.
- Data S1 refers to unprocessed data underlying the display items in manuscript, related to Figures 1, 2, 3, 4, 5, 6, 7, and S1–S4.

EXPERIMENTAL MODEL AND SUBJECT DETAILS

Human cohorts

Subjects were recruited at the University Hospital Joan XXIII (Tarragona, Spain) and Hospital de Santa Tecla (Tarragona, Spain). All participants gave their informed consent and the study was reviewed and approved by the ethics and research committees of the respective hospitals (references CEIm 177/2018 approved on the 29th of November 2018 and CEIm 41p/2015 approved on the 31st of August 2015), in accordance with the tenets of the Declaration of Helsinki. Plasma, scWAT and vWAT were obtained from age- and gender-matched human donors undergoing non-acute surgical interventions, such as hernia or cholecystectomy, in a scheduled routine surgery. Donors were classified according to their BMI as lean or obese, following World Health Organization criteria[109] (lean BMI $\leq$25 kg/m^2 and obese BMI $\geq$30 kg/m^2). Anthropometric and biochemical variables from the cohort are detailed in Table S2.

Mouse lines

Adipocyte cell-specific *Sucnr1* knockout mice (Ad-*Sucnr1* KO) were generated by breeding *Adipoq*-Cre mice (kindly provided by G. Sabio, CNIC, Madrid, Spain) with *Sucnr1*$^{fl/fl}$ mice.[34] Cre-negative *Sucnr1*$^{fl/fl}$ littermates were used as controls. Mice were genotyped by PCR; genotyping of *Sucnr1*$^{fl/fl}$ mice resulted in a 450-bp product for the *loxP*-targeted allele and a 700-bp product for the *Adipoq*-Cre allele. All genotypes were generated on a pure C57BL/6 background. Mice were housed at the Faculty of Medicine and Health Science animal facility of Universitat Rovira i Virgili, under controlled conditions of 12-h light/dark cycles at 22°C and *ad libitum* access to NCD (3.1% fat; SAFE diets, A04) or HFD (60% fat; Research diets, D12492), unless specified, beginning at 8 weeks of age

UNIVERSITAT ROVIRA I VIRGILI
Metabolic Impact of the Succinate/SUCNR1 Axis in Adipocytes: Insights into Circadian and Leptin Regulation
TERESA VILLANUEVA CARMONA

until sacrifice. Male mice were weighed weekly. At the end of the study, animals were fasted overnight, killed by cervical dislocation, and blood and tissues were collected and immediately frozen. Plasma was obtained from global *Sucnr1* KO[3] and wild-type mice (C57BL/6; Charles River, Barcelona, Spain) used as controls, as well as from Ad-*Sucnr1* KO and *Sucnr1*$^{fl/fl}$ mice, after an overnight fast ± a 3-h refed. Adipose tissue was collected from 10–12-week-old male B6.129-*Arntl*^{tm1Bra}/J heterozygous knockout mice (#009100; RRID: IMSR_JAX:009100; *Bmal1* KO) purchased from The Jackson Laboratory (Bar Harbor, ME) and C57BL/6J wild-type mice were used as controls. The *Bmal1* expression levels were confirmed by qPCR in liver: 0.55±0.03 in *Bmal1* KO *vs* 1.00±0.11 in WT, p=0.002; and in rWAT: 0.65±0.03 in *Bmal1* KO *vs* 1.00±0.09 in WT, p=0.005. All animal studies were supervised and approved by the Universitat Rovira i Virgili Animal Welfare and Governmental Ethics Committee (reference 10970). All animal procedures conformed to European Union Directive 86/609/EEC and recommendation 2007/526/EC regarding the protection of animals used for experimental and other scientific purposes, enacted under Spanish law 1201/2005.

Mouse adipose tissue explants

Mouse WAT from at least three mice was freshly isolated and cleaned with phosphate buffered-saline (PBS; Hyclone, GE Healthcare Life Sciences, Logan, UT) containing 1% antibiotic/antimycotic solution (Hyclone) and pooled. For leptin secretion analysis, tissues (0.2 g) were transferred into 1 mL of DMEM/F12 (Gibco, Life Technologies Limited, Paisley, UK) for 24 h at 37°C and 5% CO_2. Supernatants were then collected and stored at -20 °C for further analysis. For western blot experiments, tissues (0.8 g) were cultured in 24-well plates with Krebs Ringer Bicarbonate HEPES (KRBH) buffer containing 120 mM NaCl, 5 mM KCl, 2 mM $CaCl_2$, 1 mM $MgCl_2$, 25 mM $NaHCO_3$, and 5.5 mM HEPES, and supplemented with 0.1% bovine serum albumin (BSA, Sigma-Aldrich, St Louis, MO) for 2 h, and treated with 100 μM *c*ESA (TCI chemicals, Tokyo, Japan) or 400 μM succinic acid (Sigma-Aldrich) for 10 min. For gene expression studies, tissues (0.8g) were cultured in 24-well plates with KRBH buffer supplemented with 0.1% BSA for 2 h and treated with 400 μM succinic acid for 6 h.

Primary mASCs and mature adipocytes

WAT was collected from Ad-*Sucnr1* KO and *Sucnr1*$^{fl/fl}$ mice, weighed, and pooled according to WAT localization and genotype. Tissues were cut into small pieces, extensively washed with PBS to remove debris, and treated with 0.2% collagenase (Sigma-Aldrich) in PBS and 1% BSA for 1 h at 37°C with gentle agitation. Digested samples were centrifuged at 300 g for 10 min to separate adipocytes from the stromal vascular fraction (SVF). Mature adipocytes were carefully removed from the upper part of the solution and centrifuged at 300 g for 5 min. Adipocytes were then cultured in 12-well plates with DMEM/F12 supplemented with 10% fetal bovine serum (FBS, Hyclone) for 24 h at 37°C and 5% CO_2, and treated with 400 μM succinic acid for 6 h. The cell pellet containing the SVF was re-suspended in DMEM/F12 supplemented with 10% FBS and 1% antibiotic/antimycotic solution. Mouse ASCs were incubated at 37°C and 5% CO_2 and the medium was replaced 24 h after seeding to remove non-adherent cells. All experiments were performed in cells at passage 3.

Primary mouse BM-MSCs

Tibias and femurs from mice were dissected and cleaned with PBS. Bones were cut to allow flushing of bone-marrow contents using a 20-G needle attached to a syringe, and the pellet was cultured in DMEM-High Glucose medium (Hyclone) supplemented with 15% FBS and 1% antibiotic/antimycotic solution in a humidified cell culture incubator at 37°C with 5% CO_2. Non-adherent cells were removed after 24 h with subsequent media changes every 2–3 days until BM-MSCs reached confluence.

Primary hASCs

Human ASCs were isolated as described[110] from scWAT biopsies of lean and obese donors, which included 4 females (n=2 lean, BMI 20.3±0.7 kg/m^2; n=2 obese, BMI 32.9±0.7 kg/m^2). Briefly, adipose tissue was washed with PBS and then treated with 0.1% collagenase in PBS + 1% BSA for 1 h at 37°C with gentle agitation. Digested samples were centrifuged at 300 g at 4°C for 5 min to separate the SVF. The SVF was resuspended and cultured in DMEM/F12 supplemented with 10% FBS and 1% antibiotic/antimycotic solution, and frozen. Cells were stored in the IISPV BioBank (PT17/0015/0029) registered at the National Register of Biobanks (registration number #C.0003609). Differentiation of hASCs to mature white adipocytes was performed following a published protocol.[111] In brief, differentiation induction medium was used for confluent hASCs, containing DMEM/F12, 10% FBS, 1% antibiotic/antimycotic solution, DMEM-High Glucose, dexamethasone (1 μM), biotin (33 μM), calcium pantothenate (17 μM), 3-isobutyl-1-methylxanthine (IBMX; 500 μM), insulin (100 nM), and rosiglitazone (5 μM) (all from Sigma-Aldrich). After 4 days, the medium was changed every two days to supplemented DMEM/F12-DMEM-High Glucose medium only containing dexamethasone, biotin, and calcium pantothenate until day 14 of differentiation. Once differentiated, cells were serum deprived for 2 h with FBS-free medium containing 0.2% BSA, and treated with 400 μM succinic acid or 100 μM *c*ESA.

3T3-L1 cell line

Murine embryonic 3T3-L1 preadipose cells (CL-173^{TM}; RRID: CVCL-0123; ATCC, Manassas, VA) were cultured in DMEM-High Glucose medium supplemented with 10% FBS and 1% antibiotic/antimycotic solution in a humidified cell culture incubator at 37°C with 5% CO_2. Confluent cultures were treated for 2 days in the same medium containing the differentiation inducers 0.25 μM dexamethasone, 0.5 mM IBMX, 5 μg/mL insulin, and 1 μM rosiglitazone. Cells were then cultured for 2 days in growth medium supplemented with 5 μg/mL insulin and 1 μM rosiglitazone, and then in growth medium alone for the subsequent days.

UNIVERSITAT ROVIRA I VIRGILI
Metabolic Impact of the Succinate/SUCNR1 Axis in Adipocytes: Insights into Circadian and Leptin Regulation
TERESA VILLANUEVA CARMONA

At day 9–10 of differentiation, cells were rested for 2 h in FBS-free medium containing 0.2% BSA and then treated with succinic acid, cESA, or 5-aminoimidazole-4-carboxamide ribonucleotide (AICAR; Sigma-Aldrich). In studies using phosphatase inhibitors, cells were pre-treated for 30 min with SP600125 (MedChemExpress, Monmouth Junction, NJ), SB202190 (MedChemExpress) or compound C (Calbiochem, San Diego, CA).

HEK 293 cell line

Human embryonic kidney (HEK) 293 cells were obtained from ATCC (CRL-1573™; RRID: CVCL_0045). Cells were cultured in DMEM-High Glucose supplemented with 10% FBS and 1% antibiotics/antimycotics solution.

METHOD DETAILS

Indirect calorimetry

Indirect calorimetry was performed as described[112] using a 16-chamber TSE Phenomaster monitoring system (TSE Systems GmbH, Bad Homburg, Germany). Individually caged mice were acclimatized in the measuring room for three days before the onset of experiments. Oxygen consumption and CO_2 production were directly measured over a period of 48 to 72 h. From these data, the RER and EE were calculated according to the formula RER = V_{CO2}/V_{O2}; EE = (3.185 + 1.232 * RER) * V_{O2}.

Locomotor activity and food intake

Locomotor activity and food intake were monitored during the indirect calorimetry experiments. Horizontal locomotor activity of mice moving freely in their cages was continuously registered using an infrared photocell beam grid. Food and water intake were automatically monitored using built-in sensors located in each cage, and were available *ad libitum* unless stated otherwise.

Quantitative Magnetic Resonance Imaging

Fat mass

The relative amount of fat in each animal was calculated using qMRI. Mice were anaesthetized with 1.5–2% isoflurane in oxygen and MRI was performed with a 7.0T 16 cm bore Bruker Biospect MRI system equipped with a quadrature 40-mm coil and a 90-mm gradient coil insert (maximum intensity 360 G/cm) (Bruker Medical GmbH, Ettlingen, Germany). Body temperature and respiratory rate were monitored during the MRI studies using a rectal probe and a gating system for small animals (SA Instruments, Inc., Stony Brook, NY), respectively. T2-weighted spin echo images were obtained with a rapid acquisition with relaxation enhancement (RARE) sequence. Axial and coronal images were obtained for each animal. For axial planes, two set of images were acquired consecutively with and without fat suppression module. For coronal planes, fat images were obtained by applying a frequency selective radiofrequency pulse at a high-field offset of 1000–1100 Hz with respect to the water signal to excite the fat protons only. The acquisition parameters were as follows: repetition time, 3200 ms; echo time 44 ms; number of averages 2; matrix, 256 × 256 within a field of view of 50 × 50 mm; number of slices, 14 for horizontal and 36 for coronal orientations; slice thickness, 1.5 mm, without gap. Image analysis was carried out using NIH ImageJ software (RRID: SCR_003070). For each animal, the total fat volume was calculated and converted to grams by assuming a density of adipose tissue of 0.9 g/mL.[113] Fat mass was expressed as a percentage relative to the total weight of the animal.

In vivo *proton magnetic resonance spectroscopy*

Non-localized ^{1}H-MRS was performed using a single pulse sequence without water suppression and with a repetition time of 2 s (128 averages). Spectroscopic data were acquired using 2018 points and 7.5 KHz spectral width. The intensities of the water and fat signals were calculated using Mnova software (Mestrelab Research, Santiago de Compostela, Spain) and a relative concentration of fat/water was measured in every case.

Muscle volume

We performed MRI as described[114] using the equipment described above. T2-weighted spin echo images were acquired with a rapid acquisition with relaxation enhancement sequence in axial and coronal orientations with the following parameters: TR=3000 ms, TE=11.57 ms, RARE factor=8, Av=12, FOV=2.5 cm, acquisition matrix=256×256 corresponding to an in-plane resolution of 97× 97 μm^2, slice thickness=1 mm without gap between slices. Hind limb images were analyzed with ImageJ software on 5 consecutive slices without gaps, and values from both limbs were obtained and added to generate a single value for each mouse. For axial planes, the first slice was located in the dorsal direction following the one showing the entire length of the tibia. For coronal planes, the stack started at the third slice distal to the tibial plateau. In each slice, regions of interest (ROIs) were manually traced in each projection, and areas of hyper- or hypointense signal corresponding to fat or bone, respectively, were excluded.

Glucose and insulin tolerance tests

Mice were subjected to a glucose-tolerance test after a 6-h fast, receiving an intraperitoneal load of glucose solution (2 g/kg). Glucose levels were determined from blood samples taken from the tail vein at 0, 15, 30, 60, and 120 min using a handheld glucometer (Accu-Chek glucose reader; Roche, Mannheim, Germany). For intraperitoneal insulin-tolerance testing, mice were fasted for 3 h and injected with insulin (0.75 U/kg). Glucose was measured as described above.

UNIVERSITAT ROVIRA I VIRGILI
Metabolic Impact of the Succinate/SUCNR1 Axis in Adipocytes: Insights into Circadian and Leptin Regulation
TERESA VILLANUEVA CARMONA

Effect of oral succinate on circulating leptin

Ad-*Sucnr1* KO and *Sucnr1*$^{fl/fl}$ mice were fasted overnight before oral administration of 500 mg/kg of disodium succinate (Sigma-Aldrich). Blood samples were collected from the tail after 0, 2, 4, and 6 h post-gavage, and plasma was obtained for leptin determination.

In vivo lipolysis inhibition

Mice fed NCD (8-week-old) or HFD (14-week-old, 8 weeks on HFD-feeding) were treated with 200 μmol/kg of ATGLi (Cayman Chemical, Ann Arbor, MI) or corn oil as vehicle (Sigma-Aldrich) by oral gavage once daily for two weeks. Body weight and food intake were monitored daily. At the end of the study, animals were fasted overnight, killed by cervical dislocation, and tissues were collected.

Chronic leptin treatment

Ad-*Sucnr1* KO mice (8-week-old) fed NCD were intraperitoneally injected with 0.5 mg/kg leptin (Sigma-Aldrich) or PBS (as vehicle) twice daily (8:00 am and 7:00 pm) for 4 weeks. Body weight and food intake were monitored daily before leptin injection. Control mice were pair-fed to leptin-treated mice. At the end of the study, animals were fasted overnight, killed by cervical dislocation, and tissues were collected.

Feeding studies and leptin sensitivity tests

To study the gene expression in the transition from fasted to fed state, mice were fasted for 24 h, then one-half of the mice were sacrificed and the other one-half were refed for 12 h before sacrifice. For western-blot studies, mice were singly housed and acclimatized for 3 days prior to the study. Mice were fasted for 24 h, then one-half of the mice were sacrificed and the other one-half were refed for 20 minutes. For leptin sensitivity tests, mice were acclimatized by subjecting them to handling and sham injections. Mice were fasted overnight and intraperitoneally injected with 3 μg/g of mouse leptin (R&D Systems, Minneapolis, MN) or PBS. After 1 h, mice were sacrificed. In all cases, the hypothalamus was collected and immediately frozen. Alternatively, leptin sensitivity on body weight and food intake was analyzed in Ad-*Sucnr1* KO and *Sucnr1*$^{fl/fl}$ mice intraperitoneally injected with 0.5 mg/kg leptin or PBS (as vehicle) twice daily (8:00 am and 7:00 pm) for 4 days, and body weight and food intake were monitored daily before leptin injection.

Microcomputed tomography

Tibias from 22-week-old NCD-fed mice, and from mice fed HFD for 13 weeks (21-weeks old) were dissected, cleaned of soft tissue, and fixed in 4% paraformaldehyde (PFA; Sigma-Aldrich) for 24 h at 4°C. Samples were placed in PBS for 24 h at 4°C and subsequently placed in 20% sodium azide (Thermo Scientific, Rockford, IL) diluted in PBS at 4°C until analysis. High-resolution images from the tibia were acquired using a computerized microtomography imaging system (SkyScan 1272, Bruker microCT, Kontich, Belgium) in accordance with recommendations from the American Society of Bone and Mineral Research. Samples were scanned in air at 70 kV and a power of 10 W (143 μA) with an exposure time of 2700 ms, using a 1-mm aluminum filter and an isotropic voxel size of 11 μm. Two-dimensional images were obtained every 1° of a 180° rotation and were subsequently reconstructed using NRecon reconstruction software and analyzed with a CT-Analyzer (SkyScan). For trabecular measurements manual ROIs were selected, starting 0.6 mm from the growth plate of the tibiae and extending to the diaphysis for 2 mm. For cortical parameters analysis, a 3-mm section starting from the bifurcation of the fibula was selected. A Gaussian noise filter was applied for reconstruction and a global binary threshold was manually established at 15 for trabecular analysis and at 50 for cortical analysis.

Ex vivo lipolysis determination

Mouse eWAT tissues (0.8 g) were cultured in 24-well plates with KRBH buffer supplemented with 0.1% free-fatty acid-BSA. Lipolysis was induced with 1 μM isoproterenol (Sigma-Aldrich) and explants were also treated with 100 μM *c*ESA for 3 h. Lipolysis was determined by measuring glycerol released in the culture medium (Free Glycerol Reagent, Sigma-Aldrich).

Brown adipocyte differentiation of mASCs

Mouse ASCs were cultured in 6-well plates with a brown adipocyte induction medium containing DMEM/F12 supplemented with 10% FBS, 15 mM HEPES, 1 nM insulin, 100 μM IBMX, 1 μM dexamethasone, and 3 μM rosiglitazone. After 4 days, the medium was replaced with the absence of insulin until day 10 of differentiation. To evaluate lipids, cells were fixed with 4% PFA for 15 min, washed with distilled water, and stained for 45 min with Oil Red O (Sigma-Aldrich). Lipid vesicles were photographed using a light microscope equipped with a Zeiss AxioCam MRM (Zeiss, Germany) and ZEN Digital Imaging for Light Microscopy v3.1 software (blue edition; RRID: SCR_013672; Zeiss). The stain was eluted using isopropanol for 5 min and the optical density was read at 540 nm.

Osteoblast differentiation of BM-MSCs

BM-MSCs were cultured in 12-well plates with DMEM-High Glucose containing 10 mM β-glycerol phosphate, 100 mM dexamethasone, and 0.5 mM L-ascorbic acid (all from Sigma-Aldrich) for 2 weeks. Differentiated BM-MSCs were fixed in 4% PFA and washed in distilled water. The cells were incubated with 1% Alizarin red S staining solution (pH 4.1; Sigma-Aldrich) at room temperature for 45 min. Excess staining was washed in distilled water and mineralization alterations were photographed using a light microscope

UNIVERSITAT ROVIRA I VIRGILI
Metabolic Impact of the Succinate/SUCNR1 Axis in Adipocytes: Insights into Circadian and Leptin Regulation
TERESA VILLANUEVA CARMONA

equipped with a Zeiss AxioCam MRM and ZEN Digital Imaging for Light Microscopy v3.1 software (blue edition). The stain was eluted with 10% hexadecylpyridinium chloride (Sigma-Aldrich) and the optical density was read at 540 nm.

Cell fractionation assay

3T3-L1 differentiated adipocytes were lysed in homogenization buffer (20 mM Tris-HCl, 2 mM EDTA, 2 mM EGTA, 1 mM phenylmethylsulfonyl fluoride (PMSF), 10 mM 2-mercaptoethanol, 10 μg/L aprotinin, and 10 μg/mL leupeptin) followed by mechanical disruption using a Dounce homogenizer. Total lysates were centrifuged at 1300 rpm for 10 min after which the pellets containing nuclei were collected.

Biochemical parameters

Plasma triglycerides and non-esterified fatty acids were determined enzymatically using commercial kits adapted to a COBAS 6000 autoanalyzer (Roche Diagnostics, Rotkreuz, Switzerland). Leptin levels were determined from plasma or cell conditioned medium using the Leptin Quantikine ELISA (mouse or human) (R&D Systems, Minneapolis, MN). For succinate determination, human plasma samples were filtered (10-kDa) and succinate levels were measured using the fluorometric Succinate Assay Kit (Sigma Aldrich), following the manufacturer's instructions.[10] Tissular succinate accumulation was determined in 20 mg of eWAT, using the Succinate Colorimetric Assay Kit (Sigma-Aldrich), following the manufacturer's instructions.

Gene-expression analysis

Total RNA was extracted from tissues or cells using TRIzol Reagent (Invitrogen, Carlsbad, CA). cDNA was generated using the High-capacity cDNA Reverse Transcription kit (Applied Biosystems, Carlsbad, CA), and was subjected to quantitative real-time PCR amplification on a 7900HT Fast Real-Time PCR System using the TaqMan Gene Expression Assay (Applied Biosystems; Table S6). *B2m* and *RNA18S5* were used as housekeeping genes for mice and human samples, respectively. Relative expression was calculated using the comparative Ct method ($2^{-\Delta\Delta Ct}$).

Transcriptome analysis by RNA sequencing

RNA sequencing was performed on vWAT from 5 *Sucnr1*$^{fl/fl}$ mice and 5 Ad-*Sucnr1* KO mice. RNA was extracted using TRIzol reagent and further purified/DNase treated with the RNeasy Mini Kit (Qiagen, Hilden, Germany). Samples were sequenced at Centro Nacional de Análisis Genómico (CNAG-CRG, Barcelona, Spain). Libraries were prepared using the TruSeq Stranded Total RNA Library Prep kit (Human/Mouse/Rat 96 samples, Illumina, San Diego, CA) according to the manufacturer's protocol, to convert total RNA into a library of template molecules of known strand origin and suitable for subsequent cluster generation and DNA sequencing. Briefly, 300 ng of total RNA were used to remove ribosomal RNA (rRNA) using biotinylated, target-specific oligos combined with Ribo-Zero rRNA removal beads. An extra step using Sera-Mag beads (GE Healthcare/Thermo, Chicago, IL) was added to Illumina protocol to improve rRNA depletion. After the rRNA is depleted, the remaining RNA is purified with RNAClean XP beads (Beckman Coulter, Brea, CA). Following purification, the RNA is fragmented into small pieces using divalent cations under elevated temperature, and primed with random hexamers for cDNA synthesis. Then, the cleaved RNA fragments were copied into first strand cDNA using reverse transcriptase (SuperScript II, Invitrogen, Carlsbad, CA) and random primers. After that, second strand cDNA was synthesized, removing the RNA template and synthesizing a replacement strand, incorporating dUTP in place of dTTP to generate dscDNA using DNA Polymerase I and RNase H. These cDNA fragments then had the addition of a single 'A' base to the 3'ends of the blunt fragments to prevent them from ligating to one another during the adapter ligation. A corresponding single T nucleotide on the 3' end of the adapter provides a complementary overhang for ligating the adapter to the fragments ensuring a low rate of chimera (concatenated template) formation. Subsequent ligation of the multiple indexing adapter to the ends of the dscDNA was performed after A-tailing. Finally, PCR selectively enriched those DNA fragments that had adapter molecules on both ends and amplified the amount of DNA in the library. The PCR was performed with a PCR Primer Cocktail that anneals to the ends of the adapters. Final libraries were analyzed using Bioanalyzer DNA 1000 or Fragment Analyzer Standard Sensitivity (Agilent, Santa Clara, CA) to estimate the quantity and validate the size distribution, and were then quantified by qPCR using the KAPA Library Quantification Kit KK4835 (Roche, Basel, Switzerland) prior to sequencing. Libraries were sequenced 1 x 51+8+8 bp to at least 60 million reads per sample on the Illumina NextSeq2000 platform.

Read files for each sample were subsequently downloaded and collated into a single FASTQ file. FastQC (version 0.11.9; RRID: SCR_014583; BaseSpace Labs, Illumina) was used to evaluate the quality of raw read data and identify problematic features (inappropriate GC content, over-represented sequences, and/or low-quality scores). Reads were mapped against *Mus musculus* reference genome (GRCm38.p6) using STAR software (v2.5.2; RRID: SCR_004463),[100] and were assigned to genes using feature Counts from the Bioconductor package Rsubread (v2.8.2; RRID: SCR_016945).[101] All RNA sequencing data have been uploaded to Gene Expression Omnibus GEO: .

Western blotting

Cells and tissues were lysed and homogenized in M-PER buffer (Thermo Scientific) containing Halt Protease and Phosphatase Inhibitor Cocktails (Thermo Scientific). Protein concentration was determined with the BCA Protein Assay Kit (Thermo Scientific). Equal amounts of total protein were separated in SDS-polyacrylamide gel electrophoresis, transferred to Immobilon-P PDVF membranes (Merck Millipore, Burlington, MA) and blocked. Immunoblot analysis was performed with polyclonal antibodies against

UNIVERSITAT ROVIRA I VIRGILI
Metabolic Impact of the Succinate/SUCNR1 Axis in Adipocytes: Insights into Circadian and Leptin Regulation
TERESA VILLANUEVA CARMONA

phospho(p)-AKT (Ser473) (RRID: AB_331168), p-AKT (Thr308) (RRID: AB_329828), p-C/EBPα (Ser21) (RRID: AB_2077882), p-GSK3α/β (Ser21/9) (RRID: AB_329830), p-p44/42 MAPK (Erk1/2) (Thr202/Tyr204) (RRID: AB_331646), and p-SAPK/JNK (Thr183/Tyr185) (RRID: AB_331659), p-BMAL1 (Ser42) (RRID: AB_2798348), and BMAL (RRID: AB_10675117); or with monoclonal antibodies against p-AMPKα (Thr172) (RRID: AB_331250), p-IGF-I Receptor β (Tyr1135/1136)/Insulin Receptor β (Tyr1150/1151) (19H7) (RRID: AB_331253), p-p38 MAPK (Thr180/Tyr182) (RRID: AB_2139682), and p-STAT3 (Tyr705) (RRID: AB_2491009). All antibodies were from Cell Signaling Technology (Danvers, MA) except for a monoclonal antibody against β-ACTIN (Sigma-Aldrich; RRID: AB_476692) and a polyclonal anti-LAMIN A/C (Santa Cruz Biotechnology, Dallas, TX; RRID: AB_648152), which were used as loading controls, and the anti-BMAL1 antibody (Abcam, Cambridge, UK). Membranes were incubated with the respective anti-HRP secondary antibodies and visualized with the Immobilon ECL Ultra Western HRP Substrate (Merck Millipore). Band intensity was captured using the iBright CL1000 Imaging System equipped with iBright Analysis Software (RRID: SCR_017632; Invitrogen, Waltham, MA).

Histology

Blocks of paraffin-embedded tissues from mice were sectioned at 5-μm, deparaffinized, rehydrated, and stained with Harris hematoxylin (StatLab Medical Products, McKinney, TX) and eosin (Sigma-Aldrich). For UCP1 immunohistochemistry, tissue sections were heated for 10 min in 10 mM Tris, 1 mM EDTA, and 0.05% Tween-20 (Sigma-Aldrich), and then blocked for 30 min with a solution of 1% H_2O_2 (Sigma-Aldrich). To block non-specific binding, sections were incubated with 0.2% gelatin (Sigma-Aldrich), 2% BSA, and 2% FBS in PBS for 30 min at room temperature. Incubation with the primary antibody (1:500 UCP1, polyclonal; Abcam; RRID: AB_2241462) was performed overnight, followed by incubation with a secondary anti-rabbit antibody (1:250, Amersham ECL, GE Healthcare) for 1 h, and with Vectastain ABC (Vector Laboratories, Burlingame, CA) for 1 h (all incubations were performed in a humid chamber at room temperature). Finally, the slides were stained with the DAB peroxidase substrate kit (Vector Laboratories) for 4 min and counterstained with Mayer's hematoxylin solution (Sigma-Aldrich) for 1.5 min. Images were viewed using a Leica DM4 B microscope (Wetzlar, Germany) and image acquisition was performed using Leica microsystems imaging software. Adipocyte size analysis was performed using the Adiposoft plug-in of ImageJ.

For bone histological preparations, samples were fixed in 4% PFA for 24 h at 4°C, decalcified in 14% EDTA (pH 7.4) for 6 weeks, and embedded in paraffin. Samples were cut into 5-μm sections and stained with H&E for osteocyte and osteoblast quantification, or with tartrate-resistant acid phosphatase (TRAP) for osteoclasts. For TRAP staining, deparaffinized and rehydrated slides were incubated with naphthol AS-BI phosphate (Sigma-Aldrich) for 1 h at 37°C and osteoclasts were developed with pararosaniline hydrochloride (Sigma-Aldrich) for 3 min. The rest of the tissue was counterstained with 0.02% fast green solution (Sigma-Aldrich) for 45 seconds. Cells were quantified from images captured using Nikon Eclipse E800 Micorscope (RRID: SCR_020326; Nikon, Tokyo, Japan).

Luciferase reporter assay

To analyze BMAL1 promoter activity, 10 ng of pBMAL-LUC (kindly provided by S. Yamazaki, UT Southwestern Medical Center; and K. Eckel-Mahan, University of Texas)[99] and pCMV6-human SUCNR1 (GFP-tagged; Origene, Rockville, MD) were co-transfected into $10^5/cm^2$ HEK293 cells using 0.15 μL of Lipofectamine 3000, according to the manufacturer's protocol. Twenty-four hours post-transfection, cells were treated with SR1078 (Calbiochem)–a selective agonist of retinoic acid receptor-related orphan receptor α/γ (RORα/RORγ)–which is a BMAL1 activator. Forty-three hours post-transfection, cells were deprived of serum for 2 h with FBS-free medium containing 0.2% BSA, and treated with 100 μM *c*ESA. Luminescence was measured 48 h post-transfection using the Nano-Glo® Dual-Luciferase® Reporter Assay System (Promega, Madison, WI), according to the manufacturer's manual.

The pGL3-Basic plasmid (promoter-less; Promega) was used in each experiment to determine the basal levels of luciferase expression (designated as Luc). Cells were also co-transfected with pNL1.1.PGK[Nluc/PGK] vector (Promega) and NanoLuc® Luciferase measurements were used to normalize experiments for transfection efficiency. Each construct was tested in three independent transfection experiments. Luminescence was read with the Varioscan Lux plate reader (Thermo Scientific), in a white 96-well plate.

QUANTIFICATION AND STATISTICAL ANALYSIS

Shapiro-Wilk normality tests were performed to assess Gaussian distribution. When data followed Gaussian distribution, the unpaired two-tailed t-test was used to compare differences between two groups, whereas a one-way ANOVA with Dunnet's post-test was used to compare groups to a control group. For data that did not follow Gaussian distribution, the non-parametric Mann-Whitney two-tailed test was used to compare the differences between two groups, whereas the Kruskal-Wallis test followed by Dunn's multiple comparisons test was used to compare groups to a control group. Two-way ANOVA was performed in time-course analyses of body weight, GTT and ITT. GraphPad Prism 8 software for Windows (RRID: SCR_002798; San Diego, CA) was used to perform all statistical analyses. A $p<0.05$ was considered statistically significant. In box-and-whiskers plots, the center line depicts the median, box limits represent upper and lower quartiles, and whiskers show the min to max range. In time-course graphs, data are presented as mean±SEM. In violin plots, lines represent median and quartiles.

For mass-dependent measurements such as energy expenditure and food intake, a Generalized Linear Model (GLM) was performed to test for a significant interaction between genotype and body weight as per recommendations by Mina and colleagues,[115] using R software v4.2.0[102] (RRID: SCR_001905). If no statistically significant interaction effect was observed, we then performed an

UNIVERSITAT ROVIRA I VIRGILI
Metabolic Impact of the Succinate/SUCNR1 Axis in Adipocytes: Insights into Circadian and Leptin Regulation
TERESA VILLANUEVA CARMONA

ANCOVA without interaction and with body weight as the covariate. In the special case of a significant genotype effect but no significant body weight effect, the model was simplified to one-way ANOVA. Indirect calorimetry measurements not associated with mass, such as RER, were analyzed by one-way ANOVA. For time-course statistical analysis, measurements were averaged per animal on the second day, allowing for one day of acclimatization. Regression-based plots was performed using ggplot2 R package v3.3.6[103] (RRID: SCR_014601) and ggpubr R package v0.4.0 (RRID: SCR_021139).

For clinical data, associations between quantitative variables were evaluated using the Spearman correlation, and multiple linear regression analyses were employed (stepwise forward selection procedures) to determine which variables were independent factors. All variables associated in the univariate analysis with leptin gene expression were included in their respective models. Regression analyses were performed using IBM SPSS Statistics (v27.0; RRID: SCR_002865; Armonk, NY).

RNA sequencing analysis and data visualization were performed using R software v4.1.2.[102] Principal component analysis was conducted using the limma package (v3.50.1; RRID: SCR_010943)[104] to investigate technical batch noise. No sample was excluded from analysis. Normalization and differential expression analysis were performed using the R/Bioconductor package DESeq2 (v1.34.0; RRID: SCR_015687)[105] and *p-value*s were adjusted for multiple comparisons using the Benjamini-Hochberg procedure (fold change>1.25, adjusted $p<0.05$). Pathway enrichment analysis was performed with rotation gene set tests/Gene Set Analysis (ROAST-GSA, version 1.03.2), a hybrid of methods that combines the statistical inference based on limma and rotations from ROAST[106] and the re-standardized MaxMean statistic from GSA.[107] The Bioconductor R package org.Hs.eg.db (RRID:SCR_006442) was used to annotate genes according to Kyoto Encyclopedia of Genes and Genomes (KEGG) pathways.[108] *P*-values were adjusted for multiple comparisons using the Benjamini-Hochberg procedure and enriched pathways were considered significantly different if the adjusted *p-value* <0.25.

Cell Metabolism, Volume *35*

Supplemental information

SUCNR1 signaling in adipocytes controls energy metabolism by modulating circadian clock and leptin expression

Teresa Villanueva-Carmona, Lídia Cedó, Ana Madeira, Victòria Ceperuelo-Mallafré, M.-Mar Rodríguez-Peña, Catalina Núñez-Roa, Elsa Maymó- Masip, Maria Repollés-de-Dalmau, Joan Badia, Noelia Keiran, Mercedes Mirasierra, Carolina Pimenta-Lopes, Joan Sabadell-Basallote, Ramón Bosch, Laura Caubet, Joan Carles Escolà- Gil, José-Manuel Fernández-Real, Nuria Vilarrasa, Francesc Ventura, Mario Vallejo, Joan Vendrell, and Sonia Fernández-Veledo

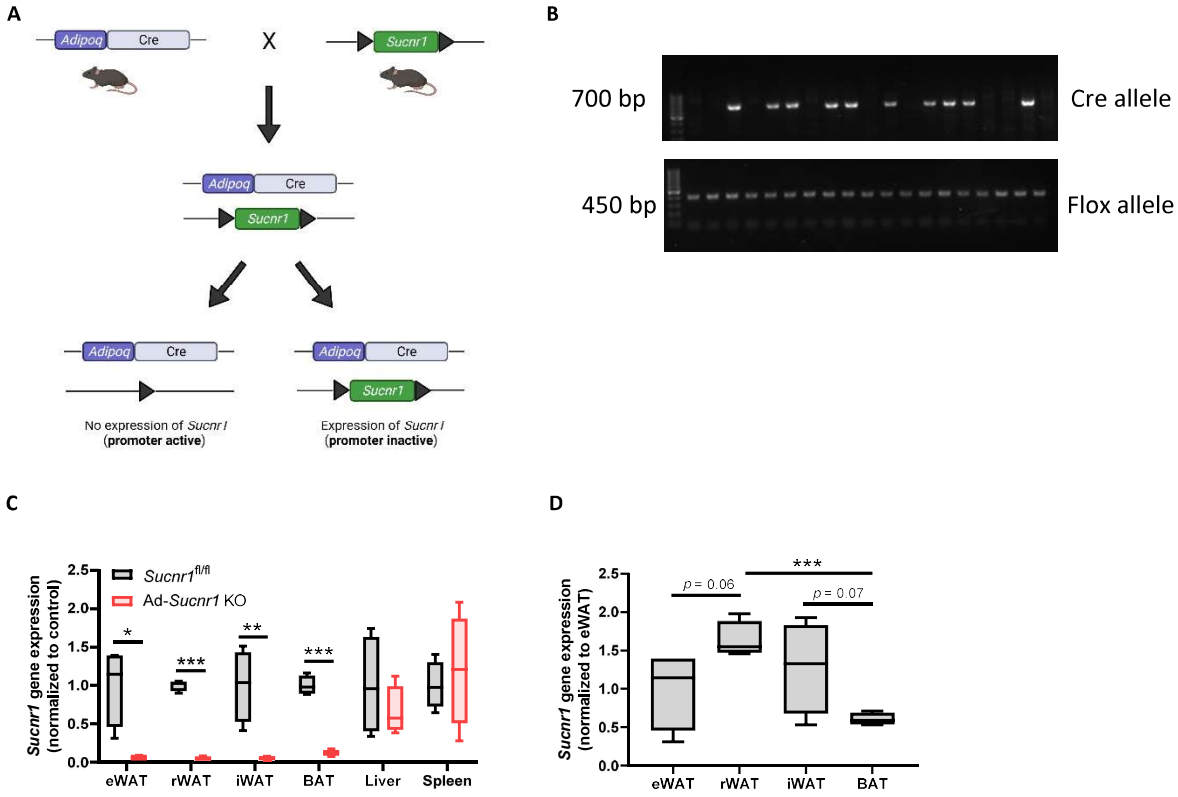

Figure S1. Generation of adipocyte-specific deletion of *Sucnr1* in mice. (Related to Figure 1) (A) Generation and **(B)** genotyping of *Sucnr1*$^{fl/fl}$ and Ad-*Sucnr1* KO mice (Cre allele=700 bp; Flox allele=450 bp). **(C)** qPCR analysis of *Sucnr1* in eWAT, rWAT, iWAT, BAT, liver, and spleen in Ad-*Sucnr1* KO mice and in age-matched *Sucnr1*$^{fl/fl}$ littermates (n=3–4/group). **(D)** *Sucnr1* expression in eWAT, rWAT, iWAT, and BAT in *Sucnr1*$^{fl/fl}$ mice (n=4 mice/tissue). Data are presented as box and whiskers plots showing median, first and third quartiles and maximum and minimum values; * $p<0.05$, ** $p<0.01$; *** $p<0.001$ (Unpaired *t*-test in bar graphs).

UNIVERSITAT ROVIRA I VIRGILI
Metabolic Impact of the Succinate/SUCNR1 Axis in Adipocytes: Insights into Circadian and Leptin Regulation
TERESA VILLANUEVA CARMONA

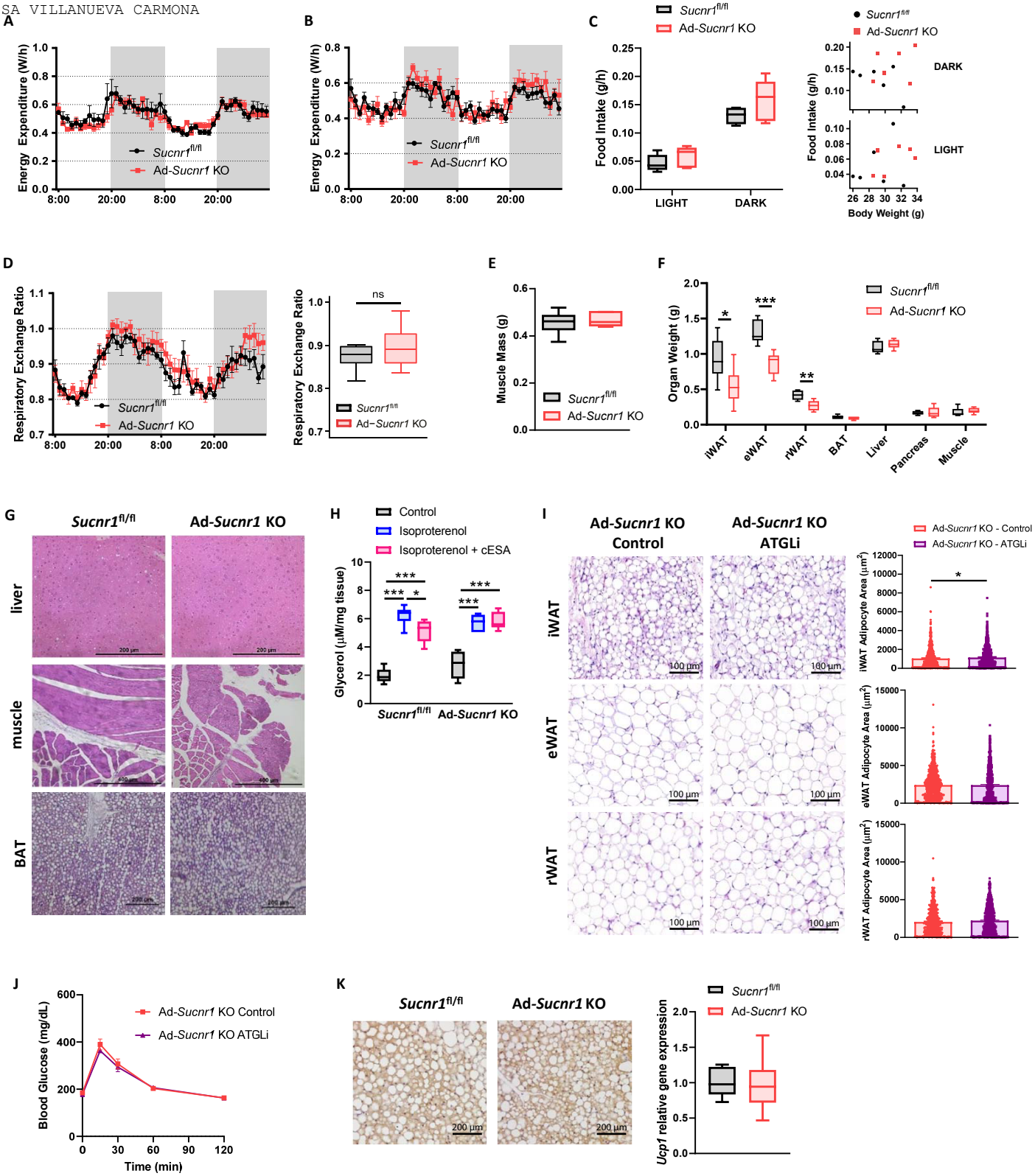

Figure S2. Metabolic phenotype of mice with conditional adipocyte deletion of *Sucnr1*. (Related to Figure 1). (A) EE at 12 weeks of life (ANCOVA, weight p=0.008 and genotype p=0.152). **(B)** EE (ANCOVA, weight p=0.875 and genotype p=0.549); **(C)** food intake during light and dark hours (left) and regression-based plot of food intake and body weight as covariate (right)(ANCOVA, genotype p=0.881 and 0.139 in light and dark respectively); and **(D)** RER (ANOVA, p=0.345 at week 20 of life (n=6 *Sucnr1*$^{fl/fl}$; n=6 Ad-*Sucnr1* KO). **(E)** qMRI quantification of muscle mass (n=8 *Sucnr1*$^{fl/fl}$; n=6 Ad-*Sucnr1* KO) at week 12 of life. **(F)** Organ weight at 29 weeks (n=5–6 mice/group). **(G)** Representative H&E staining of liver, muscle, and BAT. **(H)** Determination of lipolysis in eWAT explants from *Sucnr1*$^{fl/fl}$ and Ad-*Sucnr1* KO mice, measuring glycerol released in the absence or presence of isoproterenol and *c*ESA (n=6) (scale bars, 200 µm and 400 µm). **(I)** Representative H&E staining of iWAT, eWAT, and rWAT; quantification of adipocyte area (scale bars, 100 µm); and **(J)** GTT in Ad-*Sucnr1* KO mice treated with ATGLi or vehicle (corn oil) for 2 weeks (n=3 mice/group). **(K)** Representative images of UCP1 immunohistochemistry (scale bars, 200 µm), and *Ucp1* relative gene expression in BAT (n=5 *Sucnr1*$^{fl/fl}$; n=6 Ad-*Sucnr1* KO). Data are presented as box and whiskers plots showing median, first and third quartiles and maximum and minimum values, or as mean±SEM; * p<0.05; ** p<0.01; *** p<0.001 (Unpaired *t*-test, Mann-Whitney test, or one-way ANOVA in box and whiskers graphs and two-way ANOVA in **J**).

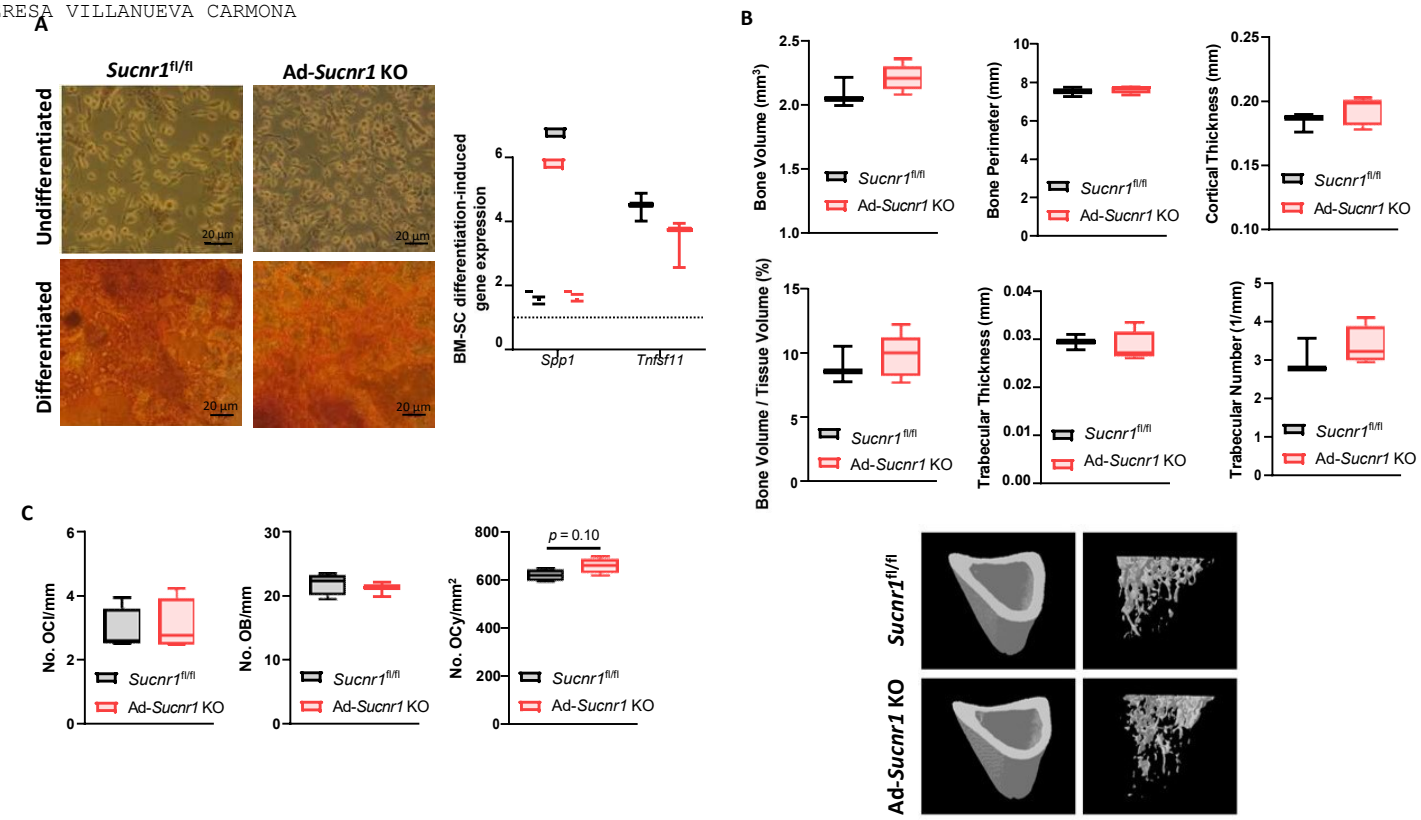

Figure S3. Bone mass phenotype in mice with conditional adipocyte deletion of *Sucnr1* on high-fat diet. (Related to Figure 3) (A) Representative images of Alizarin red S staining of undifferentiated and differentiated bone marrow-mesenchymal stem cells from *Sucnr1*$^{fl/fl}$ and Ad-*Sucnr1* KO mice (scale bars, 20 µm); and fold change of osteogenesis markers gene expression induced by differentiation (n=3). **(B)** Microcomputed tomography analysis and representative images of cortical and trabecular tibia (n=3 *Sucnr1*$^{fl/fl}$; n=5 Ad-*Sucnr1* KO); and **(C)** quantification of the number of osteoclasts (Ocl), osteoblasts (OB), and osteocytes (Ocy) (n=3–4/group) of *Sucnr1*$^{fl/fl}$ and Ad-*Sucnr1* KO mice fed HFD for 12 weeks. Data are presented as box and whisker plots showing median, first and third quartiles and maximum and minimum values (Unpaired *t*-test or Mann-Whitney test).

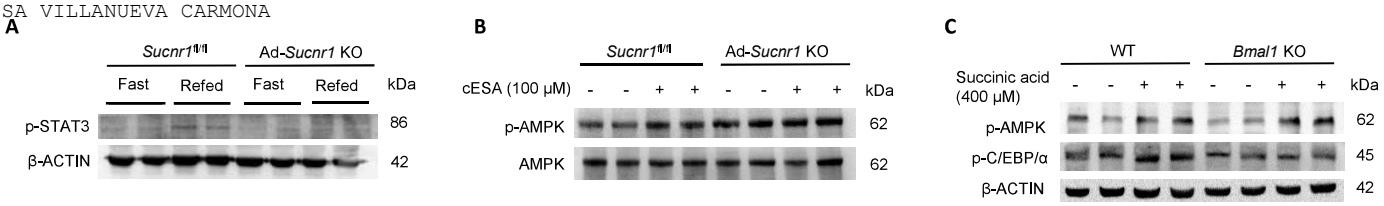

Figure S4. Signalling pathways regulated by fasted-to-fed transition and SUCNR1 activation. (Related to Figures 4, 5, and 6). (A) Representative immunoblot images of p-STAT3 in hypothalamus from *Sucnr1*$^{fl/fl}$ and Ad-*Sucnr1* KO mice in fasted and refed. β-ACTIN was used as a loading control (n=2). **(B)** Representative immunoblot images of p-AMPK in WAT explants from *Sucnr1*$^{fl/fl}$ and Ad-*Sucnr1* KO mice treated with cESA. Total AMPK was used as a loading control (n=2). **(C)** Representative immunoblot images of phosphorylated kinases in iWAT explants from WT and Bmal1 KO mice treated with succinic acid. β-ACTIN was used as a loading control (n=2).

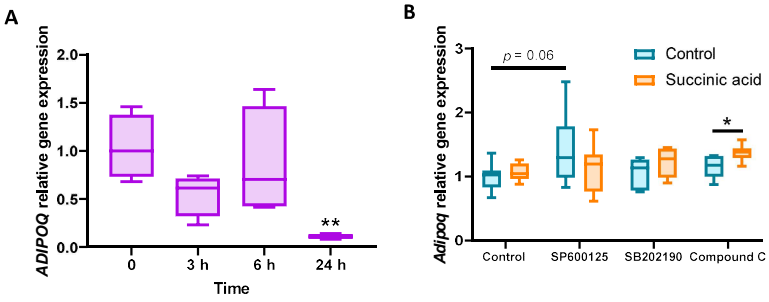

Figure S5. Succinate-SUCNR1 signaling does not control adiponectin expression. (Related to Figure 5) (A) *ADIPOQ* relative gene expression in hASCs treated with 100 μM *c*ESA (n=4). **(B)** *Adipoq* relative gene expression in differentiated 3T3-L1 cells treated with inhibitors of JNK (SP600125), p38 MAPK (SB202190), or AMPK (compound C), and co-treated with 400 μM succinic acid for 3 h (n=6–9). Data are presented as box and whiskers plots showing median, first and third quartiles and maximum and minimum values. * p <0.05; ** p<0.01 (one-way ANOVA followed by Dunnett's multiple comparisons test *vs* control or Unpaired *t*-test).

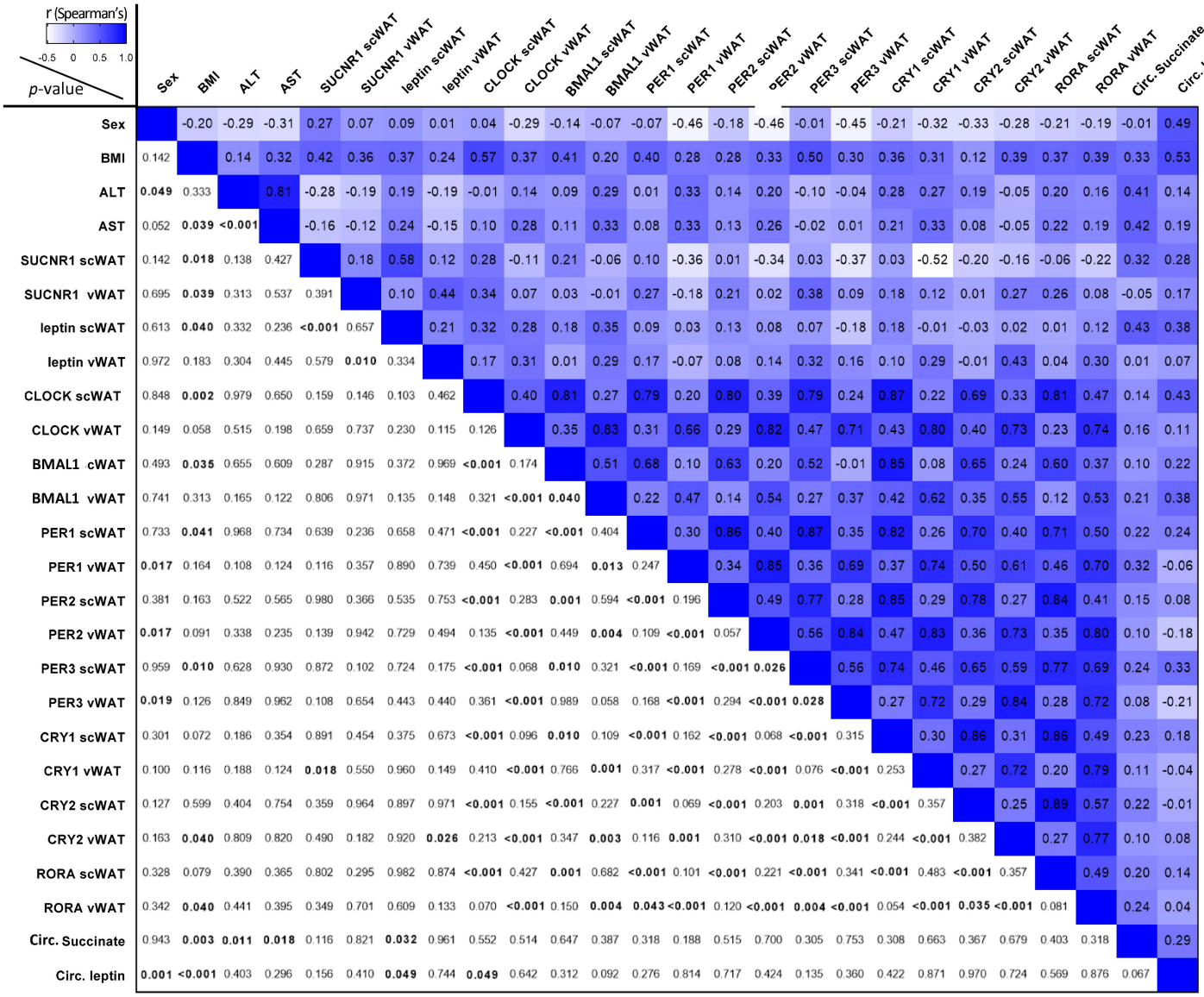

	Sex	BMI	ALT	AST	SUCNR1 scWAT	SUCNR1 vWAT	leptin scWAT	leptin vWAT	CLOCK scWAT	CLOCK vWAT	BMAL1 scWAT	BMAL1 vWAT	PER1 scWAT	PER1 vWAT	PER2 scWAT	PER2 vWAT	PER3 scWAT	PER3 vWAT	CRY1 scWAT	CRY1 vWAT	CRY2 scWAT	CRY2 vWAT	RORA scWAT	RORA vWAT	Circ. Succinate	Circ. leptin
Sex		-0.20	-0.29	-0.31	0.27	0.07	0.09	0.01	0.04	-0.29	-0.14	-0.07	-0.07	-0.46	-0.18	-0.46	-0.01	-0.45	-0.21	-0.32	-0.33	-0.28	-0.21	-0.19	-0.01	0.49
BMI	0.142		0.14	0.32	0.42	0.36	0.37	0.24	0.57	0.37	0.41	0.20	0.40	0.28	0.28	0.33	0.50	0.30	0.36	0.31	0.12	0.39	0.37	0.39	0.33	0.53
ALT	**0.049**	0.333		0.81	-0.28	-0.19	0.19	-0.19	-0.01	0.14	0.09	0.29	0.01	0.33	0.14	0.20	-0.10	-0.04	0.28	0.27	0.19	-0.05	0.20	0.16	0.41	0.14
AST	0.052	**0.039**	**<0.001**		-0.16	-0.12	0.24	-0.15	0.10	0.28	0.11	0.33	0.08	0.33	0.13	0.26	-0.02	0.01	0.21	0.33	0.08	-0.05	0.22	0.19	0.42	0.19
SUCNR1 scWAT	0.142	**0.018**	0.138	0.427		0.18	0.58	0.12	0.28	-0.11	0.21	-0.06	0.10	-0.36	0.01	-0.34	0.03	-0.37	0.03	-0.52	-0.20	-0.16	-0.06	-0.22	0.32	0.28
SUCNR1 vWAT	0.695	**0.039**	0.313	0.537	0.391		0.10	0.44	0.34	0.07	0.03	-0.01	0.27	-0.18	0.21	0.02	0.38	0.09	0.18	0.12	0.01	0.27	0.26	0.08	-0.05	0.17
leptin scWAT	0.613	**0.040**	0.332	0.236	**<0.001**	0.657		0.21	0.32	0.28	0.18	0.35	0.09	0.03	0.13	0.08	0.07	-0.18	0.18	-0.01	-0.03	0.02	0.01	0.12	0.43	0.38
leptin vWAT	0.972	0.183	0.304	0.445	0.579	**0.010**	0.334		0.17	0.31	0.01	0.29	0.17	-0.07	0.08	0.14	0.32	0.16	0.10	0.29	-0.01	0.43	0.04	0.30	0.01	0.07
CLOCK scWAT	0.848	**0.002**	0.979	0.650	0.159	0.146	0.103	0.462		0.40	0.81	0.27	0.79	0.20	0.80	0.39	0.79	0.24	0.87	0.22	0.69	0.33	0.81	0.47	0.14	0.43
CLOCK vWAT	0.149	0.058	0.515	0.198	0.659	0.737	0.230	0.115	0.126		0.35	0.83	0.31	0.66	0.29	0.82	0.47	0.71	0.43	0.80	0.40	0.73	0.23	0.74	0.16	0.11
BMAL1 cWAT	0.493	**0.035**	0.655	0.609	0.287	0.915	0.372	0.969	**<0.001**	0.174		0.51	0.68	0.10	0.63	0.20	0.52	-0.01	0.85	0.08	0.65	0.24	0.60	0.37	0.10	0.22
BMAL1 vWAT	0.741	0.313	0.165	0.122	0.806	0.971	0.135	0.148	0.321	**<0.001**	**0.040**		0.22	0.47	0.14	0.54	0.27	0.37	0.42	0.62	0.35	0.55	0.12	0.53	0.21	0.38
PER1 scWAT	0.733	**0.041**	0.968	0.734	0.639	0.236	0.658	0.471	**<0.001**	0.227	**<0.001**	0.404		0.30	0.86	0.40	0.87	0.35	0.82	0.26	0.70	0.40	0.71	0.50	0.22	0.24
PER1 vWAT	**0.017**	0.164	0.108	0.124	0.116	0.357	0.890	0.739	0.450	**<0.001**	0.694	**0.013**	0.247		0.34	0.85	0.36	0.69	0.37	0.74	0.50	0.61	0.46	0.70	0.32	-0.06
PER2 scWAT	0.381	0.163	0.522	0.565	0.980	0.366	0.535	0.753	**<0.001**	0.283	**0.001**	0.594	**<0.001**	0.196		0.49	0.77	0.28	0.85	0.29	0.78	0.27	0.84	0.41	0.15	0.08
PER2 vWAT	**0.017**	0.091	0.338	0.235	0.139	0.942	0.729	0.494	0.135	**<0.001**	0.449	**0.004**	0.109	**<0.001**	0.057		0.56	0.84	0.47	0.83	0.36	0.73	0.35	0.80	0.10	-0.18
PER3 scWAT	0.959	**0.010**	0.628	0.930	0.872	0.102	0.724	0.175	**<0.001**	0.068	**0.010**	0.321	**<0.001**	0.169	**<0.001**	**0.026**		0.56	0.74	0.46	0.65	0.59	0.77	0.69	0.24	0.33
PER3 vWAT	**0.019**	0.126	0.849	0.962	0.108	0.654	0.443	0.440	0.361	**<0.001**	0.989	0.058	0.168	**<0.001**	0.294	**<0.001**	**0.028**		0.27	0.72	0.29	0.84	0.28	0.72	0.08	-0.21
CRY1 scWAT	0.301	0.072	0.186	0.354	0.891	0.454	0.375	0.673	**<0.001**	0.096	**0.010**	0.109	**<0.001**	0.162	**<0.001**	0.068	**<0.001**	0.315		0.30	0.86	0.31	0.86	0.49	0.23	0.18
CRY1 vWAT	0.100	0.116	0.188	0.124	**0.018**	0.550	0.960	0.149	0.410	**<0.001**	0.766	**0.001**	0.317	**<0.001**	0.278	**<0.001**	0.076	**<0.001**	0.253		0.27	0.72	0.20	0.79	0.11	-0.04
CRY2 scWAT	0.127	0.599	0.404	0.754	0.359	0.964	0.897	0.971	**<0.001**	0.155	**<0.001**	0.227	**0.001**	0.069	**<0.001**	0.203	**0.001**	0.318	**<0.001**	0.357		0.25	0.89	0.57	0.22	-0.01
CRY2 vWAT	0.163	**0.040**	0.809	0.820	0.490	0.182	0.920	**0.026**	0.213	**<0.001**	0.347	**0.003**	0.116	**0.001**	0.310	**<0.001**	**0.018**	**<0.001**	0.244	**<0.001**	0.382		0.27	0.77	0.10	0.08
RORA scWAT	0.328	0.079	0.390	0.365	0.802	0.295	0.982	0.874	**<0.001**	0.427	**0.001**	0.682	**<0.001**	0.101	**<0.001**	0.221	**<0.001**	0.341	**<0.001**	0.483	**<0.001**	0.357		0.49	0.20	0.14
RORA vWAT	0.342	**0.040**	0.441	0.395	0.349	0.701	0.609	0.133	0.070	**<0.001**	0.150	**0.004**	**0.043**	**<0.001**	0.120	**<0.001**	**0.004**	**<0.001**	0.054	**<0.001**	**0.035**	**<0.001**	0.081		0.24	0.04
Circ. Succinate	0.943	**0.003**	**0.011**	**0.018**	0.116	0.821	**0.032**	0.961	0.552	0.514	0.647	0.387	0.318	0.188	0.515	0.700	0.305	0.753	0.308	0.663	0.367	0.679	0.403	0.318		0.29
Circ. leptin	**0.001**	**<0.001**	0.403	0.296	0.156	0.410	**0.049**	0.744	**0.049**	0.642	0.312	0.092	0.276	0.814	0.717	0.424	0.135	0.360	0.422	0.871	0.970	0.724	0.569	0.876	0.067	

Figure S6. Spearman's correlation matrix between clinical, biochemical, and gene expression variables of the human cohort (Related to Figure 7). The variables depicted only include the significant correlations determined for the biochemical and gene expression variables in Figure 6a. Spearman correlation coefficients and *p*-values are reported for the pairing of variables indicated on the y-axis *vs*. x-axis. Color scale ranges from white (r = −0.5) to blue (r = 1). *P*-values <0.05 were considered to be statistically significant. Abbreviations: ALT, alanine aminotransferase; AST, aspartate aminotransferase; BMAL1, brain and muscle aryl hydrocarbon receptor nuclear translocator-like protein 1; BMI, body mass index; Circ. leptin; circulating leptin; Circ. Succinate, circulating succinate; CLOCK, circadian locomotor output cycles kaput; CRY, cryptochrome; PER, period; RORA, retinoic acid receptor-related orphan receptor alpha; scWAT, subcutaneous white adipose tissue; SUCNR1, succinate receptor 1; vWAT, visceral white adipose tissue.

Table S1 – RNAseq differential gene expression of epididymal white adipose tissue from Ad-*Sucnr1* KO vs *Sucnr1*$^{fl/fl}$ mice. Adjusted *p*-value <0.05.

(Related to Figure 6).

	Symbol	Entrez	Fold change.shrinked	Adjusted *p*-value
Up-regulated genes	*Gm24382*	115489788	34.308	0.0001
	Zfp949	71640	2.637	< 0.0001
	Gsta4	14860	2.469	< 0.0001
	Sh2b2	23921	1.904	0.0002
	Tmem179	104885	1.904	0.0012
	Lrrc15	74488	1.898	0.0069
	6430571L13Rik	235599	1.857	0.0042
	Vwc2	319922	1.829	0.0020
	Ciart	229599	1.828	0.0003
	Cd164l2	69655	1.810	0.0020
	Syde2	214804	1.771	0.0003
	Mc5r	17203	1.665	0.0113
	Tef	21685	1.626	< 0.0001
	Per3	18628	1.621	< 0.0001
	Klf15	66277	1.619	0.0020
	Dbp	13170	1.614	0.0018
	Col6a6	245026	1.580	0.0016
	Pcsk4	18551	1.556	0.0062
	Gpd1	14555	1.535	0.0126
	Per1	18626	1.530	0.0018
	Lrp12	239393	1.528	0.0025
	Ppargc1b	170826	1.516	0.0006
	Per2	18627	1.504	0.0012
	B630019A10Rik	105246089	1.492	0.0191
	Gpr135	238252	1.491	0.0074
	Adora1	11539	1.466	0.0077
	Slc36a2	246049	1.460	0.0246
	Dcun1d3	233805	1.454	0.0010
	Hif3a	53417	1.443	0.0300
	Fam117a	215512	1.425	0.0010
	Myorg	329828	1.420	0.0104
	Cpn2	71756	1.418	0.0204
	Gys1	14936	1.403	0.0170
	Acsl1	14081	1.403	0.0259
	Tob2	57259	1.401	0.0006
	C730002L08Rik	320155	1.396	0.0306
	Rgma	244058	1.387	0.0204
	A530016L24Rik	319942	1.386	0.0317
	Kctd6	71393	1.370	0.0088
	Ppara	19013	1.366	0.0364
	Sccpdh	109232	1.364	0.0321
	Mlxipl	58805	1.361	0.0025
	Bcat2	12036	1.344	0.0187
	Lpin1	14245	1.343	0.0407
	Nr1d2	353187	1.339	< 0.0001
	Gm36210	102640043	1.339	0.0384
	Oscp1	230751	1.334	0.0392
	Ranbp9	56705	1.332	0.0236
	Fam214a	235493	1.331	0.0418
	Prodh	19125	1.329	0.0321
	Txnrd3	232223	1.325	0.0246
	4933406C10Rik	74076	1.320	0.0316
	Arl4a	11861	1.319	0.0418
	Gys2	232493	1.313	0.0433
	Gm34408	102637649	1.308	0.0349
	Rfc4	106344	1.296	0.0277
	Pard6g	93737	1.295	0.0418
	Fbxo3	57443	1.287	< 0.0001
	Eif4a2	13682	1.285	0.0010
	Hemk1	69536	1.281	0.0042
	Micall1	27008	1.279	0.0046
	Tmem53	68777	1.278	0.0494
	Ing2	69260	1.269	0.0012
	Clcn2	12724	1.276	0.0635
	Lonrf1	244421	1.260	0.0294

Table S1 (continued)

	Symbol	Entrez	Fold change.shrinked	Adjusted *p*-value
Down-regulated genes	*Lcp1*	18826	-1.251	0.0364
	Srp54b	665155	-1.256	< 0.0001
	Srp54a	24067	-1.257	< 0.0001
	Itm2c	64294	-1.266	0.0277
	Selp	20344	-1.269	0.0499
	Atoh8	71093	-1.269	0.0499
	Mthfsl	100039707	-1.272	0.0150
	Dll1	13388	-1.292	0.0282
	Slc7a7	20540	-1.300	0.0069
	Rims1	116837	-1.304	0.0279
	Cnn1	12797	-1.312	0.0277
	Ifi44	99899	-1.320	0.0465
	Plvap	84094	-1.328	0.0232
	Etl4	208618	-1.329	0.0279
	Lpcat2	270084	-1.344	0.0413
	Dusp4	319520	-1.347	0.0346
	Arhgap20	244867	-1.355	0.0010
	Mall	228576	-1.371	0.0277
	Adm	11535	-1.384	0.0057
	Srprb	20818	-1.391	< 0.0001
	Foxs1	14239	-1.394	0.0235
	Gm47283	170942	-1.396	0.0087
	Akr1b7	11997	-1.437	0.0171
	Gm13710	672763	-1.446	0.0012
	Gm7972	666190	-1.453	0.0289
	Mapkapk3	102626	-1.458	0.0205
	Pcdh12	53601	-1.543	0.0130
	Sh3bgrl2	212531	-1.545	0.0018
	Ier5	15939	-1.607	0.0017
	Abhd14b	76491	-1.677	< 0.0001
	Spon2	100689	-1.772	0.0039
	Ppm1m	67905	-2.060	< 0.0001
	Cldn5	12741	-2.072	< 0.0001
	Adamts4	240913	-2.390	< 0.0001
	Arntl	11865	-2.546	< 0.0001
	Rpl29	19944	-3.374	< 0.0001
	Sucnr1	84112	-18.897	< 0.0001
	Ptgs2	19225	-22.624	0.0011

Table S2 – Anthropometric and Biochemical Variables from the Human Cohort. (Related to Figure 7).

Variables	Lean	Obese
n	22	34
Sex (female/male)	17/5	18/16
Age (years)	51.4 ± 15.7	52.3 ± 12.3
BMI (kg/m^2)	22.5 ± 2.0	34.5 ± 3.67***
Glucose (mmol/L)	4.9 ± 0.8	5.3 ± 0.9
Total cholesterol (mmol/L)	4.8 ± 0.7	5.0 ± 1.0
HDLc (mmol/L)	1.6 ± 0.3	1.2 ± 0.3***
LDLc (mmol/L)	2.9 ± 0.6	3.2 ± 0.8
Triglycerides (mmol/L)	0.9 ± 0.4	1.9 ± 1.1***
Insulin (pmol/L)	35.8 ± 12.0	104.8 ± 43.0*
HOMA-IR	1.2 ± 0.6	3.8 ± 1.6*
GGT (µkat/L)	0.9 ± 2.0	2.0 ± 4.6**
ALT (µkat/L)	0.5 ± 0.7	0.5 ± 0.6
AST (µkat/L)	0.3 ± 0.2	0.5 ± 0.4*
Circulating Succinate (µmol/L)	54.8 ± 39.0	102.9 ± 79.0*
Circulating Leptin (µg/L)	10.1 ± 7.6	27.7 ± 21.9***

Abbreviations: ALT, Alanine Aminotransferase; AST, Aspartate Aminotransferase; BMI, body mass index; GGT, Gamma Glutamyltransferase; LDLc, low-density lipoprotein cholesterol; HDLc, high-density lipoprotein cholesterol; HOMA-IR, Homeostatic Model Assessment for Insulin Resistance. Results are expressed as mean ± SD. * p-value <0.05; ** p-value <0.01; and *** p-value <0.001 (Unpaired t-test or Mann-Whitney test).

Table S3 – Regressions Coefficients for predicting circulating leptin levels. (Related to Figure S6).

Circulating leptin (R=0.812; R^2=0.660)					
	B (non-standardized)	**SE**	**95% CI**	**Beta (standardized)**	***p*-value**
Constant	-37.501	11.293	-60.863 – -14.139	-	<0.01
Sex	17.841	3.802	9.976 – 25.705	0.584	<0.001
BMI	0.831	0.313	0.184 – 1.478	0.359	<0.05
***LEP* scWAT**	2.261	1.078	0.030 – 4.491	0.286	<0.05

Variables included in the model: age, glucose, body mass index (BMI), and *LEP* expression in subcutaneous white adipose tissue (scWAT).

Table S4 – Regressions Coefficients for predicting *LEP* expression in human subcutaneous adipose tissue. (Related to Figure S6).

***LEP* expression in scWAT (R=0.487; R^2=0.544)**					
	B (non-standardized)	**SE**	**95% CI**	**Beta (standardized)**	***p*-value**
Constant	2.986	1.185	0.521-5.451	-	0.020
***SUCNR1* scWAT**	0.434	0.149	0.124-0.743	0.450	<0.01
Circulating Leptin	0.058	0.020	0.017-0.098	0.454	<0.01
Age	-0.050	0.021	-0.094-0.006	-0.353	0.029

Variables included in the model: Body mass index, sex, circulating succinate, *SUCNR1* expression in human subcutaneous white adipose tissue (scWAT), circulating leptin, and age.

Table S5 – Regressions Coefficients for predicting *LEP* expression in human visceral adipose tissue. (Related to Figure S6).

***LEP* expression i vWAT (R=0.470; R^2=(.221)**					
	B (non-standardized)	**SE**	**95% CI**	**Beta (standardized)**	***p*-value**
Constant	0.868	0.235	0.388-1.348	-	<0.001
***SUCNR1* vWAT**	0.277	0.095	0.083-0.471	0.470	<0.01

Variables included in the model: age, sex, and *SUCNR1* expression in visceral white adipose tissue (vWAT).

Table S6 – Taqman Gene Expression Assay References. (Related to STAR Methods).

Gene Name	Mouse	Human
B2m	Mm00437762_m1	
RNA18S5		Hs03928985_g1
Sucnr1* / *SUCNR1	Mm02620543_s1	Hs00908230_m1
Lep* / *LEP	Mm00434759_m1	Hs00174877_m1
Adipoq* / *ADIPOQ	Mm00456425_m1	Hs00605917_m1
Ucp1	Mm01244861_m1	
Cidea	Mm00432554_m1	
Tnfsf11	Mm00441906_m1	
Spp1	Mm00436767_m1	
Npy	Mm01410146_m1	
Agrp	Mm00475829_g1	
Pparg	Mm00440940_m1	
Fasn	Mm00662319_m1	
Slc2a4	Mm00436615_m1	
Bmal1* / *BMAL1	Mm00500223_m1	Hs00154147_m1
CLOCK		Hs00231857_m1
Rora* / *RORA	Mm01173766_m1	Hs00536545_m1
Per1* / *PER1	Mm00501813_m1	Hs00242988_m1
Per2* / *PER2	Mm00478099_m1	Hs00256143_m1
Per3* / *PER3	Mm00478120_m1	Hs00213466_m1
CRY1		Hs00172734_m1
CRY2		Hs00323654_m1

STUDY 2

Protocol for the in vitro isolation and culture of mature adipocytes and white adipose tissue explants from humans and mice

Villanueva-Carmona T, Cedó L, Núñez-Roa C, Maymó-Masip E, Vendrell J, Fernández-Veledo S.

ABSTRACT

WAT explant culture allows for the *ex vivo* study of this tissue, preserving its structural integrity and properties. Concurrently, the isolation of mature adipocytes supports research into adipocyte metabolism and hormonal regulation. Here, we outline a protocol for the extraction, isolation, and processing of mature adipocytes, alongside the cultivation of WAT explants from human and mouse samples. We describe the procedures for WAT retrieval, explant culture, tissue digestion, and adipocyte separation. Following these steps, we provide detailed procedures for culturing isolated mature adipocytes. For comprehensive details on the implementation of this protocol, please see Villanueva-Carmona et al. (2023). This detailed protocol is crucial for maintaining the functionality of adipocytes and WAT during experiments, ensuring accurate results.

UNIVERSITAT ROVIRA I VIRGILI
Metabolic Impact of the Succinate/SUCNR1 Axis in Adipocytes: Insights into Circadian and Leptin Regulation
TERESA VILLANUEVA CARMONA

STAR Protocols

CellPress
OPEN ACCESS

Protocol

Protocol for the *in vitro* isolation and culture of mature adipocytes and white adipose tissue explants from humans and mice

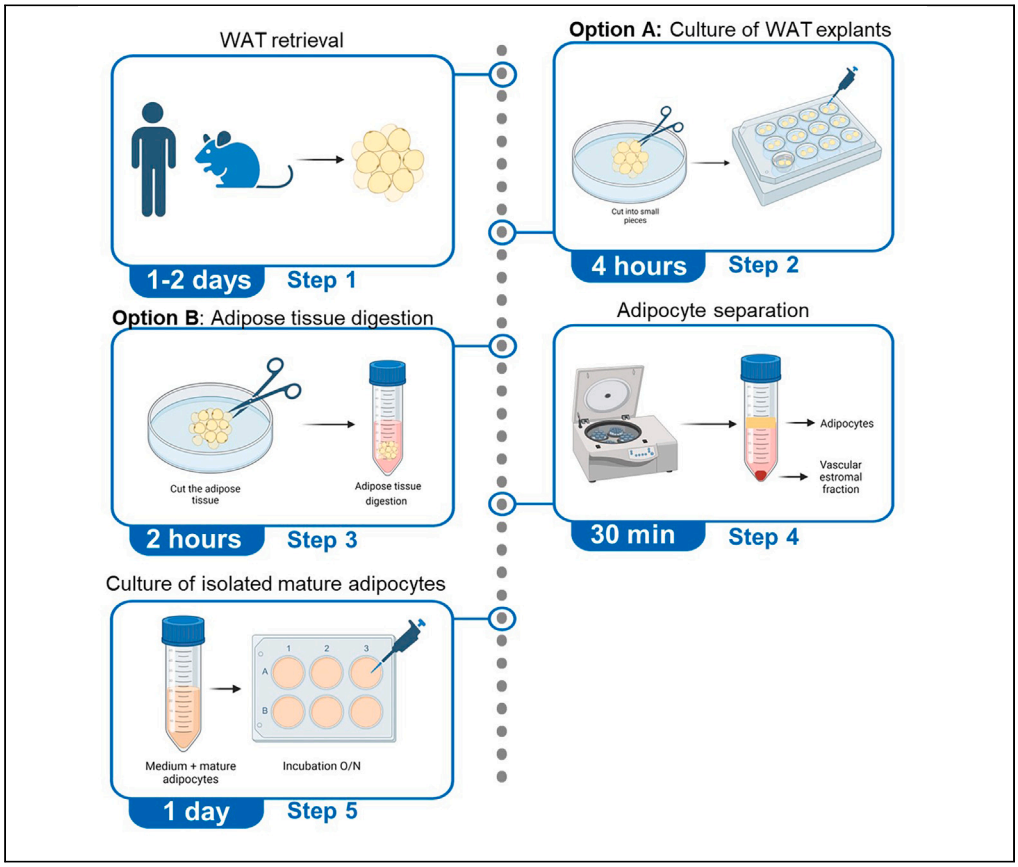

White adipose tissue (WAT) explants culture allows the study of this tissue *ex vivo*, maintaining its structure and properties. Concurrently, isolating mature adipocytes facilitates research into fat cell metabolism and hormonal regulation. Here, we present a protocol for obtaining, isolating, and processing mature adipocytes, alongside the cultivation of WAT explants from humans and mice. We describe steps for WAT retrieval, culturing of WAT explants, WAT digestion, and adipocytes separation. We then detail procedures for culturing isolated mature adipocytes.

Publisher's note: Undertaking any experimental protocol requires adherence to local institutional guidelines for laboratory safety and ethics.

Teresa Villanueva-Carmona, Lídia Cedó, Catalina Núñez-Roa, Elsa Maymó-Masip, Joan Vendrell, Sonia Fernández-Veledo

sonia.fernandez@iispv.cat

Highlights

Isolation and culture of mature adipocytes and white adipose tissue explants

Protocol applicable to white adipose tissue from rodents and humans

Step-by-step details on adipose tissue digestion and adipocyte separation

Villanueva-Carmona et al., STAR Protocols 4, 102693 December 15, 2023 © 2023 The Author(s).
https://doi.org/10.1016/j.xpro.2023.102693

UNIVERSITAT ROVIRA I VIRGILI
Metabolic Impact of the Succinate/SUCNR1 Axis in Adipocytes: Insights into Circadian and Leptin Regulation
TERESA VILLANUEVA CARMONA

STAR Protocols

CellPress
OPEN ACCESS

Protocol

Protocol for the *in vitro* isolation and culture of mature adipocytes and white adipose tissue explants from humans and mice

Teresa Villanueva-Carmona,[1,2,3,4] Lídia Cedó,[1,2] Catalina Núñez-Roa,[1,2] Elsa Maymó-Masip,[1,2] Joan Vendrell,[1,2,3] and Sonia Fernández-Veledo[1,2,4,5,*]

[1]Department of Endocrinology and Nutrition, Research Unit, Institut d'Investigació Sanitària Pere Virgili (IISPV), Hospital Universitari de Tarragona Joan XXIII, 43005 Tarragona, Spain

[2]CIBER de Diabetes y Enfermedades Metabólicas Asociadas (CIBERDEM), Instituto de Salud Carlos III, 28029 Madrid, Spain

[3]Department of Medicine and Surgery, Universitat Rovira i Virgili (URV), 43201 Reus, Spain

[4]Technical contact: teresa.villanueva@iispv.cat

[5]Lead contact

*Correspondence: sonia.fernandez@iispv.cat
https://doi.org/10.1016/j.xpro.2023.102693

SUMMARY

White adipose tissue (WAT) explants culture allows the study of this tissue *ex vivo*, maintaining its structure and properties. Concurrently, isolating mature adipocytes facilitates research into fat cell metabolism and hormonal regulation. Here, we present a protocol for obtaining, isolating, and processing mature adipocytes, alongside the cultivation of WAT explants from humans and mice. We describe steps for WAT retrieval, culturing of WAT explants, WAT digestion, and adipocytes separation. We then detail procedures for culturing isolated mature adipocytes.
For complete details on the use and execution of this protocol, please refer to Villanueva-Carmona et al. (2023).[1]

BEFORE YOU BEGIN

The following protocol outlines the detailed procedures for the isolation and culture of mature adipocytes and WAT explants from adult mice and humans. It has been successfully utilized with various types of WAT, including subcutaneous, epididymal, and retroperitoneal, in both lean and diet-induced obese mice, as well as in a variety of genetically modified mouse models. As such, this approach can be customized for different WAT sites and rodent species, and it is also applicable to humans, both in lean and obese conditions. For the collection of WAT from mice, please follow steps 1-6; and for the collection of human WAT, please follow step 7, in before you begin section.

Institutional permissions

All animal experiments involved in these studies were overseen and approved by the Universitat Rovira i Virgili Animal Welfare and Governmental Ethics Committee (ref. 10970). All animal procedures adhered to the guidelines provided by the European Union Directive 86/609/EEC and recommendation 2007/526/EC pertaining to the protection of animals used for experimental and other scientific purposes, which are enacted under Spanish law 1201/2005.

All study participants were recruited from University Hospital Joan XXIII and Hospital de Santa Tecla, both located in Tarragona, Spain. Each individual provided informed consent, with the study receiving approval from the respective hospitals' ethics and research committees (references CEIm 177/2018 approved on the 29th of November 2018 and CEIm 41p/2015 approved on the 31st of August 2015). The study's procedures adhered to the ethical guidelines stated in the Declaration of Helsinki.

This is an open access article under the CC BY-NC-ND license (http://creativecommons.org/licenses/by-nc-nd/4.0/).

UNIVERSITAT ROVIRA I VIRGILI
Metabolic Impact of the Succinate/SUCNR1 Axis in Adipocytes: Insights into Circadian and Leptin Regulation
TERESA VILLANUEVA CARMONA

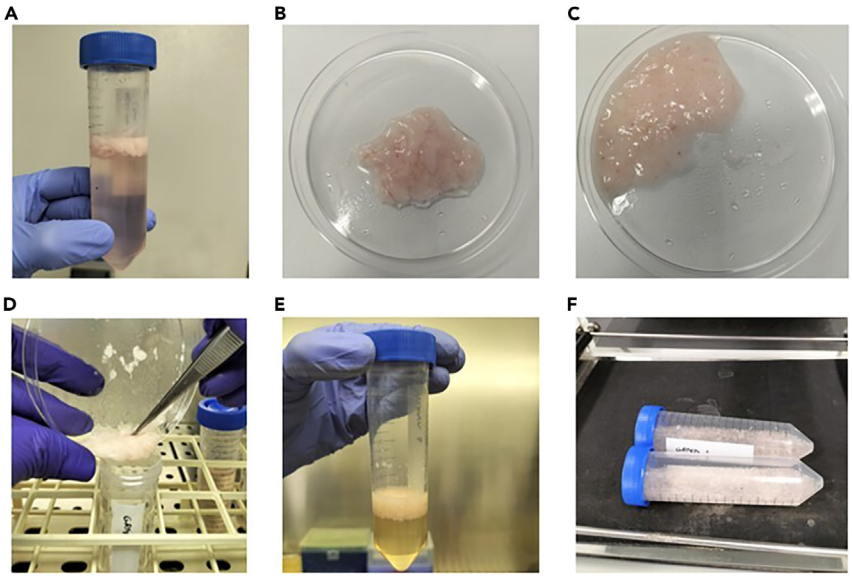

Figure 1. Process of digestion of adipose tissue

(A) Adipose tissue stored in a PBS solution supplemented with 1% Ab/Am.

(B) Tissue placed in a sterile Petri dish containing PBS with 1% Ab/Am.

(C) Adipose tissue minced.

(D and E) Transfer of the minced tissue into a sterile falcon tube containing the collagenase solution.

(F) Incubation for 1 h at 37 ºC on an orbital shaker with the collagenase solution.

Mouse euthanasia and white adipose tissue retrieval

Timing: 1 h

1. Humanely euthanize the mouse via cervical dislocation or other institutionally approved methods.

   Note: Depending on the experimental approach, mice may need to undergo a fasting period.

2. Sterilize the abdominal region with 70% ethanol.
3. Make an incision in the abdomen to expose the internal organs.
4. Using sterile scissors and forceps, harvest the desired adipose tissue depots.
5. Rinse each collected tissue with phosphate-buffered saline (PBS) supplemented with 1% antibiotic/antimycotic solution.
6. Pool the tissues of at least three mice from the same group, sorted by tissue type, into a 50 mL Falcon tube containing PBS supplemented with 1% antibiotic/antimycotic solution.

   ⚠ CRITICAL: The harvested adipose tissue can be stored in a PBS solution supplemented with antibiotics until it is ready for use (should not exceed 2–3 h). This solution aids in preserving the tissue's viability while guarding against bacterial or microbial contamination (Figure 1A).

   Note: Adipose tissue provides a versatile substrate for research studies, particularly in the field of metabolism. It can be utilized as tissue explants or by isolating mature adipocytes, with each approach offering unique advantages and insights. When adipose tissue explants are used, small sections of tissue are cultured *ex vivo*. This approach retains the native structure and heterogeneity of the tissue, allowing for the investigation of cell-cell and cell-matrix

UNIVERSITAT ROVIRA I VIRGILI
Metabolic Impact of the Succinate/SUCNR1 Axis in Adipocytes: Insights into Circadian and Leptin Regulation
TERESA VILLANUEVA CARMONA

interactions.[2] On the other hand, mature adipocyte isolation involves processing the adipose tissue to extract these specialized cells. This strategy enables more targeted experiments to be conducted, focusing on the metabolic activities and regulatory mechanisms of the adipocytes themselves. However, it does not offer the complexity of cell interactions present within the tissue. Thus, the choice between adipose tissue explants and mature adipocyte isolation largely depends on the research objectives and the level of cellular complexity required in the experimental design.

Collection of human white adipose tissue

Timing: 30 min

The procedures outlined below are applicable not only to mouse adipose tissue but also to human samples. Human adipose tissue samples were collected from age- and gender-matched donors undergoing non-acute surgical procedures, such as hernia or cholecystectomy, in a scheduled routine surgery. Donors were classified based on their BMI as either lean (BMI < 25 kg/m^2) or obese (BMI $\geq$ 30 kg/m^2), following the criteria set by the World Health Organization (WHO).

7. Collect adipose tissue samples, and immediately place them into a sterile container with PBS supplemented with 1% antibiotic/antimycotic solution to ensure their integrity and prevent any contamination.

KEY RESOURCES TABLE

REAGENT or RESOURCE	SOURCE	IDENTIFIER
Chemicals, peptides, and recombinant proteins		
Phosphate-buffered saline (PBS)	Hyclone (GE HealthCare Life Sciences)	Cat.#SH30028.02
2-[4-(2-Hydroxyethyl)Piperazin-1-Yl] Ethanesulfonic Acid (HEPES)	Fisher Scientific	Cat.#BP310-1; CAS ID: 7365-45-9
Bovine serum albumin (BSA)	Sigma-Aldrich	Cat.#A7030; CAS ID: 9048-46-8
Collagenase from *Clostridium histolyticum*	Sigma-Aldrich	Cat.#C0130; CAS ID: 9001-12-1
Experimental Models: Organisms/Strains		
Adult male C57BL/6 wild-type mice	Charles River	C57BL/6
Biological samples		
Human adipose tissue	IISPV Biobank (PT17/0015/0029)	N/A
Other		
Antibiotic/antimycotic solution	Hyclone (GE HealthCare Life Sciences)	Cat.#SV30079.01
Fetal bovine serum (FBS)	Hyclone (GE HealthCare Life Sciences)	Cat.#SH30071.03
DMEM/F12 medium	Gibco (Life Technologies Limited)	Cat.#31330-038

STEP-BY-STEP METHOD DETAILS

For culture of white adipose tissue explants, please follow steps 1–6. For mature adipocyte isolation and culture, proceed with steps 7–27.

Culture of white adipose tissue explants

Timing: 4 h

UNIVERSITAT ROVIRA I VIRGILI
Metabolic Impact of the Succinate/SUCNR1 Axis in Adipocytes: Insights into Circadian and Leptin Regulation
TERESA VILLANUEVA CARMONA

The culture of WAT explants is an essential procedure that allows us to mimic and study the tissue's natural environment. This method helps preserve the cellular structure and functions, providing valuable insights into adipose tissue biology.[2] Sterile techniques must be upheld throughout the entire process to reduce the risk of contamination and its potential adverse effects on cell viability.

1. With sterile scissors, dissect the adipose tissue into small, uniformly sized pieces of approximately 40 mg each.
2. Gently place two of the pre-cut adipose tissue pieces into each well of a 24-well plate containing 350 μL of DMEM/F12 medium, supplemented with 0.2% of BSA. Ensure that the explants are fully immersed in the medium.
3. Place the culture dishes with the adipose tissue explants in a cell culture incubator set to 37°C and 5% CO_2 for 1–2 h.

   Note: Tissue should rest for at least 1 h before proceeding, but not longer than 2 h.

4. Check the culture under a microscope to assess the integrity of the adipose tissue explants.
5. Perform any necessary experiments or treatments based on your experimental design.

   Note: Cell culture incubations or treatments should be performed in a cell culture incubator.

   Note: The viability of adipose tissue explants can exhibit variability, typically spanning from several hours up to approximately 24 h under experimental conditions. During this time, various metabolic processes can be studied such as the uptake and release of nutrients or the response to hormones, as well as gene expression analysis.

6. After the treatment, you may collect the conditioned medium from the adipose tissue explants. This medium can be utilized in experiments like ELISAs to analyze secreted proteins. Alternatively, you can also collect the adipose tissue itself for further studies, such as RNA expression or Western Blot analyses.

   Note: Your decision to collect either the conditioned medium or the adipose tissue depends on your research objectives and experimental requirements.

   Note: Performing experiments involving adipose tissue explants are conducted within an incubator, as it provides a controlled environment that mimics the physiological conditions necessary for maintaining the viability and functionality of the tissue explants.

Adipose tissue digestion

Timing: 2 h

In addition to studying WAT explants, isolating mature adipocytes, which are key in fat storage, release, and hormonal regulation,[3] can be a focal point of your study. The digestion of adipose tissue allows you to isolate these cells for subsequent investigation. This procedure entails the disruption of the extracellular matrix and connective tissue, resulting in the liberation of individual cells for further investigation.[4] Using a cell culture hood throughout the entire process is essential to ensure sterility. After euthanizing the animal and harvesting the adipose tissue, the following are the steps for adipose tissue digestion:

7. Weigh each adipose tissue separately.
8. Place the excised tissue in a sterile petri dish containing PBS with 1% antibiotic/antimycotic solution (Figure 1B).
9. Cut the adipose tissue into small pieces using sterile scissors and forceps (Figure 1C).

UNIVERSITAT ROVIRA I VIRGILI
Metabolic Impact of the Succinate/SUCNR1 Axis in Adipocytes: Insights into Circadian and Leptin Regulation
TERESA VILLANUEVA CARMONA

10. Transfer the minced tissue to a new sterile petri dish containing PBS. Repeat this step twice for a total of three consecutive washes.

Note: This step helps eliminate impurities and contaminants, thereby creating a suitable environment for experimentation.

11. Adjust the collagenase concentration based on the tissue weight. For 2 g of collected WAT adipose tissue, we use 10 mL of PBS containing 1% BSA and 0.2% collagenase.

Note: The collagenase solution plays a crucial role in enzymatically dissociating cells from tissue fragments, enabling the isolation of target cells.

12. Transfer the minced tissue into a sterile 50 mL Falcon tube containing the collagenase solution (Figure 1D).
13. Incubate the tube for 30 min–1 h at 37°C on an orbital shaker set at 200 rpm. This allows for the collagenase enzyme to digest the tissue (Figure 1E).

Note: In the context of this particular protocol, subcutaneous WAT may undergo incubation for a maximum duration of 1 h during the digestion process. Conversely, visceral WAT is incubated with collagenase solution for a period not exceeding 30 min. This shorter digestion time for visceral WAT aims to mitigate the risk of excessive adipocyte breakdown.

⚠ CRITICAL: Be sure to optimize the digestion time for your specific adipose tissue and experimental needs. Extended digestion may lead to increased adipocyte death, whereas inadequate digestion could result in incomplete tissue dissociation.[4] Consider running pilot experiments to determine the optimal digestion time for your tissue type.

Adipocyte separation

Timing: 30 min

Upon completion of the digestion process (Figure 2A), the subsequent steps focus on segregating the mature adipocytes from the stromal vascular fraction (SVF) and tissue remnants.

14. Centrifuge the digested samples at 300 g for 5 min at 22°C (Figure 2B).
15. Invert the tube to facilitate thorough phase mixing (Figure 2C).
16. Repeat the centrifugation step under the same conditions (Figure 2D).

Note: This centrifugation step will separate the different components of the tissue suspension based on their sedimentation rates.

17. Collect the mature adipocytes from the top portion of the centrifuge tube (Figure 3A) and carefully transfer them into a new 15 mL Falcon tube with a Pasteur pipette (Figure 3B).
18. Rinse the adipocytes with 8–9 mL of PBS to guarantee the removal of remaining impurities or residual solutions (Figure 3C).
19. Centrifuge the Falcon tube containing PBS and adipocytes at 300 g for 5 min at 22°C (Figure 3D).
20. Cautiously collect the mature adipocytes from the upper layer using a pipette for subsequent analysis or culture (Figures 3E and 3F).

Note: It's crucial to note that the SVF pellet, derived from the separation procedure, is not only significant for isolating mature adipocytes but also for isolating other essential components, including stem cells, macrophages, and endothelial cells, among others.[5]

UNIVERSITAT ROVIRA I VIRGILI
Metabolic Impact of the Succinate/SUCNR1 Axis in Adipocytes: Insights into Circadian and Leptin Regulation
TERESA VILLANUEVA CARMONA

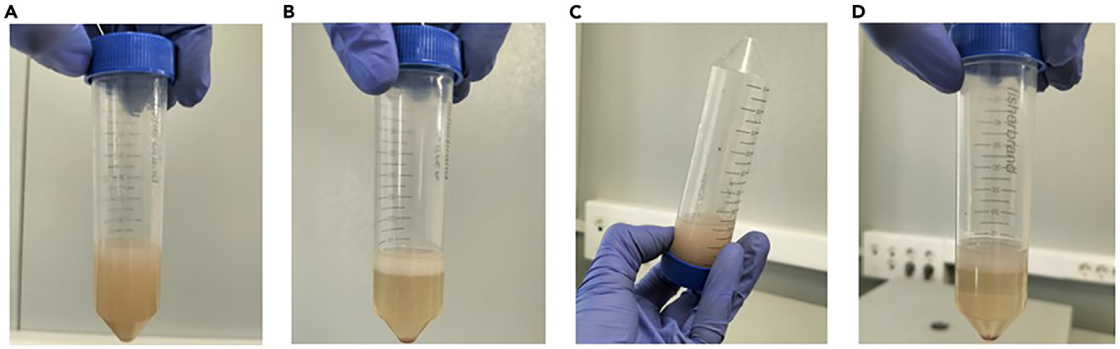

Figure 2. Separation of mature adipocytes
(A) Adipose tissue after incubation with the collagenase solution.
(B) Digested samples after the first centrifugation.
(C) Inverted tube to facilitate complete mixing of phases.
(D) Separation of mature adipocytes (arrow) from SVF and tissue remnants after centrifugation.

Cultivation of isolated mature adipocytes

Timing: 1 day

This section provides detailed steps for the cultivation and collection of isolated mature adipocytes, enabling further analysis and experimental studies.

21. Based on the experimental plan, seed the appropriate quantity of mature adipocytes in culture dishes or plates containing DMEM/F12 supplemented with 10% FBS and 1% antibiotic/antimycotic solution (Figures 4A and 4B).

Note: Owing to the heterogeneous size distribution of mature adipocytes, precise cell counting, and seeding densities become challenging to determine. The number of seeded wells is based on the total weight of the adipose tissue instead. In this specific protocol, using a 12-well plate, we recommend placing the adipocytes isolated from 1 g of tissue into each individual well.

⚠ CRITICAL: To achieve uniform dispersion of mature adipocytes across the culture plate, it is imperative to thoroughly homogenize them with the medium before seeding. Adipocytes have a tendency to float, and without adequate mixing, they might not distribute evenly within the plate, potentially affecting the success of the culture establishment.

22. Place the adipocytes in a cell culture incubator for 18 h, maintaining an environment of 37°C and 5% CO_2.
23. In line with the experimental schedule, continue with the planned assays, treatments, or experiments.
24. Collect the mature adipocytes with the medium and centrifuge at 400 g for 5 min at 22°C.
25. Post-centrifugation, cautiously collect the adipocytes that have floated to the top (Figure 4C).
26. Rinse these with PBS and repeat the centrifugation at 400 g for 5 min at 22°C.
27. Recover the mature adipocytes from the uppermost layer using a micropipette to perform the subsequent analysis or freeze at −80°C in an Eppendorf for preservation.

⚠ CRITICAL: It is important to note that the viability and functionality of the adipocytes might decrease as the duration of the culture extends. As such, it is standard practice to use mature adipocytes in experiments within the first 48 h post-isolation to ensure optimal functionality and responsiveness of the cells.

UNIVERSITAT ROVIRA I VIRGILI
Metabolic Impact of the Succinate/SUCNR1 Axis in Adipocytes: Insights into Circadian and Leptin Regulation
TERESA VILLANUEVA CARMONA

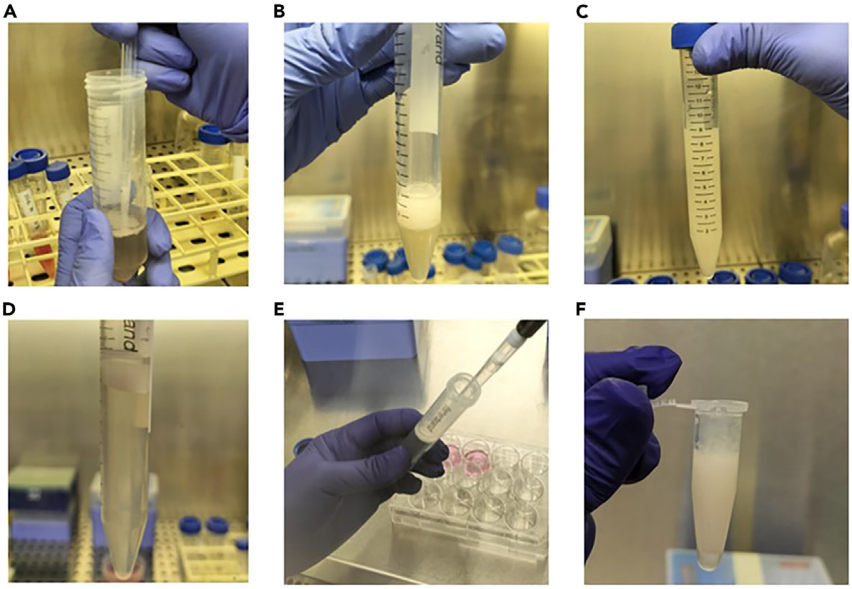

Figure 3. Collection of isolated mature adipocytes

(A) Process of recovering the mature adipocytes from the top portion of the centrifuge tube.
(B) Mature adipocytes transferred into a new 15 mL Falcon tube.
(C) Adipocytes rinsed with PBS.
(D) Falcon tube containing PBS and adipocytes after centrifugation.
(E and F) Collection of mature adipocytes from the upper layer into an Eppendorf tube.

Note: While not a mandatory step in the protocol, the visual examination of adipocytes under a microscope can be enriched by investigating the maturity of adipocytes through analyzing typical markers like PPARG, FASN, and GLUT4, among others. The analysis of mature adipocytes can take place either immediately before or after freezing. In this scenario, frozen adipocytes can maintain RNA and protein quality for several months to a year when preserved at −80°C. As a result, RNA and/or protein extraction can be conducted during this timeframe.

EXPECTED OUTCOMES

The protocol for isolating and culturing mature adipocytes aims for several key outcomes. These encompass the successful isolation of viable and functional mature adipocytes, preservation of their distinct morphology, lipid content during culture, preservation of their metabolic activity, responsiveness to stimuli, and retention of gene expression profiles relevant to adipocyte function. Additionally, culturing mature adipocytes enables the study of adipocyte-specific processes, such as lipid metabolism or adipokine secretion.

With white adipose tissue explants, one primary anticipated result is the preservation of the tissue's cellular architecture, crucial for examining cell morphology, cell-to-cell communication, and tissue-specific functions.

LIMITATIONS

This protocol describes the successful technique of isolating and culturing mature adipocytes and white adipose tissue explants. However, some limitations are noteworthy. Firstly, the presence of multiple cell types, including preadipocytes, immune, and vascular cells, can impact cell growth and overall tissue complexity. While *in vitro* systems are useful, they may not fully replicate the intricate *in vivo* microenvironment.

UNIVERSITAT ROVIRA I VIRGILI
Metabolic Impact of the Succinate/SUCNR1 Axis in Adipocytes: Insights into Circadian and Leptin Regulation
TERESA VILLANUEVA CARMONA

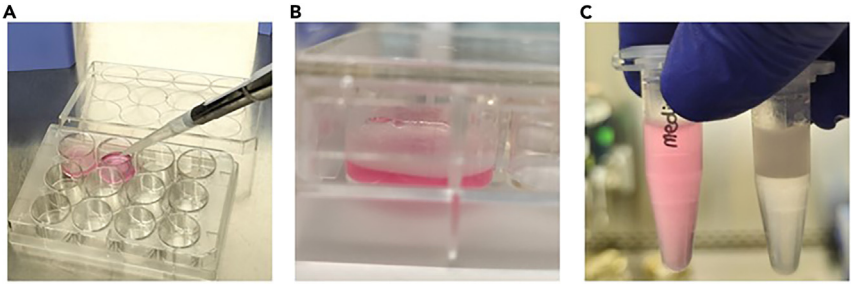

Figure 4. Process of cultivation of mature adipocytes
(A and B) Mature adipocytes seeded in culture dishes.
(C) Culture medium and mature adipocytes collected in Eppendorf tubes.

During the culture process, cells may experience phenotypic changes or gene expression alterations, potentially affecting their characteristics and behavior. Careful optimization of culture conditions - incorporating appropriate culture media, supplements, and techniques - is crucial for preserving cell viability and functionality. Furthermore, cell viability and function may decrease over time in long-term culture, requiring close monitoring. Moreover, acquiring large amounts of mature adipocytes or white adipose tissue for experimentation can be challenging due to variations in tissue abundance and accessibility, making standardized and consistent sample collection difficult.

Recognizing these constraints is important when designing experiments, interpreting results, and developing strategies to improve the reliability and relevance of adipose tissue research.

TROUBLESHOOTING

Problem 1

Low cell viability - related to step 13.

Potential solution

This can be caused by several factors. Sterile techniques must be upheld throughout the entire process to minimize contamination and its negative impact on cell viability. The digestion time and temperature during tissue dissociation need careful optimization as insufficient or excessive digestion can affect cell viability.

Problem 2

Inconsistencies arising from adipose tissue source - related to step 4 in before you begin section.

Potential solution

Adipose tissue depots vary in their cell yield and adipocyte maturity. Visceral adipose tissue typically contains larger adipocytes, indicative of greater maturity and higher lipid content, compared to subcutaneous adipose tissue. In contrast, subcutaneous adipose tissue, more vascularized than visceral adipose tissue, contains smaller, less mature adipocytes.[6] This increased vascularization can influence the ease of isolation and subsequent adipocyte culture, potentially leading to a higher yield of viable cells. Furthermore, the procedure is effective for normal adipose tissue function, but its effectiveness might differ in a situation involving a pathological condition, such as obesity. It's crucial to fine-tune the procedure if the pathological situation impacts adipose tissue. Therefore, choosing the adipose tissue depot for isolation depends on the specific research question and objectives.

Problem 3

Determining the number of mice required for the experiment - related to step 6 in before you begin section.

UNIVERSITAT ROVIRA I VIRGILI
Metabolic Impact of the Succinate/SUCNR1 Axis in Adipocytes: Insights into Circadian and Leptin Regulation
TERESA VILLANUEVA CARMONA

Potential solution

Striking a balance between scientific objectives and ethical considerations is crucial, aiming to minimize the number of mice utilized while achieving statistically significant results. A strategy known as sample pooling could help minimize the number of mice required for isolating and culturing mature adipocytes. This approach involves combining adipose tissue samples from multiple mice to generate a larger pool of cells or explants for the experiment. This method maximized tissue utilization from each mouse, enabling robust results while minimizing the overall number of mice used in the study.

RESOURCE AVAILABILITY

Lead contact

Further information and requests for resources and reagents should be directed to and will be fulfilled by the lead contact, Sonia Fernández Veledo (sonia.fernandez@iispv.cat).

Materials availability

The present study did not produce any novel or distinct reagents.

Data and code availability

No datasets were generated for this protocol.

ACKNOWLEDGMENTS

This research received financial support from multiple sources. Specifically, we acknowledge the Spanish Ministry of Science and Innovation MCIN/AEI/10.13039/501100011033 for the grants RTI2018-093919-B-100 and PID2021-122480OB-100 (to S.F.-V.) and PID2020-119030RJ-I00 (to L.C.). We also acknowledge the ISCIII for the support provided to J.V. (PI20/00338). All these grants are co-founded by the European Regional Development Fund (ERDF). Our research also received financial support from "La Caixa" Foundation (ID 100010434) under grant agreement LCF/PR/HR20/52400013 (to S.F.-V.). Both S.F.-V. and J.V. acknowledge support from the Agency for Management of University Research Grants of the Generalitat de Catalunya (2021 SGR 01409, 2021 SGR 0089). Additionally, our research was supported by the CIBER–Consorcio Centro de Investigation Biomédica en Red (CB07708/0012) from ISCIII. We express gratitude to our laboratory colleagues for their ongoing support.

AUTHOR CONTRIBUTIONS

Conceptualization, T.V.-C., L.C., J.V., S.F.-V.; methodology, T.V.-C., L.C., C.N.-R., E.M.-M.; validation, T.V.-C., L.C., C.N.-R., E.M.-M.; writing—original draft, T.V.-C., L.C., J.V., S.F.-V.; writing—review and editing, J.V., S.F.-V.; funding acquisition, J.V., S.F.-V.; supervision, J.V., S.F.-V.

DECLARATION OF INTERESTS

The authors declare no competing interests.

REFERENCES

1. Villanueva-Carmona, T., Cedó, L., Madeira, A., Ceperuelo-Mallafré, V., Rodríguez-Peña, M.M., Núñez-Roa, C., Maymó-Masip, E., Repollés-de-Dalmau, M., Badia, J., Keiran, N., et al. (2023). SUCNR1 signaling in adipocytes controls energy metabolism by modulating circadian clock and leptin expression. Cell Metab. *35*, 601–619.e10. https://doi.org/10.1016/j.cmet.2023.03.004.

2. Thalmann, S., Juge-Aubry, C.E., and Meier, C.A. (2008). Explant cultures of white adipose tissue. Methods Mol. Biol. *456*, 195–199. https://doi.org/10.1007/978-1-59745-245-8_14.

3. Luo, L., and Liu, M. (2016). Adipose tissue in control of metabolism. J. Endocrinol. *231*, R77–R99. https://doi.org/10.1530/JOE-16-0211.

4. Kilroy, G., Dietrich, M., Wu, X., Gimble, J.M., and Floyd, Z.E. (2018). Isolation of Murine Adipose-Derived Stromal/Stem Cells for Adipogenic Differentiation or Flow Cytometry-Based Analysis. Methods Mol. Biol. *1773*, 137–146. https://doi.org/10.1007/978-1-4939-7799-4_11.

5. Ramakrishnan, V.M., and Boyd, N.L. (2018). The Adipose Stromal Vascular Fraction as a Complex Cellular Source for Tissue Engineering Applications. Tissue Eng. Part B Rev. *24* (4), 289–299. https://doi.org/10.1089/ten.TEB.2017.0061.

6. Harvey, I., Boudreau, A., and Stephens, J.M. (2020). Adipose tissue in health and disease. Open Biol. *10*, 200291. https://doi.org/10.1098/rsob.200291.

DISCUSSION

AT is a highly dynamic and multifunctional metabolic organ essential for maintaining whole-body energy homeostasis by producing various adipokines, including leptin, which plays a pivotal role in regulating appetite, energy expenditure, and body weight[333,631]. Various physiological and environmental factors, such as nutritional status, energy intake, and fat mass, are known to influence leptin levels[632].

While leptin plays a vital role in regulating energy balance, the precise factors and mechanisms that control its production are still not fully understood[203]. In fact, some authors have suggested that leptin produced by fat cells is steadily released into the bloodstream, reflecting the long-term energy reserves of the body. Meanwhile, leptin derived from the stomach has been identified as a key player in the immediate post-meal increase in circulating leptin levels[340]. Notably, gastric leptin is resistant to degradation in the digestive tract, ensuring its function after secretion[633]. The stomach-derived leptin has been associated with the short-term regulation of digestion, including delaying gastric emptying, aiding nutrient absorption in the intestines, and stimulating the secretion of gastric, intestinal, and pancreatic hormones. In contrast, leptin secreted by white adipocytes primarily influences the hypothalamus, playing a significant role in the long-term regulation of food intake[634].

The succinate/SUCNR1 axis has garnered increasing scientific attention due to its emerging roles in both pathological and physiological processes[3]. Originally viewed as a metabolic intermediate within the TCA cycle, succinate is now recognized as a pivotal signaling molecule that influences cellular physiology and pathophysiology via its receptor, SUCNR1. This axis is implicated in a variety of pathological conditions, including hypertension, ischemia-reperfusion injury, inflammation, and metabolic disorders including obesity and T2DM[3,13,14,146,635]. However, recent studies have shown that physiological stimuli such as exercise[71], food ingestion[111], or cold exposure[109] can transiently increase extracellular succinate levels, suggesting that succinate might act as a hormone-like metabolite. This finding extends its importance beyond its previously understood pathological roles[3]. In fact, emerging evidence indicates that the succinate/SUCNR1 axis plays crucial roles in essential physiological processes, such as glucose regulation, insulin secretion, and AT lipolysis, underscoring its importance in both health and disease[3]. Despite SUCNR1 is expressed at relatively low levels in some tissues, its involvement in these essential physiological functions highlights its potential as a therapeutic target for a variety of disorders. Nonetheless, many aspects of SUCNR1 role in metabolic regulation are still not fully understood, highlighting the need for further research to unravel the complete role of succinate as a signaling molecule and the mechanisms of the succinate/SUCNR1 axis in various health contexts.

This doctoral thesis investigates the previously unexplored connection between the succinate/SUCNR1 axis and the endocrine adipocyte function. SUCNR1 is highly expressed in WAT, with notably high levels in isolated adipocytes[26]. Findings from a cluster analysis revealed that SUCNR1 plays a significant role in regulating lipolysis in

WAT, implying that succinate signaling may influence energy homeostasis[26]. Subsequent studies, including those by McCreath and others, have confirmed these findings, establishing that the succinate/SUCNR1 axis inhibits lipolysis in WAT, as evidenced by studies involving the global *Sucnr1* KO mice[13,26], which highlighted the complex role of SUCNR1 in regulating energy homeostasis and lipid metabolism[26].

McCreath and colleagues' pioneering research uncovered that SUCNR1 influences both adipose mass and glucose homeostasis, with its effects differing based on the pathophysiological context. *Sucnr1* KO mice displayed a leaner phenotype on a standard diet, characterized by reduced WAT size, increased energy expenditure, and improved glucose tolerance. When challenge with a HFD, these mice initially lost weight but later showed weight gain similar to WT controls, along with increased WAT and signs of hyperglycemia and reduced pancreatic insulin secretion, underscoring the complex effects of SUCNR1 deletion[13]. In contrast, Van Diepen and colleagues reported improved glucose tolerance and reduced macrophage infiltration in AT in their global *Sucnr1* KO model under HFD conditions, without significant differences in body weight compared to controls[15]. These discrepancies between studies likely arise from variations in dietary interventions, as well as distinct strategies used to generate the respective *Sucnr1* KO models, highlighting the importance of using tissue-specific KO models to fully understand the functionality of receptors and pathways that are unique to certain tissues.

Furthermore, while SUCNR1 expression in BAT is minimal, succinate plays a crucial role in modulating BAT function[13], enhancing its thermogenic properties which are essential for energy expenditure and maintaining body temperature. Under obesogenic conditions, brown adipocytes exhibit the capability to modulate extracellular succinate levels in the liver through the action of UCP1. This process represents a novel mechanism by which BAT might contribute to metabolic health by potentially mitigating liver inflammation associated with metabolic disorders[120].

Given that SUCNR1 is expressed in a wide range of tissues, it is likely that this receptor plays a complex role in maintaining metabolic homeostasis. Gaining a greater understanding of how SUCNR1 functions in different tissues will be crucial for fully appreciating its influence on metabolic health and the development of related diseases.

To explore the intricate role of SUCNR1 in WAT function, we employed genetically modified mice with *Sucnr1* specifically deleted in adipocytes, referred to as Ad-*Sucnr1* KO mice. We have identified that disturbances in succinate/SUCNR1 signaling in adipocytes influence the regulation of WAT mass and glucose homeostasis, with outcomes that vary depending to nutritional conditions. This observed phenotype closely aligns with the metabolic disturbances observed in mice lacking global *Sucnr1* expression[13]. Traditionally, the prevailing hypothesis have primarily attributed these effects to the anti-lipolytic effects of SUCNR1, thereby promoting uncontrolled fat

breackdown"[13,27]. However, beyond its anti-lipolytic effects, our findings reveal an additional critical function of succinate/SUCNR1 signaling in adipocytes: the regulation of the circadian clock and leptin expression. This regulatory role is essential for maintaining overall energy homeostasis and shed light on the intricate mechanisms governing adipocyte biology and metabolic regulation. This dichotomous effect underscores the multifaceted role of SUCNR1 in adipocyte biology, where it functions both as an inhibitor of lipolysis during metabolic stress and as a crucial regulator of leptin and circadian rhythms under normal nutritional conditions.

1. IMPACT OF *SUCNR1* DELETION ON METABOLIC HEALTH

Deletion of *Sucnr1* in adipocytes leads to notable changes in metabolic health, as shown in Ad-*Sucnr1* KO mice. On a NCD, these mice exhibited reduced body weight gain and lower fat mass. Interestingly, despite the decrease in adiposity, we did not observe the usual ectopic storage of TGs in non-ATs, a phenomenon normally associated to metabolic dysfunctions including IR and fatty liver disease. Instead, mice lacking *Sucnr1* specifically in the adipocytes presented enhanced glucose tolerance and higher RER, indicating a shift in energy utilization from lipids to carbohydratess[636,637].

Contrary to initial expectations based on models in which unrepressed lipolysis typically correlates with elevated serum lipid levels[638–640], both global *Sucnr1* KO[13] and adipocyte-specific *Sucnr1* KO did not demonstrate such lipid elevation under NCD conditions. Moreover, when we inhibited lipolysis in these mice by treating them with Atglistatin, no effect was observed on fat mass or glucose tolerance. These results suggested that the favorable phenotype observed in Ad-*Sucnr1* KO mice in NCD was not driven by lipolysis, pointing to the involvement of other mechanisms underlying their improved metabolic condition.

Notably, the absence of *Sucnr1* in adipocytes promoted WAT browning, a metabolic process associated with reduced weight gain and improved glucose tolerance[641,642]. The mechanism underlying this shift from white to brown fat is driven by an increased capacity of adipocyte precursors to differentiate into brown adipocytes. This differentiation appears to be influenced by the local accumulation of succinate, which is known to be a key inducer of brown-like adipocyte progenitors within WAT[113]. In line with this, succinate has been identified also as a critical regulator of thermogenesis in brown adipocytes by enhancing ROS production within mitochondria through SDH oxidation. This ROS production is essential for UCP1 activation, which facilitates the thermogenic processes in brown adipocytes. Additionally, brown adipocytes demonstrate a unique capability to sequester succinate from the bloodstream, suggesting a systemic mechanism by which succinate influences energy expenditure and metabolic regulation[109]. In addition, recent findings from our research group have shown

that succinate can activate WAT browning in ASCs in pathological conditions such as Crohn disease[643].

Despite exhibiting reduced fat mass and body weight gain, young Ad-*Sucnr1* KO mice display higher body weight than control mice, a finding previously reported but unexplored in global *Sucnr1* KO mice[13]. This disparity in body weight was not consequence of differences in lean mass but could partially result from the increase in bone mass observed in Ad-*Sucnr1* KO mice. Specifically, Ad-*Sucnr1* KO mice have higher levels of cortical bone and a greater number of osteoblasts and osteocytes. Given that bone mass constitutes approximately 5% of total body weight in mice, the observed 10% increase in bone mass among these mice does not completely account for the 5-10% greater body weight. Nevertheless, it is important to highlight the significant growth in tibia length, which serves as a critical indicator of longitudinal development in Ad-*Sucnr1* KO mice. Other experimental models involving specific gene deletions in adipocytes have also observed a negative correlation between WAT levels and bone mass, but these studies indicated that this phenotype is caused by disruptions in MSC differentiation[644–646]. However, in our model, we did not find differences in BM-MSCs differentiation to osteoblasts between Ad-*Sucnr1* KO mice and control mice.

Another factor that regulates bone mass is leptin[647,648]. Remarkably, Ad-*Sucnr1* KO mice showed hypoleptinemia, significantly attenuated circulating leptin responses during refeeding, and a disturbed hypothalamic response during the transition from fasting to feeding. Altogether, these factors may represent a critical influence on the observed changes in bone density and overall body weight in these mice, supporting the idea that leptin act as a central negative regulator of bone mass[398].

Leptin has been extensively studied for its impact on bone mass metabolism. *In vitro* studies have demonstrated that leptin directly stimulates the differentiation of stromal cells into osteoblasts[403] and inhibits osteoclastogenesis, but interestingly, mature osteoclasts appear to be unaffected[396]. Furthermore, deficiency in leptin signaling leads to significant reductions in bone volume and density[649]. Nonetheless, i*n vivo* studies reveal that the effects of leptin on bone are complex and mediated through central and peripheral mechanisms that can have opposing outcomes. Specifically, central administration of leptin has been shown to induce bone loss in both leptin-deficient and WT mice[398], while peripheral leptin, on the other hand, promotes bone mass by stimulating bone formation and reducing resorption[650]. This discrepancy highlights the importance of the site and mode of leptin action in determining its overall impact on bone health.

Human studies are even more conflicting, with some studies suggesting that leptin positively influences bone mass and density[651,652], and others indicating that high leptin levels can be detrimental[653,654]. This negative regulation is particularly evident in the context of obesity, where elevated leptin levels (hyperleptinemia) are associated with

reduced bone mass likely due to the presence of leptin resistance[405,406,655]. Our research with Ad-*Sucnr1* KO mice supports the idea that chronic leptin deficiency can have a positive effect on bone mass, consistent with previous findings of a negative relationship between leptin and bone health[656].

Interestingly, we also demonstrate that the typical postnatal leptin surge that occurs in mice, which is essential for fat mass accumulation in adulthood and development of hypothalamic feeding circuits[657], shows a declining trend in Ad-*Sucnr1* KO mice compared to their control littermates. This reduced leptin surge correlated with the observed lower fat mass and higher food intake in Ad-*Sucnr1* KO mice. Overall, our findings suggest that *Sucnr1* deficiency in adipocytes may indirectly influence postnatal growth and development.

Furthermore, the hypoleptinemia observed in Ad-*Sucnr1* KO mice plays a significant role in their favorable metabolic profile. Although leptin replacement therapy was administered to restore physiological leptin levels, resulting in increased adipocyte size and a slight worsening of glucose tolerance, it is important to note that these changes did not lead to the development of a pathological phenotype. This suggests that while leptin influences certain metabolic parameters, its effects do not necessarily translate into adverse health outcomes in this context.

Collectively, these results indicate that reduced leptin levels, coupled with the induction of WAT browning rather than unrestrained lipolysis, significantly contribute to the favorable metabolic profile observed in Ad-*Sucnr1* KO mice under NCD conditions.

2. METABOLIC EFFECT OF ADIPOCYTE *SUCNR1* IN HFD MICE

In response to overnutrition, the regulatory landscape of SUCNR1 undergoes significant alterations, leading to complex outcomes that closely resemble those observed in the global *Sucnr1* KO model[13,15]. When investigating the impact of HFD feeding on Ad-*Sucnr1* KO mice, our data revealed an opposite metabolic phenotype compared to that observed in NCD. Obese mice fed HFD showed a tendency towards increase fat mass and heightened hepatic steatosis. This metabolic dysregulation, accompanied by impaired glucose tolerance, parallels findings reported by McCreath and colleges[13] and is attributed to the unrestrained lipolysis. In this context, pharmacological inhibition of lipolysis by ATGLi significantly ameliorated HFD-induced glucose intolerance and hepatic steatosis in Ad-*Sucnr1* KO mice, indicating that lipolysis is a key factor in the metabolic phenotype of Ad-*Sucnr1* KO mice under conditions of overnutrition.

Moreover, in our study, Ad-*Sucnr1* KO mice exhibited completely opposite behaviors in carbohydrate metabolism when subjected to either a NCD or HFD. These opposing phenotypes were reflected in the RER, which was consistent with the observed differences in glucose tolerance and insulin sensitivity. It is well-established that glucose tolerance is generally linked to carbohydrates being the preferred energy source when glucose tolerance is optimal[636,637]. Conversely, in conditions of glucose intolerance, such as those seen in diet-induced obesity, there is a shift towards lipid utilization, reflected by a decrease in RER values.

In contrast to the phenotype observed under NCD, Ad-*Sucnr1* KO mice fed HFD did not exhibit lower leptin levels or increased hyperphagia. Instead, we observed a reduction in food intake in Ad-*Sucnr1* KO mice, but this reduction was confined to the light period. During the dark period, when mice are typically most active and consume the majority of their food, even under HFD conditions, this reduction was not evident, suggesting a disruption in their behavioral rhythms.

Additionally, we investigated the bone phenotype in mice fed HFD. While there are many discrepancies in the literature, as previously noted, HFD usually has mild deleterious effects on bone mass[658,659]. Our study revealed that bone mass changes in Ad-*Sucnr1* KO mice under a HFD were less pronounced, with no significant differences in bone parameters compared to NCD mice. As previously illustrated, we propose that the adipocyte-specific deletion of *Sucnr1* indirectly affects postnatal growth and bone development through disruptions in leptin levels. This effect appears to diminish with age and exposure to a high-calorie diet, conditions under which leptin differences between genotypes are not observed.

3. SUCCINATE AS A HORMONE-LIKE METABOLITE

3.1. LEPTIN REGULATION VIA SUCCINATE/SUCNR1 IN ADIPOCYTES

The landmark discovery of leptin as an adipocyte-secreted hormone in the 1990s firmly established AT as an active endocrine organ involved in the regulation of appetite and body weight[203]. Since then, extensive research has shed light on the molecular mechanisms through which leptin operates in peripheral tissues and the CNS, significantly enhancing our understanding of leptin resistance, particularly in the context of obesity[660]. It is well-documented that leptin levels are influenced by various physiological and environmental factors, including nutritional status, energy intake, and fat mass[632]. However, the specific regulatory factors that govern leptin production in adipocytes remain largely unknown[203], and some authors have even proposed that leptin is produced constitutively by adipocytes, with the postprandial regulation of leptin potentially influenced by signals from the gastric mucosa related to appetite.

Our research, focusing on the role of SUCNR1 disruption in adipocytes, provides compelling evidence that succinate functions as a hormone-like metabolite, significantly influencing leptin production within adipocytes. This finding introduces a novel physiological and molecular mechanism in adipocyte biology, highlighting the complex interplay between metabolic signals and endocrine function in AT.

In vitro studies using murine 3T3-L1 adipocytes have been instrumental in demonstrating that the *in vivo* observations are directly linked to the activation of SUCNR1 in adipocytes. These findings confirm that SUCNR1 plays a direct role in regulating leptin expression, further solidifying our understanding of its crucial function in maintaining energy homeostasis[111]. Our results demonstrated that leptin expression is modulated through a specific signaling pathway involving SUCNR1, AMPKα, and JNK. This finding uncovers a unique mechanism by which succinate regulates leptin production through distinct signalling pathways that were previously described in other cell types.

The variability in signaling outcomes is likely due to SUCNR1 differential coupling with various Gα-proteins across tissues, showcasing the complexity of SUCNR1 signaling[3]. For instance, in kidneys, SUCNR1 interacts with $G\alpha_q$ to activate ERK1/2 and produce prostaglandins, affecting blood pressure[19]. In cardiomyocytes, SUCNR1 enhances calcium transients and the ERK pathway, contributing to cardiac hypertrophy[143]. In pancreatic β-cells, it promotes insulin secretion by increasing calcium levels and activating PKC[25]. Further research is essential to elucidate the precise Gα-proteins involved in SUCNR1 signaling across different tissues.

Our observations reveal that SUCNR1 activation in adipocytes leads to the activation of MAPK signaling pathways, including key members such as ERK1/2 and JNK. These pathways have been extensively studied in the context of SUCNR1 activation and are

known to mediate various physiological effects. For example, research has shown that SUCNR1 influences the succinate-induced release of VEGF in the retinal ganglion cells through the MAPK/COX-2/PGE_2 signaling cascade[662]. Unexpectedly, we also discovered that SUCNR1 activation in adipocytes stimulates AMPK, a critical regulator of energy metabolism that usually reprograms metabolism by downregulating anabolic pathways, which are involved in biosynthesis and growth, and upregulating catabolic activities, which are crucial for energy production and metabolic homeostasis[663].

Despite its importance in terms of energy homeostasis, the role of AMPK in AT remains poorly documented and controversial. Traditionally, AMPK activation in AT has been associated with conditions such as fasting[664,665] and physical exercise[666]. However, recent findings reveal that AMPK is also activated in response to food intake and, in contrast to skeletal muscle, in which AMPK stimulation promotes glucose transport to provide ATP as a fuel[667], AMPK stimulation inhibits insulin-stimulated glucose transport in adipocytes to conserve ATP under conditions of cellular stress[668,669]. This process is crucial for maintaining energy homeostasis and is particularly stimulated postprandially. Beyond its role in glucose uptake, AMPK activation in adipocytes inhibits lipolysis[670,671], mirroring the effects of insulin but also succinate. The dual role of AMPK in enhancing glucose uptake and inhibiting lipolysis underscores its comprehensive function in AT.

Research have shown that the influence of AMPK on adipocyte metabolism extends beyond leptin, affecting other key hormones and proteins as well. For instance, AICAR, a direct activator of AMPK, has been shown to increase adiponectin expression in human AT[672,673]. Moreover, both adiponectin[673,674] and leptin[675] have been identified as activators of AMPK in adipocytes, suggesting a bidirectional relationship between these adipokines and AMPK signaling pathways.

3.2. CIRCADIAN CLOCK: SUCCINATE/SUCNR1 IMPLICATION

Additionally, our research has identified that SUCNR1 activation controls leptin expression via the circadian clock in AT. This finding is consistent with studies from Kettner and colleagues, who demonstrated that leptin expression, which exhibits diurnal variation both in humans and rodents[481,676], is regulated by an AT-specific peripheral clock via the CLOCK-BMAL1-C/EBPα pathway[485]. Given that several signaling molecules known to influence circadian rhythms act through GCPRs[677–679], it is not surprising that a GPCR like SUCNR1, whose agonist might be associated with dietary intake, could also regulate circadian rhythm. These GPCRs and their downstream signaling cascades are involved in the modulation of the molecular clock components and can influence the phase and period of the circadian clock, thereby linking metabolic signals to circadian regulation[680–683]. For example, members of the GPCR family B1, especially the VPAC2 receptor in mammals and its functional homologue PDFR in *Drosophila*, have been

associated with the regulation of circadian rhythms and sleep in a wide range of species[684].

In our study, the deletion of *Sucnr1* in adipocytes resulted in disruptions in the expression profiles of core-clock genes, which corresponded with altered feeding behaviors in mice fed either NCD or HFD. Although no direct data currently exist on the circadian rhythmicity of circulating succinate, it is well established that succinate levels are regulated by food intake[111,112] and follow a circadian pattern in saliva[685]. Peripheral tissues, including AT, are known to respond to nutritional cues and nutrient sensors independently of the central circadian clock, thereby playing a critical role in regulating nutrient uptake and metabolism[468,686,687]. Given these insights, it is plausible to hypothesize that succinate acts as an internal physiological signal, not only regulating lipid metabolism[13,27] but also influencing the circadian period.

Published datasets on the circadian transcriptome of AT have shown inconsistent results[688–691], likely due to species-specific variations and methodological challenges. Nonetheless, research on the circadian transcriptome in human WAT under standardized conditions have shown clear circadian variations in the TCA cycle[688]. This observation underscores a significant link between metabolic processes and circadian rhythms. Further supporting this connection, analysis of *Sucnr1* gene expression profiles in major tissues from the CircadiOmics database[692] has revealed a pronounced circadian pattern in primates, particularly baboons. These findings align with our study and suggest that the mechanisms we have identified may be conserved across different species.

Our study has elucidated a novel signaling pathway where succinate, through a SUCNR1-AMPKα-JNK-dependent mechanism, regulates leptin expression via the BMAL1-C/EBPα-pathway. This discovery highlights the complex interplay between metabolic signals and the circadian clock in AT, suggesting that succinate acts as a crucial mediator in this regulatory network. We observed that the deletion of the *Bmal1* gene resulted in a diminished response to succinate-induced phosphorylation of C/EBPα. This finding supports existing evidence that the BMAL1/CLOCK complex is crucial for stimulating C/EBPα-mediated transcription of leptin[485].

Similar to other metabolic sensors such as SIRT1[693] and PPARs[694], AMPK modulate the activity of core clock components leading to adjustments in the circadian cycle based on energy availability[695]. Our findings demonstrate that AMPK activation in adipocytes increases BMAL1 expression, consistent with previous studies indicating the role of AMPK in regulating clock gene expression. Specifically, AMPK promotes BMAL1 expression by facilitating the degradation of PER2[696] and destabilization of the core clock protein CRY1[697]. In essence, our findings underscore the pivotal role of SUCNR1 and AMPK in regulating not just the circadian rhythm but also leptin expression in adipocyte physiology.

3.3. IMPACT OF THE SUCCINATE/SUCNR1 AXIS IN HUMAN AT

Our findings establish a critical link between obesity-associated hyperleptinemia in humans and SUCNR1 overexpression in adipocytes, positioning SUCNR1 as a key determinant of leptin production in AT. We observed that adipocytes derived from precursor cells of individuals with obesity secrete more leptin in response to SUCNR1 activation compared to those from lean individuals, which aligns with the well-documented phenomenon of hyperleptinemia in obesity, where elevated leptin levels occur despite the presence of leptin resistance[698]. This suggests that SUCNR1 not only influences leptin production in AT but also play a role in the dysregulation of leptin signaling observed in obesity. These results are consistent with prior research, which demonstrated that both circulating succinate and SUCNR1 levels in adipocytes are elevated in individuals with obesity[14,37]. In line with this, other GPCRs, such as GPR43, have also been implicated in the regulation of leptin secretion in AT. GPR43 activation acetate, which is another intermediate in the TCA cycle like succinate, has been shown to increase leptin production in mesenteric adipocytes, whereas other ligands, such as butyrate, do not have the same effect[699]. Thus, while SUCNR1 is a crucial player, the overactivation of other GPCRs involved in metabolic regulation could also contribute to the hyperleptinemia observed in the context of obesity.

Over the past two decades, a growing body of research has identified several novel factors contributing to obesity and its related metabolic diseases, such as insufficient sleep and circadian misalignment[700,701]. This disruption of the circadian rhythm and eventual disruption of circadian clock functioning has been strongly linked to metabolic disorders[702]. Our data indicate that individuals with obesity not only have elevated levels of circulating succinate and leptin but also show a significant upregulation in the expression of core circadian clock genes, such as *CLOCK* and *BMAL1*, particularly in vWAT. Supporting this, research have demonstrated that, in HFD-induced obesity, CLOCK expression levels are increased, and PPARα increases BMAL1 transcription in the WAT of individuals with obesity. As a result, disruption in clock genes lead to dyslipidemia, IR and obesity[703].

The integration of this findings in human individuals reinforces the pivotal role of the succinate/SUCNR1 axis in regulating leptin expression, particularly through its interactions with the circadian clock in AT. Thus, these insights provide a comprehensive framework for further research into the role of SUCNR1 in obesity and its potential impact on both metabolic and circadian health.

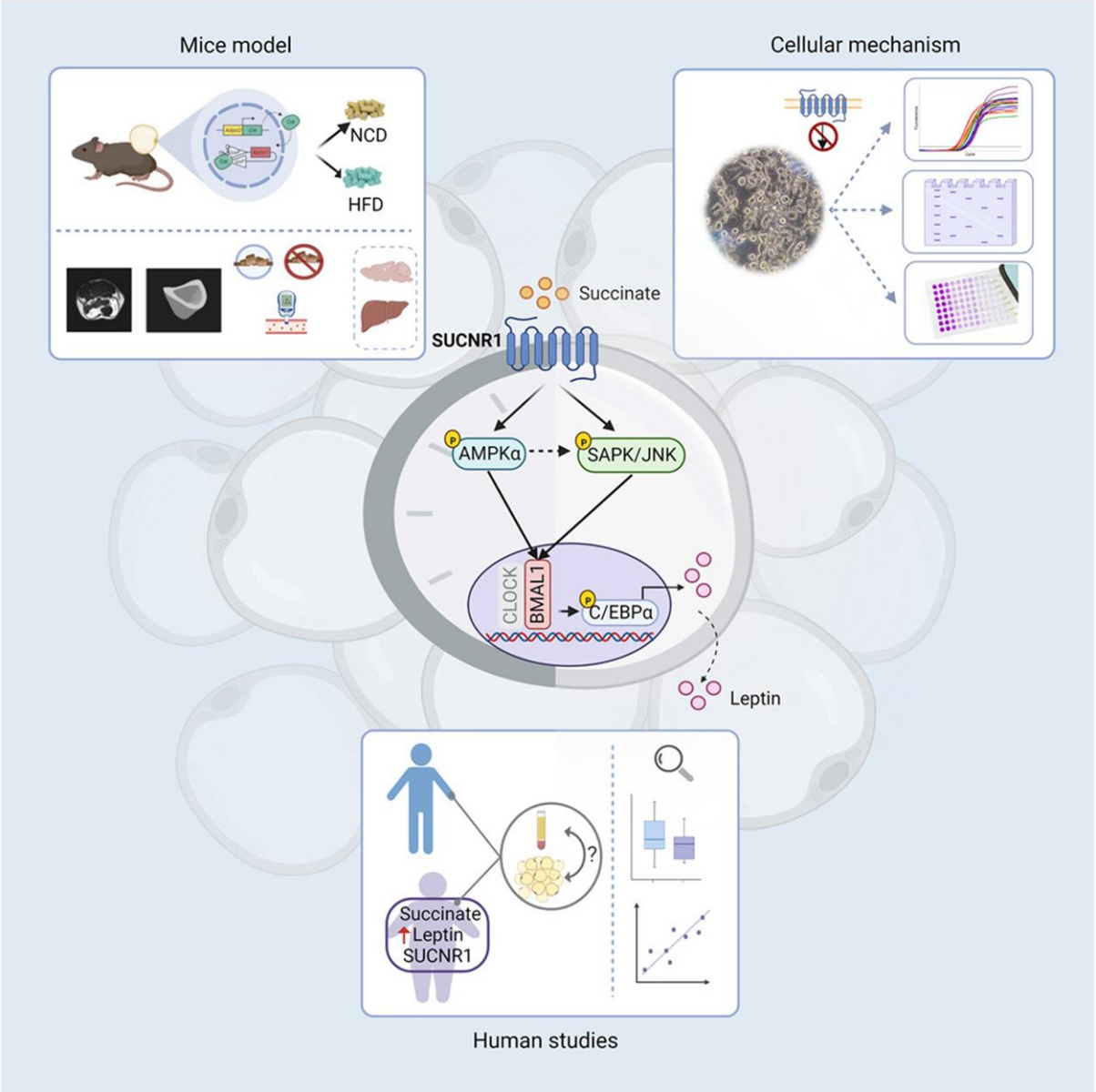

Figure 33. Overview of the succinate/SUCNR1 Interaction in adipocytes. This figure outlines the comprehensive experimental strategy adopted in this research, using *in vitro* cell models, a mouse model with adipocyte-specific *Sucnr1* KO, and a human cohort. These combined methods confirm the primary hypothesis of this thesis: the interaction between succinate and the SUCNR1 receptor in adipocytes regulates the circadian rhythm and leptin expression. Image from Biorender.

4. OBESITY-LINKED DISTURBANCES IN SUCCINATE/SUCNR1 AXIS

In the context of obesity, our study has identified significant disruptions in the succinate/SUCNR1 pathway, which are intricately connected to the elevated leptin levels commonly observed in obesity. Previous research from our group has also highlighted disturbances in this pathway in relation to inflammation associated with obesity[14]. We know today that succinate, a metabolite with pro-inflammatory properties, plays also a crucial role in resolving inflammation through signaling via the SUCNR1 receptor [14,108,171]. Nonetheless, our findings indicate that this mechanism is compromised in obesity. Specifically, ATMs from subjects with obesity exhibit reduced expression of SUCNR1 and anti-inflammatory markers, such as PPARγ, despite the presence of elevated circulating succinate levels. This state, referred to as "succinate resistance," suggests a diminished capacity for these cells to respond to succinate and resolve inflammation. This dysregulation likely contributes to the persistent inflammatory state observed in obesity, highlighting a potential underlying mechanism for the associated metabolic dysfunction[14].

Conversely, as previously mentioned, our research showed that adipocytes in individuals with obesity exhibit higher levels of *SUCNR1* expression, which significantly enhances their sensitivity to succinate and promotes increased leptin secretion. This phenomenon results in the excessive production of leptin in the context of obesity, leading to hyperleptinemia, which subsequently triggers leptin resistance. This resistance disrupts the ability of the body to effectively regulate both appetite and energy expenditure, thereby exacerbating the process of weight gain. Thus, our findings indicate that obesity is characterized by the hyperactivation of succinate/SUCNR1 signaling in adipocytes, leading to elevated leptin production. Thus, both the hyperactivation of SUCNR1 in adipocytes and the inhibition of the pathway resolutive functions in AT derived-macrophages are detrimental in the context of obesity. These dual disruptions highlight the complexity of targeting the succinate/SUCNR1 signaling in obesity.

Furthermore, recent findings from our group revealed that the succinate/SUCNR1 axis plays a dual role in liver pathology. In the early stages, it acts as a protective mechanism in the progression from MAFLD to NASH, helping to counteract inflammation and cellular stress. However, this protective role can become detrimental over time, as persistent activation of this pathway may lead to excessive fibrosis and contribute to the worsening of the disease[28]. A similar dual role is observed in pancreatic β-cells during prediabetic stages. Initially, succinate hyperactivation triggers increased insulin production to compensate for IR. However, as the disease progresses, this response becomes impaired, with succinate postprandial effects eventually diminishing[25]. Thus, while the succinate/SUCNR1 axis initially helps manage stress both in liver and

pancreatic β-cells, its persistent activation can ultimately exacerbate disease progression[25,28].

5. RESEARCH INSIGHTS AND FUTURE DIRECTIONS

The research presented in this thesis significantly advances the understanding of the succinate/SUCNR1 axis, establishing it as a pivotal component of the metabolic-sensing machinery that enables adipocytes to coordinate metabolic responses to nutrient intake. The role of succinate as a signaling molecule becomes particularly evident during the transition from a fasted to a fed state. During this transition, fluctuations in circulating succinate levels might serve physiological functions in AT, extending beyond the regulation of lipolysis to encompass the modulation of leptin production and circadian clock by adipocytes through SUCNR1 signaling. In the context of obesity, the succinate/SUCNR1 axis becomes dysregulated, leading to a cascade of metabolic disturbances. Elevated levels of circulating succinate, coupled with altered SUCNR1 expression, contribute to obesity-related metabolic disturbances, including hyperleptinemia. Our research underscores the dual role of succinate/SUCNR1 axis in adipocytes under normal metabolic regulation and pathological states such as obesity.

In this scenario, our findings underscore the potential of SUCNR1 as a promising therapeutic target for addressing leptin dysregulation in patients with obesity. In individuals with obesity, the normal feedback mechanism that regulates food intake, partly mediated by leptin, is often impaired, leading to uncontrolled appetite and further weight gain[517]. Our research suggests that modulating the succinate/SUCNR1 pathway could play a crucial role in restoring leptin levels to their physiological norm.

Nonetheless, further research is needed due to the broad expression of SUCNR1 and its pleiotropic functions[3]. As previously outlined, while the succinate/SUCNR1 axis is crucial for resolving inflammation[14,171], its activation can also have pro-inflammatory effects in the acute phase of the immune response[5,56]. Therefore, directly targeting SUCNR1 to restore leptin secretion and sensitivity in patients with obesity may not be the most effective course, given the receptor diverse roles and potential off-target impacts. An emerging strategy involves mitigating elevated levels of circulating succinate, particularly from its intestinal source. This approach could potentially avoid the unintended consequences of broad SUCNR1 activation, such as exacerbating inflammation[48].

By decreasing succinate levels, we hypothesize that the activation of SUCNR1 could be reduced, potentially leading to a normalization of leptin secretion and sensitivity. This approach could counteract the hyperleptinemia and leptin resistance commonly observed in obesity, thereby improving the regulatory mechanisms of appetite and energy expenditure, contributing to a more effective management of obesity. Moreover,

this strategy might mitigate some of the metabolic complications associated with obesity, such as IR and chronic inflammation, and it could be valuable in preventing the development of CVD and T2DM, conditions that are closely linked to obesity[496].

In summary, our study proposes that targeting the succinate/SUCNR1 pathway could be a viable strategy for restoring leptin function and addressing the underlying metabolic disturbances in obesity. Further research into this pathway could pave the way for the development of new treatments that not only focus on weight loss but also improve overall metabolic health. Currently, our research group is undertaking a new project to further investigate the interplay and mutual influence between the succinate/SUCNR1 axis and the molecular clock, both under physiological conditions and in the context of obesity. Disruptions in circadian rhythms are known to contribute to metabolic disorders and restoring or synchronizing these rhythms by targeting the succinate/SUCNR1 pathway could be an effective approach in treating obesity. Additionally, this approach may also hold promise for restoring SUCNR1 function for addressing other metabolic disorders. For instance, it could be useful for enhance insulin secretion in T2DM patients, potentially improving glycemic control and reducing reliance on insulin therapy[25]. However, an exhaustive investigation is required to understand the detailed mechanics of this signaling pathway in improving metabolic health and treating metabolic disorders.

CONCLUSIONS

1. Conditional adipocyte deletion of *Sucnr1* in mice fed NCD results in **decreased adipose** mass and **improved metabolic health** due to both reduced leptin levels and the induction of WAT browning.

2. Mice lacking *Sucnr1* in adipocytes exhibit **hepatic fat accumulation** and **glucose intolerance** on HFD primarily driven by the anti-lipolytic properties of SUCNR1.

3. Succinate/SUCNR1 signaling modulates leptin expression in adipocytes via a mechanism involving the circadian clock in an **AMPK/JNK/BMAL1-C/EBP-α-**dependent manner.

4. Obesity-associated hyperleptinemia is associated with an overactivation of the succinate/SUCNR1 pathway in humans.

OVERALL CONCLUSION

The succinate/SUCNR1 signaling pathway in adipocytes is crucial for the regulation of metabolic processes, particularly influencing lipid metabolism and endocrine functions within AT, with its dysregulation significantly contributing to obesity-related metabolic disturbances.

REFERENCES

1. Krebs HA, Johnson WA. The role of citric acid in intermediate metabolism in animal tissues. *FEBS Lett*. 1980;117 Suppl:K1-10. doi:10.4159/harvard.9780674366701.c143

2. PubChem. Succinic Acid. Accessed July 8, 2024. https://pubchem.ncbi.nlm.nih.gov/compound/1110

3. Fernández-Veledo S, Ceperuelo-Mallafré V, Vendrell J. Rethinking succinate: an unexpected hormone-like metabolite in energy homeostasis. *Trends Endocrinol Metab TEM*. 2021;32(9):680-692. doi:10.1016/j.tem.2021.06.003

4. He W, Miao FJP, Lin DCH, et al. Citric acid cycle intermediates as ligands for orphan G-protein-coupled receptors. *Nature*. 2004;429(6988):188-193. doi:10.1038/nature02488

5. Littlewood-Evans A, Sarret S, Apfel V, et al. GPR91 senses extracellular succinate released from inflammatory macrophages and exacerbates rheumatoid arthritis. *J Exp Med*. 2016;213(9):1655-1662. doi:10.1084/jem.20160061

6. Saraiva AL, Veras FP, Peres RS, et al. Succinate receptor deficiency attenuates arthritis by reducing dendritic cell traffic and expansion of Th17 cells in the lymph nodes. *FASEB J Off Publ Fed Am Soc Exp Biol*. Published online June 12, 2018:fj201800285. doi:10.1096/fj.201800285

7. Li Y, Liu Y, Wang C, et al. Succinate induces synovial angiogenesis in rheumatoid arthritis through metabolic remodeling and HIF-1α/VEGF axis. *Free Radic Biol Med*. 2018;126:1-14. doi:10.1016/j.freeradbiomed.2018.07.009

8. Macias-Ceja DC, Ortiz-Masiá D, Salvador P, et al. Succinate receptor mediates intestinal inflammation and fibrosis. *Mucosal Immunol*. 2019;12(1):178-187. doi:10.1038/s41385-018-0087-3

9. Favret S, Binet F, Lapalme E, et al. Deficiency in the metabolite receptor SUCNR1 (GPR91) leads to outer retinal lesions. *Aging*. 2013;5(6):427-444. doi:10.18632/aging.100563

10. Mu X, Zhao T, Xu C, et al. Oncometabolite succinate promotes angiogenesis by upregulating VEGF expression through GPR91-mediated STAT3 and ERK activation. *Oncotarget*. 2017;8(8):13174-13185. doi:10.18632/oncotarget.14485

11. Zhao T, Mu X, You Q. Succinate: An initiator in tumorigenesis and progression. *Oncotarget*. 2017;8(32):53819-53828. doi:10.18632/oncotarget.17734

12. Li X, Xie L, Qu X, et al. GPR91, a critical signaling mechanism in modulating pathophysiologic processes in chronic illnesses. *FASEB J Off Publ Fed Am Soc Exp Biol*. 2020;34(10):13091-13105. doi:10.1096/fj.202001037R

13. McCreath KJ, Espada S, Gálvez BG, et al. Targeted disruption of the SUCNR1 metabolic receptor leads to dichotomous effects on obesity. *Diabetes*. 2015;64(4):1154-1167. doi:10.2337/db14-0346

14. Keiran N, Ceperuelo-Mallafré V, Calvo E, et al. SUCNR1 controls an anti-inflammatory program in macrophages to regulate the metabolic response to obesity. *Nat Immunol*. 2019;20(5):581-592. doi:10.1038/s41590-019-0372-7

15. van Diepen JA, Robben JH, Hooiveld GJ, et al. SUCNR1-mediated chemotaxis of macrophages aggravates obesity-induced inflammation and diabetes. *Diabetologia*. 2017;60(7):1304-1313. doi:10.1007/s00125-017-4261-z

16. Atallah R, Gindlhuber J, Platzer W, et al. SUCNR1 Is Expressed in Human Placenta and Mediates Angiogenesis: Significance in Gestational Diabetes. *Int J Mol Sci*. 2021;22(21):12048. doi:10.3390/ijms222112048

17. Aguiar CJ, Rocha-Franco JA, Sousa PA, et al. Succinate causes pathological cardiomyocyte hypertrophy through GPR91 activation. *Cell Commun Signal CCS*. 2014;12:78. doi:10.1186/s12964-014-0078-2

18. Robben JH, Fenton RA, Vargas SL, et al. Localization of the succinate receptor in the distal nephron and its signaling in polarized MDCK cells. *Kidney Int*. 2009;76(12):1258-1267. doi:10.1038/ki.2009.360

19. Vargas SL, Toma I, Kang JJ, Meer EJ, Peti-Peterdi J. Activation of the succinate receptor GPR91 in macula densa cells causes renin release. *J Am Soc Nephrol JASN*. 2009;20(5):1002-1011. doi:10.1681/ASN.2008070740

20. Toma I, Kang JJ, Sipos A, et al. Succinate receptor GPR91 provides a direct link between high glucose levels and renin release in murine and rabbit kidney. *J Clin Invest*. 2008;118(7):2526-2534. doi:10.1172/JCI33293

21. Sapieha P, Sirinyan M, Hamel D, et al. The succinate receptor GPR91 in neurons has a major role in retinal angiogenesis. *Nat Med*. 2008;14(10):1067-1076. doi:10.1038/nm.1873

22. Hu J, Wu Q, Li T, Chen Y, Wang S. Inhibition of high glucose-induced VEGF release in retinal ganglion cells by RNA interference targeting G protein-coupled receptor 91. *Exp Eye Res*. 2013;109:31-39. doi:10.1016/j.exer.2013.01.011

23. Li YH, Choi DH, Lee EH, Seo SR, Lee S, Cho EH. Sirtuin 3 (SIRT3) Regulates α-Smooth Muscle Actin (α-SMA) Production through the Succinate Dehydrogenase-G Protein-coupled Receptor 91 (GPR91) Pathway in Hepatic Stellate Cells. *J Biol Chem*. 2016;291(19):10277-10292. doi:10.1074/jbc.M115.692244

24. Liu XJ, Xie L, Du K, et al. Succinate-GPR-91 Receptor Signaling Is Responsible for Nonalcoholic Steatohepatitis-Associated Fibrosis: Effects of DHA Supplementation. *Liver Int Off J Int Assoc Study Liver*. 2020;40(4):830-843. doi:10.1111/liv.14370

25. Sabadell-Basallote J, Astiarraga B, Castaño C, et al. SUCNR1 regulates insulin secretion and glucose elevates the succinate response in people with prediabetes. *J Clin Invest*. Published online May 7, 2024:e173214. doi:10.1172/JCI173214

26. Regard JB, Sato IT, Coughlin SR. Anatomical profiling of G protein-coupled receptor expression. *Cell*. 2008;135(3):561-571. doi:10.1016/j.cell.2008.08.040

27. An YA, Chen S, Deng Y, et al. The mitochondrial dicarboxylate carrier prevents hepatic lipotoxicity by inhibiting white adipocyte lipolysis. *J Hepatol*. 2021;75(2):387-399. doi:10.1016/j.jhep.2021.03.006

28. Marsal-Beltran A, Rodríguez-Castellano A, Astiarraga B, et al. Protective effects of the succinate/SUCNR1 axis on damaged hepatocytes in NAFLD. *Metabolism*. 2023;145:155630. doi:10.1016/j.metabol.2023.155630

29. Wang T, Xu Y, Yuan Y, et al. Succinate induces skeletal muscle fiber remodeling via SUCNR1 signaling. *EMBO Rep*. 2019;20(9):e47892. doi:10.15252/embr.201947892

30. Fernández-Veledo S, Vendrell J. Gut microbiota-derived succinate: Friend or foe in human metabolic diseases? *Rev Endocr Metab Disord*. 2019;20(4):439-447. doi:10.1007/s11154-019-09513-z

31. Zhang W, Lang R. Succinate metabolism: a promising therapeutic target for inflammation, ischemia/reperfusion injury and cancer. *Front Cell Dev Biol*. 2023;11. doi:10.3389/fcell.2023.1266973

32. Tretter L, Patocs A, Chinopoulos C. Succinate, an intermediate in metabolism, signal transduction, ROS, hypoxia, and tumorigenesis. *Biochim Biophys Acta*. 2016;1857(8):1086-1101. doi:10.1016/j.bbabio.2016.03.012

33. Alabduladhem TO, Bordoni B. Physiology, Krebs Cycle. In: *StatPearls*. StatPearls Publishing; 2024. Accessed April 12, 2024. http://www.ncbi.nlm.nih.gov/books/NBK556032/

34. Akram M. Citric acid cycle and role of its intermediates in metabolism. *Cell Biochem Biophys*. 2014;68(3):475-478. doi:10.1007/s12013-013-9750-1

35. Huang H, Li G, He Y, et al. Cellular succinate metabolism and signaling in inflammation: implications for therapeutic intervention. *Front Immunol*. 2024;15. doi:10.3389/fimmu.2024.1404441

36. Geiger O, Sanchez-Flores A, Padilla-Gomez J, Degli Esposti M. Multiple approaches of cellular metabolism define the bacterial ancestry of mitochondria. *Sci Adv*. 2023;9(32):eadh0066. doi:10.1126/sciadv.adh0066

37. Serena C, Ceperuelo-Mallafré V, Keiran N, et al. Elevated circulating levels of succinate in human obesity are linked to specific gut microbiota. *ISME J*. 2018;12(7):1642-1657. doi:10.1038/s41396-018-0068-2

38. Reichardt N, Duncan SH, Young P, et al. Phylogenetic distribution of three pathways for propionate production within the human gut microbiota. *ISME J*. 2014;8(6):1323-1335. doi:10.1038/ismej.2014.14

39. Imdad S, Lim W, Kim JH, Kang C. Intertwined Relationship of Mitochondrial Metabolism, Gut Microbiome and Exercise Potential. *Int J Mol Sci*. 2022;23(5):2679. doi:10.3390/ijms23052679

40. Cummings JH, Pomare EW, Branch WJ, Naylor CP, Macfarlane GT. Short chain fatty acids in human large intestine, portal, hepatic and venous blood. *Gut*. 1987;28(10):1221-1227. doi:10.1136/gut.28.10.1221

41. De Vadder F, Kovatcheva-Datchary P, Zitoun C, Duchampt A, Bäckhed F, Mithieux G. Microbiota-Produced Succinate Improves Glucose Homeostasis via Intestinal Gluconeogenesis. *Cell Metab*. 2016;24(1):151-157. doi:10.1016/j.cmet.2016.06.013

42. Meijer-Severs GJ, van Santen E. Short-chain fatty acids and succinate in feces of healthy human volunteers and their correlation with anaerobe cultural counts. *Scand J Gastroenterol*. 1987;22(6):672-676. doi:10.3109/00365528709011141

43. Bringaud F, Biran M, Millerioux Y, Wargnies M, Allmann S, Mazet M. Combining reverse genetics and nuclear magnetic resonance-based metabolomics unravels trypanosome-specific metabolic pathways. *Mol Microbiol*. 2015;96(5):917-926. doi:10.1111/mmi.12990

44. Louis P, Flint HJ. Formation of propionate and butyrate by the human colonic microbiota. *Environ Microbiol*. 2017;19(1):29-41. doi:10.1111/1462-2920.13589

45. Faith JJ, Ahern PP, Ridaura VK, Cheng J, Gordon JI. Identifying gut microbe-host phenotype relationships using combinatorial communities in gnotobiotic mice. *Sci Transl Med*. 2014;6(220):220ra11. doi:10.1126/scitranslmed.3008051

46. Nagao-Kitamoto H, Shreiner AB, Gillilland MG, et al. Functional Characterization of Inflammatory Bowel Disease-Associated Gut Dysbiosis in Gnotobiotic Mice. *Cell Mol Gastroenterol Hepatol*. 2016;2(4):468-481. doi:10.1016/j.jcmgh.2016.02.003

47. Kim YG, Sakamoto K, Seo SU, et al. Neonatal acquisition of Clostridia species protects against colonization by bacterial pathogens. *Science*. 2017;356(6335):315-319. doi:10.1126/science.aag2029

48. Huber-Ruano I, Calvo E, Mayneris-Perxachs J, et al. Orally administered Odoribacter laneus improves glucose control and inflammatory profile in obese mice by depleting circulating succinate. *Microbiome*. 2022;10:135. doi:10.1186/s40168-022-01306-y

49. Ariake K, Ohkusa T, Sakurazawa T, et al. Roles of mucosal bacteria and succinic acid in colitis caused by dextran sulfate sodium in mice. *J Med Dent Sci*. 2000;47(4):233-241.

50. Macy JM, Ljungdahl LG, Gottschalk G. Pathway of succinate and propionate formation in Bacteroides fragilis. *J Bacteriol*. 1978;134(1):84-91. doi:10.1128/jb.134.1.84-91.1978

51. Pybus V, Onderdonk AB. The Effect of pH on Growth and Succinate Production by Prevotella bivia. *Microb Ecol Health Dis*. 1996;9(1):19-25. doi:10.3109/08910609609167725

52. Trautmann A, Schleicher L, Koch A, Günther J, Steuber J, Seifert J. A shift towards succinate-producing Prevotella in the ruminal microbiome challenged with monensin. *PROTEOMICS*. 2023;23(21-22):2200121. doi:10.1002/pmic.202200121

53. Wei Y han, Ma X, Zhao JC, Wang XQ, Gao CQ. Succinate metabolism and its regulation of host-microbe interactions. *Gut Microbes*. 15(1):2190300. doi:10.1080/19490976.2023.2190300

54. Watanabe Y, Nagai F, Morotomi M. Characterization of Phascolarctobacterium succinatutens sp. nov., an Asaccharolytic, Succinate-Utilizing Bacterium Isolated from Human Feces. *Appl Environ Microbiol*. 2012;78(2):511-518. doi:10.1128/AEM.06035-11

55. Ferreyra JA, Wu KJ, Hryckowian AJ, Bouley DM, Weimer BC, Sonnenburg JL. Gut microbiota-produced succinate promotes C. difficile infection after antibiotic treatment or motility disturbance. *Cell Host Microbe*. 2014;16(6):770-777. doi:10.1016/j.chom.2014.11.003

56. Rubic T, Lametschwandtner G, Jost S, et al. Triggering the succinate receptor GPR91 on dendritic cells enhances immunity. *Nat Immunol*. 2008;9(11):1261-1269. doi:10.1038/ni.1657

57. De Vadder F, Kovatcheva-Datchary P, Goncalves D, et al. Microbiota-generated metabolites promote metabolic benefits via gut-brain neural circuits. *Cell*. 2014;156(1-2):84-96. doi:10.1016/j.cell.2013.12.016

58. Kovatcheva-Datchary P, Nilsson A, Akrami R, et al. Dietary Fiber-Induced Improvement in Glucose Metabolism Is Associated with Increased Abundance of Prevotella. *Cell Metab*. 2015;22(6):971-982. doi:10.1016/j.cmet.2015.10.001

59. Banerjee A, Herring CA, Chen B, et al. Succinate Produced by Intestinal Microbes Promotes Specification of Tuft Cells to Suppress Ileal Inflammation. *Gastroenterology*. 2020;159(6):2101-2115.e5. doi:10.1053/j.gastro.2020.08.029

60. Zhao L, Lou H, Peng Y, Chen S, Fan L, Li X. Elevated levels of circulating short-chain fatty acids and bile acids in type 2 diabetes are linked to gut barrier disruption and disordered gut microbiota. *Diabetes Res Clin Pract*. 2020;169:108418. doi:10.1016/j.diabres.2020.108418

61. Fernández-Veledo S, Marsal-Beltran A, Vendrell J. Type 2 diabetes and succinate: unmasking an age-old molecule. *Diabetologia*. 2024;67(3):430-442. doi:10.1007/s00125-023-06063-7

62. Tannahill GM, Curtis AM, Adamik J, et al. Succinate is an inflammatory signal that induces IL-1β through HIF-1α. *Nature*. 2013;496(7444):238-242. doi:10.1038/nature11986

63. Mills E, O'Neill LAJ. Succinate: a metabolic signal in inflammation. *Trends Cell Biol*. 2014;24(5):313-320. doi:10.1016/j.tcb.2013.11.008

64. Grimolizzi F, Arranz L. Multiple faces of succinate beyond metabolism in blood. *Haematologica*. 2018;103(10):1586-1592. doi:10.3324/haematol.2018.196097

65. Chouchani ET, Pell VR, Gaude E, et al. Ischaemic accumulation of succinate controls reperfusion injury through mitochondrial ROS. *Nature*. 2014;515(7527):431-435. doi:10.1038/nature13909

66. Jitrapakdee S, Maurice MSt, Rayment I, Cleland WW, Wallace JC, Attwood PV. Structure, Mechanism and Regulation of Pyruvate Carboxylase. *Biochem J*. 2008;413(3):369-387. doi:10.1042/BJ20080709

67. Wilson KA, Han Y, Zhang M, et al. Inter-relations between 3-hydroxypropionate and propionate metabolism in rat liver: relevance to disorders of propionyl-CoA metabolism. *Am J Physiol - Endocrinol Metab*. 2017;313(4):E413-E428. doi:10.1152/ajpendo.00105.2017

68. Encyclopedia of the Human Brain - 1st Edition | Elsevier Shop. Accessed April 12, 2024. https://shop.elsevier.com/books/encyclopedia-of-the-human-brain/ramachandran/978-0-08-054803-6

69. Kuo CC, Wu JY, Wu KK. Cancer-derived extracellular succinate: a driver of cancer metastasis. *J Biomed Sci*. 2022;29(1):93. doi:10.1186/s12929-022-00878-z

70. Selak MA, Armour SM, MacKenzie ED, et al. Succinate links TCA cycle dysfunction to oncogenesis by inhibiting HIF-alpha prolyl hydroxylase. *Cancer Cell*. 2005;7(1):77-85. doi:10.1016/j.ccr.2004.11.022

71. Reddy A, Bozi LHM, Yaghi OK, et al. pH-Gated Succinate Secretion Regulates Muscle Remodeling in Response to Exercise. *Cell*. 2020;183(1):62-75.e17. doi:10.1016/j.cell.2020.08.039

72. Mizuarai S, Miki S, Araki H, Takahashi K, Kotani H. Identification of dicarboxylate carrier Slc25a10 as malate transporter in de novo fatty acid synthesis. *J Biol Chem*. 2005;280(37):32434-32441. doi:10.1074/jbc.M503152200

73. Huypens P, Pillai R, Sheinin T, et al. The dicarboxylate carrier plays a role in mitochondrial malate transport and in the regulation of glucose-stimulated insulin secretion from rat pancreatic beta cells. *Diabetologia*. 2011;54(1):135-145. doi:10.1007/s00125-010-1923-5

74. Shoshan-Barmatz V, Ben-Hail D. VDAC, a multi-functional mitochondrial protein as a pharmacological target. *Mitochondrion*. 2012;12(1):24-34. doi:10.1016/j.mito.2011.04.001

75. Murphy MP, O'Neill LAJ. Krebs Cycle Reimagined: The Emerging Roles of Succinate and Itaconate as Signal Transducers. *Cell*. 2018;174(4):780-784. doi:10.1016/j.cell.2018.07.030

76. Mills EL, Kelly B, Logan A, et al. Succinate Dehydrogenase Supports Metabolic Repurposing of Mitochondria to Drive Inflammatory Macrophages. *Cell*. 2016;167(2):457-470.e13. doi:10.1016/j.cell.2016.08.064

77. Semenza GL. Hypoxia-Inducible Factors in Physiology and Medicine. *Cell*. 2012;148(3):399-408. doi:10.1016/j.cell.2012.01.021

78. Epstein AC, Gleadle JM, McNeill LA, et al. C. elegans EGL-9 and mammalian homologs define a family of dioxygenases that regulate HIF by prolyl hydroxylation. *Cell*. 2001;107(1):43-54. doi:10.1016/s0092-8674(01)00507-4

79. Koivunen P, Hirsilä M, Remes AM, Hassinen IE, Kivirikko KI, Myllyharju J. Inhibition of hypoxia-inducible factor (HIF) hydroxylases by citric acid cycle intermediates: possible links between cell metabolism and stabilization of HIF. *J Biol Chem*. 2007;282(7):4524-4532. doi:10.1074/jbc.M610415200

80. Watts ER, Walmsley SR. Inflammation and Hypoxia: HIF and PHD Isoform Selectivity. *Trends Mol Med*. 2019;25(1):33-46. doi:10.1016/j.molmed.2018.10.006

81. Yang Q, Liu R, Yu Q, Bi Y, Liu G. Metabolic regulation of inflammasomes in inflammation. *Immunology*. 2019;157(2):95-109. doi:10.1111/imm.13056

82. Li Y, Zheng JY, Liu JQ, et al. Succinate/NLRP3 Inflammasome Induces Synovial Fibroblast Activation: Therapeutical Effects of Clematichinenoside AR on Arthritis. *Front Immunol*. 2016;7:532. doi:10.3389/fimmu.2016.00532

83. Cervera AM, Bayley JP, Devilee P, McCreath KJ. Inhibition of succinate dehydrogenase dysregulates histone modification in mammalian cells. *Mol Cancer*. 2009;8:89. doi:10.1186/1476-4598-8-89

84. Xiao M, Yang H, Xu W, et al. Inhibition of α-KG-dependent histone and DNA demethylases by fumarate and succinate that are accumulated in mutations of FH and SDH tumor suppressors. *Genes Dev*. 2012;26(12):1326-1338. doi:10.1101/gad.191056.112

85. Deng YH, Zhang XX, Tao CY, et al. Succinylation profiles of brain injury after intracerebral hemorrhage. *PLOS ONE*. 2021;16(11):e0259798. doi:10.1371/journal.pone.0259798

86. Wang H, Lu J, Gao WC, et al. Donepezil down-regulates propionylation, 2-hydroxyisobutyrylation, butyrylation, succinylation, and crotonylation in the brain of bilateral common carotid artery occlusion-induced vascular dementia rats. *Clin Exp Pharmacol Physiol*. 2020;47(10):1731-1739. doi:10.1111/1440-1681.13352

87. Zhou B, Du Y, Xue Y, Miao G, Wei T, Zhang P. Identification of Malonylation, Succinylation, and Glutarylation in Serum Proteins of Acute Myocardial Infarction Patients. *Proteomics Clin Appl*. 2020;14(1):e1900103. doi:10.1002/prca.201900103

88. Ye J, Li J. First analyses of lysine succinylation proteome and overlap between succinylation and acetylation in Solenopsis invicta Buren (Hymenoptera: Formicidae). *BMC Genomics*. 2022;23(1):61. doi:10.1186/s12864-021-08285-8

89. Huang Z, He L, Sang W, Wang L, Huang Q, Lei C. Potential role of lysine succinylation in the response of moths to artificial light at night stress. *Ecotoxicol Environ Saf*. 2021;220:112334. doi:10.1016/j.ecoenv.2021.112334

90. Zhao G, Zhen J, Liu X, et al. Protein post-translational modification by lysine succinylation: Biochemistry, biological implications, and therapeutic opportunities. *Genes Dis*. 2022;10(4):1242-1262. doi:10.1016/j.gendis.2022.03.009

91. Xu H, Wu M, Ma X, Huang W, Xu Y. Function and Mechanism of Novel Histone Posttranslational Modifications in Health and Disease. *BioMed Res Int*. 2021;2021:6635225. doi:10.1155/2021/6635225

92. Smestad J, Erber L, Chen Y, Maher LJ. Chromatin Succinylation Correlates with Active Gene Expression and Is Perturbed by Defective TCA Cycle Metabolism. *iScience*. 2018;2:63-75. doi:10.1016/j.isci.2018.03.012

93. Yokoyama A, Katsura S, Sugawara A. Biochemical Analysis of Histone Succinylation. *Biochem Res Int*. 2017;2017:8529404. doi:10.1155/2017/8529404

94. Wang Y, Guo YR, Xing D, Tao YJ, Lu Z. Supramolecular assembly of KAT2A with succinyl-CoA for histone succinylation. *Cell Discov*. 2018;4(1):1-4. doi:10.1038/s41421-018-0048-8

95. Rardin MJ, He W, Nishida Y, et al. SIRT5 regulates the mitochondrial lysine succinylome and metabolic networks. *Cell Metab*. 2013;18(6):920-933. doi:10.1016/j.cmet.2013.11.013

96. Smith BJ, Brandão-Teles C, Zuccoli GS, et al. Protein Succinylation and Malonylation as Potential Biomarkers in Schizophrenia. *J Pers Med*. 2022;12(9):1408. doi:10.3390/jpm12091408

97. Ning Q, Ma Z, Zhao X, Yin M. SSKM_Succ: A Novel Succinylation Sites Prediction Method Incorporating K-Means Clustering With a New Semi-Supervised Learning Algorithm. *IEEE/ACM Trans Comput Biol Bioinform*. 2022;19(1):643-652. doi:10.1109/TCBB.2020.3006144

98. Yang Y, Tapias V, Acosta D, et al. Altered succinylation of mitochondrial proteins, APP and tau in Alzheimer's disease. *Nat Commun*. 2022;13(1):159. doi:10.1038/s41467-021-27572-2

99. Zhong Q, Xiao X, Qiu Y, et al. Protein posttranslational modifications in health and diseases: Functions, regulatory mechanisms, and therapeutic implications. *MedComm*. 2023;4(3):e261. doi:10.1002/mco2.261

100. Sreedhar A, Wiese EK, Hitosugi T. Enzymatic and metabolic regulation of lysine succinylation. *Genes Dis*. 2019;7(2):166-171. doi:10.1016/j.gendis.2019.09.011

101. Anzai N, Kanai Y, Endou H. Organic anion transporter family: current knowledge. *J Pharmacol Sci*. 2006;100(5):411-426. doi:10.1254/jphs.crj06006x

102. Pajor AM. Sodium-coupled dicarboxylate and citrate transporters from the SLC13 family. *Pflugers Arch*. 2014;466(1):119-130. doi:10.1007/s00424-013-1369-y

103. Khamaysi A, Anbtawee-Jomaa S, Fremder M, et al. Systemic Succinate Homeostasis and Local Succinate Signaling Affect Blood Pressure and Modify Risks for Calcium Oxalate Lithogenesis. *J Am Soc Nephrol JASN*. 2019;30(3):381-392. doi:10.1681/ASN.2018030277

104. Bento JL, Palmer ND, Zhong M, et al. Heterogeneity in gene loci associated with type 2 diabetes on human chromosome 20q13.1. *Genomics*. 2008;92(4):226-234. doi:10.1016/j.ygeno.2008.06.004

105. Nigam SK. The SLC22 Transporter Family: A Paradigm for the Impact of Drug Transporters on Metabolic Pathways, Signaling, and Disease. *Annu Rev Pharmacol Toxicol*. 2018;58:663-687. doi:10.1146/annurev-pharmtox-010617-052713

106. Lozano E, Briz O, Macias RIR, Serrano MA, Marin JJG, Herraez E. Genetic Heterogeneity of SLC22 Family of Transporters in Drug Disposition. *J Pers Med*. 2018;8(2):14. doi:10.3390/jpm8020014

107. Schumann T, König J, Henke C, et al. Solute Carrier Transporters as Potential Targets for the Treatment of Metabolic Disease. *Pharmacol Rev*. 2020;72(1):343-379. doi:10.1124/pr.118.015735

108. Peruzzotti-Jametti L, Bernstock JD, Vicario N, et al. Macrophage-Derived Extracellular Succinate Licenses Neural Stem Cells to Suppress Chronic Neuroinflammation. *Cell Stem Cell*. 2018;22(3):355-368.e13. doi:10.1016/j.stem.2018.01.020

109. Mills EL, Pierce KA, Jedrychowski MP, et al. Accumulation of succinate controls activation of adipose tissue thermogenesis. *Nature*. 2018;560(7716):102-106. doi:10.1038/s41586-018-0353-2

110. Hochachka PW, Dressendorfer RH. Succinate accumulation in man during exercise. *Eur J Appl Physiol*. 1976;35(4):235-242. doi:10.1007/BF00423282

111. Astiarraga B, Martínez L, Ceperuelo-Mallafré V, et al. Impaired Succinate Response to a Mixed Meal in Obesity and Type 2 Diabetes Is Normalized After Metabolic Surgery. *Diabetes Care*. 2020;43(10):2581-2587. doi:10.2337/dc20-0460

112. Shrestha A, Müllner E, Poutanen K, Mykkänen H, Moazzami AA. Metabolic changes in serum metabolome in response to a meal. *Eur J Nutr*. 2017;56(2):671-681. doi:10.1007/s00394-015-1111-y

113. Liu K, Lin L, Li Q, et al. Scd1 controls de novo beige fat biogenesis through succinate-dependent regulation of mitochondrial complex II. *Proc Natl Acad Sci*. 2020;117(5):2462-2472. doi:10.1073/pnas.1914553117

114. Ives SJ, Zaleski KS, Slocum C, et al. The effect of succinic acid on the metabolic profile in high-fat diet-induced obesity and insulin resistance. *Physiol Rep*. 2020;8(21):e14630. doi:10.14814/phy2.14630

115. Sadagopan N, Li W, Roberds SL, et al. Circulating succinate is elevated in rodent models of hypertension and metabolic disease. *Am J Hypertens*. 2007;20(11):1209-1215. doi:10.1016/j.amjhyper.2007.05.010

116. Ozturk BE. Understanding Ischemic Retinopathies: The Role of Succinate and Its Receptor in Retinal Pigment Epithelium. *Adv Exp Med Biol*. 2023;1415:527-531. doi:10.1007/978-3-031-27681-1_77

117. Yan XL, Liu XC, Zhang YN, et al. Succinate aggravates intestinal injury in mice with necrotizing enterocolitis. *Front Cell Infect Microbiol*. 2022;12:1064462. doi:10.3389/fcimb.2022.1064462

118. Osuna-Prieto FJ, Martinez-Tellez B, Ortiz-Alvarez L, et al. Elevated plasma succinate levels are linked to higher cardiovascular disease risk factors in young adults. *Cardiovasc Diabetol*. 2021;20:151. doi:10.1186/s12933-021-01333-3

119. Correa PRAV, Kruglov EA, Thompson M, Leite MF, Dranoff JA, Nathanson MH. Succinate is a paracrine signal for liver damage. *J Hepatol*. 2007;47(2):262-269. doi:10.1016/j.jhep.2007.03.016

120. Mills EL, Harmon C, Jedrychowski MP, et al. UCP1 governs liver extracellular succinate and inflammatory pathogenesis. *Nat Metab*. 2021;3(5):604-617. doi:10.1038/s42255-021-00389-5

121. Nguyen G, Park SY, Le CT, Park WS, Choi DH, Cho EH. Metformin ameliorates activation of hepatic stellate cells and hepatic fibrosis by succinate and GPR91 inhibition. *Biochem Biophys Res Commun*. 2018;495(4):2649-2656. doi:10.1016/j.bbrc.2017.12.143

122. Ceperuelo-Mallafré V, Llauradó G, Keiran N, et al. Preoperative Circulating Succinate Levels as a Biomarker for Diabetes Remission After Bariatric Surgery. *Diabetes Care*. 2019;42(10):1956-1965. doi:10.2337/dc19-0114

123. Liu L, Liu L, Wang J, Zheng Q, Jin B, Sun L. Differentiation of gestational diabetes mellitus by nuclear magnetic resonance-based metabolic plasma analysis. *J Biomed Res*. 2021;35(5):351-360. doi:10.7555/JBR.35.20200191

124. Rawat A, Misra G, Saxena M, et al. 1H NMR based serum metabolic profiling reveals differentiating biomarkers in patients with diabetes and diabetes-related complication. *Diabetes Metab Syndr*. 2019;13(1):290-298. doi:10.1016/j.dsx.2018.09.009

125. Park S, Kim OH, Lee K, et al. Plasma and urinary extracellular vesicle microRNAs and their related pathways in diabetic kidney disease. *Genomics*. 2022;114(4):110407. doi:10.1016/j.ygeno.2022.110407

126. Hu J, Li T, Du X, Wu Q, Le YZ. G protein-coupled receptor 91 signaling in diabetic retinopathy and hypoxic retinal diseases. *Vision Res*. 2017;139:59-64. doi:10.1016/j.visres.2017.05.001

127. Younossi ZM, Marchesini G, Pinto-Cortez H, Petta S. Epidemiology of Nonalcoholic Fatty Liver Disease and Nonalcoholic Steatohepatitis: Implications for Liver Transplantation. *Transplantation*. 2019;103(1):22-27. doi:10.1097/TP.0000000000002484

128. Chashmniam S, Ghafourpour M, Farimani AR, Gholami A, Ghoochani BFNM. Metabolomic Biomarkers in the Diagnosis of Non-Alcoholic Fatty Liver Disease. *Hepat Mon*. 2019;19(9). doi:10.5812/hepatmon.92244

129. Deen PMT, Robben JH. Succinate receptors in the kidney. *J Am Soc Nephrol JASN*. 2011;22(8):1416-1422. doi:10.1681/ASN.2010050481

130. Pu M, Zhang J, Hong F, et al. The pathogenic role of succinate-SUCNR1: a critical function that induces renal fibrosis via M2 macrophage. *Cell Commun Signal CCS*. 2024;22(1):78. doi:10.1186/s12964-024-01481-5

131. Pu M, Zhang J, Zeng Y, et al. Succinate-SUCNR1 induces renal tubular cell apoptosis. *Am J Physiol-Cell Physiol*. 2023;324(2):C467-C476. doi:10.1152/ajpcell.00327.2022

132. Kato K, Matsubara T, Sakamoto N. Correlation between myocardial blood flow and tissue succinate during acute ischemia. *Nagoya J Med Sci*. 1994;57(1-4):43-50.

133. Chen L, Huang M. Oncometabolites in cancer: from cancer cells to the tumor microenvironment. *Holist Integr Oncol*. 2024;3(1):26. doi:10.1007/s44178-024-00096-7

134. Hobert JA, Mester JL, Moline J, Eng C. Elevated plasma succinate in PTEN, SDHB, and SDHD mutation-positive individuals. *Genet Med Off J Am Coll Med Genet*. 2012;14(6):616-619. doi:10.1038/gim.2011.63

135. Aghamir SMK, Heshmat R, Ebrahimi M, Ketabchi SE, Parichehreh Dizaji S, Khatami F. The Impact Of Succinate Dehydrogenase Gene (SDH) Mutations In Renal Cell Carcinoma (RCC): A Systematic Review. *OncoTargets Ther*. 2019;12(null):7929-7940. doi:10.2147/OTT.S207460

136. Ibrahim A, Chopra S. Succinate Dehydrogenase–Deficient Gastrointestinal Stromal Tumors. *Arch Pathol Lab Med*. 2019;144(5):655-660. doi:10.5858/arpa.2018-0370-RS

137. Letouzé E, Martinelli C, Loriot C, et al. SDH Mutations Establish a Hypermethylator Phenotype in Paraganglioma. *Cancer Cell*. 2013;23(6):739-752. doi:10.1016/j.ccr.2013.04.018

138. Xiao Z, Liu S, Ai F, et al. SDHB downregulation facilitates the proliferation and invasion of colorectal cancer through AMPK functions excluding those involved in the modulation of aerobic glycolysis. *Exp Ther Med*. 2018;15(1):864-872. doi:10.3892/etm.2017.5482

139. Sciacovelli M, Guzzo G, Morello V, et al. The mitochondrial chaperone TRAP1 promotes neoplastic growth by inhibiting succinate dehydrogenase. *Cell Metab*. 2013;17(6):988-999. doi:10.1016/j.cmet.2013.04.019

140. Wu JY, Huang TW, Hsieh YT, et al. Cancer-Derived Succinate Promotes Macrophage Polarization and Cancer Metastasis via Succinate Receptor. *Mol Cell*. 2020;77(2):213-227.e5. doi:10.1016/j.molcel.2019.10.023

141. Terra X, Ceperuelo-Mallafré V, Merma C, et al. Succinate Pathway in Head and Neck Squamous Cell Carcinoma: Potential as a Diagnostic and Prognostic Marker. *Cancers*. 2021;13(7):1653. doi:10.3390/cancers13071653

142. Wittenberger T, Schaller HC, Hellebrand S. An expressed sequence tag (EST) data mining strategy succeeding in the discovery of new G-protein coupled receptors. *J Mol Biol*. 2001;307(3):799-813. doi:10.1006/jmbi.2001.4520

143. Aguiar CJ, Andrade VL, Gomes ERM, et al. Succinate modulates Ca(2+) transient and cardiomyocyte viability through PKA-dependent pathway. *Cell Calcium*. 2010;47(1):37-46. doi:10.1016/j.ceca.2009.11.003

144. Fasciani I, Carli M, Petragnano F, et al. GPCRs in Intracellular Compartments: New Targets for Drug Discovery. *Biomolecules*. 2022;12(10):1343. doi:10.3390/biom12101343

145. Sanchez M, Hamel D, Bajon E, et al. The Succinate Receptor SUCNR1 Resides at the Endoplasmic Reticulum and Relocates to the Plasma Membrane in Hypoxic Conditions. *Cells*. 2022;11(14):2185. doi:10.3390/cells11142185

146. Krzak G, Willis CM, Smith JA, Pluchino S, Peruzzotti-Jametti L. Succinate Receptor 1: An Emerging Regulator of Myeloid Cell Function in Inflammation. *Trends Immunol*. 2021;42(1):45-58. doi:10.1016/j.it.2020.11.004

147. Katritch V, Cherezov V, Stevens RC. Structure-function of the G protein-coupled receptor superfamily. *Annu Rev Pharmacol Toxicol*. 2013;53:531-556. doi:10.1146/annurev-pharmtox-032112-135923

148. Gilissen J, Jouret F, Pirotte B, Hanson J. Insight into SUCNR1 (GPR91) structure and function. *Pharmacol Ther*. 2016;159:56-65. doi:10.1016/j.pharmthera.2016.01.008

149. Zhang J, Zhang K, Gao ZG, et al. Agonist-bound structure of the human P2Y12 receptor. *Nature*. 2014;509(7498):119-122. doi:10.1038/nature13288

150. Zhang D, Gao ZG, Zhang K, et al. Two disparate ligand-binding sites in the human P2Y1 receptor. *Nature*. 2015;520(7547):317-321. doi:10.1038/nature14287

151. Yang D, Zhou Q, Labroska V, et al. G protein-coupled receptors: structure- and function-based drug discovery. *Signal Transduct Target Ther*. 2021;6(1):7. doi:10.1038/s41392-020-00435-w

152. Hilger D, Masureel M, Kobilka BK. Structure and dynamics of GPCR signaling complexes. *Nat Struct Mol Biol*. 2018;25(1):4-12. doi:10.1038/s41594-017-0011-7

153. Schneider J, Korshunova K, Musiani F, Alfonso-Prieto M, Giorgetti A, Carloni P. Predicting ligand binding poses for low-resolution membrane protein models: Perspectives from multiscale simulations. *Biochem Biophys Res Commun*. 2018;498(2):366-374. doi:10.1016/j.bbrc.2018.01.160

154. Zhong X, Kriz R, Seehra J, Kumar R. N-linked glycosylation of platelet P2Y12 ADP receptor is essential for signal transduction but not for ligand binding or cell surface expression. *FEBS Lett*. 2004;562(1-3):111-117. doi:10.1016/S0014-5793(04)00191-7

155. Geubelle P, Gilissen J, Dilly S, et al. Identification and pharmacological characterization of succinate receptor agonists. *Br J Pharmacol*. 2017;174(9):796-808. doi:10.1111/bph.13738

156. Bhuniya D, Umrani D, Dave B, et al. Discovery of a potent and selective small molecule hGPR91 antagonist. *Bioorg Med Chem Lett*. 2011;21(12):3596-3602. doi:10.1016/j.bmcl.2011.04.091

157. Haffke M, Fehlmann D, Rummel G, et al. Structural basis of species-selective antagonist binding to the succinate receptor. *Nature*. 2019;574(7779):581-585. doi:10.1038/s41586-019-1663-8

158. Pierce KL, Premont RT, Lefkowitz RJ. Seven-transmembrane receptors. *Nat Rev Mol Cell Biol*. 2002;3(9):639-650. doi:10.1038/nrm908

159. Calebiro D, Koszegi Z, Lanoiselée Y, Miljus T, O'Brien S. G protein-coupled receptor-G protein interactions: a single-molecule perspective. *Physiol Rev*. 2021;101(3):857-906. doi:10.1152/physrev.00021.2020

160. Peterson YK, Luttrell LM. The Diverse Roles of Arrestin Scaffolds in G Protein-Coupled Receptor Signaling. *Pharmacol Rev*. 2017;69(3):256-297. doi:10.1124/pr.116.013367

161. Xu Z, Shao Z. Dynamic mechanism of GPCR-mediated β-arrestin: a potential therapeutic agent discovery of biased drug. *Signal Transduct Target Ther*. 2022;7(1):283. doi:10.1038/s41392-022-01140-6

162. Kohout TA, Lefkowitz RJ. Regulation of G protein-coupled receptor kinases and arrestins during receptor desensitization. *Mol Pharmacol*. 2003;63(1):9-18. doi:10.1124/mol.63.1.9

163. Lefkowitz RJ, Shenoy SK. Transduction of receptor signals by beta-arrestins. *Science*. 2005;308(5721):512-517. doi:10.1126/science.1109237

164. Yang L, Yu D, Fan HH, et al. Triggering the succinate receptor GPR91 enhances pressure overload-induced right ventricular hypertrophy. *Int J Clin Exp Pathol*. 2014;7(9):5415-5428.

165. Montano MM, Desjardins CL, Doughman YQ, et al. Inducible re-expression of HEXIM1 causes physiological cardiac hypertrophy in the adult mouse. *Cardiovasc Res*. 2013;99(1):74-82. doi:10.1093/cvr/cvt086

166. Li YH, Woo SH, Choi DH, Cho EH. Succinate causes α-SMA production through GPR91 activation in hepatic stellate cells. *Biochem Biophys Res Commun*. 2015;463(4):853-858. doi:10.1016/j.bbrc.2015.06.023

167. Thor D. G protein-coupled receptors as regulators of pancreatic islet functionality. *Biochim Biophys Acta Mol Cell Res*. 2022;1869(5):119235. doi:10.1016/j.bbamcr.2022.119235

168. Seino S, Sugawara K, Yokoi N, Takahashi H. β-Cell signalling and insulin secretagogues: A path for improved diabetes therapy. *Diabetes Obes Metab*. 2017;19 Suppl 1:22-29. doi:10.1111/dom.12995

169. Gilissen J, Geubelle P, Dupuis N, Laschet C, Pirotte B, Hanson J. Forskolin-free cAMP assay for Gi-coupled receptors. *Biochem Pharmacol*. 2015;98(3):381-391. doi:10.1016/j.bcp.2015.09.010

170. Sundström L, Greasley PJ, Engberg S, Wallander M, Ryberg E. Succinate receptor GPR91, a Gα(i) coupled receptor that increases intracellular calcium concentrations through PLCβ. *FEBS Lett*. 2013;587(15):2399-2404. doi:10.1016/j.febslet.2013.05.067

171. Trauelsen M, Hiron TK, Lin D, et al. Extracellular succinate hyperpolarizes M2 macrophages through SUCNR1/GPR91-mediated Gq signaling. *Cell Rep*. 2021;35(11):109246. doi:10.1016/j.celrep.2021.109246

172. Tang X, Rönnberg E, Säfholm J, et al. Activation of succinate receptor 1 boosts human mast cell reactivity and allergic bronchoconstriction. *Allergy*. 2022;77(9):2677-2687. doi:10.1111/all.15245

173. Mancini AD, Poitout V. The fatty acid receptor FFA1/GPR40 a decade later: how much do we know? *Trends Endocrinol Metab TEM*. 2013;24(8):398-407. doi:10.1016/j.tem.2013.03.003

174. Itoh Y, Kawamata Y, Harada M, et al. Free fatty acids regulate insulin secretion from pancreatic beta cells through GPR40. *Nature*. 2003;422(6928):173-176. doi:10.1038/nature01478

175. Li T, Hu J, Du S, Chen Y, Wang S, Wu Q. ERK1/2/COX-2/PGE2 signaling pathway mediates GPR91-dependent VEGF release in streptozotocin-induced diabetes. *Mol Vis*. 2014;20:1109-1121.

176. Hakak Y, Lehmann-Bruinsma K, Phillips S, et al. The role of the GPR91 ligand succinate in hematopoiesis. *J Leukoc Biol*. 2009;85(5):837-843. doi:10.1189/jlb.1008618

177. Högberg C, Gidlöf O, Tan C, et al. Succinate independently stimulates full platelet activation via cAMP and phosphoinositide 3-kinase-β signaling. *J Thromb Haemost*. 2011;9(2):361-372. doi:10.1111/j.1538-7836.2010.04158.x

178. Ariza AC, Deen PMT, Robben JH. The Succinate Receptor as a Novel Therapeutic Target for Oxidative and Metabolic Stress-Related Conditions. *Front Endocrinol*. 2012;3:22. doi:10.3389/fendo.2012.00022

179. Ryan DG, Murphy MP, Frezza C, et al. Coupling Krebs cycle metabolites to signalling in immunity and cancer. *Nat Metab*. 2019;1:16-33. doi:10.1038/s42255-018-0014-7

180. Fremder M, Kim SW, Khamaysi A, et al. A transepithelial pathway delivers succinate to macrophages, thus perpetuating their pro-inflammatory metabolic state. *Cell Rep*. 2021;36(6):109521. doi:10.1016/j.celrep.2021.109521

181. Trauelsen M, Rexen Ulven E, Hjorth SA, et al. Receptor structure-based discovery of non-metabolite agonists for the succinate receptor GPR91. *Mol Metab*. 2017;6(12):1585-1596. doi:10.1016/j.molmet.2017.09.005

182. Mauer J, Chaurasia B, Goldau J, et al. Signaling by IL-6 promotes alternative activation of macrophages to limit endotoxemia and obesity-associated resistance to insulin. *Nat Immunol*. 2014;15(5):423-430. doi:10.1038/ni.2865

183. Gudgeon N, Munford H, Bishop EL, et al. Succinate uptake by T cells suppresses their effector function via inhibition of mitochondrial glucose oxidation. *Cell Rep*. 2022;40(7):111193. doi:10.1016/j.celrep.2022.111193

184. Nastasi C, Willerlev-Olsen A, Dalhoff K, et al. Inhibition of succinate dehydrogenase activity impairs human T cell activation and function. *Sci Rep*. 2021;11(1):1458. doi:10.1038/s41598-020-80933-7

185. Li H, Tan H, Liu Z, et al. Succinic acid exacerbates experimental autoimmune uveitis by stimulating neutrophil extracellular traps formation via SUCNR1 receptor. *Br J Ophthalmol*. 2023;107(11):1744-1749. doi:10.1136/bjophthalmol-2021-320880

186. Saltiel AR, Olefsky JM. Inflammatory mechanisms linking obesity and metabolic disease. *J Clin Invest*. 2017;127(1):1-4. doi:10.1172/JCI92035

187. Lei W, Ren W, Ohmoto M, et al. Activation of intestinal tuft cell-expressed Sucnr1 triggers type 2 immunity in the mouse small intestine. *Proc Natl Acad Sci U S A*. 2018;115(21):5552-5557. doi:10.1073/pnas.1720758115

188. Chakrabarti P, Kim JY, Singh M, et al. Insulin Inhibits Lipolysis in Adipocytes via the Evolutionarily Conserved mTORC1-Egr1-ATGL-Mediated Pathway. *Mol Cell Biol*. 2013;33(18):3659-3666. doi:10.1128/MCB.01584-12

189. Chouchani ET, Kazak L, Spiegelman BM. New Advances in Adaptive Thermogenesis: UCP1 and Beyond. *Cell Metab*. 2019;29(1):27-37. doi:10.1016/j.cmet.2018.11.002

190. Diehl J, Gries B, Pfeil U, et al. Expression and localization of GPR91 and GPR99 in murine organs. *Cell Tissue Res*. 2016;364(2):245-262. doi:10.1007/s00441-015-2318-1

191. Nadjsombati MS, McGinty JW, Lyons-Cohen MR, et al. Detection of Succinate by Intestinal Tuft Cells Triggers a Type 2 Innate Immune Circuit. *Immunity*. 2018;49(1):33-41.e7. doi:10.1016/j.immuni.2018.06.016

192. Saoi M, Percival M, Nemr C, Li A, Gibala M, Britz-McKibbin P. Characterization of the Human Skeletal Muscle Metabolome for Elucidating the Mechanisms of Bicarbonate Ingestion on Strenuous Interval Exercise. *Anal Chem*. 2019;91(7):4709-4718. doi:10.1021/acs.analchem.9b00149

193. Huffman KM, Koves TR, Hubal MJ, et al. Metabolite signatures of exercise training in human skeletal muscle relate to mitochondrial remodelling and cardiometabolic fitness. *Diabetologia*. 2014;57(11):2282-2295. doi:10.1007/s00125-014-3343-4

194. Wang T, Xu YQ, Yuan YX, et al. Succinate induces skeletal muscle fiber remodeling via SUNCR1 signaling. *EMBO Rep*. 2019;20(9):e47892. doi:10.15252/embr.201947892

195. Xu G, Yuan Y, Luo P, et al. Acute Succinate Administration Increases Oxidative Phosphorylation and Skeletal Muscle Explosive Strength via SUCNR1. *Front Vet Sci*. 2022;8:808863. doi:10.3389/fvets.2021.808863

196. Guo Y, Cho SW, Saxena D, Li X. Multifaceted Actions of Succinate as a Signaling Transmitter Vary with Its Cellular Locations. *Endocrinol Metab*. 2020;35(1):36-43. doi:10.3803/EnM.2020.35.1.36

197. Abdelmoez AM, Dmytriyeva O, Zurke YX, et al. Cell selectivity in succinate receptor SUCNR1/GPR91 signaling in skeletal muscle. *Am J Physiol Endocrinol Metab*. 2023;324(4):E289-E298. doi:10.1152/ajpendo.00009.2023

198. Emont MP, Jacobs C, Essene AL, et al. A single-cell atlas of human and mouse white adipose tissue. *Nature*. 2022;603(7903):926-933. doi:10.1038/s41586-022-04518-2

199. Ghesmati Z, Rashid M, Fayezi S, Gieseler F, Alizadeh E, Darabi M. An update on the secretory functions of brown, white, and beige adipose tissue: Towards therapeutic applications. *Rev Endocr Metab Disord*. 2024;25(2):279-308. doi:10.1007/s11154-023-09850-0

200. Richard AJ, White U, Elks CM, Stephens JM. Adipose Tissue: Physiology to Metabolic Dysfunction. In: Feingold KR, Anawalt B, Blackman MR, et al., eds. *Endotext*. MDText.com, Inc.; 2000. Accessed July 17, 2024. http://www.ncbi.nlm.nih.gov/books/NBK555602/

201. Lee JH, Park A, Oh KJ, Lee SC, Kim WK, Bae KH. The Role of Adipose Tissue Mitochondria: Regulation of Mitochondrial Function for the Treatment of Metabolic Diseases. *Int J Mol Sci*. 2019;20(19):4924. doi:10.3390/ijms20194924

202. Scherer PE. Adipose tissue: from lipid storage compartment to endocrine organ. *Diabetes*. 2006;55(6):1537-1545. doi:10.2337/db06-0263

203. Zhang Y, Proenca R, Maffei M, Barone M, Leopold L, Friedman JM. Positional cloning of the mouse obese gene and its human homologue. *Nature*. 1994;372(6505):425-432. doi:10.1038/372425a0

204. Liu X, Zhang Z, Song Y, Xie H, Dong M. An update on brown adipose tissue and obesity intervention: Function, regulation and therapeutic implications. *Front Endocrinol*. 2023;13:1065263. doi:10.3389/fendo.2022.1065263

205. Carobbio S, Pellegrinelli V, Vidal-Puig A. Adipose Tissue Function and Expandability as Determinants of Lipotoxicity and the Metabolic Syndrome. *Adv Exp Med Biol*. 2017;960:161-196. doi:10.1007/978-3-319-48382-5_7

206. Luo L, Liu M. Adipose tissue in control of metabolism. *J Endocrinol*. 2016;231(3):R77-R99. doi:10.1530/JOE-16-0211

207. Ziqubu K, Dludla PV, Mthembu SXH, et al. An insight into brown/beige adipose tissue whitening, a metabolic complication of obesity with the multifactorial origin. *Front Endocrinol*. 2023;14:1114767. doi:10.3389/fendo.2023.1114767

208. de Lange P, Lombardi A, Silvestri E, et al. Physiological Approaches Targeting Cellular and Mitochondrial Pathways Underlying Adipose Organ Senescence. *Int J Mol Sci*. 2023;24(14):11676. doi:10.3390/ijms241411676

209. Ikeda K, Maretich P, Kajimura S. The Common and Distinct Features of Brown and Beige Adipocytes. *Trends Endocrinol Metab TEM*. 2018;29(3):191-200. doi:10.1016/j.tem.2018.01.001

210. Emont MP, Rosen ED. Exploring the heterogeneity of white adipose tissue in mouse and man. *Curr Opin Genet Dev*. 2023;80:102045. doi:10.1016/j.gde.2023.102045

211. Avtanski D, Hadzi-Petrushev N, Josifovska S, Mladenov M, Reddy V. Emerging technologies in adipose tissue research. *Adipocyte*. 12(1):2248673. doi:10.1080/21623945.2023.2248673

212. Granneman JG, Li P, Zhu Z, Lu Y. Metabolic and cellular plasticity in white adipose tissue I: effects of beta3-adrenergic receptor activation. *Am J Physiol Endocrinol Metab*. 2005;289(4):E608-616. doi:10.1152/ajpendo.00009.2005

213. Medina-Gómez G. Mitochondria and endocrine function of adipose tissue. *Best Pract Res Clin Endocrinol Metab*. 2012;26(6):791-804. doi:10.1016/j.beem.2012.06.002

214. Cinti S. Transdifferentiation properties of adipocytes in the adipose organ. *Am J Physiol Endocrinol Metab*. 2009;297(5):E977-986. doi:10.1152/ajpendo.00183.2009

215. McNeill BT, Suchacki KJ, Stimson RH. MECHANISMS IN ENDOCRINOLOGY: Human brown adipose tissue as a therapeutic target: warming up or cooling down? *Eur J Endocrinol*. 2021;184(6):R243-R259. doi:10.1530/EJE-20-1439

216. Diaz MB, Herzig S, Vegiopoulos A. Thermogenic adipocytes: from cells to physiology and medicine. *Metabolism*. 2014;63(10):1238-1249. doi:10.1016/j.metabol.2014.07.002

217. Zwick RK, Guerrero-Juarez CF, Horsley V, Plikus MV. Anatomical, physiological and functional diversity of adipose tissue. *Cell Metab*. 2018;27(1):68-83. doi:10.1016/j.cmet.2017.12.002

218. Sharp LZ, Shinoda K, Ohno H, et al. Human BAT possesses molecular signatures that resemble beige/brite cells. *PloS One*. 2012;7(11):e49452. doi:10.1371/journal.pone.0049452

219. Rosenwald M, Perdikari A, Rülicke T, Wolfrum C. Bi-directional interconversion of brite and white adipocytes. *Nat Cell Biol*. 2013;15(6):659-667. doi:10.1038/ncb2740

220. Altshuler-Keylin S, Shinoda K, Hasegawa Y, et al. Beige Adipocyte Maintenance Is Regulated by Autophagy-Induced Mitochondrial Clearance. *Cell Metab*. 2016;24(3):402-419. doi:10.1016/j.cmet.2016.08.002

221. Friedenstein AJ, Petrakova KV, Kurolesova AI, Frolova GP. Heterotopic of bone marrow. Analysis of precursor cells for osteogenic and hematopoietic tissues. *Transplantation*. 1968;6(2):230-247.

222. da Silva Meirelles L, Chagastelles PC, Nardi NB. Mesenchymal stem cells reside in virtually all post-natal organs and tissues. *J Cell Sci*. 2006;119(Pt 11):2204-2213. doi:10.1242/jcs.02932

223. Zuk PA, Zhu M, Mizuno H, et al. Multilineage cells from human adipose tissue: implications for cell-based therapies. *Tissue Eng*. 2001;7(2):211-228. doi:10.1089/107632701300062859

224. Zuk PA, Zhu M, Ashjian P, et al. Human Adipose Tissue Is a Source of Multipotent Stem Cells. *Mol Biol Cell*. 2002;13(12):4279-4295. doi:10.1091/mbc.E02-02-0105

225. Badimon L, Cubedo J. Adipose tissue depots and inflammation: effects on plasticity and resident mesenchymal stem cell function. *Cardiovasc Res*. 2017;113(9):1064-1073. doi:10.1093/cvr/cvx096

226. Mimeault M, Hauke R, Batra SK. Stem cells: a revolution in therapeutics-recent advances in stem cell biology and their therapeutic applications in regenerative medicine and cancer therapies. *Clin Pharmacol Ther*. 2007;82(3):252-264. doi:10.1038/sj.clpt.6100301

227. Zimmerlin L, Donnenberg VS, Pfeifer ME, et al. Stromal vascular progenitors in adult human adipose tissue. *Cytom Part J Int Soc Anal Cytol*. 2010;77(1):22-30. doi:10.1002/cyto.a.20813

228. Nellinger S, Kluger PJ. How Mechanical and Physicochemical Material Characteristics Influence Adipose-Derived Stem Cell Fate. *Int J Mol Sci*. 2023;24(4):3551. doi:10.3390/ijms24043551

229. Farmer SR. Regulation of PPARgamma activity during adipogenesis. *Int J Obes 2005*. 2005;29 Suppl 1:S13-16. doi:10.1038/sj.ijo.0802907

230. Bruderer M, Richards RG, Alini M, Stoddart MJ. Role and regulation of RUNX2 in osteogenesis. *Eur Cell Mater*. 2014;28:269-286. doi:10.22203/ecm.v028a19

231. Yi SW, Kim HJ, Oh HJ, et al. Gene expression profiling of chondrogenic differentiation by dexamethasone-conjugated polyethyleneimine with SOX trio genes in stem cells. *Stem Cell Res Ther*. 2018;9(1):341. doi:10.1186/s13287-018-0998-7

232. Ahmad B, Vohra MS, Saleemi MA, Serpell CJ, Fong IL, Wong EH. Brown/Beige adipose tissues and the emerging role of their secretory factors in improving metabolic health: The batokines. *Biochimie*. 2021;184:26-39. doi:10.1016/j.biochi.2021.01.015

233. Sanchez-Gurmaches J, Hung CM, Sparks CA, Tang Y, Li H, Guertin DA. PTEN loss in the Myf5 lineage redistributes body fat and reveals subsets of white adipocytes that arise from Myf5 precursors. *Cell Metab*. 2012;16(3):348-362. doi:10.1016/j.cmet.2012.08.003

234. Lepper C, Fan CM. Inducible lineage tracing of Pax7-descendant cells reveals embryonic origin of adult satellite cells. *Genes N Y N 2000*. 2010;48(7):424-436. doi:10.1002/dvg.20630

235. Timmons JA, Wennmalm K, Larsson O, et al. Myogenic gene expression signature establishes that brown and white adipocytes originate from distinct cell lineages. *Proc Natl Acad Sci U S A*. 2007;104(11):4401-4406. doi:10.1073/pnas.0610615104

236. Bourgeois C, Gorwood J, Barrail-Tran A, et al. Specific Biological Features of Adipose Tissue, and Their Impact on HIV Persistence. *Front Microbiol*. 2019;10:2837. doi:10.3389/fmicb.2019.02837

237. Seydel KB, Milner DA, Kamiza SB, Molyneux ME, Taylor TE. The distribution and intensity of parasite sequestration in comatose Malawian children. *J Infect Dis*. 2006;194(2):208-205. doi:10.1086/505078

238. Rosen ED, MacDougald OA. Adipocyte differentiation from the inside out. *Nat Rev Mol Cell Biol*. 2006;7(12):885-896. doi:10.1038/nrm2066

239. Peirce V, Carobbio S, Vidal-Puig A. The different shades of fat. *Nature*. 2014;510(7503):76-83. doi:10.1038/nature13477

240. Gesta S, Tseng YH, Kahn CR. Developmental origin of fat: tracking obesity to its source. *Cell*. 2007;131(2):242-256. doi:10.1016/j.cell.2007.10.004

241. Tseng YH, Kokkotou E, Schulz TJ, et al. New role of bone morphogenetic protein 7 in brown adipogenesis and energy expenditure. *Nature*. 2008;454(7207):1000-1004. doi:10.1038/nature07221

242. Harms MJ, Ishibashi J, Wang W, et al. Prdm16 is required for the maintenance of brown adipocyte identity and function in adult mice. *Cell Metab*. 2014;19(4):593-604. doi:10.1016/j.cmet.2014.03.007

243. Wang W, Kissig M, Rajakumari S, et al. Ebf2 is a selective marker of brown and beige adipogenic precursor cells. *Proc Natl Acad Sci*. 2014;111(40):14466-14471. doi:10.1073/pnas.1412685111

244. Rui L. Brown and Beige Adipose Tissues in Health and Disease. *Compr Physiol*. 2017;7(4):1281-1306. doi:10.1002/cphy.c170001

245. Rosenwald M, Wolfrum C. The origin and definition of brite versus white and classical brown adipocytes. *Adipocyte*. 2014;3(1):4-9. doi:10.4161/adip.26232

246. Merlin J, Evans BA, Dehvari N, Sato M, Bengtsson T, Hutchinson DS. Could burning fat start with a brite spark? Pharmacological and nutritional ways to promote thermogenesis. *Mol Nutr Food Res*. 2016;60(1):18-42. doi:10.1002/mnfr.201500251

247. Lihua W, Yiran L, Feng H, Zhongyu Z. The potential mechanisms of white adipose tissue browning: a novel target for the treatment of obesity. *Nutr Hosp*. Published online 2022:411-424.

248. Rohm M, Sommerfeld A, Strzoda D, et al. Transcriptional cofactor TBLR1 controls lipid mobilization in white adipose tissue. *Cell Metab*. 2013;17(4):575-585. doi:10.1016/j.cmet.2013.02.010

249. Langin D. In and out: adipose tissue lipid turnover in obesity and dyslipidemia. *Cell Metab*. 2011;14(5):569-570. doi:10.1016/j.cmet.2011.10.003

250. Kershaw EE, Flier JS. Adipose tissue as an endocrine organ. *J Clin Endocrinol Metab*. 2004;89(6):2548-2556. doi:10.1210/jc.2004-0395

251. Yu YH, Ginsberg HN. Adipocyte signaling and lipid homeostasis: sequelae of insulin-resistant adipose tissue. *Circ Res*. 2005;96(10):1042-1052. doi:10.1161/01.RES.0000165803.47776.38

252. Trim WV, Lynch L. Immune and non-immune functions of adipose tissue leukocytes. *Nat Rev Immunol*. 2022;22(6):371-386. doi:10.1038/s41577-021-00635-7

253. Sakers A, De Siqueira MK, Seale P, Villanueva CJ. Adipose-tissue plasticity in health and disease. *Cell*. 2022;185(3):419-446. doi:10.1016/j.cell.2021.12.016

254. Chusyd DE, Wang D, Huffman DM, Nagy TR. Relationships between Rodent White Adipose Fat Pads and Human White Adipose Fat Depots. *Front Nutr*. 2016;3:10. doi:10.3389/fnut.2016.00010

255. Vitali A, Murano I, Zingaretti MC, Frontini A, Ricquier D, Cinti S. The adipose organ of obesity-prone C57BL/6J mice is composed of mixed white and brown adipocytes. *J Lipid Res*. 2012;53(4):619-629. doi:10.1194/jlr.M018846

256. Zhang M, Hu T, Zhang S, Zhou L. Associations of Different Adipose Tissue Depots with Insulin Resistance: A Systematic Review and Meta-analysis of Observational Studies. *Sci Rep*. 2015;5:18495. doi:10.1038/srep18495

257. Chait A, den Hartigh LJ. Adipose Tissue Distribution, Inflammation and Its Metabolic Consequences, Including Diabetes and Cardiovascular Disease. *Front Cardiovasc Med*. 2020;7:22. doi:10.3389/fcvm.2020.00022

258. Coelho M, Oliveira T, Fernandes R. Biochemistry of adipose tissue: an endocrine organ. *Arch Med Sci AMS*. 2013;9(2):191-200. doi:10.5114/aoms.2013.33181

259. Arner P. Differences in Lipolysis between Human Subcutaneous and Omental Adipose Tissues. *Ann Med*. Published online January 1, 1995. doi:10.3109/07853899709002451

260. Kwon H, Kim D, Kim JS. Body Fat Distribution and the Risk of Incident Metabolic Syndrome: A Longitudinal Cohort Study. *Sci Rep*. 2017;7(1):10955. doi:10.1038/s41598-017-09723-y

261. Powell-Wiley TM, Poirier CP, Burke VCLE, et al. Obesity and Cardiovascular Disease. *Circulation*. 2021;143(21):e984-e1010. doi:10.1161/CIR.0000000000000973

262. Hale LP. Histologic and molecular assessment of human thymus. *Ann Diagn Pathol*. 2004;8(1):50-60. doi:10.1016/j.anndiagpath.2003.11.006

263. Coín Aragüez L, Murri M, Oliva Olivera W, et al. Thymus fat as an attractive source of angiogenic factors in elderly subjects with myocardial ischemia. *Age Dordr Neth*. 2013;35(4):1263-1275. doi:10.1007/s11357-012-9418-6

264. Weisberg SP, McCann D, Desai M, Rosenbaum M, Leibel RL, Ferrante AW. Obesity is associated with macrophage accumulation in adipose tissue. *J Clin Invest*. 2003;112(12):1796-1808. doi:10.1172/JCI19246

265. Lumeng CN, Bodzin JL, Saltiel AR. Obesity induces a phenotypic switch in adipose tissue macrophage polarization. *J Clin Invest*. 2007;117(1):175-184. doi:10.1172/JCI29881

266. Ferrante AW. The immune cells in adipose tissue. *Diabetes Obes Metab*. 2013;15 Suppl 3(0 3):34-38. doi:10.1111/dom.12154

267. Lee MW, Odegaard JI, Mukundan L, et al. Activated type 2 innate lymphoid cells regulate beige fat biogenesis. *Cell*. 2015;160(1-2):74-87. doi:10.1016/j.cell.2014.12.011

268. Brestoff JR, Kim BS, Saenz SA, et al. Group 2 innate lymphoid cells promote beiging of white adipose tissue and limit obesity. *Nature*. 2015;519(7542):242-246. doi:10.1038/nature14115

269. Tang W, Zeve D, Suh JM, et al. White fat progenitor cells reside in the adipose vasculature. *Science*. 2008;322(5901):583-586. doi:10.1126/science.1156232

270. Spalding KL, Arner E, Westermark PO, et al. Dynamics of fat cell turnover in humans. *Nature*. 2008;453(7196):783-787. doi:10.1038/nature06902

271. Rigamonti A, Brennand K, Lau F, Cowan CA. Rapid cellular turnover in adipose tissue. *PloS One*. 2011;6(3):e17637. doi:10.1371/journal.pone.0017637

272. Cartier A, Lemieux I, Alméras N, Tremblay A, Bergeron J, Després JP. Visceral obesity and plasma glucose-insulin homeostasis: contributions of interleukin-6 and tumor necrosis factor-alpha in men. *J Clin Endocrinol Metab*. 2008;93(5):1931-1938. doi:10.1210/jc.2007-2191

273. Trayhurn P. Origins and early development of the concept that brown adipose tissue thermogenesis is linked to energy balance and obesity. *Biochimie*. 2017;134:62-70. doi:10.1016/j.biochi.2016.09.007

274. Aherne W, Hull D. Brown adipose tissue and heat production in the newborn infant. *J Pathol Bacteriol*. 1966;91(1):223-234. doi:10.1002/path.1700910126

275. Heaton JM. The distribution of brown adipose tissue in the human. *J Anat*. 1972;112(Pt 1):35-39.

276. Yeung HWD, Grewal RK, Gonen M, Schöder H, Larson SM. Patterns of (18)F-FDG uptake in adipose tissue and muscle: a potential source of false-positives for PET. *J Nucl Med Off Publ Soc Nucl Med*. 2003;44(11):1789-1796.

277. Virtanen KA, Lidell ME, Orava J, et al. Functional brown adipose tissue in healthy adults. *N Engl J Med*. 2009;360(15):1518-1525. doi:10.1056/NEJMoa0808949

278. van Marken Lichtenbelt WD, Vanhommerig JW, Smulders NM, et al. Cold-activated brown adipose tissue in healthy men. *N Engl J Med*. 2009;360(15):1500-1508. doi:10.1056/NEJMoa0808718

279. Cypess AM, Lehman S, Williams G, et al. Identification and importance of brown adipose tissue in adult humans. *N Engl J Med*. 2009;360(15):1509-1517. doi:10.1056/NEJMoa0810780

280. Carpentier AC, Blondin DP, Haman F, Richard D. Brown Adipose Tissue—A Translational Perspective. *Endocr Rev*. 2023;44(2):143-192. doi:10.1210/endrev/bnac015

281. Fedorenko A, Lishko PV, Kirichok Y. Mechanism of Fatty-Acid-Dependent UCP1 Uncoupling in Brown Fat Mitochondria. *Cell*. 2012;151(2):400-413. doi:10.1016/j.cell.2012.09.010

282. Harb E, Kheder O, Poopalasingam G, Rashid R, Srinivasan A, Izzi-Engbeaya C. Brown adipose tissue and regulation of human body weight. *Diabetes Metab Res Rev*. 2023;39(1):e3594. doi:10.1002/dmrr.3594

283. Collins S, Kuhn CM, Petro AE, Swick AG, Chrunyk BA, Surwit RS. Role of leptin in fat regulation. *Nature*. 1996;380(6576):677. doi:10.1038/380677a0

284. Commins SP, Marsh DJ, Thomas SA, et al. Norepinephrine is required for leptin effects on gene expression in brown and white adipose tissue. *Endocrinology*. 1999;140(10):4772-4778. doi:10.1210/endo.140.10.7043

285. Commins SP, Watson PM, Padgett MA, Dudley A, Argyropoulos G, Gettys TW. Induction of uncoupling protein expression in brown and white adipose tissue by leptin. *Endocrinology*. 1999;140(1):292-300. doi:10.1210/endo.140.1.6399

286. Scarpace PJ, Matheny M, Pollock BH, Tümer N. Leptin increases uncoupling protein expression and energy expenditure. *Am J Physiol*. 1997;273(1 Pt 1):E226-230. doi:10.1152/ajpendo.1997.273.1.E226

287. Schnabl K, Li Y, Klingenspor M. The gut hormone secretin triggers a gut-brown fat-brain axis in the control of food intake. *Exp Physiol*. 2020;105(8):1206-1213. doi:10.1113/EP087878

288. Wang P, Loh KH, Wu M, et al. A leptin–BDNF pathway regulating sympathetic innervation of adipose tissue. *Nature*. 2020;583(7818):839-844. doi:10.1038/s41586-020-2527-y

289. Qiao L, Yoo H sun, Bosco C, et al. Adiponectin reduces thermogenesis by inhibiting brown adipose tissue activation in mice. *Diabetologia*. 2014;57(5):1027-1036. doi:10.1007/s00125-014-3180-5

290. Yoneshiro T, Wang Q, Tajima K, et al. BCAA catabolism in brown fat controls energy homeostasis through SLC25A44. *Nature*. 2019;572(7771):614-619. doi:10.1038/s41586-019-1503-x

291. Zeng X, Ye M, Resch JM, et al. Innervation of Thermogenic Adipose Tissue via a Calsyntenin-3β/S100b Axis. *Nature*. 2019;569(7755):229-235. doi:10.1038/s41586-019-1156-9

292. Bel JS, Tai TC, Khaper N, Lees SJ. Mirabegron: The most promising adipose tissue beiging agent. *Physiol Rep*. 2021;9(5). doi:10.14814/phy2.14779

293. Ma L, Xiong L, Huang G. Effects of mirabegron on brown adipose tissue and metabolism in humans: A systematic review and meta-analysis. *Eur J Clin Pharmacol*. 2024;80(3):317-333. doi:10.1007/s00228-023-03614-0

294. Saito M, Yoneshiro T. Capsinoids and related food ingredients activating brown fat thermogenesis and reducing body fat in humans. *Curr Opin Lipidol*. 2013;24(1):71-77. doi:10.1097/MOL.0b013e32835a4f40

295. Osuna-Prieto FJ, Martinez-Tellez B, Sanchez-Delgado G, et al. Activation of Human Brown Adipose Tissue by Capsinoids, Catechins, Ephedrine, and Other Dietary Components: A Systematic Review. *Adv Nutr*. 2019;10(2):291-302. doi:10.1093/advances/nmy067

296. Chang SH, Song NJ, Choi JH, Yun UJ, Park KW. Mechanisms underlying UCP1 dependent and independent adipocyte thermogenesis. *Obes Rev Off J Int Assoc Study Obes*. 2019;20(2):241-251. doi:10.1111/obr.12796

297. Roesler A, Kazak L. UCP1-independent thermogenesis. *Biochem J*. 2020;477(3):709-725. doi:10.1042/BCJ20190463

298. Ikeda K, Yamada T. UCP1 Dependent and Independent Thermogenesis in Brown and Beige Adipocytes. *Front Endocrinol*. 2020;11. doi:10.3389/fendo.2020.00498

299. Stanford KI, Middelbeek RJW, Townsend KL, et al. Brown adipose tissue regulates glucose homeostasis and insulin sensitivity. *J Clin Invest*. 2013;123(1):215-223. doi:10.1172/JCI62308

300. Zhang W, Bi S. Hypothalamic Regulation of Brown Adipose Tissue Thermogenesis and Energy Homeostasis. *Front Endocrinol*. 2015;6:136. doi:10.3389/fendo.2015.00136

301. Saito M, Okamatsu-Ogura Y, Matsushita M, et al. High incidence of metabolically active brown adipose tissue in healthy adult humans: effects of cold exposure and adiposity. *Diabetes*. 2009;58(7):1526-1531. doi:10.2337/db09-0530

302. Merklin RJ. Growth and distribution of human fetal brown fat. *Anat Rec*. 1974;178(3):637-645. doi:10.1002/ar.1091780311

303. Loncar D. Development of thermogenic adipose tissue. *Int J Dev Biol*. 1991;35(3):321-333.

304. Cypess AM, Weiner LS, Roberts-Toler C, et al. Activation of human brown adipose tissue by a β3-adrenergic receptor agonist. *Cell Metab*. 2015;21(1):33-38. doi:10.1016/j.cmet.2014.12.009

305. Torres Irizarry VC, Jiang Y, He Y, Xu P. Hypothalamic Estrogen Signaling and Adipose Tissue Metabolism in Energy Homeostasis. *Front Endocrinol*. 2022;13:898139. doi:10.3389/fendo.2022.898139

306. Wu J, Boström P, Sparks LM, et al. Beige adipocytes are a distinct type of thermogenic fat cell in mouse and human. *Cell*. 2012;150(2):366-376. doi:10.1016/j.cell.2012.05.016

307. Jespersen NZ, Larsen TJ, Peijs L, et al. A classical brown adipose tissue mRNA signature partly overlaps with brite in the supraclavicular region of adult humans. *Cell Metab*. 2013;17(5):798-805. doi:10.1016/j.cmet.2013.04.011

308. Ikeda K, Kang Q, Yoneshiro T, et al. UCP1-independent signaling involving SERCA2b-mediated calcium cycling regulates beige fat thermogenesis and systemic glucose homeostasis. *Nat Med*. 2017;23(12):1454-1465. doi:10.1038/nm.4429

309. Kazak L, Chouchani ET, Jedrychowski MP, et al. A creatine-driven substrate cycle enhances energy expenditure and thermogenesis in beige fat. *Cell*. 2015;163(3):643-655. doi:10.1016/j.cell.2015.09.035

310. Anderson CM, Kazantzis M, Wang J, et al. Dependence of Brown Adipose Tissue Function on CD36-Mediated Coenzyme Q Uptake. *Cell Rep*. 2015;10(4):505-515. doi:10.1016/j.celrep.2014.12.048

311. Betz MJ, Enerbäck S. Human Brown Adipose Tissue: What We Have Learned So Far. *Diabetes*. 2015;64(7):2352-2360. doi:10.2337/db15-0146

312. García-Martín R, Alexaki VI, Qin N, et al. Adipocyte-Specific Hypoxia-Inducible Factor 2α Deficiency Exacerbates Obesity-Induced Brown Adipose Tissue Dysfunction and Metabolic Dysregulation. *Mol Cell Biol*. 2016;36(3):376-393. doi:10.1128/MCB.00430-15

313. Lombardi A, Senese R, De Matteis R, et al. 3,5-Diiodo-L-Thyronine Activates Brown Adipose Tissue Thermogenesis in Hypothyroid Rats. *PLoS ONE*. 2015;10(2):e0116498. doi:10.1371/journal.pone.0116498

314. Gallerand A, Stunault MI, Merlin J, et al. Brown adipose tissue monocytes support tissue expansion. *Nat Commun*. 2021;12(1). doi:10.1038/s41467-021-25616-1

315. Sun W, Dong H, Balaz M, et al. snRNA-seq reveals a subpopulation of adipocytes that regulates thermogenesis. *Nature*. 2020;587(7832):98-102. doi:10.1038/s41586-020-2856-x

316. Bertola A, Gallerand A, Ivanov S. Immune cell involvement in brown adipose tissue functions. *Discov Immunol*. 2022;1(1):kyac007. doi:10.1093/discim/kyac007

317. McKay RM, McKay JP, Avery L, Graff JM. C elegans: a model for exploring the genetics of fat storage. *Dev Cell*. 2003;4(1):131-142. doi:10.1016/s1534-5807(02)00411-2

318. Van Vleet ES, Candileri S, McNeillie J, Reinhardt SB, Conkright ME, Zwissler A. Neutral lipid components of eleven species of Caribbean sharks. *Comp Biochem Physiol B*. 1984;79(4):549-554. doi:10.1016/0305-0491(84)90364-x

319. Miller JM, Oligino T, Pazdera M, López AJ, Hoshizaki DK. Identification of fat-cell enhancer regions in Drosophila melanogaster. *Insect Mol Biol*. 2002;11(1):67-77. doi:10.1046/j.0962-1075.2001.00310.x

320. Birsoy K, Festuccia WT, Laplante M. A comparative perspective on lipid storage in animals. *J Cell Sci*. 2013;126(Pt 7):1541-1552. doi:10.1242/jcs.104992

321. Sethi JK, Vidal-Puig AJ. Thematic review series: adipocyte biology. Adipose tissue function and plasticity orchestrate nutritional adaptation. *J Lipid Res*. 2007;48(6):1253-1262. doi:10.1194/jlr.R700005-JLR200

322. Kersten S. Physiological regulation of lipoprotein lipase. *Biochim Biophys Acta*. 2014;1841(7):919-933. doi:10.1016/j.bbalip.2014.03.013

323. Fielding BA, Frayn KN. Lipoprotein lipase and the disposition of dietary fatty acids. *Br J Nutr*. 1998;80(6):495-502. doi:10.1017/s0007114598001585

324. Frayn KN. Adipose tissue as a buffer for daily lipid flux. *Diabetologia*. 2002;45(9):1201-1210. doi:10.1007/s00125-002-0873-y

325. Ferré P, Foufelle F. SREBP-1c transcription factor and lipid homeostasis: clinical perspective. *Horm Res*. 2007;68(2):72-82. doi:10.1159/000100426

326. Zechner R, Strauss JG, Haemmerle G, Lass A, Zimmermann R. Lipolysis: pathway under construction. *Curr Opin Lipidol*. 2005;16(3):333-340. doi:10.1097/01.mol.0000169354.20395.1c

327. Kuriyama H, Shimomura I, Kishida K, et al. Coordinated regulation of fat-specific and liver-specific glycerol channels, aquaporin adipose and aquaporin 9. *Diabetes*. 2002;51(10):2915-2921. doi:10.2337/diabetes.51.10.2915

328. Carmen GY, Víctor SM. Signalling mechanisms regulating lipolysis. *Cell Signal*. 2006;18(4):401-408. doi:10.1016/j.cellsig.2005.08.009

329. Nielsen TS, Jessen N, Jørgensen JOL, Møller N, Lund S. Dissecting adipose tissue lipolysis: molecular regulation and implications for metabolic disease. *J Mol Endocrinol*. 2014;52(3):R199-222. doi:10.1530/JME-13-0277

330. Haemmerle G, Zimmermann R, Hayn M, et al. Hormone-sensitive lipase deficiency in mice causes diglyceride accumulation in adipose tissue, muscle, and testis. *J Biol Chem*. 2002;277(7):4806-4815. doi:10.1074/jbc.M110355200

331. Zimmermann R, Strauss JG, Haemmerle G, et al. Fat mobilization in adipose tissue is promoted by adipose triglyceride lipase. *Science*. 2004;306(5700):1383-1386. doi:10.1126/science.1100747

332. Saponaro C, Gaggini M, Carli F, Gastaldelli A. The Subtle Balance between Lipolysis and Lipogenesis: A Critical Point in Metabolic Homeostasis. *Nutrients*. 2015;7(11):9453-9474. doi:10.3390/nu7115475

333. Friedman JM, Halaas JL. Leptin and the regulation of body weight in mammals. *Nature*. 1998;395(6704):763-770. doi:10.1038/27376

334. Rosen ED, Spiegelman BM. What we talk about when we talk about fat. *Cell*. 2014;156(1-2):20-44. doi:10.1016/j.cell.2013.12.012

335. Parimisetty A, Dorsemans AC, Awada R, Ravanan P, Diotel N, Lefebvre d'Hellencourt C. Secret talk between adipose tissue and central nervous system via secreted factors-an emerging frontier in the neurodegenerative research. *J Neuroinflammation*. 2016;13(1):67. doi:10.1186/s12974-016-0530-x

336. Waki H, Tontonoz P. Endocrine functions of adipose tissue. *Annu Rev Pathol*. 2007;2:31-56. doi:10.1146/annurev.pathol.2.010506.091859

337. Scherer PE, Williams S, Fogliano M, Baldini G, Lodish HF. A novel serum protein similar to C1q, produced exclusively in adipocytes. *J Biol Chem*. 1995;270(45):26746-26749. doi:10.1074/jbc.270.45.26746

338. Fasshauer M, Blüher M. Adipokines in health and disease. *Trends Pharmacol Sci*. 2015;36(7):461-470. doi:10.1016/j.tips.2015.04.014

339. Blüher M, Mantzoros CS. From leptin to other adipokines in health and disease: facts and expectations at the beginning of the 21st century. *Metabolism*. 2015;64(1):131-145. doi:10.1016/j.metabol.2014.10.016

340. Bado A, Levasseur S, Attoub S, et al. The stomach is a source of leptin. *Nature*. 1998;394(6695):790-793. doi:10.1038/29547

341. Wang J, Liu R, Hawkins M, Barzilai N, Rossetti L. A nutrient-sensing pathway regulates leptin gene expression in muscle and fat. *Nature*. 1998;393(6686):684-688. doi:10.1038/31474

342. Sobhani I, Bado A, Vissuzaine C, et al. Leptin secretion and leptin receptor in the human stomach. *Gut*. 2000;47(2):178-183. doi:10.1136/gut.47.2.178

343. Hansen GH, Niels-Christiansen LL, Danielsen EM. Leptin and the obesity receptor (OB-R) in the small intestine and colon: a colocalization study. *J Histochem Cytochem Off J Histochem Soc*. 2008;56(7):677-685. doi:10.1369/jhc.2008.950782

344. Jamaluddin MS, Weakley SM, Yao Q, Chen C. Resistin: functional roles and therapeutic considerations for cardiovascular disease. *Br J Pharmacol*. 2012;165(3):622-632. doi:10.1111/j.1476-5381.2011.01369.x

345. Goralski KB, McCarthy TC, Hanniman EA, et al. Chemerin, a novel adipokine that regulates adipogenesis and adipocyte metabolism. *J Biol Chem*. 2007;282(38):28175-28188. doi:10.1074/jbc.M700793200

346. Mattern A, Zellmann T, Beck-Sickinger AG. Processing, signaling, and physiological function of chemerin. *IUBMB Life*. 2014;66(1):19-26. doi:10.1002/iub.1242

347. Loskutoff DJ, Samad F. The adipocyte and hemostatic balance in obesity: studies of PAI-1. *Arterioscler Thromb Vasc Biol*. 1998;18(1):1-6. doi:10.1161/01.atv.18.1.1

348. Boucher J, Masri B, Daviaud D, et al. Apelin, a newly identified adipokine up-regulated by insulin and obesity. *Endocrinology*. 2005;146(4):1764-1771. doi:10.1210/en.2004-1427

349. Saddi-Rosa P, Oliveira CS, Giuffrida FM, Reis AF. Visfatin, glucose metabolism and vascular disease: a review of evidence. *Diabetol Metab Syndr*. 2010;2:21. doi:10.1186/1758-5996-2-21

350. Deng Y, Scherer PE. Adipokines as novel biomarkers and regulators of the metabolic syndrome. *Ann N Y Acad Sci*. 2010;1212:E1-E19. doi:10.1111/j.1749-6632.2010.05875.x

351. Rosen ED, Spiegelman BM. Adipocytes as regulators of energy balance and glucose homeostasis. *Nature*. 2006;444(7121):847-853. doi:10.1038/nature05483

352. Halaas JL, Gajiwala KS, Maffei M, et al. Weight-reducing effects of the plasma protein encoded by the obese gene. *Science*. 1995;269(5223):543-546. doi:10.1126/science.7624777

353. Ramos-Lobo AM, Donato J. The role of leptin in health and disease. *Temp Multidiscip Biomed J*. 2017;4(3):258-291. doi:10.1080/23328940.2017.1327003

354. Saladin R, De Vos P, Guerre-Millo M, et al. Transient increase in obese gene expression after food intake or insulin administration. *Nature*. 1995;377(6549):527-529. doi:10.1038/377527a0

355. Sinha MK, Ohannesian JP, Heiman ML, et al. Nocturnal rise of leptin in lean, obese, and non-insulin-dependent diabetes mellitus subjects. *J Clin Invest*. 1996;97(5):1344-1347.

356. Maffei M, Halaas J, Ravussin E, et al. Leptin levels in human and rodent: measurement of plasma leptin and ob RNA in obese and weight-reduced subjects. *Nat Med*. 1995;1(11):1155-1161. doi:10.1038/nm1195-1155

357. Pelleymounter MA, Cullen MJ, Baker MB, et al. Effects of the obese gene product on body weight regulation in ob/ob mice. *Science*. 1995;269(5223):540-543. doi:10.1126/science.7624776

358. Jørgensen JO, Vahl N, Dall R, Christiansen JS. Resting metabolic rate in healthy adults: relation to growth hormone status and leptin levels. *Metabolism*. 1998;47(9):1134-1139. doi:10.1016/s0026-0495(98)90289-x

359. Meister B. Control of food intake via leptin receptors in the hypothalamus. *Vitam Horm*. 2000;59:265-304. doi:10.1016/s0083-6729(00)59010-4

360. Sahu A. Evidence suggesting that galanin (GAL), melanin-concentrating hormone (MCH), neurotensin (NT), proopiomelanocortin (POMC) and neuropeptide Y (NPY) are targets of leptin signaling in the hypothalamus. *Endocrinology*. 1998;139(2):795-798. doi:10.1210/endo.139.2.5909

361. Arvaniti K, Huang Q, Richard D. Effects of leptin and corticosterone on the expression of corticotropin-releasing hormone, agouti-related protein, and proopiomelanocortin in the brain of ob/ob mouse. *Neuroendocrinology*. 2001;73(4):227-236. doi:10.1159/000054639

362. López M, Seoane L, García MC, et al. Leptin regulation of prepro-orexin and orexin receptor mRNA levels in the hypothalamus. *Biochem Biophys Res Commun*. 2000;269(1):41-45. doi:10.1006/bbrc.2000.2245

363. Kumano S, Matsumoto H, Takatsu Y, Noguchi J, Kitada C, Ohtaki T. Changes in hypothalamic expression levels of galanin-like peptide in rat and mouse models support that it is a leptin-target peptide. *Endocrinology*. 2003;144(6):2634-2643. doi:10.1210/en.2002-221113

364. Kristensen P, Judge ME, Thim L, et al. Hypothalamic CART is a new anorectic peptide regulated by leptin. *Nature*. 1998;393(6680):72-76. doi:10.1038/29993

365. Bariohay B, Lebrun B, Moyse E, Jean A. Brain-derived neurotrophic factor plays a role as an anorexigenic factor in the dorsal vagal complex. *Endocrinology*. 2005;146(12):5612-5620. doi:10.1210/en.2005-0419

366. Tartaglia LA, Dembski M, Weng X, et al. Identification and expression cloning of a leptin receptor, OB-R. *Cell*. 1995;83(7):1263-1271. doi:10.1016/0092-8674(95)90151-5

367. Bjørbaek C, Uotani S, da Silva B, Flier JS. Divergent signaling capacities of the long and short isoforms of the leptin receptor. *J Biol Chem*. 1997;272(51):32686-32695. doi:10.1074/jbc.272.51.32686

368. Tartaglia LA. The leptin receptor. *J Biol Chem*. 1997;272(10):6093-6096. doi:10.1074/jbc.272.10.6093

369. Münzberg H, Huo L, Nillni EA, Hollenberg AN, Bjørbaek C. Role of signal transducer and activator of transcription 3 in regulation of hypothalamic proopiomelanocortin gene expression by leptin. *Endocrinology*. 2003;144(5):2121-2131. doi:10.1210/en.2002-221037

370. El-Haschimi K, Pierroz DD, Hileman SM, Bjørbaek C, Flier JS. Two defects contribute to hypothalamic leptin resistance in mice with diet-induced obesity. *J Clin Invest*. 2000;105(12):1827-1832. doi:10.1172/JCI9842

371. Münzberg H, Flier JS, Bjørbaek C. Region-specific leptin resistance within the hypothalamus of diet-induced obese mice. *Endocrinology*. 2004;145(11):4880-4889. doi:10.1210/en.2004-0726

372. Mantzoros CS, Qu D, Frederich RC, et al. Activation of beta(3) adrenergic receptors suppresses leptin expression and mediates a leptin-independent inhibition of food intake in mice. *Diabetes*. 1996;45(7):909-914. doi:10.2337/diab.45.7.909

373. Trayhurn P, Duncan JS, Rayner DV. Acute cold-induced suppression of ob (obese) gene expression in white adipose tissue of mice: mediation by the sympathetic system. *Biochem J*. 1995;311(Pt 3):729-733.

374. Fonseca-Alaniz MH, Takada J, Alonso-Vale MIC, Lima FB. Adipose tissue as an endocrine organ: from theory to practice. *J Pediatr (Rio J)*. 2007;83(5 Suppl):S192-203. doi:10.2223/JPED.1709

375. Tsai M, Asakawa A, Amitani H, Inui A. Stimulation of leptin secretion by insulin. *Indian J Endocrinol Metab*. 2012;16(Suppl 3):S543-S548. doi:10.4103/2230-8210.105570

376. Shimizu H, Shimomura Y, Nakanishi Y, et al. Estrogen increases in vivo leptin production in rats and human subjects. *J Endocrinol*. 1997;154(2):285-292. doi:10.1677/joe.0.1540285

377. Bruun JM, Pedersen SB, Kristensen K, Richelsen B. Effects of pro-inflammatory cytokines and chemokines on leptin production in human adipose tissue in vitro. *Mol Cell Endocrinol*. 2002;190(1-2):91-99. doi:10.1016/s0303-7207(02)00007-2

378. Martínez-Sánchez N. There and Back Again: Leptin Actions in White Adipose Tissue. *Int J Mol Sci*. 2020;21(17):6039. doi:10.3390/ijms21176039

379. Chen XX, Yang T. Roles of leptin in bone metabolism and bone diseases. *J Bone Miner Metab*. 2015;33(5):474-485. doi:10.1007/s00774-014-0569-7

380. de Candia P, Prattichizzo F, Garavelli S, Alviggi C, La Cava A, Matarese G. The pleiotropic roles of leptin in metabolism, immunity, and cancer. *J Exp Med*. 2021;218(5):e20191593. doi:10.1084/jem.20191593

381. D'souza AM, Neumann UH, Glavas MM, Kieffer TJ. The glucoregulatory actions of leptin. *Mol Metab*. 2017;6(9):1052-1065. doi:10.1016/j.molmet.2017.04.011

382. Bennett BD, Solar GP, Yuan JQ, Mathias J, Thomas GR, Matthews W. A role for leptin and its cognate receptor in hematopoiesis. *Curr Biol*. 1996;6(9):1170-1180. doi:10.1016/S0960-9822(02)70684-2

383. Signore AP, Zhang F, Weng Z, Gao Y, Chen J. Leptin neuroprotection in the CNS: mechanisms and therapeutic potentials. *J Neurochem*. 2008;106(5):1977-1990. doi:10.1111/j.1471-4159.2008.05457.x

384. Procaccini C, La Rocca C, Carbone F, De Rosa V, Galgani M, Matarese G. Leptin as immune mediator: Interaction between neuroendocrine and immune system. *Dev Comp Immunol*. 2017;66:120-129. doi:10.1016/j.dci.2016.06.006

385. Caprio M, Fabbrini E, Isidori AM, Aversa A, Fabbri A. Leptin in reproduction. *Trends Endocrinol Metab*. 2001;12(2):65-72. doi:10.1016/S1043-2760(00)00352-0

386. Flier JS, Harris M, Hollenberg AN. Leptin, nutrition, and the thyroid: the why, the wherefore, and the wiring. *J Clin Invest*. 2000;105(7):859-861. doi:10.1172/JCI9725

387. Bouloumié A, Drexler HCA, Lafontan M, Busse R. Leptin, the Product of Ob Gene, Promotes Angiogenesis. *Circ Res*. 1998;83(10):1059-1066. doi:10.1161/01.RES.83.10.1059

388. Beltowski J. Role of leptin in blood pressure regulation and arterial hypertension. *J Hypertens*. 2006;24(5):789. doi:10.1097/01.hjh.0000222743.06584.66

389. Shek EW, Brands MW, Hall JE. Chronic Leptin Infusion Increases Arterial Pressure. *Hypertension*. 1998;31(1):409-414. doi:10.1161/01.HYP.31.1.409

390. Cakir B, Kasimay O, Devseren E, Yeğen BC. Leptin inhibits gastric emptying in rats: role of CCK receptors and vagal afferent fibers. *Physiol Res*. 2007;56(3):315-322. doi:10.33549/physiolres.930865

391. La leptina es una hormona producida por las células adiposas que ayuda a regular el apetito, el control del metabolismo, la homeostasis energética, la activación de las células inmunes, y la otra función. Sistema endocrino humano. 123RF. Accessed July 21, 2024. https://es.123rf.com/photo_44567679_la-leptina-es-una-hormona-producida-por-las-células-adiposas-que-ayuda-a-regular-el-apetito-el.html

392. Motyl KJ, Rosen CJ. Understanding leptin-dependent regulation of skeletal homeostasis. *Biochimie*. 2012;94(10):2089-2096. doi:10.1016/j.biochi.2012.04.015

393. Beresford JN. Osteogenic stem cells and the stromal system of bone and marrow. *Clin Orthop*. 1989;(240):270-280.

394. Thomas T. The complex effects of leptin on bone metabolism through multiple pathways. *Curr Opin Pharmacol*. 2004;4(3):295-300. doi:10.1016/j.coph.2004.01.009

395. Steppan CM, Crawford DT, Chidsey-Frink KL, Ke H, Swick AG. Leptin is a potent stimulator of bone growth in ob/ob mice. *Regul Pept*. 2000;92(1-3):73-78. doi:10.1016/s0167-0115(00)00152-x

396. Cornish J, Callon KE, Bava U, et al. Leptin directly regulates bone cell function in vitro and reduces bone fragility in vivo. *J Endocrinol*. 2002;175(2):405-415. doi:10.1677/joe.0.1750405

397. Amling M, Takeda S, Karsenty G. A neuro (endo)crine regulation of bone remodeling. *BioEssays News Rev Mol Cell Dev Biol*. 2000;22(11):970-975. doi:10.1002/1521-1878(200011)22:11<970::AID-BIES3>3.0.CO;2-L

398. Ducy P, Amling M, Takeda S, et al. Leptin inhibits bone formation through a hypothalamic relay: a central control of bone mass. *Cell*. 2000;100(2):197-207. doi:10.1016/s0092-8674(00)81558-5

399. Elefteriou F, Ahn JD, Takeda S, et al. Leptin regulation of bone resorption by the sympathetic nervous system and CART. *Nature*. 2005;434(7032):514-520. doi:10.1038/nature03398

400. Zuo C, Huang Y, Bajis R, et al. Osteoblastogenesis regulation signals in bone remodeling. *Osteoporos Int J Establ Result Coop Eur Found Osteoporos Natl Osteoporos Found USA*. 2012;23(6):1653-1663. doi:10.1007/s00198-012-1909-x

401. Kishida Y, Hirao M, Tamai N, et al. Leptin regulates chondrocyte differentiation and matrix maturation during endochondral ossification. *Bone*. 2005;37(5):607-621. doi:10.1016/j.bone.2005.05.009

402. Cheng M, Li T, Li W, Chen Y, Xu W, Xu L. Leptin can promote mineralization and up-regulate RANKL mRNA expression in osteoblasts from adult female SD rats. *Int J Clin Exp Pathol*. 2018;11(3):1610-1619.

403. Thomas T, Gori F, Khosla S, Jensen MD, Burguera B, Riggs BL. Leptin acts on human marrow stromal cells to enhance differentiation to osteoblasts and to inhibit differentiation to adipocytes. *Endocrinology*. 1999;140(4):1630-1638. doi:10.1210/endo.140.4.6637

404. Kim GS, Hong JS, Kim SW, et al. Leptin induces apoptosis via ERK/cPLA2/cytochrome c pathway in human bone marrow stromal cells. *J Biol Chem*. 2003;278(24):21920-21929. doi:10.1074/jbc.M204598200

405. Hamrick MW, Della-Fera MA, Choi YH, Pennington C, Hartzell D, Baile CA. Leptin treatment induces loss of bone marrow adipocytes and increases bone formation in leptin-deficient ob/ob mice. *J Bone Miner Res Off J Am Soc Bone Miner Res*. 2005;20(6):994-1001. doi:10.1359/JBMR.050103

406. Ealey KN, Fonseca D, Archer MC, Ward WE. Bone abnormalities in adolescent leptin-deficient mice. *Regul Pept*. 2006;136(1-3):9-13. doi:10.1016/j.regpep.2006.04.013

407. Liu Y, Qian SW, Tang Y, Tang QQ. The secretory function of adipose tissues in metabolic regulation. *Life Metab*. 2024;3(2):loae003. doi:10.1093/lifemeta/loae003

408. Navarro-Perez J, Vidal-Puig A, Carobbio S. Recent developments in adipose tissue-secreted factors and their target organs. *Curr Opin Genet Dev*. 2023;80:102046. doi:10.1016/j.gde.2023.102046

409. Kahn CR, Wang G, Lee KY. Altered adipose tissue and adipocyte function in the pathogenesis of metabolic syndrome. *J Clin Invest*. 2019;129(10):3990-4000. doi:10.1172/JCI129187

410. Steppan CM, Wang J, Whiteman EL, Birnbaum MJ, Lazar MA. Activation of SOCS-3 by resistin. *Mol Cell Biol*. 2005;25(4):1569-1575. doi:10.1128/MCB.25.4.1569-1575.2005

411. Hivert MF, Sullivan LM, Fox CS, et al. Associations of adiponectin, resistin, and tumor necrosis factor-alpha with insulin resistance. *J Clin Endocrinol Metab*. 2008;93(8):3165-3172. doi:10.1210/jc.2008-0425

412. Park HK, Kwak MK, Kim HJ, Ahima RS. Linking resistin, inflammation, and cardiometabolic diseases. *Korean J Intern Med*. 2017;32(2):239-247. doi:10.3904/kjim.2016.229

413. Yang Q, Graham TE, Mody N, et al. Serum retinol binding protein 4 contributes to insulin resistance in obesity and type 2 diabetes. *Nature*. 2005;436(7049):356-362. doi:10.1038/nature03711

414. Thompson SJ, Sargsyan A, Lee SA, et al. Hepatocytes Are the Principal Source of Circulating RBP4 in Mice. *Diabetes*. 2017;66(1):58-63. doi:10.2337/db16-0286

415. Lee SA, Yuen JJ, Jiang H, Kahn BB, Blaner WS. Adipocyte-specific overexpression of retinol-binding protein 4 causes hepatic steatosis in mice. *Hepatol Baltim Md*. 2016;64(5):1534-1546. doi:10.1002/hep.28659

416. Balli U, Bozkurt Dogan S, Ongoz Dede F, Sertoglu E, Keles GC. The levels of visceral adipose tissue-derived serpin, omentin-1 and tumor necrosis factor-α in the gingival crevicular fluid of obese patients following periodontal therapy. *J Oral Sci*. 2016;58(4):465-473. doi:10.2334/josnusd.16-0212

417. Ravussin A, Youm YH, Sander J, et al. Loss of Nucleobindin-2 Causes Insulin Resistance in Obesity without Impacting Satiety or Adiposity. *Cell Rep*. 2018;24(5):1085-1092.e6. doi:10.1016/j.celrep.2018.06.112

418. Bouchard L, Faucher G, Tchernof A, et al. Comprehensive genetic analysis of the dipeptidyl peptidase-4 gene and cardiovascular disease risk factors in obese individuals. *Acta Diabetol*. 2009;46(1):13-21. doi:10.1007/s00592-008-0049-4

419. Li X, Liao M, Shen R, et al. Plasma Asprosin Levels Are Associated with Glucose Metabolism, Lipid, and Sex Hormone Profiles in Females with Metabolic-Related Diseases. *Mediators Inflamm*. 2018;2018:7375294. doi:10.1155/2018/7375294

420. Huang H, Song TJ, Li X, et al. BMP signaling pathway is required for commitment of C3H10T1/2 pluripotent stem cells to the adipocyte lineage. *Proc Natl Acad Sci*. 2009;106(31):12670-12675. doi:10.1073/pnas.0906266106

421. Schulz TJ, Huang TL, Tran TT, et al. Identification of inducible brown adipocyte progenitors residing in skeletal muscle and white fat. *Proc Natl Acad Sci U S A*. 2011;108(1):143-148. doi:10.1073/pnas.1010929108

422. Donath MY, Shoelson SE. Type 2 diabetes as an inflammatory disease. *Nat Rev Immunol*. 2011;11(2):98-107. doi:10.1038/nri2925

423. Kanda H, Tateya S, Tamori Y, et al. MCP-1 contributes to macrophage infiltration into adipose tissue, insulin resistance, and hepatic steatosis in obesity. *J Clin Invest*. 2006;116(6):1494-1505. doi:10.1172/JCI26498

424. Yore MM, Syed I, Moraes-Vieira PM, et al. Discovery of a class of endogenous mammalian lipids with anti-diabetic and anti-inflammatory effects. *Cell*. 2014;159(2):318-332. doi:10.1016/j.cell.2014.09.035

425. Lynes MD, Leiria LO, Lundh M, et al. The cold-induced lipokine 12,13-diHOME promotes fatty acid transport into brown adipose tissue. *Nat Med*. 2017;23(5):631-637. doi:10.1038/nm.4297

426. Duisenbek A, Lopez-Armas GC, Pérez M, et al. Insights into the Role of Plasmatic and Exosomal microRNAs in Oxidative Stress-Related Metabolic Diseases. *Antioxidants*. 2023;12(6):1290. doi:10.3390/antiox12061290

427. Ludwig N, Leidinger P, Becker K, et al. Distribution of miRNA expression across human tissues. *Nucleic Acids Res*. 2016;44(8):3865-3877. doi:10.1093/nar/gkw116

428. Mori MA, Thomou T, Boucher J, et al. Altered miRNA processing disrupts brown/white adipocyte determination and associates with lipodystrophy. *J Clin Invest*. 2014;124(8):3339-3351. doi:10.1172/JCI73468

429. Herrera BM, Lockstone HE, Taylor JM, et al. MicroRNA-125a is over-expressed in insulin target tissues in a spontaneous rat model of Type 2 Diabetes. *BMC Med Genomics*. 2009;2:54. doi:10.1186/1755-8794-2-54

430. Sun L, Xie H, Mori MA, et al. Mir193b-365 is essential for brown fat differentiation. *Nat Cell Biol*. 2011;13(8):958-965. doi:10.1038/ncb2286

431. Benavides-Aguilar JA, Torres-Copado A, Isidoro-Sánchez J, et al. The Regulatory Role of MicroRNAs in Obesity and Obesity-Derived Ailments. *Genes*. 2023;14(11):2070. doi:10.3390/genes14112070

432. Thomou T, Mori MA, Dreyfuss JM, et al. Adipose-derived circulating miRNAs regulate gene expression in other tissues. *Nature*. 2017;542(7642):450-455. doi:10.1038/nature21365

433. Ying W, Riopel M, Bandyopadhyay G, et al. Adipose Tissue Macrophage-Derived Exosomal miRNAs Can Modulate In Vivo and In Vitro Insulin Sensitivity. *Cell*. 2017;171(2):372-384.e12. doi:10.1016/j.cell.2017.08.035

434. Can U, Buyukinan M, Yerlikaya FH. The investigation of circulating microRNAs associated with lipid metabolism in childhood obesity. *Pediatr Obes*. 2016;11(3):228-234. doi:10.1111/ijpo.12050

435. Willeit P, Skroblin P, Moschen AR, et al. Circulating MicroRNA-122 Is Associated With the Risk of New-Onset Metabolic Syndrome and Type 2 Diabetes. *Diabetes*. 2017;66(2):347-357. doi:10.2337/db16-0731

436. Castaño C, Kalko S, Novials A, Párrizas M. Obesity-associated exosomal miRNAs modulate glucose and lipid metabolism in mice. *Proc Natl Acad Sci U S A*. 2018;115(48):12158-12163. doi:10.1073/pnas.1808855115

437. Kong L, Zhu J, Han W, et al. Significance of serum microRNAs in pre-diabetes and newly diagnosed type 2 diabetes: a clinical study. *Acta Diabetol*. 2011;48(1):61-69. doi:10.1007/s00592-010-0226-0

438. Sun K, Chang X, Yin L, et al. Expression and DNA methylation status of microRNA-375 in patients with type 2 diabetes mellitus. *Mol Med Rep*. 2014;9(3):967-972. doi:10.3892/mmr.2013.1872

439. Latreille M, Herrmanns K, Renwick N, et al. miR-375 gene dosage in pancreatic β-cells: implications for regulation of β-cell mass and biomarker development. *J Mol Med*. 2015;93(10):1159-1169. doi:10.1007/s00109-015-1296-9

440. Karolina DS, Tavintharan S, Armugam A, et al. Circulating miRNA Profiles in Patients with Metabolic Syndrome. *J Clin Endocrinol Metab*. 2012;97(12):E2271-E2276. doi:10.1210/jc.2012-1996

441. Deng Z bin, Poliakov A, Hardy RW, et al. Adipose tissue exosome-like vesicles mediate activation of macrophage-induced insulin resistance. *Diabetes*. 2009;58(11):2498-2505. doi:10.2337/db09-0216

442. Zhang Y, Mei H, Chang X, Chen F, Zhu Y, Han X. Adipocyte-derived microvesicles from obese mice induce M1 macrophage phenotype through secreted miR-155. *J Mol Cell Biol*. 2016;8(6):505-517. doi:10.1093/jmcb/mjw040

443. Reppert SM, Weaver DR. Coordination of circadian timing in mammals. *Nature*. 2002;418(6901):935-941. doi:10.1038/nature00965

444. Takahashi JS. Transcriptional architecture of the mammalian circadian clock. *Nat Rev Genet*. 2017;18(3):164-179. doi:10.1038/nrg.2016.150

445. Johnston JD, Ordovás JM, Scheer FA, Turek FW. Circadian Rhythms, Metabolism, and Chrononutrition in Rodents and Humans123. *Adv Nutr*. 2016;7(2):399-406. doi:10.3945/an.115.010777

446. Albrecht U. The mammalian circadian clock: a network of gene expression. *Front Biosci J Virtual Libr*. 2004;9:48-55. doi:10.2741/1196

447. Albrecht U, Eichele G. The mammalian circadian clock. *Curr Opin Genet Dev*. 2003;13(3):271-277. doi:10.1016/s0959-437x(03)00055-8

448. Richards J, Gumz ML. Advances in understanding the peripheral circadian clocks. *FASEB J Off Publ Fed Am Soc Exp Biol*. 2012;26(9):3602-3613. doi:10.1096/fj.12-203554

449. Lamia KA, Storch KF, Weitz CJ. Physiological significance of a peripheral tissue circadian clock. *Proc Natl Acad Sci U S A*. 2008;105(39):15172-15177. doi:10.1073/pnas.0806717105

450. Sadacca LA, Lamia KA, deLemos AS, Blum B, Weitz CJ. An intrinsic circadian clock of the pancreas is required for normal insulin release and glucose homeostasis in mice. *Diabetologia*. 2011;54(1):120-124. doi:10.1007/s00125-010-1920-8

451. Paschos GK, Ibrahim S, Song WL, et al. Obesity in mice with adipocyte-specific deletion of clock component Arntl. *Nat Med*. 2012;18(12):1768-1777. doi:10.1038/nm.2979

452. Shostak A, Meyer-Kovac J, Oster H. Circadian regulation of lipid mobilization in white adipose tissues. *Diabetes*. 2013;62(7):2195-2203. doi:10.2337/db12-1449

453. Dyar KA, Ciciliot S, Wright LE, et al. Muscle insulin sensitivity and glucose metabolism are controlled by the intrinsic muscle clock. *Mol Metab*. 2014;3(1):29-41. doi:10.1016/j.molmet.2013.10.005

454. Patke A, Young MW, Axelrod S. Molecular mechanisms and physiological importance of circadian rhythms. *Nat Rev Mol Cell Biol*. 2020;21(2):67-84. doi:10.1038/s41580-019-0179-2

455. Bunger MK, Wilsbacher LD, Moran SM, et al. Mop3 is an essential component of the master circadian pacemaker in mammals. *Cell*. 2000;103(7):1009-1017. doi:10.1016/s0092-8674(00)00205-1

456. Vitaterna MH, King DP, Chang AM, et al. Mutagenesis and mapping of a mouse gene, Clock, essential for circadian behavior. *Science*. 1994;264(5159):719-725. doi:10.1126/science.8171325

457. Ko CH, Takahashi JS. Molecular components of the mammalian circadian clock. *Hum Mol Genet*. 2006;15 Spec No 2:R271-277. doi:10.1093/hmg/ddl207

458. Gallego M, Virshup DM. Post-translational modifications regulate the ticking of the circadian clock. *Nat Rev Mol Cell Biol*. 2007;8(2):139-148. doi:10.1038/nrm2106

459. Siepka SM, Yoo SH, Park J, et al. Circadian mutant Overtime reveals F-box protein FBXL3 regulation of cryptochrome and period gene expression. *Cell*. 2007;129(5):1011-1023. doi:10.1016/j.cell.2007.04.030

460. Yoo SH, Mohawk JA, Siepka SM, et al. Competing E3 ubiquitin ligases govern circadian periodicity by degradation of CRY in nucleus and cytoplasm. *Cell*. 2013;152(5):1091-1105. doi:10.1016/j.cell.2013.01.055

461. Zhao M, Lu D, Chen M, Wu B. Introduction to Mammalian Circadian Clock System. In: Wu B, Lu D, Dong D, eds. *Circadian Pharmacokinetics*. Springer; 2020:1-21. doi:10.1007/978-981-15-8807-5_1

462. Preitner N, Damiola F, Lopez-Molina L, et al. The orphan nuclear receptor REV-ERBalpha controls circadian transcription within the positive limb of the mammalian circadian oscillator. *Cell*. 2002;110(2):251-260. doi:10.1016/s0092-8674(02)00825-5

463. Ueda HR, Chen W, Adachi A, et al. A transcription factor response element for gene expression during circadian night. *Nature*. 2002;418(6897):534-539. doi:10.1038/nature00906

464. Pickel L, Sung HK. Feeding Rhythms and the Circadian Regulation of Metabolism. *Front Nutr*. 2020;7:39. doi:10.3389/fnut.2020.00039

465. Fagiani F, Di Marino D, Romagnoli A, et al. Molecular regulations of circadian rhythm and implications for physiology and diseases. *Signal Transduct Target Ther*. 2022;7(1):41. doi:10.1038/s41392-022-00899-y

466. Minnetti M, Hasenmajer V, Pofi R, Venneri MA, Alexandraki KI, Isidori AM. Fixing the broken clock in adrenal disorders: focus on glucocorticoids and chronotherapy. *J Endocrinol*. 2020;246(2):R13-R31. doi:10.1530/JOE-20-0066

467. Mure LS, Le HD, Benegiamo G, et al. Diurnal transcriptome atlas of a primate across major neural and peripheral tissues. *Science*. 2018;359(6381):eaao0318. doi:10.1126/science.aao0318

468. Eckel-Mahan K, Sassone-Corsi P. Metabolism and the circadian clock converge. *Physiol Rev*. 2013;93(1):107-135. doi:10.1152/physrev.00016.2012

469. Yoo SH, Yamazaki S, Lowrey PL, et al. PERIOD2::LUCIFERASE real-time reporting of circadian dynamics reveals persistent circadian oscillations in mouse peripheral tissues. *Proc Natl Acad Sci U S A*. 2004;101(15):5339-5346. doi:10.1073/pnas.0308709101

470. Granados-Fuentes D, Prolo LM, Abraham U, Herzog ED. The suprachiasmatic nucleus entrains, but does not sustain, circadian rhythmicity in the olfactory bulb. *J Neurosci Off J Soc Neurosci*. 2004;24(3):615-619. doi:10.1523/JNEUROSCI.4002-03.2004

471. Granados-Fuentes D, Tseng A, Herzog ED. A circadian clock in the olfactory bulb controls olfactory responsivity. *J Neurosci Off J Soc Neurosci*. 2006;26(47):12219-12225. doi:10.1523/JNEUROSCI.3445-06.2006

472. Yan J, Wang H, Liu Y, Shao C. Analysis of gene regulatory networks in the mammalian circadian rhythm. *PLoS Comput Biol*. 2008;4(10):e1000193. doi:10.1371/journal.pcbi.1000193

473. Zhang R, Lahens NF, Ballance HI, Hughes ME, Hogenesch JB. A circadian gene expression atlas in mammals: implications for biology and medicine. *Proc Natl Acad Sci U S A*. 2014;111(45):16219-16224. doi:10.1073/pnas.1408886111

474. Tahara Y, Shibata S. Circadian rhythms of liver physiology and disease: experimental and clinical evidence. *Nat Rev Gastroenterol Hepatol*. 2016;13(4):217-226. doi:10.1038/nrgastro.2016.8

475. Vollmers C, Gill S, DiTacchio L, Pulivarthy SR, Le HD, Panda S. Time of feeding and the intrinsic circadian clock drive rhythms in hepatic gene expression. *Proc Natl Acad Sci U S A*. 2009;106(50):21453-21458. doi:10.1073/pnas.0909591106

476. Bray MS, Young ME. Circadian rhythms in the development of obesity: potential role for the circadian clock within the adipocyte. *Obes Rev Off J Int Assoc Study Obes*. 2007;8(2):169-181. doi:10.1111/j.1467-789X.2006.00277.x

477. Gavrila A, Peng CK, Chan JL, Mietus JE, Goldberger AL, Mantzoros CS. Diurnal and ultradian dynamics of serum adiponectin in healthy men: comparison with leptin, circulating soluble leptin receptor, and cortisol patterns. *J Clin Endocrinol Metab*. 2003;88(6):2838-2843. doi:10.1210/jc.2002-021721

478. Weyer C, Funahashi T, Tanaka S, et al. Hypoadiponectinemia in obesity and type 2 diabetes: close association with insulin resistance and hyperinsulinemia. *J Clin Endocrinol Metab*. 2001;86(5):1930-1935. doi:10.1210/jcem.86.5.7463

479. Iwabu M, Yamauchi T, Okada-Iwabu M, et al. Adiponectin and AdipoR1 regulate PGC-1alpha and mitochondria by Ca(2+) and AMPK/SIRT1. *Nature*. 2010;464(7293):1313-1319. doi:10.1038/nature08991

480. Mootha VK, Lindgren CM, Eriksson KF, et al. PGC-1alpha-responsive genes involved in oxidative phosphorylation are coordinately downregulated in human diabetes. *Nat Genet*. 2003;34(3):267-273. doi:10.1038/ng1180

481. Bodosi B, Gardi J, Hajdu I, Szentirmai E, Obal F, Krueger JM. Rhythms of ghrelin, leptin, and sleep in rats: effects of the normal diurnal cycle, restricted feeding, and sleep deprivation. *Am J Physiol Regul Integr Comp Physiol*. 2004;287(5):R1071-1079. doi:10.1152/ajpregu.00294.2004

482. Kalsbeek A, Fliers E, Romijn JA, et al. The suprachiasmatic nucleus generates the diurnal changes in plasma leptin levels. *Endocrinology*. 2001;142(6):2677-2685. doi:10.1210/endo.142.6.8197

483. Shea SA, Hilton MF, Orlova C, Ayers RT, Mantzoros CS. Independent circadian and sleep/wake regulation of adipokines and glucose in humans. *J Clin Endocrinol Metab*. 2005;90(5):2537-2544. doi:10.1210/jc.2004-2232

484. Simon C, Gronfier C, Schlienger JL, Brandenberger G. Circadian and ultradian variations of leptin in normal man under continuous enteral nutrition: relationship to sleep and body temperature. *J Clin Endocrinol Metab*. 1998;83(6):1893-1899. doi:10.1210/jcem.83.6.4864

485. Kettner NM, Mayo SA, Hua J, Lee C, Moore DD, Fu L. Circadian Dysfunction Induces Leptin Resistance in Mice. *Cell Metab*. 2015;22(3):448-459. doi:10.1016/j.cmet.2015.06.005

486. Marcheva B, Ramsey KM, Buhr ED, et al. Disruption of the clock components CLOCK and BMAL1 leads to hypoinsulinaemia and diabetes. *Nature*. 2010;466(7306):627-631. doi:10.1038/nature09253

487. Wu T, Ni Y, Dong Y, et al. Regulation of circadian gene expression in the kidney by light and food cues in rats. *Am J Physiol Regul Integr Comp Physiol*. 2010;298(3):R635-641. doi:10.1152/ajpregu.00578.2009

488. Eckel RH, York DA, Rössner S, et al. Prevention Conference VII: Obesity, a worldwide epidemic related to heart disease and stroke: executive summary. *Circulation*. 2004;110(18):2968-2975. doi:10.1161/01.CIR.0000140086.88453.9A

489. Obesity and overweight. Accessed April 14, 2024. https://www.who.int/news-room/fact-sheets/detail/obesity-and-overweight

490. World Obesity Atlas 2023. World Obesity Federation. Accessed April 14, 2024. https://www.worldobesity.org/resources/resource-library/world-obesity-atlas-2023

491. Mackenbach JP, Stirbu I, Roskam AJR, et al. Socioeconomic inequalities in health in 22 European countries. *N Engl J Med*. 2008;358(23):2468-2481. doi:10.1056/NEJMsa0707519

492. Garawi F, Devries K, Thorogood N, Uauy R. Global differences between women and men in the prevalence of obesity: is there an association with gender inequality? *Eur J Clin Nutr*. 2014;68(10):1101-1106. doi:10.1038/ejcn.2014.86

493. Kanter R, Caballero B. Global gender disparities in obesity: a review. *Adv Nutr Bethesda Md*. 2012;3(4):491-498. doi:10.3945/an.112.002063

494. Lin X, Li H. Obesity: Epidemiology, Pathophysiology, and Therapeutics. *Front Endocrinol*. 2021;12:706978. doi:10.3389/fendo.2021.706978

495. Romieu I, Dossus L, Barquera S, et al. Energy balance and obesity: what are the main drivers? *Cancer Causes Control CCC*. 2017;28(3):247-258. doi:10.1007/s10552-017-0869-z

496. Thorpe KE, Yang Z, Long KM, Garvey WT. The impact of weight loss among seniors on Medicare spending. *Health Econ Rev*. 2013;3(1):7. doi:10.1186/2191-1991-3-7

497. Müller TD, Blüher M, Tschöp MH, DiMarchi RD. Anti-obesity drug discovery: advances and challenges. *Nat Rev Drug Discov*. 2022;21(3):201-223. doi:10.1038/s41573-021-00337-8

498. GBD 2015 Obesity Collaborators, Afshin A, Forouzanfar MH, et al. Health Effects of Overweight and Obesity in 195 Countries over 25 Years. *N Engl J Med*. 2017;377(1):13-27. doi:10.1056/NEJMoa1614362

499. Sarwer DB, Hanson AJ, Voeller J, Steffen K. Obesity and Sexual Functioning. *Curr Obes Rep*. 2018;7(4):301-307. doi:10.1007/s13679-018-0319-6

500. Gutierrez SB, Quispe KO. Weight gain and physical inactivity during the COVID-19 pandemic. *Rev Panam Salud Pública*. 2021;45:e136. doi:10.26633/RPSP.2021.136

501. Stumvoll M, Goldstein BJ, van Haeften TW. Type 2 diabetes: principles of pathogenesis and therapy. *Lancet Lond Engl*. 2005;365(9467):1333-1346. doi:10.1016/S0140-6736(05)61032-X

502. Weyer C, Bogardus C, Mott DM, Pratley RE. The natural history of insulin secretory dysfunction and insulin resistance in the pathogenesis of type 2 diabetes mellitus. *J Clin Invest*. 1999;104(6):787-794. doi:10.1172/JCI7231

503. Chatterjee S, Khunti K, Davies MJ. Type 2 diabetes. *Lancet Lond Engl*. 2017;389(10085):2239-2251. doi:10.1016/S0140-6736(17)30058-2

504. Chan JM, Rimm EB, Colditz GA, Stampfer MJ, Willett WC. Obesity, fat distribution, and weight gain as risk factors for clinical diabetes in men. *Diabetes Care*. 1994;17(9):961-969. doi:10.2337/diacare.17.9.961

505. Han TS, Feskens EJ, Lean ME, Seidell JC. Associations of body composition with type 2 diabetes mellitus. *Diabet Med J Br Diabet Assoc*. 1998;15(2):129-135. doi:10.1002/(SICI)1096-9136(199802)15:2<129::AID-DIA535>3.0.CO;2-2

506. Freeman AM, Acevedo LA, Pennings N. Insulin Resistance. In: *StatPearls*. StatPearls Publishing; 2024. Accessed August 18, 2024. http://www.ncbi.nlm.nih.gov/books/NBK507839/

507. Cerf ME. Beta Cell Dysfunction and Insulin Resistance. *Front Endocrinol*. 2013;4:37. doi:10.3389/fendo.2013.00037

508. Zheng Y, Ley SH, Hu FB. Global aetiology and epidemiology of type 2 diabetes mellitus and its complications. *Nat Rev Endocrinol*. 2018;14(2):88-98. doi:10.1038/nrendo.2017.151

509. Slawik M, Vidal-Puig AJ. Adipose tissue expandability and the metabolic syndrome. *Genes Nutr*. 2007;2(1):41-45. doi:10.1007/s12263-007-0014-9

510. Virtue S, Vidal-Puig A. Adipose tissue expandability, lipotoxicity and the Metabolic Syndrome — An allostatic perspective. *Biochim Biophys Acta BBA - Mol Cell Biol Lipids*. 2010;1801(3):338-349. doi:10.1016/j.bbalip.2009.12.006

511. Unger RH, Clark GO, Scherer PE, Orci L. Lipid homeostasis, lipotoxicity and the metabolic syndrome. *Biochim Biophys Acta*. 2010;1801(3):209-214. doi:10.1016/j.bbalip.2009.10.006

512. Rohm TV, Meier DT, Olefsky JM, Donath MY. Inflammation in Obesity, Diabetes and related Disorders. *Immunity*. 2022;55(1):31-55. doi:10.1016/j.immuni.2021.12.013

513. Hossain P, Kawar B, El Nahas M. Obesity and diabetes in the developing world--a growing challenge. *N Engl J Med*. 2007;356(3):213-215. doi:10.1056/NEJMp068177

514. Wild S, Roglic G, Green A, Sicree R, King H. Global prevalence of diabetes: estimates for the year 2000 and projections for 2030. *Diabetes Care*. 2004;27(5):1047-1053. doi:10.2337/diacare.27.5.1047

515. Vilariño-García T, Polonio-González ML, Pérez-Pérez A, et al. Role of Leptin in Obesity, Cardiovascular Disease, and Type 2 Diabetes. *Int J Mol Sci*. 2024;25(4):2338. doi:10.3390/ijms25042338

516. Zhao S, Zhu Y, Schultz RD, et al. Partial Leptin Reduction as an Insulin Sensitization and Weight Loss Strategy. *Cell Metab*. 2019;30(4):706-719.e6. doi:10.1016/j.cmet.2019.08.005

517. Zelissen PMJ, Stenlof K, Lean MEJ, et al. Effect of three treatment schedules of recombinant methionyl human leptin on body weight in obese adults: a randomized, placebo-controlled trial. *Diabetes Obes Metab*. 2005;7(6):755-761. doi:10.1111/j.1463-1326.2005.00468.x

518. Ahima RS, Flier JS. Leptin. *Annu Rev Physiol*. 2000;62:413-437. doi:10.1146/annurev.physiol.62.1.413

519. Liu J, Lai F, Hou Y, Zheng R. Leptin signaling and leptin resistance. *Med Rev*. 2022;2(4):363-384. doi:10.1515/mr-2022-0017

520. Expression of leptin receptor isoforms in rat brain microvessels - PubMed. Accessed July 21, 2024. https://pubmed.ncbi.nlm.nih.gov/9681499/

521. Banks WA, Kastin AJ, Huang W, Jaspan JB, Maness LM. Leptin enters the brain by a saturable system independent of insulin. *Peptides*. 1996;17(2):305-311. doi:10.1016/0196-9781(96)00025-3

522. Chen H, Charlat O, Tartaglia LA, et al. Evidence that the diabetes gene encodes the leptin receptor: identification of a mutation in the leptin receptor gene in db/db mice. *Cell*. 1996;84(3):491-495. doi:10.1016/s0092-8674(00)81294-5

523. Peng J, Yin L, Wang X. Central and peripheral leptin resistance in obesity and improvements of exercise. *Horm Behav*. 2021;133:105006. doi:10.1016/j.yhbeh.2021.105006

524. Sáinz N, Barrenetxe J, Moreno-Aliaga MJ, Martínez JA. Leptin resistance and diet-induced obesity: central and peripheral actions of leptin. *Metabolism*. 2015;64(1):35-46. doi:10.1016/j.metabol.2014.10.015

525. Zhao S, Li N, Xiong W, et al. Leptin Reduction as a Required Component for Weight Loss. *Diabetes*. 2023;73(2):197-210. doi:10.2337/db23-0571

526. Adamovich Y, Rousso-Noori L, Zwighaft Z, et al. Circadian clocks and feeding time regulate the oscillations and levels of hepatic triglycerides. *Cell Metab*. 2014;19(2):319-330. doi:10.1016/j.cmet.2013.12.016

527. Sridhar GR, Sanjana NSN. Sleep, circadian dysrhythmia, obesity and diabetes. *World J Diabetes*. 2016;7(19):515-522. doi:10.4239/wjd.v7.i19.515

528. Gao M, Huang X, Song BL, Yang H. The biogenesis of lipid droplets: Lipids take center stage. *Prog Lipid Res*. 2019;75:100989. doi:10.1016/j.plipres.2019.100989

529. Villanueva JE, Livelo C, Trujillo AS, et al. Time-restricted feeding restores muscle function in Drosophila models of obesity and circadian-rhythm disruption. *Nat Commun*. 2019;10(1):2700. doi:10.1038/s41467-019-10563-9

530. Baron KG, Reid KJ, Kim T, et al. Circadian timing and alignment in healthy adults: associations with BMI, body fat, caloric intake and physical activity. *Int J Obes 2005*. 2017;41(2):203-209. doi:10.1038/ijo.2016.194

531. Liu X, Zheng C, Xu C, et al. Nighttime snacking is associated with risk of obesity and hyperglycemia in adults: a cross-sectional survey from Chinese adult teachers. *J Biomed Res*. 2017;31(6):541-547. doi:10.7555/JBR.31.20160083

532. Schäbler S, Amatobi KM, Horn M, et al. Loss of function in the Drosophila clock gene period results in altered intermediary lipid metabolism and increased susceptibility to starvation. *Cell Mol Life Sci CMLS*. 2020;77(23):4939-4956. doi:10.1007/s00018-019-03441-6

533. Meléndez-Fernández OH, Liu JA, Nelson RJ. Circadian Rhythms Disrupted by Light at Night and Mistimed Food Intake Alter Hormonal Rhythms and Metabolism. *Int J Mol Sci*. 2023;24(4):3392. doi:10.3390/ijms24043392

534. Meyer-Kovac J, Kolbe I, Ehrhardt L, et al. Hepatic gene therapy rescues high-fat diet responses in circadian Clock mutant mice. *Mol Metab*. 2017;6(6):512-523. doi:10.1016/j.molmet.2017.03.008

535. Turek FW, Joshu C, Kohsaka A, et al. Obesity and metabolic syndrome in circadian Clock mutant mice. *Science*. 2005;308(5724):1043-1045. doi:10.1126/science.1108750

536. Harfmann BD, Schroder EA, Kachman MT, Hodge BA, Zhang X, Esser KA. Muscle-specific loss of Bmal1 leads to disrupted tissue glucose metabolism and systemic glucose homeostasis. *Skelet Muscle*. 2016;6:12. doi:10.1186/s13395-016-0082-x

537. Lee J, Kim MS, Li R, et al. Loss of Bmal1 leads to uncoupling and impaired glucose-stimulated insulin secretion in β-cells. *Islets*. 2011;3(6):381-388. doi:10.4161/isl.3.6.18157

538. Perelis M, Marcheva B, Ramsey KM, et al. Pancreatic β cell enhancers regulate rhythmic transcription of genes controlling insulin secretion. *Science*. 2015;350(6261):aac4250. doi:10.1126/science.aac4250

539. Tahira K, Ueno T, Fukuda N, et al. Obesity alters the expression profile of clock genes in peripheral blood mononuclear cells. *Arch Med Sci AMS*. 2011;7(6):933-940. doi:10.5114/aoms.2011.26603

540. Touitou Y, Reinberg A, Touitou D. Association between light at night, melatonin secretion, sleep deprivation, and the internal clock: Health impacts and mechanisms of circadian disruption. *Life Sci*. 2017;173:94-106. doi:10.1016/j.lfs.2017.02.008

541. Nedeltcheva AV, Scheer FAJL. Metabolic effects of sleep disruption, links to obesity and diabetes. *Curr Opin Endocrinol Diabetes Obes*. 2014;21(4):293-298. doi:10.1097/MED.0000000000000082

542. Fuster JJ, Ouchi N, Gokce N, Walsh K. Obesity-Induced Changes in Adipose Tissue Microenvironment and Their Impact on Cardiovascular Disease. *Circ Res*. 2016;118(11):1786-1807. doi:10.1161/CIRCRESAHA.115.306885

543. Salans LB, Horton ES, Sims EA. Experimental obesity in man: cellular character of the adipose tissue. *J Clin Invest*. 1971;50(5):1005-1011. doi:10.1172/JCI106570

544. Meister BM, Hong SG, Shin J, Rath M, Sayoc J, Park JY. Healthy versus Unhealthy Adipose Tissue Expansion: the Role of Exercise. *J Obes Metab Syndr*. 2022;31(1):37-50. doi:10.7570/jomes21096

545. Kusminski CM, Bickel PE, Scherer PE. Targeting adipose tissue in the treatment of obesity-associated diabetes. *Nat Rev Drug Discov*. 2016;15(9):639-660. doi:10.1038/nrd.2016.75

546. McLaughlin T, Lamendola C, Liu A, Abbasi F. Preferential fat deposition in subcutaneous versus visceral depots is associated with insulin sensitivity. *J Clin Endocrinol Metab*. 2011;96(11):E1756-1760. doi:10.1210/jc.2011-0615

547. Snijder MB, Dekker JM, Visser M, et al. Associations of hip and thigh circumferences independent of waist circumference with the incidence of type 2 diabetes: the Hoorn Study. *Am J Clin Nutr*. 2003;77(5):1192-1197. doi:10.1093/ajcn/77.5.1192

548. Cildir G, Akıncılar SC, Tergaonkar V. Chronic adipose tissue inflammation: all immune cells on the stage. *Trends Mol Med*. 2013;19(8):487-500. doi:10.1016/j.molmed.2013.05.001

549. Kratz M, Coats BR, Hisert KB, et al. Metabolic dysfunction drives a mechanistically distinct proinflammatory phenotype in adipose tissue macrophages. *Cell Metab*. 2014;20(4):614-625. doi:10.1016/j.cmet.2014.08.010

550. Zeyda M, Farmer D, Todoric J, et al. Human adipose tissue macrophages are of an anti-inflammatory phenotype but capable of excessive pro-inflammatory mediator production. *Int J Obes 2005*. 2007;31(9):1420-1428. doi:10.1038/sj.ijo.0803632

551. McNelis JC, Olefsky JM. Macrophages, immunity, and metabolic disease. *Immunity*. 2014;41(1):36-48. doi:10.1016/j.immuni.2014.05.010

552. Cinti S, Mitchell G, Barbatelli G, et al. Adipocyte death defines macrophage localization and function in adipose tissue of obese mice and humans. *J Lipid Res*. 2005;46(11):2347-2355. doi:10.1194/jlr.M500294-JLR200

553. Murano I, Barbatelli G, Parisani V, et al. Dead adipocytes, detected as crown-like structures, are prevalent in visceral fat depots of genetically obese mice. *J Lipid Res*. 2008;49(7):1562-1568. doi:10.1194/jlr.M800019-JLR200

554. Apovian CM, Bigornia S, Mott M, et al. Adipose macrophage infiltration is associated with insulin resistance and vascular endothelial dysfunction in obese subjects. *Arterioscler Thromb Vasc Biol*. 2008;28(9):1654-1659. doi:10.1161/ATVBAHA.108.170316

555. Mansuy-Aubert V, Zhou QL, Xie X, et al. Imbalance between neutrophil elastase and its inhibitor α1-antitrypsin in obesity alters insulin sensitivity, inflammation, and energy expenditure. *Cell Metab*. 2013;17(4):534-548. doi:10.1016/j.cmet.2013.03.005

556. Talukdar S, Oh DY, Bandyopadhyay G, et al. Neutrophils mediate insulin resistance in mice fed a high-fat diet through secreted elastase. *Nat Med*. 2012;18(9):1407-1412. doi:10.1038/nm.2885

557. Liu J, Divoux A, Sun J, et al. Genetic deficiency and pharmacological stabilization of mast cells reduce diet-induced obesity and diabetes in mice. *Nat Med*. 2009;15(8):940-945. doi:10.1038/nm.1994

558. Kawai T, Autieri MV, Scalia R. Adipose tissue inflammation and metabolic dysfunction in obesity. *Am J Physiol-Cell Physiol*. 2021;320(3):C375-C391. doi:10.1152/ajpcell.00379.2020

559. Gealekman O, Guseva N, Hartigan C, et al. Depot-specific differences and insufficient subcutaneous adipose tissue angiogenesis in human obesity. *Circulation*. 2011;123(2):186-194. doi:10.1161/CIRCULATIONAHA.110.970145

560. Hosogai N, Fukuhara A, Oshima K, et al. Adipose tissue hypoxia in obesity and its impact on adipocytokine dysregulation. *Diabetes*. 2007;56(4):901-911. doi:10.2337/db06-0911

561. Ye J, Gao Z, Yin J, He Q. Hypoxia is a potential risk factor for chronic inflammation and adiponectin reduction in adipose tissue of ob/ob and dietary obese mice. *Am J Physiol Endocrinol Metab*. 2007;293(4):E1118-1128. doi:10.1152/ajpendo.00435.2007

562. Sun K, Wernstedt Asterholm I, Kusminski CM, et al. Dichotomous effects of VEGF-A on adipose tissue dysfunction. *Proc Natl Acad Sci U S A*. 2012;109(15):5874-5879. doi:10.1073/pnas.1200447109

563. Elias I, Franckhauser S, Ferré T, et al. Adipose Tissue Overexpression of Vascular Endothelial Growth Factor Protects Against Diet-Induced Obesity and Insulin Resistance. *Diabetes*. 2012;61(7):1801-1813. doi:10.2337/db11-0832

564. Sung HK, Doh KO, Son JE, et al. Adipose vascular endothelial growth factor regulates metabolic homeostasis through angiogenesis. *Cell Metab*. 2013;17(1):61-72. doi:10.1016/j.cmet.2012.12.010

565. Shimizu I, Aprahamian T, Kikuchi R, et al. Vascular rarefaction mediates whitening of brown fat in obesity. *J Clin Invest*. 2014;124(5):2099-2112. doi:10.1172/JCI71643

566. Bošanská L, Michalský D, Lacinová Z, et al. The influence of obesity and different fat depots on adipose tissue gene expression and protein levels of cell adhesion molecules. *Physiol Res*. 2010;59(1):79-88. doi:10.33549/physiolres.931705

567. Nishimura S, Manabe I, Nagasaki M, et al. In vivo imaging in mice reveals local cell dynamics and inflammation in obese adipose tissue. *J Clin Invest*. 2008;118(2):710-721. doi:10.1172/JCI33328

568. Farb MG, Bigornia S, Mott M, et al. Reduced adipose tissue inflammation represents an intermediate cardiometabolic phenotype in obesity. *J Am Coll Cardiol*. 2011;58(3):232-237. doi:10.1016/j.jacc.2011.01.051

569. Khan T, Muise ES, Iyengar P, et al. Metabolic dysregulation and adipose tissue fibrosis: role of collagen VI. *Mol Cell Biol*. 2009;29(6):1575-1591. doi:10.1128/MCB.01300-08

570. Zhang Q, Lu C, Lu F, Liao Y, Cai J, Gao J. Challenges and opportunities in obesity: the role of adipocytes during tissue fibrosis. *Front Endocrinol*. 2024;15:1365156. doi:10.3389/fendo.2024.1365156

571. Reilly SM, Saltiel AR. Adapting to obesity with adipose tissue inflammation. *Nat Rev Endocrinol*. 2017;13(11):633-643. doi:10.1038/nrendo.2017.90

572. Ali MM, Phillips SA, Mahmoud AM. HIF1α/TET1 Pathway Mediates Hypoxia-Induced Adipocytokine Promoter Hypomethylation in Human Adipocytes. *Cells*. 2020;9(1):134. doi:10.3390/cells9010134

573. Wipff PJ, Rifkin DB, Meister JJ, Hinz B. Myofibroblast contraction activates latent TGF-beta1 from the extracellular matrix. *J Cell Biol*. 2007;179(6):1311-1323. doi:10.1083/jcb.200704042

574. Sun K, Park J, Gupta OT, et al. Endotrophin triggers adipose tissue fibrosis and metabolic dysfunction. *Nat Commun*. 2014;5:3485. doi:10.1038/ncomms4485

575. Iwayama T, Steele C, Yao L, et al. PDGFRα signaling drives adipose tissue fibrosis by targeting progenitor cell plasticity. *Genes Dev*. 2015;29(11):1106-1119. doi:10.1101/gad.260554.115

576. Spalding KL, Bernard S, Näslund E, et al. Impact of fat mass and distribution on lipid turnover in human adipose tissue. *Nat Commun*. 2017;8:15253. doi:10.1038/ncomms15253

577. Ipsen DH, Lykkesfeldt J, Tveden-Nyborg P. Molecular mechanisms of hepatic lipid accumulation in non-alcoholic fatty liver disease. *Cell Mol Life Sci CMLS*. 2018;75(18):3313-3327. doi:10.1007/s00018-018-2860-6

578. Horwitz A, Birk R. Adipose Tissue Hyperplasia and Hypertrophy in Common and Syndromic Obesity-The Case of BBS Obesity. *Nutrients*. 2023;15(15):3445. doi:10.3390/nu15153445

579. Byrne CD. Ectopic fat, insulin resistance and non-alcoholic fatty liver disease. *Proc Nutr Soc*. 2013;72(4):412-419. doi:10.1017/S0029665113001249

580. Hammarstedt A, Gogg S, Hedjazifar S, Nerstedt A, Smith U. Impaired Adipogenesis and Dysfunctional Adipose Tissue in Human Hypertrophic Obesity. *Physiol Rev*. 2018;98(4):1911-1941. doi:10.1152/physrev.00034.2017

581. Carr RM, Peralta G, Yin X, Ahima RS. Absence of Perilipin 2 Prevents Hepatic Steatosis, Glucose Intolerance and Ceramide Accumulation in Alcohol-Fed Mice. *PLOS ONE*. 2014;9(5):e97118. doi:10.1371/journal.pone.0097118

582. Samuel VT, Liu ZX, Wang A, et al. Inhibition of protein kinase Cepsilon prevents hepatic insulin resistance in nonalcoholic fatty liver disease. *J Clin Invest*. 2007;117(3):739-745. doi:10.1172/JCI30400

583. Liu L, Mei M, Yang S, Li Q. Roles of Chronic Low-Grade Inflammation in the Development of Ectopic Fat Deposition. *Mediators Inflamm*. 2014;2014:418185. doi:10.1155/2014/418185

584. Petrescu M, Vlaicu SI, Ciumărnean L, et al. Chronic Inflammation—A Link between Nonalcoholic Fatty Liver Disease (NAFLD) and Dysfunctional Adipose Tissue. *Medicina (Mex)*. 2022;58(5):641. doi:10.3390/medicina58050641

585. Brøns C, Grunnet LG. MECHANISMS IN ENDOCRINOLOGY: Skeletal muscle lipotoxicity in insulin resistance and type 2 diabetes: a causal mechanism or an innocent bystander? *Eur J Endocrinol*. 2017;176(2):R67-R78. doi:10.1530/EJE-16-0488

586. Szendroedi J, Yoshimura T, Phielix E, et al. Role of diacylglycerol activation of PKCθ in lipid-induced muscle insulin resistance in humans. *Proc Natl Acad Sci U S A*. 2014;111(26):9597-9602. doi:10.1073/pnas.1409229111

587. Wu H, Ballantyne CM. Skeletal muscle inflammation and insulin resistance in obesity. *J Clin Invest*. 127(1):43-54. doi:10.1172/JCI88880

588. Farr JN, Van Loan MD, Lohman TG, Going SB. Lower Physical Activity is Associated with Skeletal Muscle Fat Content in Girls. *Med Sci Sports Exerc*. 2012;44(7):10.1249/MSS.0b013e31824749b2. doi:10.1249/MSS.0b013e31824749b2

589. Liu D, Zhong J, Ruan Y, Zhang Z, Sun J, Chen H. The association between fat-to-muscle ratio and metabolic disorders in type 2 diabetes. *Diabetol Metab Syndr*. 2021;13(1):129. doi:10.1186/s13098-021-00748-y

590. Sharma S, Adrogue JV, Golfman L, et al. Intramyocardial lipid accumulation in the failing human heart resembles the lipotoxic rat heart. *FASEB J Off Publ Fed Am Soc Exp Biol*. 2004;18(14):1692-1700. doi:10.1096/fj.04-2263com

591. Guzzardi MA, Iozzo P. Fatty Heart, Cardiac Damage, and Inflammation. *Rev Diabet Stud RDS*. 2011;8(3):403-417. doi:10.1900/RDS.2011.8.403

592. Neeland IJ, Ross R, Després JP, et al. Visceral and ectopic fat, atherosclerosis, and cardiometabolic disease: a position statement. *Lancet Diabetes Endocrinol*. 2019;7(9):715-725. doi:10.1016/S2213-8587(19)30084-1

593. Milanese G, Silva M, Ledda RE, et al. Validity of epicardial fat volume as biomarker of coronary artery disease in symptomatic individuals: Results from the ALTER-BIO registry. *Int J Cardiol*. 2020;314:20-24. doi:10.1016/j.ijcard.2020.04.031

594. Lim S, Meigs JB. Links between ectopic fat and vascular disease in humans. *Arterioscler Thromb Vasc Biol*. 2014;34(9):1820-1826. doi:10.1161/ATVBAHA.114.303035

595. Wen Y, Chen C, Kong X, et al. Pancreatic fat infiltration, β-cell function and insulin resistance: A study of the young patients with obesity. *Diabetes Res Clin Pract*. 2022;187. doi:10.1016/j.diabres.2022.109860

596. Wagner R, Eckstein SS, Yamazaki H, et al. Metabolic implications of pancreatic fat accumulation. *Nat Rev Endocrinol*. 2022;18(1):43-54. doi:10.1038/s41574-021-00573-3

597. Lim JJ, Sequeira-Bisson IR, Yip WCY, Lu LW, Miles-Chan JL, Poppitt SD. Intra-pancreatic fat is associated with high circulating glucagon and GLP-1 concentrations following whey protein ingestion in overweight women with impaired fasting glucose: A randomised controlled trial. *Diabetes Res Clin Pract*. 2024;207. doi:10.1016/j.diabres.2023.111084

598. Galicia-Garcia U, Benito-Vicente A, Jebari S, et al. Pathophysiology of Type 2 Diabetes Mellitus. *Int J Mol Sci*. 2020;21(17):6275. doi:10.3390/ijms21176275

599. Birk RZ, Rubio-Aliaga I, Boekschoten MV, Danino H, Müller M, Daniel H. Differential regulation of pancreatic digestive enzymes during chronic high-fat diet-induced obesity in C57BL/6J mice. *Br J Nutr*. 2014;112(2):154-161. doi:10.1017/S0007114514000816

600. Foster MC, Hwang SJ, Porter SA, Massaro JM, Hoffmann U, Fox CS. Fatty kidney, hypertension, and chronic kidney disease: the Framingham Heart Study. *Hypertens Dallas Tex 1979*. 2011;58(5):784-790. doi:10.1161/HYPERTENSIONAHA.111.175315

601. Ambrosi TH, Scialdone A, Graja A, et al. Adipocyte Accumulation in the Bone Marrow during Obesity and Aging Impairs Stem Cell-Based Hematopoietic and Bone Regeneration. *Cell Stem Cell*. 2017;20(6):771-784.e6. doi:10.1016/j.stem.2017.02.009

602. Cheng X, Jiang S, Pan B, Xie W, Meng J. Ectopic and visceral fat deposition in aging, obesity, and idiopathic pulmonary fibrosis: an interconnected role. *Lipids Health Dis*. 2023;22(1):201. doi:10.1186/s12944-023-01964-3

603. Bray GA, Kim KK, Wilding JPH, World Obesity Federation. Obesity: a chronic relapsing progressive disease process. A position statement of the World Obesity Federation. *Obes Rev Off J Int Assoc Study Obes*. 2017;18(7):715-723. doi:10.1111/obr.12551

604. Burki T. European Commission classifies obesity as a chronic disease. *Lancet Diabetes Endocrinol*. 2021;9(7):418. doi:10.1016/S2213-8587(21)00145-5

605. Blüher M. Obesity: global epidemiology and pathogenesis. *Nat Rev Endocrinol*. 2019;15(5):288-298. doi:10.1038/s41574-019-0176-8

606. Carlsson LMS, Sjöholm K, Jacobson P, et al. Life Expectancy after Bariatric Surgery in the Swedish Obese Subjects Study. *N Engl J Med*. 2020;383(16):1535-1543. doi:10.1056/NEJMoa2002449

607. Adams TD, Davidson LE, Litwin SE, et al. Weight and Metabolic Outcomes 12 Years after Gastric Bypass. *N Engl J Med*. 2017;377(12):1143-1155. doi:10.1056/NEJMoa1700459

608. Blüher M, Aras M, Aronne LJ, et al. New insights into the treatment of obesity. *Diabetes Obes Metab*. 2023;25(8):2058-2072. doi:10.1111/dom.15077

609. Hauner H, Hastreiter L, Werdier D, Chen-Stute A, Scholze J, Blüher M. Efficacy and Safety of Cathine (Nor-Pseudoephedrine) in the Treatment of Obesity: A Randomized Dose-Finding Study. *Obes Facts*. 2017;10(4):407-419. doi:10.1159/000478098

610. Lucchetta RC, Riveros BS, Pontarolo R, et al. Systematic review and meta-analysis of the efficacy and safety of amfepramone and mazindol as a monotherapy for the treatment of obese or overweight patients. *Clin Sao Paulo Braz*. 2017;72(5):317-324. doi:10.6061/clinics/2017(05)10

611. Müller TD, Clemmensen C, Finan B, DiMarchi RD, Tschöp MH. Anti-Obesity Therapy: from Rainbow Pills to Polyagonists. *Pharmacol Rev*. 2018;70(4):712-746. doi:10.1124/pr.117.014803

612. Tilinca MC, Tiuca RA, Burlacu A, Varga A. A 2021 Update on the Use of Liraglutide in the Modern Treatment of "Diabesity": A Narrative Review. *Med Kaunas Lith*. 2021;57(7):669. doi:10.3390/medicina57070669

613. Wilding JPH, Batterham RL, Calanna S, et al. Once-Weekly Semaglutide in Adults with Overweight or Obesity. *N Engl J Med*. 2021;384(11):989-1002. doi:10.1056/NEJMoa2032183

614. Angelidi AM, Belanger MJ, Kokkinos A, Koliaki CC, Mantzoros CS. Novel Noninvasive Approaches to the Treatment of Obesity: From Pharmacotherapy to Gene Therapy. *Endocr Rev*. 2022;43(3):507-557. doi:10.1210/endrev/bnab034

615. Drucker DJ, Habener JF, Holst JJ. Discovery, characterization, and clinical development of the glucagon-like peptides. *J Clin Invest*. 2017;127(12):4217-4227. doi:10.1172/JCI97233

616. Heymsfield SB, Greenberg AS, Fujioka K, et al. Recombinant leptin for weight loss in obese and lean adults: a randomized, controlled, dose-escalation trial. *JAMA*. 1999;282(16):1568-1575. doi:10.1001/jama.282.16.1568

617. Brandfon S, Eylon A, Khanna D, Parmar MS. Advances in Anti-obesity Pharmacotherapy: Current Treatments, Emerging Therapies, and Challenges. *Cureus*. 15(10):e46623. doi:10.7759/cureus.46623

618. Oral EA, Simha V, Ruiz E, et al. Leptin-Replacement Therapy for Lipodystrophy. *N Engl J Med*. 2002;346(8):570-578. doi:10.1056/NEJMoa012437

619. Tchang BG, Shukla AP, Aronne LJ. Metreleptin and generalized lipodystrophy and evolving therapeutic perspectives. *Expert Opin Biol Ther*. 2015;15(7):1061-1075. doi:10.1517/14712598.2015.1052789

620. Stanek E, Pacia MZ, Kaczor A, Czamara K. The distinct phenotype of primary adipocytes and adipocytes derived from stem cells of white adipose tissue as assessed by Raman and fluorescence imaging. *Cell Mol Life Sci CMLS*. 2022;79(7):383. doi:10.1007/s00018-022-04391-2

621. Ghoneim NI, Hussein AE, El-Badri N. Isolation of Bone Marrow and Adipose-Derived Mesenchymal Stromal Cells. In: El-Badri N, ed. *Regenerative Medicine and Stem Cell Biology*. Springer International Publishing; 2020:243-264. doi:10.1007/978-3-030-55359-3_8

622. Calvo E, Keiran N, Núñez-Roa C, et al. Effects of stem cells from inducible brown adipose tissue on diet-induced obesity in mice. *Sci Rep*. 2021;11(1):13923. doi:10.1038/s41598-021-93224-6

623. Pachón-Peña G, Yu G, Tucker A, et al. Stromal stem cells from adipose tissue and bone marrow of age-matched female donors display distinct immunophenotypic profiles. *J Cell Physiol*. 2011;226(3):843-851. doi:10.1002/jcp.22408

624. Crown SB, Marze N, Antoniewicz MR. Catabolism of Branched Chain Amino Acids Contributes Significantly to Synthesis of Odd-Chain and Even-Chain Fatty Acids in 3T3-L1 Adipocytes. *PloS One*. 2015;10(12):e0145850. doi:10.1371/journal.pone.0145850

625. Del Río-Martín A, Pérez-Taboada I, Fernández-Pérez A, Moratalla R, de la Villa P, Vallejo M. Hypomorphic Expression of Pitx3 Disrupts Circadian Clocks and Prevents Metabolic Entrainment of Energy Expenditure. *Cell Rep*. 2019;29(11):3678-3692.e4. doi:10.1016/j.celrep.2019.11.027

626. Tang H, Vasselli JR, Wu EX, Boozer CN, Gallagher D. High-resolution magnetic resonance imaging tracks changes in organ and tissue mass in obese and aging rats. *Am J Physiol Regul Integr Comp Physiol*. 2002;282(3):R890-899. doi:10.1152/ajpregu.0527.2001

627. Mina AI, LeClair RA, LeClair KB, Cohen DE, Lantier L, Banks AS. CalR: A Web-Based Analysis Tool for Indirect Calorimetry Experiments. *Cell Metab*. 2018;28(4):656-666.e1. doi:10.1016/j.cmet.2018.06.019

628. R: The R Project for Statistical Computing. Accessed May 2, 2024. https://www.r-project.org/

629. Ritchie ME, Phipson B, Wu D, et al. limma powers differential expression analyses for RNA-sequencing and microarray studies. *Nucleic Acids Res*. 2015;43(7):e47. doi:10.1093/nar/gkv007

630. Love MI, Huber W, Anders S. Moderated estimation of fold change and dispersion for RNA-seq data with DESeq2. *Genome Biol*. 2014;15(12):550. doi:10.1186/s13059-014-0550-8

631. Spiegelman BM, Flier JS. Obesity and the regulation of energy balance. *Cell*. 2001;104(4):531-543. doi:10.1016/s0092-8674(01)00240-9

632. Considine RV, Sinha MK, Heiman ML, et al. Serum immunoreactive-leptin concentrations in normal-weight and obese humans. *N Engl J Med*. 1996;334(5):292-295. doi:10.1056/NEJM199602013340503

633. Kim MH, Kim H. Role of Leptin in the Digestive System. *Front Pharmacol*. 2021;12:660040. doi:10.3389/fphar.2021.660040

634. Cammisotto PG, Bendayan M. Leptin secretion by white adipose tissue and gastric mucosa. *Histol Histopathol*. 2007;22(2):199-210. doi:10.14670/HH-22.199

635. de Castro Fonseca M, Aguiar CJ, da Rocha Franco JA, Gingold RN, Leite MF. GPR91: expanding the frontiers of Krebs cycle intermediates. *Cell Commun Signal*. 2016;14(1):3. doi:10.1186/s12964-016-0126-1

636. Longo KA, Charoenthongtrakul S, Giuliana DJ, et al. Improved insulin sensitivity and metabolic flexibility in ghrelin receptor knockout mice. *Regul Pept*. 2008;150(1-3):55-61. doi:10.1016/j.regpep.2008.03.011

637. Gilbertson NM, Eichner NZM, Francois M, et al. Glucose Tolerance is Linked to Postprandial Fuel Use Independent of Exercise Dose. *Med Sci Sports Exerc*. 2018;50(10):2058-2066. doi:10.1249/MSS.0000000000001667

638. Ahmed K, Tunaru S, Tang C, et al. An autocrine lactate loop mediates insulin-dependent inhibition of lipolysis through GPR81. *Cell Metab*. 2010;11(4):311-319. doi:10.1016/j.cmet.2010.02.012

639. Zhang G, Li R, Li W, et al. Toll-like receptor 3 ablation prevented high-fat diet-induced obesity and metabolic disorder. *J Nutr Biochem*. 2021;95:108761. doi:10.1016/j.jnutbio.2021.108761

640. Tunaru S, Kero J, Schaub A, et al. PUMA-G and HM74 are receptors for nicotinic acid and mediate its anti-lipolytic effect. *Nat Med*. 2003;9(3):352-355. doi:10.1038/nm824

641. Bartelt A, Heeren J. Adipose tissue browning and metabolic health. *Nat Rev Endocrinol*. 2014;10(1):24-36. doi:10.1038/nrendo.2013.204

642. Kazak L, Chouchani ET, Lu GZ, et al. Genetic Depletion of Adipocyte Creatine Metabolism Inhibits Diet-Induced Thermogenesis and Drives Obesity. *Cell Metab*. 2017;26(4):660-671.e3. doi:10.1016/j.cmet.2017.08.009

643. Monfort-Ferré D, Caro A, Menacho M, et al. The Gut Microbiota Metabolite Succinate Promotes Adipose Tissue Browning in Crohn's Disease. *J Crohns Colitis*. 2022;16(10):1571-1583. doi:10.1093/ecco-jcc/jjac069

644. Gao H, Guo Y, Yan Q, et al. Lipoatrophy and metabolic disturbance in mice with adipose-specific deletion of kindlin-2. *JCI Insight*. 2019;4(13):e128405, 128405. doi:10.1172/jci.insight.128405

645. Corsa CAS, Walsh CM, Bagchi DP, et al. Adipocyte-Specific Deletion of Lamin A/C Largely Models Human Familial Partial Lipodystrophy Type 2. *Diabetes*. 2021;70(9):1970-1984. doi:10.2337/db20-1001

646. Urs S, Venkatesh D, Tang Y, et al. Sprouty1 is a critical regulatory switch of mesenchymal stem cell lineage allocation. *FASEB J Off Publ Fed Am Soc Exp Biol*. 2010;24(9):3264-3273. doi:10.1096/fj.10-155127

647. Upadhyay J, Farr OM, Mantzoros CS. The role of leptin in regulating bone metabolism. *Metabolism*. 2015;64(1):105-113. doi:10.1016/j.metabol.2014.10.021

648. Reid IR, Baldock PA, Cornish J. Effects of Leptin on the Skeleton. *Endocr Rev*. 2018;39(6):938-959. doi:10.1210/er.2017-00226

649. Bao D, Ma Y, Zhang X, et al. Preliminary Characterization of a Leptin Receptor Knockout Rat Created by CRISPR/Cas9 System. *Sci Rep*. 2015;5(1):15942. doi:10.1038/srep15942

650. Philbrick KA, Wong CP, Branscum AJ, Turner RT, Iwaniec UT. Leptin stimulates bone formation in ob/ob mice at doses having minimal impact on energy metabolism. *J Endocrinol*. 2017;232(3):461-474. doi:10.1530/JOE-16-0484

651. Pasco JA, Henry MJ, Kotowicz MA, et al. Serum leptin levels are associated with bone mass in nonobese women. *J Clin Endocrinol Metab*. 2001;86(5):1884-1887. doi:10.1210/jcem.86.5.7417

652. Yamauchi M, Sugimoto T, Yamaguchi T, et al. Plasma leptin concentrations are associated with bone mineral density and the presence of vertebral fractures in postmenopausal women. *Clin Endocrinol (Oxf)*. 2001;55(3):341-347. doi:10.1046/j.1365-2265.2001.01361.x

653. Ruhl CE, Everhart JE. Relationship of serum leptin concentration with bone mineral density in the United States population. *J Bone Miner Res Off J Am Soc Bone Miner Res*. 2002;17(10):1896-1903. doi:10.1359/jbmr.2002.17.10.1896

654. Odabaşi E, Ozata M, Turan M, et al. Plasma leptin concentrations in postmenopausal women with osteoporosis. *Eur J Endocrinol*. 2000;142(2):170-173. doi:10.1530/eje.0.1420170

655. Hamrick MW, Pennington C, Newton D, Xie D, Isales C. Leptin deficiency produces contrasting phenotypes in bones of the limb and spine. *Bone*. 2004;34(3):376-383. doi:10.1016/j.bone.2003.11.020

656. Karsenty G, Khosla S. The crosstalk between bone remodeling and energy metabolism: A translational perspective. *Cell Metab*. 2022;34(6):805-817. doi:10.1016/j.cmet.2022.04.010

657. LeDuc CA, Skowronski AA, Rosenbaum M. The Role of Leptin in the Development of Energy Homeostatic Systems and the Maintenance of Body Weight. *Front Physiol*. 2021;12:789519. doi:10.3389/fphys.2021.789519

658. Ali D, Figeac F, Caci A, et al. High-fat diet-induced obesity augments the deleterious effects of estrogen deficiency on bone: Evidence from ovariectomized mice. *Aging Cell*. 2022;21(12):e13726. doi:10.1111/acel.13726

659. Kim S, Henneicke H, Cavanagh LL, et al. Osteoblastic glucocorticoid signaling exacerbates high-fat-diet- induced bone loss and obesity. *Bone Res*. 2021;9:40. doi:10.1038/s41413-021-00159-9

660. Casado ME, Collado-Pérez R, Frago LM, Barrios V. Recent Advances in the Knowledge of the Mechanisms of Leptin Physiology and Actions in Neurological and Metabolic Pathologies. *Int J Mol Sci*. 2023;24(2):1422. doi:10.3390/ijms24021422

661. Cammisotto PG, Renaud C, Gingras D, Delvin E, Levy E, Bendayan M. Endocrine and exocrine secretion of leptin by the gastric mucosa. *J Histochem Cytochem Off J Histochem Soc*. 2005;53(7):851-860. doi:10.1369/jhc.5A6620.2005

662. Hu J, Li T, Du S, et al. The MAPK signaling pathway mediates the GPR91-dependent release of VEGF from RGC-5 cells. *Int J Mol Med*. 2015;36(1):130-138. doi:10.3892/ijmm.2015.2195

663. Trefts E, Shaw RJ. AMPK: restoring metabolic homeostasis over space and time. *Mol Cell*. 2021;81(18):3677-3690. doi:10.1016/j.molcel.2021.08.015

664. Daval M, Diot-Dupuy F, Bazin R, et al. Anti-lipolytic action of AMP-activated protein kinase in rodent adipocytes. *J Biol Chem*. 2005;280(26):25250-25257. doi:10.1074/jbc.M414222200

665. Sponarova J, Mustard KJ, Horakova O, et al. Involvement of AMP-activated protein kinase in fat depot-specific metabolic changes during starvation. *FEBS Lett*. 2005;579(27):6105-6110. doi:10.1016/j.febslet.2005.09.078

666. Park H, Kaushik VK, Constant S, et al. Coordinate regulation of malonyl-CoA decarboxylase, sn-glycerol-3-phosphate acyltransferase, and acetyl-CoA carboxylase by AMP-activated protein kinase in rat tissues in response to exercise. *J Biol Chem*. 2002;277(36):32571-32577. doi:10.1074/jbc.M201692200

667. Musi N, Hayashi T, Fujii N, Hirshman MF, Witters LA, Goodyear LJ. AMP-activated protein kinase activity and glucose uptake in rat skeletal muscle. *Am J Physiol Endocrinol Metab*. 2001;280(5):E677-684. doi:10.1152/ajpendo.2001.280.5.E677

668. Salt IP, Connell JM, Gould GW. 5-aminoimidazole-4-carboxamide ribonucleoside (AICAR) inhibits insulin-stimulated glucose transport in 3T3-L1 adipocytes. *Diabetes*. 2000;49(10):1649-1656. doi:10.2337/diabetes.49.10.1649

669. Sakoda H, Ogihara T, Anai M, et al. Activation of AMPK is essential for AICAR-induced glucose uptake by skeletal muscle but not adipocytes. *Am J Physiol Endocrinol Metab*. 2002;282(6):E1239-1244. doi:10.1152/ajpendo.00455.2001

670. Chuang SJ, Johanns M, Pyr Dit Ruys S, et al. AMPK activation by SC4 inhibits noradrenaline-induced lipolysis and insulin-stimulated lipogenesis in white adipose tissue. *Biochem J*. 2021;478(21):3869-3889. doi:10.1042/BCJ20210411

671. Szkudelski T, Szkudelska K. Effects of AMPK activation on lipolysis in primary rat adipocytes: studies at different glucose concentrations. *Arch Physiol Biochem*. 2017;123(1):43-49. doi:10.1080/13813455.2016.1227853

672. Lihn AS, Jessen N, Pedersen SB, Lund S, Richelsen B. AICAR stimulates adiponectin and inhibits cytokines in adipose tissue. *Biochem Biophys Res Commun*. 2004;316(3):853-858. doi:10.1016/j.bbrc.2004.02.139

673. Sell H, Dietze-Schroeder D, Eckardt K, Eckel J. Cytokine secretion by human adipocytes is differentially regulated by adiponectin, AICAR, and troglitazone. *Biochem Biophys Res Commun*. 2006;343(3):700-706. doi:10.1016/j.bbrc.2006.03.010

674. Wu X, Motoshima H, Mahadev K, Stalker TJ, Scalia R, Goldstein BJ. Involvement of AMP-activated protein kinase in glucose uptake stimulated by the globular domain of adiponectin in primary rat adipocytes. *Diabetes*. 2003;52(6):1355-1363. doi:10.2337/diabetes.52.6.1355

675. Orci L, Cook WS, Ravazzola M, et al. Rapid transformation of white adipocytes into fat-oxidizing machines. *Proc Natl Acad Sci U S A*. 2004;101(7):2058-2063. doi:10.1073/pnas.0308258100

676. Templeman I, Smith HA, Walhin JP, et al. Unacylated ghrelin, leptin, and appetite display diurnal rhythmicity in lean adults. *J Appl Physiol Bethesda Md 1985*. 2021;130(5):1534-1543. doi:10.1152/japplphysiol.00920.2020

677. Doi M, Murai I, Kunisue S, et al. Gpr176 is a Gz-linked orphan G-protein-coupled receptor that sets the pace of circadian behaviour. *Nat Commun*. 2016;7:10583. doi:10.1038/ncomms10583

678. Harmar AJ, Marston HM, Shen S, et al. The VPAC(2) receptor is essential for circadian function in the mouse suprachiasmatic nuclei. *Cell*. 2002;109(4):497-508. doi:10.1016/s0092-8674(02)00736-5

679. Liu J, Clough SJ, Hutchinson AJ, Adamah-Biassi EB, Popovska-Gorevski M, Dubocovich ML. MT1 and MT2 Melatonin Receptors: A Therapeutic Perspective. *Annu Rev Pharmacol Toxicol*. 2016;56:361-383. doi:10.1146/annurev-pharmtox-010814-124742

680. Yannielli PC, Harrington ME. Neuropeptide Y in the mammalian circadian system: effects on light-induced circadian responses. *Peptides*. 2001;22(3):547-556. doi:10.1016/s0196-9781(01)00356-4

681. McArthur AJ, Coogan AN, Ajpru S, Sugden D, Biello SM, Piggins HD. Gastrin-releasing peptide phase-shifts suprachiasmatic nuclei neuronal rhythms in vitro. *J Neurosci Off J Soc Neurosci*. 2000;20(14):5496-5502. doi:10.1523/JNEUROSCI.20-14-05496.2000

682. Takekida S, Yan L, Maywood ES, Hastings MH, Okamura H. Differential adrenergic regulation of the circadian expression of the clock genes Period1 and Period2 in the rat pineal gland. *Eur J Neurosci*. 2000;12(12):4557-4561. doi:10.1046/j.0953-816x.2000.01324.x

683. Cahill GM, Besharse JC. Resetting the circadian clock in cultured Xenopus eyecups: regulation of retinal melatonin rhythms by light and D2 dopamine receptors. *J Neurosci Off J Soc Neurosci*. 1991;11(10):2959-2971. doi:10.1523/JNEUROSCI.11-10-02959.1991

684. Kunst M, Tso MCF, Ghosh DD, Herzog ED, Nitabach MN. Rhythmic control of activity and sleep by class B1 GPCRs. *Crit Rev Biochem Mol Biol*. 2015;50(1):18-30. doi:10.3109/10409238.2014.985815

685. Dallmann R, Viola AU, Tarokh L, Cajochen C, Brown SA. The human circadian metabolome. *Proc Natl Acad Sci U S A*. 2012;109(7):2625-2629. doi:10.1073/pnas.1114410109

686. Buijs R, Salgado R, Sabath E, Escobar C. Peripheral circadian oscillators: time and food. *Prog Mol Biol Transl Sci*. 2013;119:83-103. doi:10.1016/B978-0-12-396971-2.00004-X

687. Challet E. Circadian clocks, food intake, and metabolism. *Prog Mol Biol Transl Sci*. 2013;119:105-135. doi:10.1016/B978-0-12-396971-2.00005-1

688. Christou S, Wehrens SMT, Isherwood C, et al. Circadian regulation in human white adipose tissue revealed by transcriptome and metabolic network analysis. *Sci Rep*. 2019;9(1):2641. doi:10.1038/s41598-019-39668-3

689. Loboda A, Kraft WK, Fine B, et al. Diurnal variation of the human adipose transcriptome and the link to metabolic disease. *BMC Med Genomics*. 2009;2:7. doi:10.1186/1755-8794-2-7

690. Stenvers DJ, Jongejan A, Atiqi S, et al. Diurnal rhythms in the white adipose tissue transcriptome are disturbed in obese individuals with type 2 diabetes compared with lean control individuals. *Diabetologia*. 2019;62(4):704-716. doi:10.1007/s00125-019-4813-5

691. Zvonic S, Ptitsyn AA, Conrad SA, et al. Characterization of peripheral circadian clocks in adipose tissues. *Diabetes*. 2006;55(4):962-970. doi:10.2337/diabetes.55.04.06.db05-0873

692. Ceglia N, Liu Y, Chen S, et al. CircadiOmics: circadian omic web portal. *Nucleic Acids Res*. 2018;46(W1):W157-W162. doi:10.1093/nar/gky441

693. Nakahata Y, Kaluzova M, Grimaldi B, et al. The NAD+-dependent deacetylase SIRT1 modulates CLOCK-mediated chromatin remodeling and circadian control. *Cell*. 2008;134(2):329-340. doi:10.1016/j.cell.2008.07.002

694. Chen L, Yang G. PPARs Integrate the Mammalian Clock and Energy Metabolism. *PPAR Res*. 2014;2014:653017. doi:10.1155/2014/653017

695. Jordan SD, Lamia KA. AMPK at the crossroads of circadian clocks and metabolism. *Mol Cell Endocrinol*. 2013;366(2):163-169. doi:10.1016/j.mce.2012.06.017

696. Um JH, Yang S, Yamazaki S, et al. Activation of 5'-AMP-activated kinase with diabetes drug metformin induces casein kinase Iepsilon (CKIepsilon)-dependent degradation of clock protein mPer2. *J Biol Chem*. 2007;282(29):20794-20798. doi:10.1074/jbc.C700070200

697. Lamia KA, Sachdeva UM, DiTacchio L, et al. AMPK regulates the circadian clock by cryptochrome phosphorylation and degradation. *Science*. 2009;326(5951):437-440. doi:10.1126/science.1172156

698. Knight ZA, Hannan KS, Greenberg ML, Friedman JM. Hyperleptinemia is required for the development of leptin resistance. *PloS One*. 2010;5(6):e11376. doi:10.1371/journal.pone.0011376

699. Zaibi MS, Stocker CJ, O'Dowd J, et al. Roles of GPR41 and GPR43 in leptin secretory responses of murine adipocytes to short chain fatty acids. *FEBS Lett*. 2010;584(11):2381-2386. doi:10.1016/j.febslet.2010.04.027

700. Reutrakul S, Van Cauter E. Sleep influences on obesity, insulin resistance, and risk of type 2 diabetes. *Metabolism*. 2018;84:56-66. doi:10.1016/j.metabol.2018.02.010

701. Zhu B, Shi C, Park CG, Zhao X, Reutrakul S. Effects of sleep restriction on metabolism-related parameters in healthy adults: A comprehensive review and meta-analysis of randomized controlled trials. *Sleep Med Rev*. 2019;45:18-30. doi:10.1016/j.smrv.2019.02.002

702. Engin A. Circadian Rhythms in Diet-Induced Obesity. In: Engin AB, Engin A, eds. *Obesity and Lipotoxicity*. Springer International Publishing; 2017:19-52. doi:10.1007/978-3-319-48382-5_2

703. Kaneko K, Yamada T, Tsukita S, et al. Obesity alters circadian expressions of molecular clock genes in the brainstem. *Brain Res*. 2009;1263:58-68. doi:10.1016/j.brainres.2008.12.071

ANNEX

1. SUPPLEMENTARY METHOD DETAILS

Annex Table 1. Anthropometric and Biochemical Variables from the Human Cohort.

Variables	Lean	Obese
n	22	34
Sex (female/male)	17/5	18/16
Age (years)	51.4 ± 15.7	52.3 ± 12.3
BMI (kg/m²)	22.5 ± 2.0	34.5 ± 3.67***
Glucose (mmol/L)	4.9 ± 0.8	5.3 ± 0.9
Total cholesterol (mmol/L)	4.8 ± 0.7	5.0 ± 1.0
HDLc (mmol/L)	1.6 ± 0.3	1.2 ± 0.3***
LDLc (mmol/L)	2.9 ± 0.6	3.2 ± 0.8
Triglycerides (mmol/L)	0.9 ± 0.4	1.9 ± 1.1***
Insulin (pmol/L)	35.8 ± 12.0	104.8 ± 43.0*
HOMA-IR	1.2 ± 0.6	3.8 ± 1.6*
GGT (µkat/L)	0.9 ± 2.0	2.0 ± 4.6**
ALT (µkat/L)	0.5 ± 0.7	0.5 ± 0.6
AST (µkat/L)	0.3 ± 0.2	0.5 ± 0.4*
Circulating Succinate (µmol/L)	54.8 ± 39.0	102.9 ± 79.0*
Circulating Leptin (µg/L)	10.1 ± 7.6	27.7 ± 21.9***

Abbreviations: ALT, Alanine Aminotransferase; AST, Aspartate Aminotransferase; BMI, body mass index; GGT, Gamma Glutamyltransferase; LDLc, low-density lipoprotein cholesterol; HDLc, high-density lipoprotein cholesterol; HOMA-IR, Homeostatic Model Assessment for Insulin Resistance. Results are expressed as mean ± SD. * p-value <0.05; ** p-value <0.01; and *** p-value <0.001 (Unpaired t-test or Mann-Whitney test).

Annex Table 2. List of Taqman Gene Expression Assay References

GENE NAME	MOUSE	HUMAN
B2m	Mm00437762_m1	
RNA18S5		Hs03928985_g1
Sucnr1/SUCNR1	Mm02620543_s1	Hs00908230_m1
Lep/LEP	Mm00434759_m1	Hs00174877_m1
AdipoQ/ADIPOQ	Mm00456425_m1	Hs00605917_m1
Ucp1	Mm01244861_m1	
Cidea	Mm00432554_m1	
Tnfsf11	Mm00441906_m1	
Spp1	Mm00436767_m1	
Npy	Mm01410146_m1	
Agrp	Mm00475829_g1	
Pparg	Mm00440940_m1	
Fasn	Mm00662319_m1	
Slc2a4	Mm00436615_m1	
Bmal1/BMAL1	Mm00500223_m1	Hs00154147_m1
CLOCK		Hs00231857_m1
Rora/RORA	Mm01173766_m1	Hs00536545_m1
Per1/PER1	Mm00501813_m1	Hs00242988_m1
Per2/PER2	Mm00478099_m1	Hs00256143_m1
Per3/PER3	Mm00478120_m1	Hs00213466_m1
CRY1		Hs00172734_m1
CRY2		Hs00323654_m1

Annex Table 3. List of Employed Reagents and Resources in the Study.

REAGENT OR RESOURCE	*SOURCE*	*IDENTIFIER*
Biological Samples		
hASCs	IISPV Biobank (PT17/0015/0029)	N/A
Chemicals, Peptides, And Recombinant Proteins		
PBS	Hyclone (GE Healthcare Life Sciences)	Cat.#SH30028.02
Sodium Chloride (NaCl)	Panreac	Cat.#131659.1211; CAS ID: 7647-14-5
Potassium Chloride (KCl)	Panreac	Cat.#131494; CAS ID: 7440-09-7
Calcium Chloride ($CaCl_2$)	Fisher Chemical	Cat.#1500/53; CAS ID: 10043-52-4
Magnesium Chloride ($MgCl_2$)	Sigma-Aldrich	Cat.#M8266; CAS ID: 7786-30-3
Sodium bicarbonate ($NaHCO_3$)	Merck	Cat.#6329; CAS ID: 144-55-8
2-[4-(2-Hydroxyethyl)Piperazin-1-Yl]Ethanesulfonic Acid (HEPES)	Fisher Scientific	Cat.#BP310-1; CAS ID: 7365-45-9
Bovine Serum Albumin (BSA)	Sigma-Aldrich	Cat.#A7030; CAS ID: 9048-46-8
cis-epoxysuccinic acid	TCI Chemicals	Cat.#E0449; CAS ID: 16533-72-5
Succinic acid	Sigma-Aldrich	Cat.#S9512; CAS ID: 110-15-6
Disodium succinate	Sigma-Aldrich	Cat.#W327700; CAS ID: 150-90-3
Collagenase from *Clostridium histolyticum*	Sigma-Aldrich	Cat.#C0130; CAS ID: 9001-12-1
Dexamethasone	Sigma-Aldrich	Cat.#D2915; CAS ID: 50-02-2
Biotin	Sigma-Aldrich	Cat.#B4501; CAS ID: 58-85-5

Calcium pantothenate	Sigma-Aldrich	Cat.#C8721; CAS ID: 137-08-6
IBMX	Sigma-Aldrich	Cat.#I5879; CAS ID: 28822-58-4
Insulin from bovine pancreas	Sigma-Aldrich	Cat.#I1882; CAS ID: 11070-73-8
Rosiglitazone	Sigma-Aldrich	Cat.#R2408; CAS ID: 122320-73-4
AICAR	Sigma-Aldrich	Cat.#A9978; CAS ID: 2627-69-2
SP600125	MedChemExpress	Cat.#HY-12041; CAS ID: 129-56-6
SB202190	MedChemExpress	Cat.#HY-10295; CAS ID: 152121-30-7
Compound C	Calbiochem	Cat.#171260; CAS ID: 866405-64-3
Atglistatin	Cayman Chemicals	Cat.#15284; CAS ID: 1469924-27-3
Corn oil	Sigma-Aldrich	Cat.#C8267; CAS ID: 8001-30-7
Leptin from mouse	Sigma-Aldrich	Cat.#L3772; CAS ID: 181030-10-4
rm-Leptin - recombinant mouse	R&D Systems	Cat.#498-OB
PFA 4%	Sigma-Aldrich	Cat.#1.00496.5000
Sodium azide	Thermo Scientific	Cat.#AC190380050; CAS ID: 26628-22-8
Isoproterenol	Sigma-Aldrich	Cat.#PHR2722; CAS ID: 51-30-9
Oil Red O	Sigma-Aldrich	Cat.#O0625; CAS ID: 1320-06-5
β-glycerolphosphate disodium salt	Sigma-Aldrich	Cat.#G9422; CAS ID: 154804-51-0
L-ascorbic acid	Sigma-Aldrich	Cat.#33034; CAS ID: 50-81-7
Alizarin red S	Sigma-Aldrich	Cat.#A5533; CAS ID: 130-22-3

Hexadecylpyridinium chloride	Sigma-Aldrich	Cat.#C9002; CAS ID: 6004-24-6
Tris-HCl	Fischer bioreagents	Cat.#BP153-500; CAS ID: 1185-53-1
EDTA	Sigma-Aldrich	Cat.#E6758; CAS ID: 60-00-4
Ethylene glycol-bis(2-aminoethylether)-*N,N,N′,N′*-tetraacetic acid (EGTA)	Sigma-Aldrich	Cat.#E3889; CAS ID: 67-42-5
2-mercaptoethanol	Sigma-Aldrich	Cat.#M3148; CAS ID: 60-24-2
Phenylmethylsulfonyl fluoride (PMSF)	Sigma-Aldrich	Cat.#P7626; CAS ID: 329-98-6
Aprotinin	Thermo Scientific	Cat.#78432; CAS ID: 9087-70-1
Leupeptin	Sigma-Aldrich	Cat.#L5793; CAS ID: 103476-89-7
TRIzol Reagent	Invitrogen	Cat.#15596018
RNAClean XP	Beckman Coulter	Cat.#A66514
M-PER	Thermo Scientific	Cat.#78501
Halt Phosphatase Inhibitor Cocktail 100x	Thermo Scientific	Cat.#78426
Halt Protease Inhibitor Cocktail 100x	Thermo Scientific	Cat.#78429
Harris Hematoxylin	StatLab Medical Products	Cat.#HXHHELT
Eosin	Sigma-Aldrich	Cat.#HT110216
Tween-20	Sigma-Aldrich	Cat.#P2287; CAS-ID: 9005-64-5
PERDROGEN 30% H_2O_2 (w/w)	Sigma-Aldrich	Cat.#31642; CAS ID: 7722-84-1
Gelatin, from cold water fish skin	Sigma-Aldrich	Cat.#G7765; CAS ID: 9000-70-8
Mayer's Hematoxylin	Sigma-Aldrich	Cat.#MHS32
Naphthol AS-BI phosphate	Sigma-Aldrich	Cat.#N2125; CAS ID: 1919-91-1

Pararosaniline hydrochloride	Sigma-Aldrich	Cat.#P3750; CAS ID: 569-61-9
Fast Green FCF	Sigma-Aldrich	Cat.#F7252; CAS ID: 2353-45-9
SR1078 (RORα/γ Agonist)	Sigma-Aldrich	Cat.#557352
Critical Commercial Assays		
Free Glycerol Reagent	Sigma-Aldrich	Cat.#F6428
Human Leptin Quantikine ELISA	R&D Systems	Cat.#DLP00
Quantikine ELISA Mouse/Rat Leptin	R&D Systems	Cat.#MOB00B
Succinate Assay Kit	Sigma-Aldrich	Cat.#CB04A13
Succinate Colorimetric Assay Kit	Sigma-Aldrich	Cat.#MAK184
High-Capacity cDNA Reverse Transcription kit with RNAse inhibitor	Applied Biosysems	Cat.#4374966
RNeasy Mini Kit	Qiagen	Cat.#74106
TruSeq Stranded Total RNA Library Prep kit	Illumina	Cat.#20020597
Reverse transcriptase SuperScript II	Invitrogen	Cat.#10328062
KAPA Library Quantification Kit KK4835	Roche	Cat.#07960204001
Pierce BCA Protein Assay Kit	Thermo Scientific	Cat.#23225
Immobilon ECL Ultra Western HRP Substrate	Merck Millipore	Cat.#WBULS0500
Vectastain ABC	Vector Laboratories	Cat.#SK-4000
DAB peroxidase substrate kit	Vector Laboratories	Cat.#SK-4100
Nano-Glo® Dual-Luciferase® Reporter Assay System	Promega	Cat.#N1610
Deposited Data		
RNA sequencing data	Gene Expression Omnibus (GEO)	Accession number: GSE200749
Experimental Models: Cell Lines		

3T3-L1 cell line	ATCC	CL-173™; RRID: CVCL_0123
HEK 293 cell line	ATCC	CRL-1573™; RRID: CVCL_0045
Experimental Models: Organisms/Strains		
Adipoq-Cre mice	kindly provided by G.Sabio, CNIC, Madrid, Spain	N/A
Sucnr1$^{fl/fl}$ mice	Keiran et al., 2019	N/A
Sucnr1 KO mice	McCreath et al., 2015	N/A
C57BL/6 wild-type mice	Charles River	N/A
B6.129-*Arntl*^{tm1Bra}/J	The Jackson Laboratory	Strain: #009100; RRID: IMSR_JAX:009100
Oligonucleotides		
Taqman Gene Expression Assays	Applied Biosystems	See Table 5
Recombinant Dna		
pBMAL1-LUC	kindly provided by S. Yamazaki (UT Southwestern Medical Center) and K. Eckel-Mahan (University of Texas) Yeom et al., 2010	N/A
pCMV6-human SUCNR1 (GFP-tagged)	Origene	Cat.#RC205888
pGL3-Basic	Promega	Cat.#E1751
pNL1.1.PGK[Nluc/PGK]	Promega	Cat.#N1441
Software And Algorithms		
ImageJ software 1.53k	National Institutes of Health, USA	RRID: SCR_003070
Mnova software	Mestrelab Research	N/A
NRecon resontruction software	SkyScan	N/A
CT-Analyzer	SkyScan	N/A
ZEN Digital Imaging for Light Microscopy v 3.1 (blue edition)	Zeiss	RRID: SCR_013672
Bioanalyzer DNA 1000	Agilent	N/A
Fragment Analyzer Standard Sensitivity	Agilent	N/A

FastQC v0.11.9	BaseSpace Labs	RRID: SCR_014583
STAR software v 2.5.2	Dobin et al., 2013	RRID: SCR_004463
Rsubread package v 2.8.2	Liao et al., 2019	RRID: SCR_016945
iBright Analysis Software	Invitrogen	RRID: SCR_017632
Leica microsystems imaging software	Leica	N/A
Adiposoft plug-in (Image J)	Natrional Institutes of Health, USA	N/A
Nikon Eclipse E800 microscope	Nikon	RRID: SCR_020326
Graphpad Prism 8	Graphpad Software	RRID: SCR_002798
R software v4.2.0	R Core Team, 2022	RRID: SCR_001905
ggplot2 R package v3.3.6	Wickham, 2016	RRID: SCR_014601
ggpubr R package v0.4.0	N/A	RRID: SCR_021139
IBM SPSS Statistics v 27.0	IBM Corp	RRID: SCR_002865
R software v 4.1.2	R Core Team, 2022	RRID: SCR_001905
limma package v 3.50.1	Ritchie et al., 2015	RRID: SCR_010943
R/Bioconductor package DESeq2 v 1.34.0	Love et al., 2014	RRID: SCR_015687
ROAST-GSA v 1.03.2	Wu et al., 2010 Efron and Tibshirani, 2007	N/A
Bioconductor R package org.Hs.eg.db	Carlson, 2019	RRID:SCR_006442
Other		
NCD	SAFE diets	Cat.#A04
HFD 60% fat	Research diets	Cat.#D12492
DMEM/F12 medium	Gibco (Life Technologies Limited)	Cat.#31330-038
DMEM-High glucose	Hyclone (GE Healthcare Life Sciences)	Cat.#SH30081.01
FBS	Hyclone (GE Healthcare Life Sciences)	Cat.#SH30071.03
Antibiotic/antimycotic solution	Hyclone (GE Healthcare Life Sciences)	Cat.#SV30079.01
Immobilon-P PVDF membrane	Merck Millipore	Cat.#IPVH00010

2. POSTERS AND ORAL COMMUNICATIONS

21st MetNet Meeting of the Catalan Society of Biology, 03/2021.

- ✓ Oral presentation entitled: "Metabolic phenotype of adipocyte specific SUCNR1 knockout mice: deciphering new metabolic functions for succinate".
- ✓ Barcelona (Spain).

First Conference for Young Researchers organized by the Rovira i Virgili University and IISPV, 11/2021.

- ✓ Moderator and oral presentation entitled: "Ad-Sucnr1 KO mice and new metabolic functions for succinate/SUCNR1".
- ✓ Rovira I Virgili University, Reus (Spain).

Pint of Science, 05/2022.

- ✓ Scientific dissemination about stem cells.
- ✓ Tarragona (Spain)

44th Congress of the SEBBM (Spanish Society of Biochemistry and Molecular Biology), 09/2022.

- ✓ Poster entitled: "SUCNR1 signaling in adipocytes controls energy homeostasis by modulating leptin".
- ✓ Málaga (Spain).

XIII CIBERDEM Annual Meeting, 11/2022.

- ✓ Poster entitled: "SUCNR1 signaling in adipocytes controls energy homeostasis by modulating circadian clock and leptin expression".
- ✓ Mataró (Spain).

45th Congress of the SEBBM (Spanish Society of Biochemistry and Molecular Biology), 09/2023.

- ✓ Poster and oral presentation entitled: "Colonic succinate stimulates GLP-1 secretion in the gastrointestinal tract via SUCNR1".
- ✓ Zaragoza (Spain).

Lunenfeld-Tanenbaum Research Institute (LTRI) Seminar, 10/2023.

- ✓ Oral presentation entitled: "Colonic succinate stimulates GLP-1 secretion in the gastrointestinal tract via SUCNR1".
- ✓ Mount Sinai Hospital, Toronto (Canada).

European Research Night, 2020-2022.

Workshop:

- ✓ "Ageing, obesity and diabetes: our Achilles heel in the face of Covid-19" (11/2020).
- ✓ "From the inside out, the fat you don't see" (09/2021).
- ✓ "Learn what fat does to our body: the good, the bad and the unknown" (09/2022).

Scientific seminars of DIAMET group, 2021-2024.

Oral presentations entitled:

- ✓ "Metabolic involvement of the succinate/SUCNR1 axis: in the adipocyte" (2021).
- ✓ "SUCNR1 signaling in adipocytes controls energy metabolism by modulating leptin expression" (2022).
- ✓ "Succinate/SUCNR1 axis and GLP-1 secretion in the gastrointestinal tract" (2023).
- ✓ "Diet-driven succinate production by intestinal microbiota stimulates GLP-1 secretion by colonic enteroendocrine cells via SUCNR1" (2024).

3. FELLOWSHIPS, AWARDS, AND HONORS

Predoctoral fellowship FPI (2019 call).

This doctoral thesis is carried out with the aid for predoctoral contracts for the training of FPI doctors of the 2019 call, which is associated with the project RTI2018-093919-B-I00 of Dr. Sonia Fernández Veledo.

Award for best poster at the XIII CIBERDEM Annual Meeting.

- ✓ Mataró (Barcelona)-November 10 and 11, 2022.
- ✓ Poster entitled "SUCNR1 signaling in adipocytes controls energy homeostasis by modulating leptin expression".

Nature Reviews Endocrinology "Research Highlights"

- ✓ Summary of our article published in Cell Metabolism (2023 Apr 4;35(4):601-619.e10) in the "Research Highlights" section titled: "Succinate signaling regulates leptin production in adipocytes." Nat Rev Endocrinol. 2023 Apr 17. doi: 10.1038/s41574-023-00838-z.

Mobility Grant for the 2023 URV Biomedicine PhD Program.

- ✓ This mobility grant cover expenses during the three-month predoctoral stay in Toronto with Dr. Daniel J. Drucker (09/23-12/23).
- ✓ Project entitled: "Colonic succinate stimulates GLP-1 secretion in the gastrointestinal tract via SUCNR1"

Member of the IISPV PhD Training Commission.

- ✓ Pere Virgili Health Research Institute, 11/2021-present.
- ✓ Participation in the organization of seminars and events for doctoral students.

Member of the Spanish Society of Biochemistry and Molecular Biology (SEBBM).

- ✓ 2022-present.

Member the Biomedical Network Research Center for Diabetes and Associated Metabolic Diseases (CIBERDEM).

- ✓ 2021-present.

4. RESEARCH STAYS DURING THE DOCTORAL PERIOD

Lunenfeld-Tanenbaum Research Institute, Mount Sinai Hospital, University of Toronto, Canada. 09/2023-12/2023

- ✓ Visiting predoctoral studentship training: Collaboration with the host laboratory with the project entitled: "Colonic succinate stimulates GLP-1 secretion in the gastrointestinal tract via SUCNR1". PI: Dr. Daniel J. Drucker

Alberto Sols Biomedical Research Institute (IIBM), Madrid. 04/ 2021.

- ✓ Calorimetry studies with (Phenomaster platform) and nuclear magnetic resonance (NMR) of Ad-*Sucnr1* KO transgenic mice. PI: Dr. Mario Vallejo Fernández.

Department of Physiological Sciences, University of Barcelona, Bellvitge. 05/2021.

- ✓ MicroCT analysis and bone histology of Ad-*Sucnr1* KO transgenic mice. PI: Dr. Francesc Ventura.